

**Pyrazole and Imidazole based Fluorescent Boron
Compounds: Synthesis and Study of Aggregation Induced
Enhanced Emission Properties of Tetraaryl Pyrazole
Supported Polymers and Cyclophosphazenes**

By

V.MUKUNDAM

CHEM11201104014

**National Institute of Science Education and Research,
Bhubaneswar, Odisha**

*A thesis submitted to the
Board of Studies in Chemical Sciences
In partial fulfillment of requirements
for the Degree of*

DOCTOR OF PHILOSOPHY

Of

HOMI BHABHA NATIONAL INSTITUTE

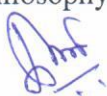
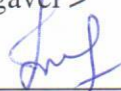
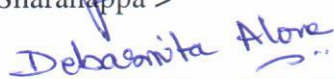


June, 2017

Homi Bhabha National Institute¹

Recommendations of the Viva Voce Committee

As members of the Viva Voce Committee, we certify that we have read the dissertation prepared by V.Mukundam entitled “Pyrazole and Imidazole based Fluorescent Boron Compounds: Synthesis and Study of Aggregation Induced Enhanced Emission Properties of Tetraaryl Pyrazole Supported Polymers and Cyclophosphazenes ” and recommend that it may be accepted as fulfilling the thesis requirement for the award of Degree of Doctor of Philosophy.

	12.10.17
Chairman - < Prof. A. Srinivasan >	Date:
	12/10/17
Guide / Convener - < Dr. V. Krishnan >	Date:
	12/10/17
Examiner - < Prof. R. Murugavel >	Date:
	12/10/17
Member 1- < Dr. U. Lourderaj >	Date:
	12/10/17
Member 2- < Dr. N. Sharanappa >	Date:
	12/10/17
Member 3- < Dr. Debasmita P. Alone >	Date:

Final approval and acceptance of this thesis is contingent upon the candidate's submission of the final copies of the thesis to HBNI.

I/We here by certify that I have read this thesis prepared under my direction and recommend that it may be accepted as fulfilling the thesis requirement.

Date: 12/10/17

Place: Bhubaneswar


<Signature>

Guide

¹ This page is to be included only for final submission after successful completion of viva voce.

STATEMENT BY AUTHOR

This dissertation has been submitted in partial fulfillment of requirements for an advanced degree at Homi Bhabha National Institute (HBNI) and is deposited in the Library to be made available to borrowers under rules of the HBNI.

Brief quotations from this dissertation are allowable without special permission, provided that accurate acknowledgement of source is made. Requests for permission for extended quotation from or reproduction of this manuscript in whole or in part may be granted by the Competent Authority of HBNI when in his or her judgment the proposed use of the material is in the interests of scholarship. In all other instances, however, permission must be obtained from the author.

V.Mukundam

DECLARATION

I, hereby declare that the investigation presented in the thesis has been carried out by me. The work is original and has not been submitted earlier as a whole or in part for a degree / diploma at this or any other Institution / University.

V.Mukundam

LIST OF PUBLICATIONS

Published

1. ***Mukundam, V.**; Dhanunjayarao, K.; Chuang, C.-N.; Kang, D.-Y.; Leung, M.-k.; Hsieh, K.-H.; Venkatasubbaiah, K. Design, synthesis, photophysical and electrochemical properties of 2-(4,5-diphenyl-1-p-aryl-1H-imidazol-2-yl)phenol-based boron complexes. *Dalton Trans.* **2015**, *44*, 10228.
2. ***Mukundam, V.**; Kumar, A.; Dhanunjayarao, K.; Ravi, A.; Peruncheralathan, S.; Venkatasubbaiah, K. Tetraaryl pyrazole polymers: Versatile synthesis, aggregation induced emission enhancement and detection of explosives. *Polym. Chem.* **2015**, *6*, 7764.
3. ***Mukundam, V.**; Dhanunjayarao, K.; Mamidala, R.; Venkatasubbaiah, K. Synthesis, characterization and aggregation induced enhanced emission properties of tetraaryl pyrazole decorated cyclophosphazenes. *J. Mater. Chem. C.* **2016**, *4*, 3523.
4. †Dhanunjayarao, K.; †**Mukundam, V.**; Venkatasubbaiah, K. Tetracoordinate imidazole-based boron complexes for the selective detection of picric acid. *Inorg. Chem.* **2016**, *55*, 11153 (†equal contribution).
5. ***Mukundam, V.**; Dhanunjayarao, K.; Samal, S.; Venkatasubbaiah, K. Substituent variation at the para-position of 2-phenol of tetraaryl substituted imidazole boron difluoride complexes: Synthesis, characterization and photophysical properties. *Asian J. Org. Chem.* **2017**, *6*, 1054
6. Mamidala, R.; **Mukundam, V.**; Dhanunjayarao, K.; Venkatasubbaiah, K. Synthesis of a cyclometalated 1,3,5-triphenylpyrazole palladium dimer and its activity towards cross coupling reactions. *Dalton Trans.* **2015**, *44*, 5805.

-
7. Dhanunjayarao, K.; **Mukundam, V.**; Ramesh, M.; Venkatasubbaiah, K. Synthesis and optical properties of salicylaldehyde-based diboron complexes. *Eur. J. Inorg. Chem.* **2014**, 539.
 8. Dhanunjayarao, K.; **Mukundam, V.**; Venkatasubbaiah, K. A highly selective ratiometric detection of F⁻ based on excited-state intramolecular proton-transfer (Imidazole) materials. *J. Mater. Chem. C* **2014**, 2, 8599.
 9. Dhanunjayarao, K.; **Mukundam, V.**; Venkatasubbaiah, K. Ratiometric sensing of fluoride anion through selective cleavage of Si-O bond. *Sensors and Actuators B* **2016**, 232, 175.
 10. Adinarayana, B.; Thomas, A. P.; Yadav, P.; Mukundam, V.; Srinivasan, A. Carbatriphyrin(3.1.1)-a distinct coordination approach of B^{III} to generate organoborane and weak C-H...B interactions. *Chem. Eur. J.* **2017**, 23, 2993.
 11. Mamidala, R.; Mukundam, V.; Dhanunjayarao, K.; Venkatasubbaiah, K. Cyclometalated palladium pre-catalyst for N-alkylation of amines using alcohols and regioselective alkylation of sulfanilamide using aryl alcohols. *Tetrahedron* **2017**, 73, 2225.

Manuscript under preparation

1. ***Mukundam, V.**; Venkatasubbaiah, K. Pyrazole based N,C- chelate organoboron compounds and its dimeric compounds with aromatic spacer.
2. ***Mukundam, V.**; Venkatasubbaiah, K. Luminescent N,C- chelate dinuclear boron compounds based on phenanthrene imidazole: Synthesis, characterization photophysical and electrochemical properties.
3. **Mukundam, V.**; Venkatasubbaiah, K. Pyrazole based tri-coordinate boron compounds for selective detection of picric acid.

* Pertaining to thesis

Conferences

1. "Synthesis and Optical Properties of Salicylaldimine-Based Diboron Complexes"- K. Dhanunjayarao, **V. Mukundam**, R. Mamidala and K. Venkatasubbaiah*in Indo-French Symposium on Functional Metal-Organics: Applications in Materials and Catalysis, February 24-26th, 2014 Organized at School of Chemical Sciences, NISER, Bhubaneswar. (**Poster Presentation**)
2. "Tetraaryl Pyrazole Supported Polymers and Cyclophosphazenes : Synthesis and Photophysical Properties"- **V. Mukundam**, K. Dhanunjayarao, R. Mamidala and K. Venkatasubbaiah* in 19th CRSI National Symposium in Chemistry July 14-16th, 2016 Organized at Department of Chemistry, University of North Bengal, Darjeeling (**Poster Presentation**)

V. Mukundam

Dedicated to my family

ACKNOWLEDGEMENTS

*I would like to express my sincere gratitude to my supervisor **Dr.V.Krishnan** for his patient guidance, insightful advice and invaluable encouragements throughout my time as his student.*

*I am thankful to **Prof. V. Chandrasekhar**, Director, NISER and also **Prof.T. K. Chandrashekar**, Founder-Director, NISER for providing the laboratory facilities, CSIR-New Delhi for financial support.*

*I would like to thank my thesis monitoring committee members **Prof. A. Srinivasan, Dr. Sharanappa Nembenna**, all other faculties in SCS NISER for their useful suggestions and **Dr.S. Peruncheralathan, Dr. Upakarasamy Lourderaj, Dr. Arun Kumar** support on several occasions.*

*I sincerely thank **Mr. Deepak, Mr. Sanjaya, Mr. Amit and Mr. Raj Kumar** for recording the single crystal X-Ray, NMR and Mass spectral analysis.*

*I am greatly indebted to **all my teachers** of school (**Shankara chari, Sridhar sir**), graduation (**Madhava rao sir**) and post-graduation who inculcated knowledge, discipline and encouragement.*

*It gives me immense pleasure to thank all those seniors, friends and juniors who made my life at NISER really enjoyable and memorable. Special mention must be made of my labmates **Dhanu, Ramesh, Ramu, Sathish, Srinibas, Samser, Shiva, Prakash, Joseph, Priybrata, Athul, Tharun, Sanket, Preeta** for their support and special thanks to my seniors **Pardhasaradhi, Milan, Ashim, Basu, Giri, Manoj, Chandu, Subba reddy, Pedda rao, Thapas, Saikat**. Also I thank **Prabhath, Somnath, Manas, Arindam, Tanmay, Mriganka, Venkat, Shiva, Surya, Ranjay, Thirupathi and Amaranth** for their help.*

*I am greatly thankful to my life partner **Sangeetha** for her understanding, support, encouragement, quite patience and unwavering love.*

*I am deeply grateful to my beloved **Amma, Nanna, Brothers and Sisters-in-law** for their unconditional love, support, sacrifices, blessings and inspiration throughout my career.*

V.Mukundam

CONTENTS

	Page No.
Synopsis	xi
List of Tables	xx
List of Schemes	xii
List of Figures	xxiii
List of Abbreviations	xxxii
Chapter 1	1
Chapter 2	47
Chapter 3	107
Chapter 4	171
Chapter 5	199
Summary	257

SYNOPSIS

First part of this chapter describes a brief introduction to fluorescent boron compounds. Boron containing organic luminescent materials can be broadly classified into two categories tri^{1,2}- and tetra³⁻⁵- coordinate boron compounds (Figure 1). Bulky aryl groups, such as the mesityl (2,4,6-trimethylphenyl), fluoromesityl (2,4,6-tris(trifluoromethylphenyl)), or triptyl (2,4,6-triisopropylphenyl) groups are necessary to stabilize the tri-coordinate boron compounds. The overlap of the empty p_z orbital of the tri-coordinate boron atom with the organic π -system leads to interesting optoelectronic properties and also enables the detection of anions such as fluoride and cyanide. Much effort has been devoted to the development of different types of tetra-coordinate boron compounds owing to their high stability towards air and moisture over tri-coordinate boron compounds. Boron dipyrromethene (BODIPYs)⁶ dyes are well known tetra-coordinate boron compounds with N,N-chelate ligands and have been used extensively as fluorescent imaging agents, chemical sensors and near-infrared emitting materials. Although BODIPYs exhibit strong fluorescence and high molar extinction coefficients, they suffer from small Stokes shift and weak solid state emissions which limits their potential application in organic light emitting diodes (OLED). Therefore, there is a need to develop novel boron complexes with a well designed structure to overcome the weakness of BODIPY. Several examples of boron fluorophores with different architectures have been reported to intrinsically exhibit better photophysical properties, not only in solution but also in the solid state. According to the chelate donor atoms, the four-coordinate boron compounds mainly classified as N,O-, N,N-, N,C-, and O,O-chelate. Recently developed this class of compounds were used as very attractive materials for various optoelectronic applications including emitters, electron transport materials, and hole blocking

materials for organic light emitting diodes (OLEDs), sensory and biological imaging materials, and photoresponsive materials³⁻⁵.

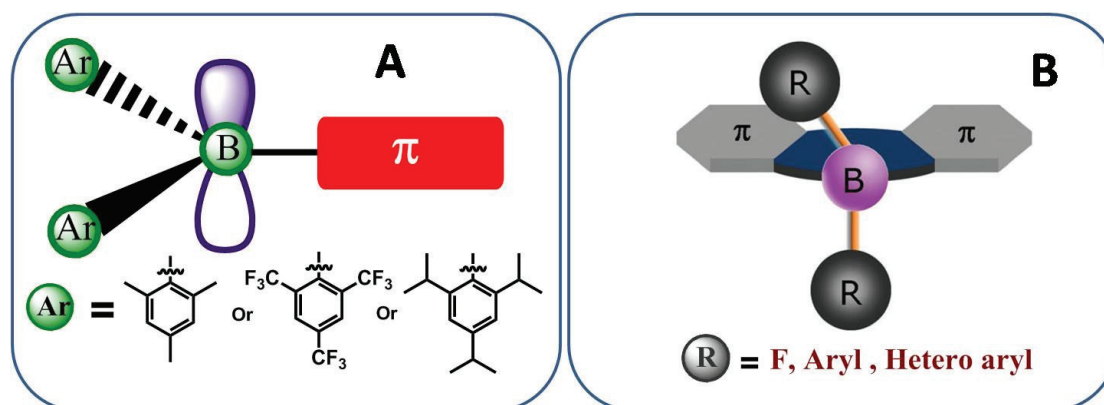


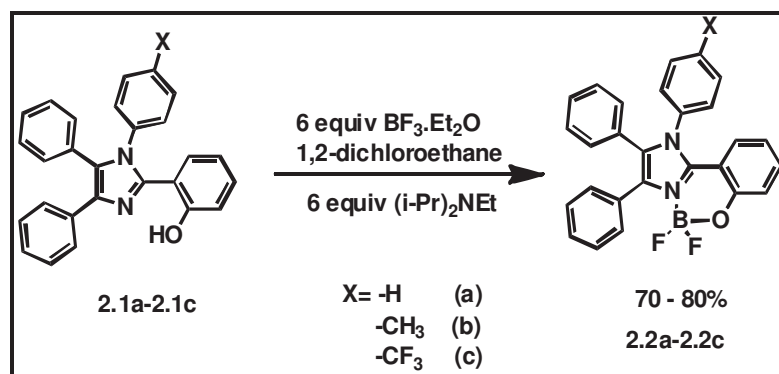
Figure 1: Structures of tri- (A) and tetra- (B) coordinate boron compounds

Part B:

Second part of this chapter deals with the introduction of Aggregation induced emission (AIE) phenomenon. Organic fluorophores generally shows strong emission in dilute solutions, however more often exhibit relatively weak emission in the solid state due to the aggregation of molecules in the solid state. This phenomenon is known as aggregation caused quenching (ACQ), which has become an obstacle in the fabrication of light emitting devices. The trouble caused by ACQ has driven researchers to develop unconventional anti ACQ luminophoric systems. The recent discovery of aggregation induced emission (AIE) by Tang's group⁷ and aggregation induced enhanced emission (AIEE) by Park's group⁸ has attracted much attention owing to their potential applications in different fields. Since these pioneering studies, a series of interesting molecules with AIE or AIEE properties have been reported and used as bioprobes, stimuli responsive nanomaterials, chemosensors and active layers in the construction of efficient organic light emitting diodes⁹.

Chapter 2: Design, synthesis, photophysical and electrochemical properties of imidazole based N,O- chelate boron complexes

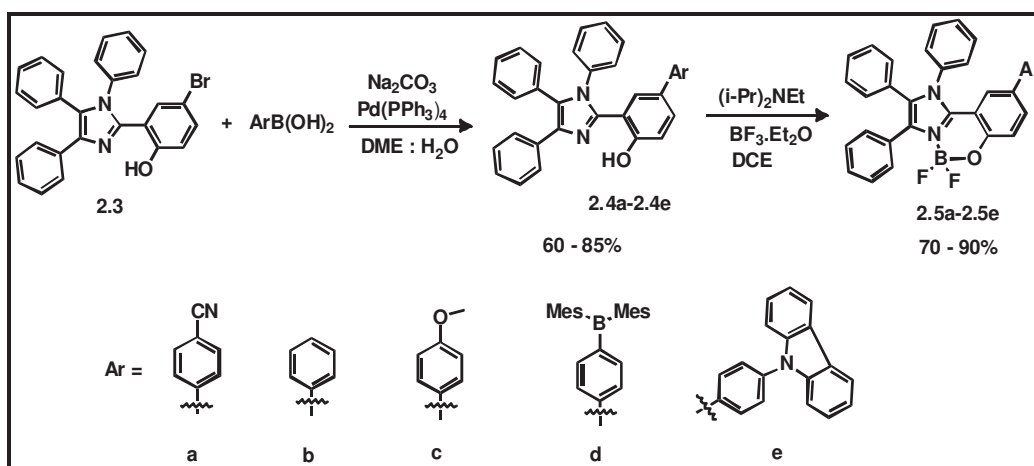
This chapter is divided into two parts. First part of this chapter describes the synthesis of 2-(4,5-diphenyl-1-p-aryl-1H-imidazol-2-yl)phenol-based boron complexes (**2.2a-2.2c**) from the excited-state intramolecular proton-transfer process celebrated tetraarylimidazoles (**2.1a-2.1c**) (scheme 1). All boron compounds were fully characterized by multinuclear NMR spectroscopy, LC-MS, thermogravimetric analysis, cyclic voltammetry and single crystal X-ray diffraction analysis (for **2.2a** & **2.2c**). Photophysical measurements of all three new boron compounds showed good quantum yields in solution and one electron electrochemical irreversible reduction. Single layer organic light emitting devices were fabricated using these boron compounds (**2.2a** - **2.2c**) as the electron transporting materials. A maximum brightness of 6450 cd m^{-2} at 12.5 V was realized when compound **2.2a** was used as an electron transporting material.



Scheme 1: Synthetic route to compounds **2.2a-2.2c**.

Second part of this chapter describes the substituent effects on the photoluminescence of imidazole boron complexes. These compounds (**2.5a-2.5e**) were synthesized using the conditions as shown in scheme 2. All five new boron complexes were characterized by multinuclear NMR spectroscopy, LC-MS, elemental analysis. Single

crystals of **2.5a**, **2.5b**, **2.5d** and **2.5e** were grown from CH₂Cl₂/hexane mixtures and analyzed by X-ray diffraction crystallography.

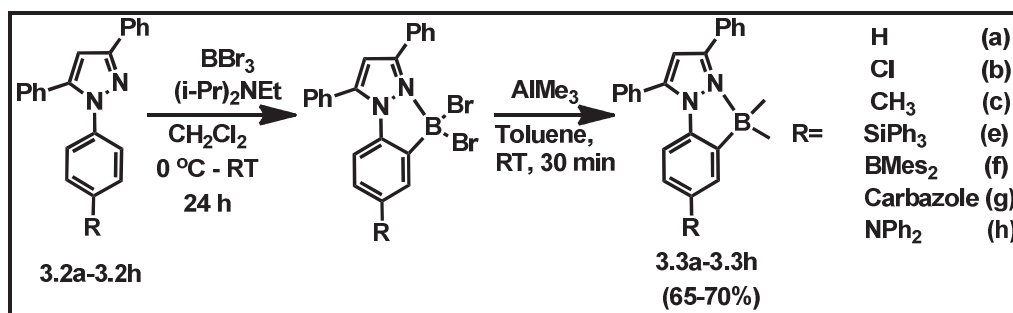


Scheme 2: Synthetic route to compounds **2.5a-2.5e**

These complexes exhibit bright blue emissions in solution with quantum yields ranging from 0.23 to 0.65 in dichloromethane at room temperature. All five boron complexes exhibit good thermal stability (decomposition starts above 300 °C) with high melting points (>270 °C). Cyclic voltammetric studies reveal that compounds **2.5b**, **2.5c**, and **2.5e** showed one electron irreversible reduction peaks where as compound **2.5a** and **2.5d** exhibited two reduction peaks due to the presence of -CN group and tri-coordinated boron respectively.

Chapter 3: Synthesis, photophysical and electrochemical properties of N,C-chelate pyrazole based boron complexes.

This chapter is divided into two parts. The first part of this chapter describe the synthesis of different substituted pyrazole based boron complexes which are shown in scheme 3. All these compounds were fully characterized by IR, HRMS, multinuclear NMR spectroscopy, electronic absorption, emission (solution), electrochemical and thermal studies. The photophysical properties of these boron compounds in dichloromethane solution reveal that they exhibit moderate quantum yields.



Scheme 3: Synthetic route to compounds **3.3a-3.3h**.

Compound **3.3g** and **3.3h** exhibited solvatochromism in the fluorescence spectra. All These compounds (**3.3a-3.3h**) exhibited one electron electrochemical irreversible reduction. Second part of this chapter deals with synthesis, characterization, photophysical, thermal and electrochemical properties of novel pyrazole based diboron complexes.

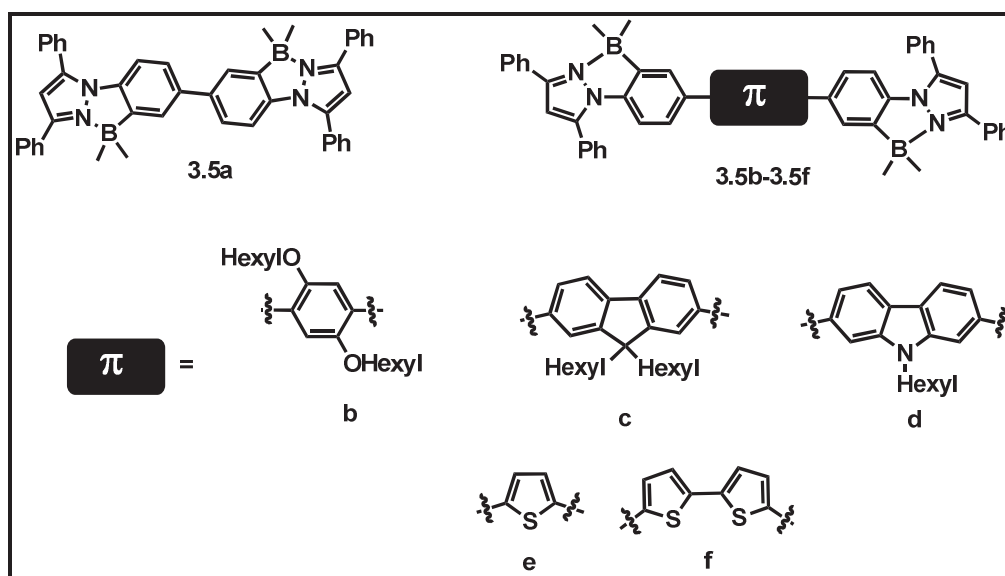


Figure 2: Pyrazole based diboron complexes.

The diboron complexes were characterized by multinuclear NMR spectroscopy, high resolution MS, and single crystal X-ray diffraction analysis (for **3.5a**, **3.5c**, **3.5e** and **3.5f**). These diboron complexes possess high thermal stabilities with decomposition temperature > 350 °C. Photophysical studies of these diboron complexes in solution and solid state reveal that they exhibit excellent quantum yields in solution and

moderate quantum yield in solid state. Emission maxima of thiophene (**3.5e**) and bithiophene (**3.5f**) spacer diboron complexes were red shifted compared to other diboron complexes.

Chapter 4: Luminescent N,C- chelate dinuclear boron complexes based on phenanthrene imidazole.

The incorporation of multiboron centers in the π -conjugated framework intensifies the emission, enhances the charge transport properties, and increases thermal stability¹⁰.

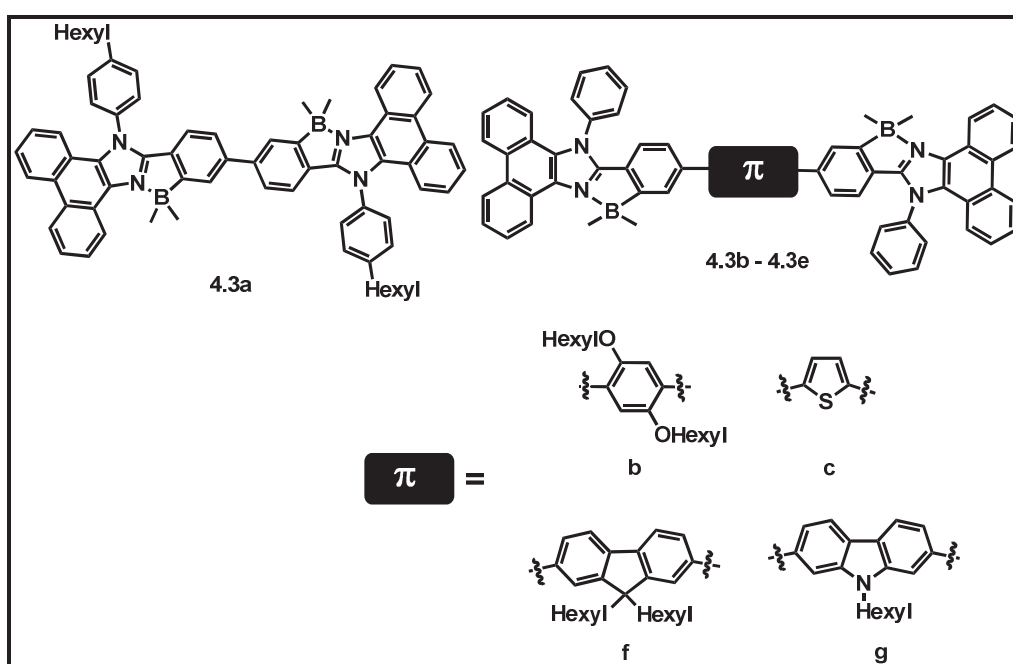


Figure 3:Phenanthrene imidazole based diboron complexes.

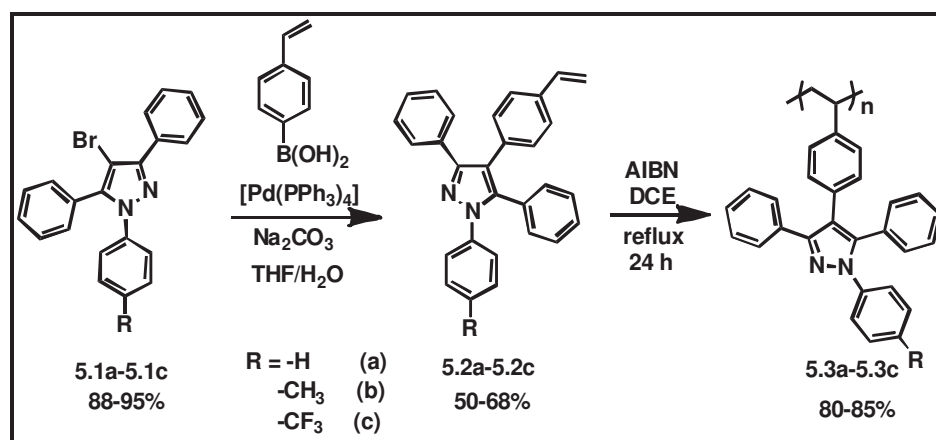
This chapter describes the synthesis of phenanthrene imidazole based diboron complexes. All the five diboron complexes were characterized by multinuclear NMR, HRMS, and single crystal X-ray diffraction analysis. These boron complexes possess very high decomposition temperature ($>390^{\circ}\text{C}$), indicative of their high thermal stabilities. Photophysical studies of these complexes reveal that these diboron compounds show strong emission with excellent quantum yields in dichloromethane and moderate quantum yields in solid state.

Chapter 5: Tetraaryl pyrazole supported polymers and cyclophosphazenes

Recently it was realized that tetraaryl pyrazoles show a significant enhancement in their light emission upon aggregation¹¹. We envisioned that the tetraaryl pyrazoles supported polymers and cyclophosphazenes might also show the AIEE phenomenon. This chapter demonstrate their synthesis, AIEE phenomenon and their application in picric acid sensing. This chapter is divided into two parts.

Part A:

First part of this chapter describe a new approach to obtain tetraaryl pyrazole polymers and their AIEE properties. The styryl containing pyrazoles were prepared according to the synthetic route shown in Scheme 4. The poly(tetraaryl pyrazole)s with moderate molecular weights were prepared from the monomers **5.2a**, **5.2b** and **5.2c** by using the standard free radical initiator, AIBN.



Scheme 4: Synthetic route to tetraaryl pyrazole polymers.

All the polymers were thermally stable ($T_d > 300\text{ }^\circ\text{C}$) and readily soluble in organic solvents such as THF, CH_2Cl_2 and $CHCl_3$. The study of the photophysical properties of the poly(tetraaryl pyrazole)s reveal that they are less emissive when dissolved in THF solution but became more emissive when aggregated, divulging that they are AIEE active. Utilizing this AIEE effect of the poly(tetraaryl pyrazole)s we exploited

them as chemosensors for the detection of explosives (picric acid) in the aggregate state.

Part B:

Cyclophosphazenes are interesting inorganic heterocycles have attracted interest because of their use as scaffolds for the design and construction of a wide variety of functional and specialty materials.

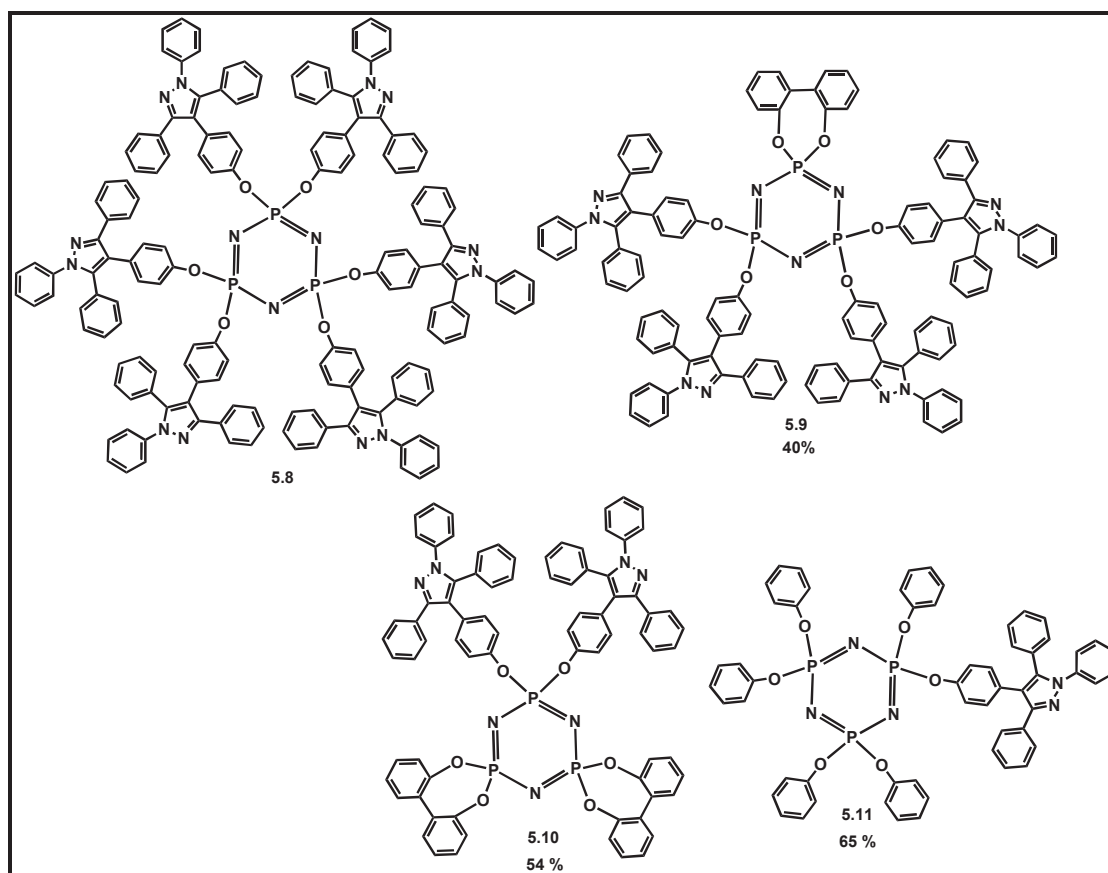


Figure 4:Hexa-(5.8), tetra-(5.9), di-(5.10) and mono-(5.11) AIEE luminogen decorated cyclophosphazenes.

Another added advantage of the cyclotriphosphazenes is its ability to serve as a small molecule model system for high polymeric phosphazenes¹¹. This part of chapter 5 describes synthesis of tetraaryl pyrazole decorated cyclophosphazenes, their AIEE properties. All compounds were characterized using multinuclear NMR spectroscopy, high resolution mass spectroscopy (HRMS) and elemental analysis. The study of the

photophysical properties of the tetraaryl pyrazole decorated cyclophosphazenes in the aggregated and non-aggregated form reveals that they exhibit the aggregation induced emission enhancement (AIEE) phenomenon. The luminogen decorated cyclophosphazenes in aggregate state used as a probe for the detection of explosive picric acid.

References:

- (1) Wade, C. R.; Broomsgrove, A. E. J.; Aldridge, S.; Gabbai, F. P. *Chem. Rev.* **2010**, *110*, 3958.
- (2) Jäkle, F. *Coord. Chem. Rev.* **2006**, *250*, 1107.
- (3) Frath, D.; Massue, J.; Ulrich, G.; Ziessel, R. *Angew. Chem. Int. Ed.* **2014**, *53*, 2290.
- (4) Li, D.; Zhang, H.; Wang, Y. *Chem. Soc. Rev.* **2013**, *42*, 8416.
- (5) Rao, Y.-L.; Wang, S. *Inorg. Chem.* **2011**, *50*, 12263.
- (6) Loudet, A.; Burgess, K. *Chem. Rev.* **2007**, *107*, 4891.
- (7) Luo, J.; Xie, Z.; Lam, J. W. Y.; Cheng, L.; Chen, H.; Qiu, C.; Kwok, H. S.; Zhan, X.; Liu, Y.; Zhu, D.; Tang, B. Z. *Chem. Commun.* **2001**, 1740.
- (8) An, B.-K.; Kwon, S.-K.; Jung, S.-D.; Park, S. Y. *J. Am. Chem. Soc.* **2002**, *124*, 14410.
- (9) Mei, J.; Leung, N. L. C.; Kwok, R. T. K.; Lam, J. W. Y.; Tang, B. Z. *Chem. Rev.* **2015**, *115*, 11718
- (10) Job, A.; Wakamiya, A.; Kehr, G.; Erker, G.; Yamaguchi, S. *Org. Lett.* **2010**, *12*, 5470.
- (11) Mukherjee, S.; Salini, P. S.; Srinivasan, A.; Peruncheralathan, S. *Chem. Commun.* **2015**, *51*, 17148.
- (12) Chandrasekhar, V. *Inorganic and organometallic polymers*. Springer, 2005.

List of tables

1	Table 2A.1	Comparison of some selected bond lengths [\AA] and bond angles [deg] for compounds 2a and 2c	53
2	Table 2A.2	Crystal data and structure refinement parameters for compounds 2a and 2c	54
3	Table 2A.3	Photophysical data of the imidazole boron compounds 2a-2c	57
4	Table 2A.4	Calculated electronic transitions for compound 2a-2c from TD-DFT (B3LYP) calculations	59
5	Table 2A.5	Electrochemical data of compounds 2a-2c	61
6	Table 2A.6	EL performances of the device 2a-2c	63
7	Table 2A.7	EL characters of the device 2a that contain different ratio of guest	63
8	Table 2B.1	Comparison of some selected bond lengths [\AA] and bond angles [deg] for compounds 3a , 3b , 3d and 3e	81
9	Table 2B.2	Comparison of deviation of boron atom from C_3NBO plane [\AA] and interplanar angles [deg] for compounds 3a , 3b , 3d and 3e	82
10	Table 2B.3	Crystal data and structure refinement parameters for compounds 3a , 3b , 3d and 3e	83
11	Table 2B.4	Photophysical data of the imidazole based boron compound 3a-3e	86
12	Table 3A.1	Comparison of selected bond lengths [\AA] and bond angles [deg] for compounds 13-19	114
13	Table 3A.2	Comparison of deviation of boron atom from $\text{C}_2\text{N}_2\text{B}$ plane [\AA] and inter planar angles [deg] for 13-19	115
14	Table 3A.3.1	Crystal data and structure refinement parameters for compounds 13-16	116
15	Table 3A.3.2	Crystal data and structure refinement parameters for compounds 17-19	117
16	Table 3A.4	Photophysical data of 12-19 in different solvents	119
17	Table 3A.5	Electrochemical data of 12-19	122
18	Table 3B.1	Comparison of selected bond lengths [\AA] and bond angles [deg] for compounds 4 , 8 , 10 and 11	149

19	Table 3B.2	Comparison of deviation of boron atom from C ₂ N ₂ B plane [Å] and inter planar angles [deg] for compounds 4, 8, 10 and 11	150
20	Table 3B.3	Crystal data and structure refinement parameters for compounds 4, 8, 10 and 11	151
21	Table 3B.4	Photophysical properties of 4 and 7-11 in various solvents at 298 K	154
22	Table 4.1	Comparison of selected bond lengths [Å] and bond angles [deg] for compounds 7- 10	179
23	Table 4.2	Comparison of deviation of boron atom from C ₃ NB plane [Å] and inter planar angles [deg] for compounds 7- 10	180
24	Table 4.3	Crystal data and structure refinement parameters for compounds 7, 8, 9 &10	181
25	Table 4.4	Photophysical properties of 7-11 in various solvents and in solid state	183
26	Table 5A.1	Crystal data and structure refinement parameters for compounds 9	206
27	Table 5A.2	Molecular Weight data for polymers 10-12 &16	206
28	Table 5A.3	Thermal data for polymers 10-12 &16	207
29	Table 5A.4	Optical properties of the monomers (7-9 &15) and polymers (10-12 &16) in the solution and aggregated state	209
30	Table 5B.1	Optical properties of the compounds 5, 6, 7 & 9	233
31	Table 5B.2	Crystal data and structure refinement parameters for compounds 3 &7	239

List of schemes

1	Scheme 2A.1	Synthetic route to the compounds 2a-2c	51
2	Scheme 2B.1	Synthesis of imidazole boron complexes 3a-3e	78
3	Scheme 3A.1	Synthesis of compounds 1-11	110
4	Scheme 3A.2	Synthesis of compounds 12-19	111
5	Scheme 3B.1	Synthesis of compound 4	142
6	Scheme 3B.2	Synthesis of compounds 7-11	143
7	Scheme 4.1	Synthesis of compounds 5 and 6	174
8	Scheme 4.2	Synthesis of compounds 8-11	175
9	Scheme 5A.1	Synthetic route for the preparation of poly(tetraaryl pyrazole)s (10-12)	202
10	Scheme 5A.2	Synthetic route for the preparation of flexible poly(tetraaryl pyrazole)	203
11	Scheme 5B.1	Synthetic pathway for compound 4	228
12	Scheme 5B.2	Synthetic pathway for compound 5, 6 and 7	231
13	Scheme 5B.3	Synthetic pathway for compound 9	232

List of figures

1	Figure 1.1	Schematic representation of(left) tri-coordinate boron; (right) tetra-coordinate boron compounds.	3
2	Figure 1.2	BODIPY dye	5
3	Figure 1.3	N,N- chelate tetra-coordinate boron complexes (1-16)	7
4	Figure 1.4	N,N- chelate tetra-coordinate boron complexes (17-40)	8
5	Figure 1.5	N,N- chelate tetra-coordinate boron complexes (41-62)	10
6	Figure 1.6	N,N- chelate tetra-coordinate boron complexes (63-70)	11
7	Figure 1.7	N,O- chelate tetra-coordinate boron complexes (71-91)	12
8	Figure 1.8	N,O- chelate tetra-coordinate boron complexes (92-104)	13
9	Figure 1.9	N,O- chelate tetra-coordinate boron complexes (105-130)	14
10	Figure 1.10	N,O- chelate tetra-coordinate boron complexes (131-148)	15
11	Figure 1.11	N,O- chelate tetra-coordinate boron complexes (149-188)	16
12	Figure 1.12	N,O- chelate tetra-coordinate boron complexes (189-201)	17
13	Figure 1.13	N,O- chelate tetra-coordinate boron complexes (202-226)	19
14	Figure 1.14	N,O- chelate tetra-coordinate boron complexes (227-234)	20
15	Figure 1.15	N,C- chelate tetra-coordinate boron compounds (235-240)	21
16	Figure 1.16	N,C- chelate tetra-coordinate boron compounds (241-250)	22
17	Figure 1.17	N,C- chelate tetra-coordinate boron compounds (251-251B)	22
18	Figure 1.18	N,C- chelate tetra-coordinate boron compounds (252-261)	23
19	Figure 1.19	N,C- chelate tetra-coordinate boron compounds (262-265)	24
20	Figure 1.20	N,C- chelate tetra-coordinate boron compounds (266-288)	25
21	Figure 1.21	N,C- chelate tetra-coordinate boron compounds (289-295)	25
22	Figure 1.22	N,C- chelate tetra-coordinate boron compounds (296-300)	26

23	Figure 1.23	N,C- chelate tetra-coordinate boron compounds (302-305)	27
24	Figure 1.24	N,C- chelate tetra-coordinate boron compounds (306-312)	27
25	Figure 1.25	N,C- chelate tetra-coordinate boron compounds (313-316)	28
26	Figure 1.26	N,C- chelate tetra-coordinate boron compounds (317-330)	29
27	Figure 1.27	N,C- chelate tetra-coordinate boron compounds (331-338)	29
28	Figure 1.28	N,C- chelate tetra-coordinate boron compounds (339-342)	30
29	Figure 1.29	(A) Planar luminophoric molecules such as perylene tend to aggregate as discs pile up, due to the strong π - π stacking interactions between the aromatic rings, which commonly turns “off” light emission. (B) Non-planar luminogenic molecules such as hexaphenylsilole (HPS) behave oppositely, with their light emissions turned “on” by aggregate formation, due to the restriction of the intramolecular rotation (RIR) of the multiple phenyl rotors against the silole stator in the aggregate state	32
30	Figure 1.30	(Left) Chemical structure of HPS. (Right) HPS solutions in acetonitrile-water mixtures containing different volume fractions of water; photographs taken under illumination of a UV lamp	33
31	Figure 1.31	Typical examples of structural motifs of AIEgens and their technological applications	34
32	Figure 1.32	Examples of the transformation from ACQ to AIE by decorating ACQphores with AIE gen (e.g., TPE)	35
33	Figure 1.33	Examples of the transformation from ACQ to AIE by replacing the one (top) or two phenyl (middle, bottom) rings of AIEgens (TPE, dimethyltetraphenylsilole, 9,10-di((E)-styryl)anthracene) with ACQphores	35

	(tirphenylamine, fluoranthene, carbazole)	
34	Figure 1.34 Examples of the transformation from ACQ to AIE by decorating ACQphores with aromatic rotors	36
35	Figure 2A.1 ^{11}B and ^{19}F NMR spectrum of compound 2c	52
36	Figure 2A.2 Molecular structures of compounds 2a , 2c (left); Thermal ellipsoids are shown at 30% probability level for 2a and 50% for 2c . Side view of 2a , 2c (right). Co-crystallized solvent molecule and hydrogen atoms are omitted for clarity	53
37	Figure 2A.3 Imidazole core numbering	54
38	Figure 2A.4 (top) Normalized UV-Vis absorption & (bottom) Normalized fluorescence spectra of compounds 2a-2c in dichloromethane (concentration = 4×10^{-5} M)	56
39	Figure 2A.5 The fluorescence photograph of compounds 2a-2c in dichloromethane solution (wavelength of light is 365 nm)	56
40	Figure 2A.6 Computed orbitals for compounds 2a-2c	58
41	Figure 2A.7 TGA curves of 2a-2c at a heating rate of 20 °C/min	60
42	Figure 2A.8 Cyclic voltammograms of compounds 2a-2c (vs. Ferrocene/Ferrocenium) with 0.1 M Bu_4NPF_6 in DMF as the supporting electrolyte (scan rate 100 mV/s)	61
43	Figure 2A.9 Schematic illustration of EL device structure	62
44	Figure 2A.10 EL characters of the device 2a-2c . (left) brightness-voltage, (right) current efficiency-current density	62
45	Figure 2A.11 EL performances of device 2a that contain different ratio of guest. (left) brightness-voltage, (right) current efficiency-current density	63
46	Figure 2B.1 Schematic representation of the skeleton of imidazole boron complexes	78
47	Figure 2B.2 ^1H NMR spectrum of compound 3d recorded in CDCl_3	79
48	Figure 2B.3 HRMS of compound 3d	79
49	Figure 2B.4 Molecular structures of 3a , 3b , 3d and 3e . Hydrogen atoms are omitted for clarity. Thermal ellipsoids are shown at the 50% probability level for 3a , 3d , 3e and	81

		30% for 3b .	
50	Figure 2B.5	Crystal-packing of 3a, 3b, 3d and 3e	82
51	Figure 2B.6	(top) Uv-Vis absorption spectra of 3a-3e in CH ₂ Cl ₂ (concentration = 4 × 10 ⁻⁵ M); (bottom) Normalized fluorescence spectra of 3a-3e in CH ₂ Cl ₂ (concentration = 4 × 10 ⁻⁵ M)	85
52	Figure 2B.7	The fluorescence photograph of compounds 3a-3e in dichloromethane solution under UV excitation ($\lambda_{\text{ex}} = 365$ nm)	85
53	Figure 2B.8	Fluorescence spectra of 3a-3e in the solid state	87
54	Figure 2B.9	Fluorescence spectra of compound 3a, 3b, 3c and 3c in different solid state ($\lambda_{\text{ex}} = 340$ nm)	87
55	Figure 2B.10	X-ray diffraction patterns of different solids of compound 3a, 3b, 3c and 3d	88
56	Figure 2B.11	Fluorescence spectra of compounds 3a, 3b, 3c and 3d recorded at various concentrations in tetrahydrofuran (THF) (excited at λ_{max})	89
57	Figure 2B.12	Computed orbitals for 3a-3e	91
58	Figure 2B.13	TGA curves of 3a-3e at heating rate of 10 °C /min	92
59	Figure 2B.14	Cyclic voltammograms of 3a, 3b, 3c, 3d, 3e in CH ₃ CN (with 0.1M Bu ₄ N(PF ₆) supporting electrolyte; scan rate 100 mV/s). Referenced relative to Fc/Fc+ couple	93
60	Figure 3A.1	HRMS spectrum of compound 14	112
61	Figure 3A.2	HRMS spectrum of compound 17	112
62	Figure 3A.3	¹ H NMR spectrum of compound 19 recorded in CDCl ₃	113
63	Figure 3A.4	¹¹ B NMR spectrum of compound 19 recorded in CDCl ₃	113
64	Figure 3A.5	Molecular structures of compound 13-19 . Hydrogen atoms have been omitted for clarity. Thermal ellipsoids are drawn at the 30% probability level	114
65	Figure 3A.6	Absorption spectra of 12-19 in dichloromethane (concentration: 4 × 10 ⁻⁵ M)	118
66	Figure 3A.7	Absorbance spectra of compounds 17 (a) and 18 (b) with increasing solvent polarity (concentration: 4 × 10 ⁻⁵ M)	118

67	Figure 3A.8	A comparison of normalized fluorescence spectra of compounds 12-19 in dichloromethane (concentration: 4×10^{-5} M).	120
68	Figure 3A.9	Normalized fluorescence spectra of compounds 17 (a) and 18 (b) with increasing solvent polarity (concentration: 4×10^{-5} M)	121
69	Figure 3A.10	The fluorescence photograph of compounds 12-19 in dichloromethane solution. Irradiation was performed with a UV lamp with a wavelength of 365 nm	121
70	Figure 3A.11	Cyclic voltammograms of 12-19 recorded in CH_3CN containing 0.1M $^n\text{Bu}_4\text{N}(\text{PF}_6)$ as supporting electrolyte; scan rate 100 mV/s. Referenced relative to Fc/Fc^+ couple.	122
71	Figure 3B.1	^1H NMR spectrum of compound 5 and 6	144
72	Figure 3B.2	^{11}B NMR spectrum of compound 5 and 6	144
73	Figure 3B.3	HRMS spectrum of compound 4	145
74	Figure 3B.4	HRMS spectrum of compound 7	146
75	Figure 3B.5	^1H NMR spectrum of compound 8 recorded in CDCl_3	146
76	Figure 3B.6	Molecular structure of compound 4 , 8 , 10 and 11 (left), side view (right). Thermal ellipsoids are drawn at 30% probability level	148
77	Figure 3B.7	Comparison of normalized absorption spectra of 4 and 7-11 in dichloromethane (concentration: 1×10^{-5} M)	153
78	Figure 3B.8	Comparison of normalized emission spectra of 4 and 7-11 in dichloromethane (concentration: 1×10^{-5} M)	153
79	Figure 3B.9	A comparison of normalized emission spectra of 4 and 7-11 in solid state	155
80	Figure 3B.10	The fluorescence photographs of compound 4,7-11 in dichloromethane solution (top) and in solid state (bottom). Irradiation was performed with a UV lamp with a wavelength of 365 nm	155
81	Figure 3B.11	TGA curves of 4 and 7-11 at a heating rate of $10^\circ\text{C}/\text{min}$	156
82	Figure 3B.12	DSC curves of 4 and 7-11 at heating rate of $10^\circ\text{C}/\text{min}$	156
83	Figure 3B.13	Cyclic voltammograms of 4 , 7-11 recorded in DMF	157

	containing 0.1M $n\text{Bu}_4\text{N}(\text{PF}_6)$ as supporting electrolyte; scan rate 100 mV/s. Referenced relative to Fc/Fc ⁺ couple	
84	Figure 4.1 ^{11}B NMR of compounds 3 and 5	175
85	Figure 4.2 ^1H NMR spectrum of compound 7	176
86	Figure 4.3 HRMS of compound 9	177
87	Figure 4.4 Molecular structure of compound 7 , 8 , 9 and 10 (left); side view (right). Thermal ellipsoids are drawn at 30% probability level	178
88	Figure 4.5 Comparison of normalized absorption spectra of 7-11 in dichloromethane (concentration: 1×10^{-5} M)	182
89	Figure 4.6 Comparison of normalized emission spectra of 7-11 in dichloromethane (concentration: 1×10^{-5} M)	183
90	Figure 4.7 Comparison of normalized emission spectra of 7-11 in solid state	184
91	Figure 4.8 The fluorescence photograph of compounds 7-11 in dichloromethane solution (top) and in solid state (bottom). Irradiation was performed with a UV lamp of a wavelength of 365 nm	184
92	Figure 4.9 TGA curves of 7-11 at heating rate of 10 °C/min	185
93	Figure 4.10 DSC curves of 7-11 at heating rate of 10 °C/min	186
94	Figure 4.11 Cyclic voltammograms of 7-11 recorded in DMF containing 0.1M $n\text{Bu}_4\text{N}(\text{PF}_6)$ as supporting electrolyte; scan rate 100 mV/s. Referenced relative to Fc/Fc ⁺ couple.	186
95	Figure 5A.1 HRMS spectrum of compound 7	204
96	Figure 5A.2 Molecular structure of 9 (left), thermal ellipsoids are drawn at the 50% probability level (Hydrogen atoms are omitted for clarity).	205
97	Figure 5A.3 ^1H NMR spectra of (top) monomer 7 & (bottom) polymer 11 in CDCl_3	205
98	Figure 5A.4 TGA curves of polymers 10-12 & 16 at heating rate of 20 °C/min	207
99	Figure 5A.5 DSC curves of polymer 10-12 & 16 at a heating rate of 20 °C/min	208

100	Figure 5A.6	(top) UV-Vis absorption spectra of polymers 10-12 & 16 (2.2 x 10 ⁻⁵ M) in THF solution. (bottom) Fluorescence spectra of polymers 10-12 & 16 (2.2 x 10 ⁻⁵ M) in THF solution	209
101	Figure 5A.7	Variation of quantum yields of polymer 10 with water fraction in the THF/H ₂ O mixture	210
102	Figure 5A.8	Fluorescence spectra of polymers 10-12 & 16 in THF/water mixtures with different water fraction (f _w). (Concentration = 2.2 x 10 ⁻⁵ M)	211
103	Figure 5A.9	Effects of water addition on Fluorescence Intensity (I) of Monomers (left) and polymers (right)	211
104	Figure 5A.10	Molecular structure of monomer 9 (left), thermal ellipsoids are drawn at the 50% probability level (Hydrogen atoms are omitted for clarity)	212
105	Figure 5A.11	Fluorescence spectra of polymer 10 (2.2 x 10 ⁻⁵ M) at different temperatures	213
106	Figure 5A.12	(left) Fluorescence quenching of Polymer 10 (2.2 x 10 ⁻⁵ M) in THF/water mixture (70:30) with various concentrations of picric acid (0, 0.25, 0.50, 0.75, 1.00, 1.25, 1.50, 1.75, 2.00, 2.25, 2.50, 3.00, 3.50, 4.50, 5.50 equiv). Stern -Volmer plot for polymer 10 using picric acid as quencher at lower concentration	213
107	Figure 5A.13	Fluorescence lifetime decay profile of polymer 10 (2.2 x 10 ⁻⁵ M) in THF/H ₂ O (30:70) mixture for different concentrations of picric acid (PA). IRF= instrument response function. λ _{ex} = 280 nm	214
108	Figure 5A.14	Colour of fluorescent strips under UV light before and after addition of different concentration of picric acid (from left to right: blank, 10 ⁻³ , 10 ⁻⁴ , 10 ⁻⁵ M (PA))	214
109	Figure 5B.1	¹ H NMR spectrum of compound 3 (top) and 4 (bottom) recorded in CDCl ₃	229
110	Figure 5B.2	HRMS of compound 6 (top) and 7 (bottom)	230
111	Figure 5B.3	³¹ P NMR spectrum of compound 5, 6, 7, 8 and 9 recorded	232

	in CDCl ₃	
112	Figure 5B.4 (left) UV-Visible spectra of compounds 5, 6, 7&9 ; (right) Normalized photoluminescence spectra (excited at 280 nm) of compounds 5, 6, 7&9	233
113	Figure 5B.5 Fluorescence spectra of compound 5, 6, 7 & 9 (4.8×10^{-6} M, excited at 280 nm) in THF/H ₂ O mixture with different water fraction (f_w).	234
114	Figure 5B.6 Relationship between PL intensity of compound 5 and different water fraction	234
115	Figure 5B.7 Effects of water addition on fluorescence intensity (I) of the compound 5, 6, 7 & 9	235
116	Figure 5B.8 Fluorescence spectra of compound 5 (4.8×10^{-6} M; excited at 280 nm) at different temperature	236
117	Figure 5B.9 Photoluminescence peak intensity of compound 7 (1.9×10^{-5} M; excited at 280 nm) vs composition of glycerol/methanol mixtures.	237
118	Figure 5B.10 UV –Vis absorption spectra of compound 7 (4.8×10^{-6} M)in H ₂ O/THF mixtures with different volume fractions of water	237
119	Figure 5B.11 Fluoresce decay of compound 5, 6, 7 & 9 in THF (red) solution and THF:H ₂ O (10:90; blue) aggregates. (2.28×10^{-5} M; excited at 280 nm)	238
120	Figure 5B.12 (left) Molecular structure of compound 3 ; (right) Packing diagram with intermolecular C-H \cdots π interactions	240
121	Figure 5B.13 (top) Molecular structure of compound 7 . (bottom) Packing diagram with intermolecular C-H \cdots π interactions	240
122	Figure 5B.14 Computed orbitals for compound 3, 7 & 9	241
123	Figure 5B.15 (left)Fluorescence quenching of compound 5 and 6 , (right) Stern-Volmer plot for compound 5 and 6 using PA as quencher at lower concentration	243
124	Figure 5B.16 Fluorescence lifetime decay profiles for compound 5, 6, 7&9 in THF/water mixture (30:70) (4.8×10^{-6} M ; λ_{ex} = 280 nm).	244

-
- 125 **Figure 5B.17** Fluorescence quenching efficiencies of compound **5** in THF:H₂O (30:70) mixture (4.8×10^{-6} M; excited at 280 nm) toward different analytes (12 eq). 245
- 126 **Figure 5B.18** Colour of fluorescent strips under UV light after the addition of different concentration of picric acid 245

List of Abbreviations

^1H NMR	Proton nuclear magnetic resonance
^{13}C NMR	Carbon-13 nuclear magnetic resonance
^{11}B NMR	Boron-11 nuclear magnetic resonance
^{19}F NMR	Fluorine-19 nuclear magnetic resonance
^{31}P NMR	Phosphorus-31 nuclear magnetic resonance
UV-Vis	Ultraviolet–Visible
ESI	Electrospray ionization
DFT	Density functional theory
TGA	Thermogravimetric analysis
DSC	Differential scanning calorimetry
HRMS	High-resolution mass spectrometry
IRF	instrument response function
GPC	Gel permeation chromatography
XRD	X-ray diffraction
GOF	Goodness of fit
PDI	Polydispersity index
OLEDs	Organic light emitting diodes
HOMO	Highest occupied molecular orbital
LUMO	Lowest unoccupied molecular orbital
eV	Electronvolt
EL	Electroluminescence
ACQ	Aggregation caused quenching
AIE	Aggregation induced emission
AIEE	Aggregation induced emission enhancement
ESIPT	Excited state intramolecular proton transfer
BODIPY	Boron dipyrromethene
M_n	Number average molecular weight
M_w	Weight average molecular weight
T_g	Glass Transition Temperature
ppm	Parts per million
CH_2Cl_2	Dichloromethane

CHCl ₃	Chloroform
DCE	1,2-Dichloroethane
CH ₃ CN	Acetonitrile
EtOH	Ethanol
THF	Tetrahydrofuran
DMF	Dimethylformamide
CDCl ₃	Deuterated chloroform
NH ₄ OAc	Ammonium acetate
AcOH	Acetic acid
Na ₂ CO ₃	Sodium carbonate
K ₂ CO ₃	Potassium carbonate
Cs ₂ CO ₃	Cesium carbonate
Na ₂ SO ₄	Sodium sulfate
CaH ₂	Calcium hydride
KBr	Potassium bromide
AlCl ₃	Aluminium chloride
BBr ₃	Boron tribromide
NaHCO ₃	Sodium bicarbonate
Bu ₄ NPF ₆	Tetrabutylammonium hexafluorophosphate
CuI	Copper(I) iodide
AlMe ₃	Trimethylaluminium
<i>n</i> -BuLi	<i>n</i> -Butyllithium
(Bpin) ₂	bis(pinacolato)diboron
<i>i</i> -Pr ₂ NEt	N,N-Diisopropylethylamine
H ₃ PO ₄	Phosphoric acid
P ₃ N ₃ Cl ₆	Hexachlorocyclotriphosphazene
NBS	N-Bromosuccinimide
AIBN	Azobisisobutyronitrile
NaH	Sodium hydride
B(O ^{<i>i</i>} Pr) ₃	Triisopropyl borate
DDQ	2, 3-Dichloro-5, 6-dicyano-1, 4-benzoquinone
Pd(PPh ₃) ₄	Tetrakis(triphenylphosphine)palladium(0)
Ir(ppy) ₃	Tris[2-phenylpyridinato-C ² ,N]iridium(III)

Pd(dppf)Cl ₂	[1,1'-Bis(diphenylphosphino)ferrocene]dichloropalladium(II)
PA	Picric acid
Mes	Mesityl

CHAPTER 1

INTRODUCTION

1.1 Fluorescent boron compounds	3
1.1.1 Tri- coordinate boron compounds	3
1.1.2 Tetra- coordinate boron compounds	4
1.1.2.1 N,N- chelate boron compounds	5
1.1.2.2 N,O- chelate boron compounds	11
1.1.2.3 N,C- chelate boron compounds	20
1.2 Aggregation induced emission	30
1.3 Scope of thesis	36
1.4 References	37

1.1 Fluorescent boron compounds

Highly emissive organic conjugated molecules have drawn increasing attention because of their potential applications in organic light emitting diodes (OLEDs), organic solid state lasers (OSLs), sensors, bioimages, and so on¹⁻⁵. Recently, it has been demonstrated that the incorporation of boron into organic conjugated frameworks offer considerable promise for the development of new functional materials with outstanding photophysical and electronic properties. In general, fluorescent boron compounds have been classified into two categories i) tri-coordinate boron compounds ii) tetra-coordinate boron compounds (Figure 1.1)

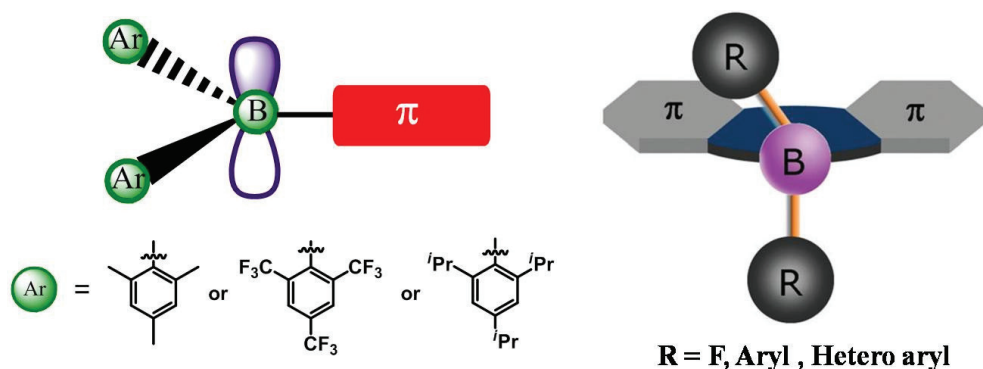


Figure 1.1: Schematic representation of (left) tri-coordinate boron; (right) tetra-coordinate boron compounds.

1.1.1 Tri-coordinate boron compounds

In tri-coordinate boron compounds, the boron atom adopts classic sp^2 hybridization with a vacant p_z orbital on it. The empty p_z orbital on the boron centre makes these compounds strong π -electron acceptor, which can lead to significant delocalization when conjugated with an adjacent organic π -system. Because of the presence of empty p_z orbital, tri-coordinate boranes are attacked by nucleophiles such as water which leads to destruction in conjugation with adjacent π -system. Bulky *ortho*-substituted aryl groups such as mesityl (2,4,6-trimethylphenyl),

fluoromesityl (2,4,6-tris(trifluoromethyl)phenyl), or triptyl (2,4,6-triisopropylphenyl) are often employed to protect the boron centre from most nucleophilic attack. The bulky aryl groups not only protect the boron centre from moisture, they can prevent intermolecular stacking, interaction in the solid state, which results in intense solid-state emission. Fluoride and cyanide can easily bind to boron centre of the inherent Lewis acidic triaryl boranes due to their smaller size, which makes this class of compounds as highly selective sensors for fluoride and cyanide^{6,7}. Apart from sensing, triaryl boranes have been used successfully as nonlinear optical materials, efficient fluorescent emitters and charge transport materials in OLEDs and fluorescent indicators in bioimaging⁸⁻¹⁰.

1.1.2 Tetra-coordinate boron compounds

In general, the tetra-coordinate boron compounds are more stable compared to tri-coordinate ones. Consequently, much effort has been devoted to the molecular design of tetra-coordinate boron compounds and has been widely used in optoelectronics including OLEDs, organic field effect transistors, photoresponsive materials, sensory and biological imaging materials¹¹⁻¹⁶. In tetra-coordinate boron compounds, the coordinative saturation of the boron centre confers increased chemical stability and rigidity, often accompanied by significantly higher fluorescence quantum yield. In most of the tetra-coordinate boron compounds, the chelate ligand is more often monoanionic in nature to produce the charge neutral boron complexes. The vital role of the Lewis acidic boron atom is to stabilize the anionic chelate ligand by forming covalent bonds with the chelate and dissipating the negative charge on the ligand. As a consequence of chelation to boron, the π -conjugation of the chelate is reinforced. The lowest unoccupied molecular orbital (LUMO) of four-coordinate boron compounds is usually localized on the π -

conjugated chelating ligand while the highest occupied molecular orbital (HOMO) is localized either at the chelating ligand or the R group (Figure 1.1) depending on the nature of the latter. The π - π^* electronic transitions of the chelate or charge transfer transition from the R group to the chelate are usually responsible for the luminescent properties of this class of compounds. Hence, variations on the chelating ligand or R group of the molecule would influence the HOMO-LUMO levels and thereby the colour of emission. The luminescent tetra-coordinate boron compounds can be broadly classified into four different types based on the chelated donor atoms, namely, (i) N,N- chelate boron compounds, (ii) N,O- chelate boron compounds, (iii) N,C- chelate boron compounds, and (iv) other chelate boron compounds like C,C-, C,O-, O,O- .

1.1.2.1 N,N- chelate boron compounds

The 4,4-difluoro-4-bora-3a,4a-diaza-s-indacene (or) boron dipyrromethene (BODIPY) dyes¹⁷⁻¹⁹ are the most well-known boron compounds with N,N- chelate ligand (Figure 1.2). In this type of compounds, out of two nitrogen atoms, one can form a covalent bond with the boron center while the other nitrogen forms a coordinate covalent bond by donating lone pair of electron to the empty p_z orbital of the boron centre. BODIPY dyes have excellent spectroscopic properties such as narrow absorption and emission bands, high molar extinction coefficients, high fluorescence quantum yields, strong chemical and photochemical stability in solution and solid state.

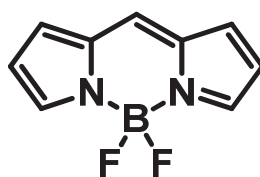


Figure 1.2: BODIPY dye.

Owing to these excellent characteristics, BODIPY dyes have been studied to a greater extent in artificial light harvesters, laser dyes, fluorescent sensors, sensitizers for solar cells, molecular photonic wires and as well as in photodynamic therapy. However, the typical BODIPY dyes are weak emissive in solid state, which limits their optoelectronic applications. The luminescence quenching of BODIPYs in solid state attributed to the undesirable π - π interactions leading to the formation of excimers and exciplexes and small Stokes shifts (400 - 600 cm^{-1} in most cases), which result in the self absorption of its own fluorescence. Efforts have been made to synthesise modified BODIPY fluorophores with pronounced Stokes shifts and better electroluminescent properties.²⁰⁻²² For example, solid state emissive BODIPYs has been achieved by decorating the classical BODIPY core with aryl groups.^{20,23}

Wang group reported N,N- chelate four-coordinate boron compounds **1-3** (Figure 1.3). The fluorescence spectra of these complexes exhibited emission maxima at 475 nm for 7-azaindolyl (**1**), 516 nm for indolyl (**2**), and 445 nm for benzoimidazolyl (**3**) derivatives, indicating that the emission maxima of these compounds were tuned with location of the N- heteroatom in the chelating ligand.^{24,25} To examine effect of substituent groups on the luminescence properties, the electron withdrawing fluoro/chloro atoms and an electron donating methoxy group were introduced to the 5-position of indole in compound **2**. The resulting compounds **4**, **5** and **6** exhibited emission maxima at 490 , 487 and 532 nm in solution, respectively, indicating that electron withdrawing groups blue shifted the emission maxima whereas the electron donating groups red shifted the emission maxima.²⁶

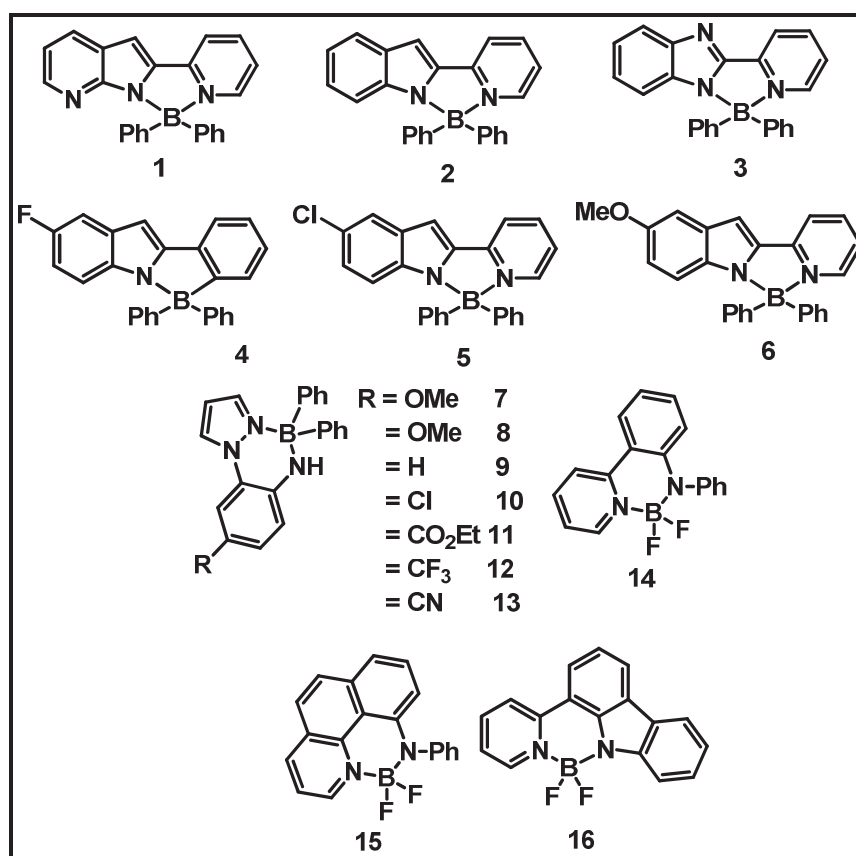


Figure 1.3: N,N- chelate tetra-coordinate boron complexes (1-16).

Gardinier and co-workers reported a series colour tunable fluorophores based on the diphenylboron complexes of (2-pyrazolyl)-4-R-anilines or BORAZANS ((boron azoanilines) (7-13) where R is the *para* substituent on the aniline ring. In their study, it was found that BORAZANS with electron-withdrawing *para*-aniline substituents exhibits higher chemical stability and blue fluorescent emission, while the BORAZANS with the electron-donating groups shift the emission to green and destabilize the compound towards hydrolysis.²⁷ Piers and co-workers reported a series of anilido-pyridine boron difluorides (14-16), which exhibits high photostability, large Stokes shifts along with high quantum yields both in solution and in the solid state.²⁸

Gomes and co-workers synthesised several fluorescent boron compounds containing 2-(N-aryl)formiminopyrrolyl ligands.

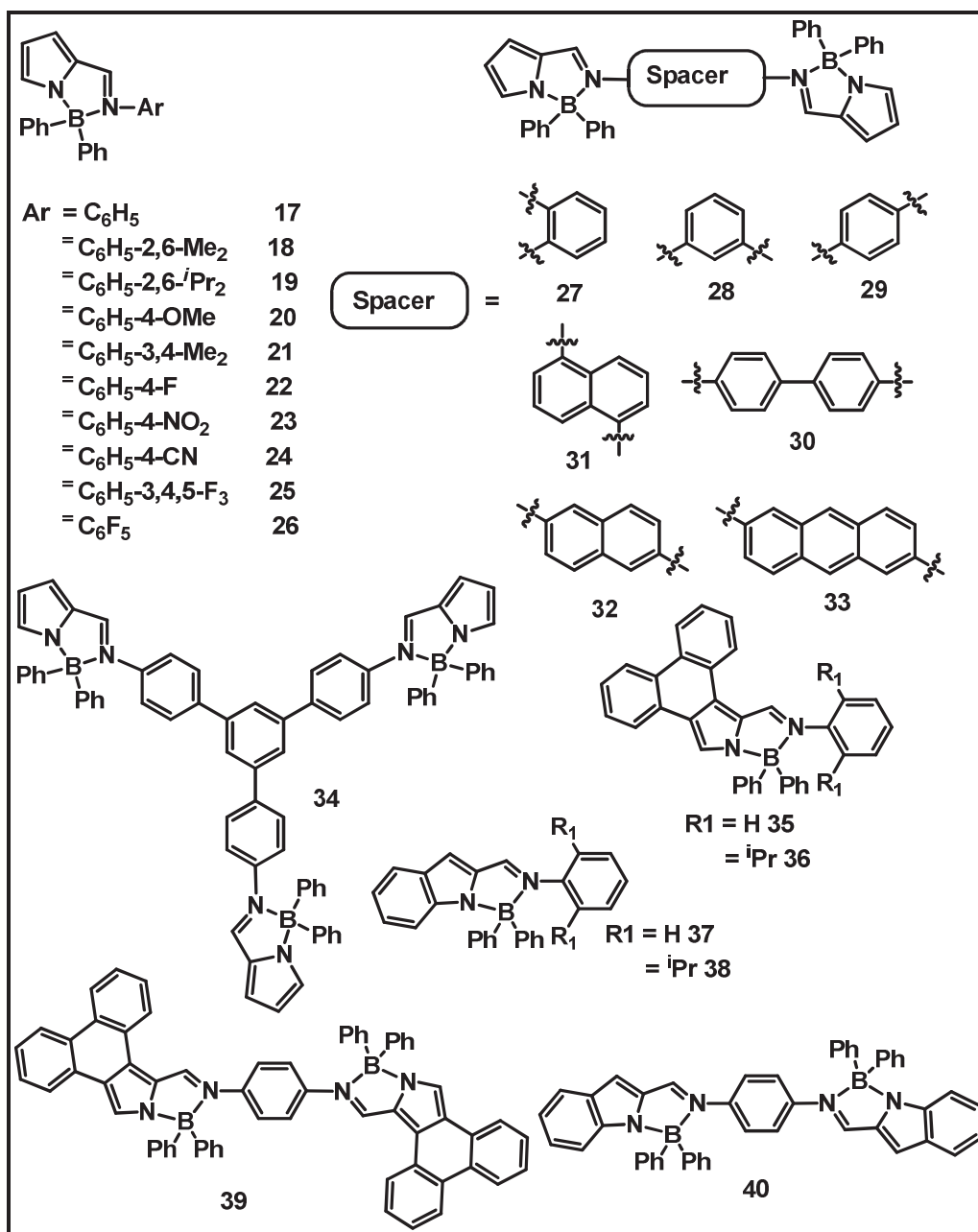


Figure 1.4: N,N- chelate tetra-coordinate boron complexes (17-40).

In mono nuclear compounds (17-26), the colour of emission could be tuned from blue to green by varying the electronic and steric nature of the N-aryl group. Further, they extended their work to synthesize bi- and tri- nuclear tetra coordinate boron complexes (27-34) by varying the length of π -conjugated spacer. These poly nuclear boron

complexes were found to be highly fluorescent; their emission colour could be tuned from blue to orange-red depending on the π -conjugation length. The bi-nuclear compounds were successfully used as the emitting layer of non-doped OLEDs.²⁹⁻³¹ Recently, the same group has reported the synthesis of boron complexes (**35-40**) containing 2-(*N*-aryl)formiminophenanthro[9,10-*c*]pyrrolyl or 2-(*N*-aryl)formiminoindolyl ligands with extended π -conjugation over the pyrrole moiety. These compounds exhibited the emission colour ranged from blue to orange.³²

Gilroy and Otten groups have synthesized several boron complexes based on formazanate ligands (**41-53**) which exhibited desirable spectroscopic and electrochemical properties. Their studies revealed that electron withdrawing substituents were shown to increase reduction potentials (E°_{red1} and E°_{red2} become more negative) and red-shifted absorption and emission maxima.³³⁻³⁶ Gilroy group also studied the effect of extended π -conjugation on the properties of BF_2 formazanate dyes (**54-59**); in their study they revealed that absorption and emission maxima were red-shifted as π -conjugation was increased, fluorescence quantum yields increased up to 10-fold.³⁷ More recently BF_2 formazanate dyes have been explored by the Gilroy and co-workers as an efficient electrochemiluminescent (ECL) emitters (**41-43**),³⁸ AIEE fluorophores (**60-62**),³⁹ fluorescent cell-imaging agents,⁴⁰ furthermore they have also incorporated into polymers.⁴¹

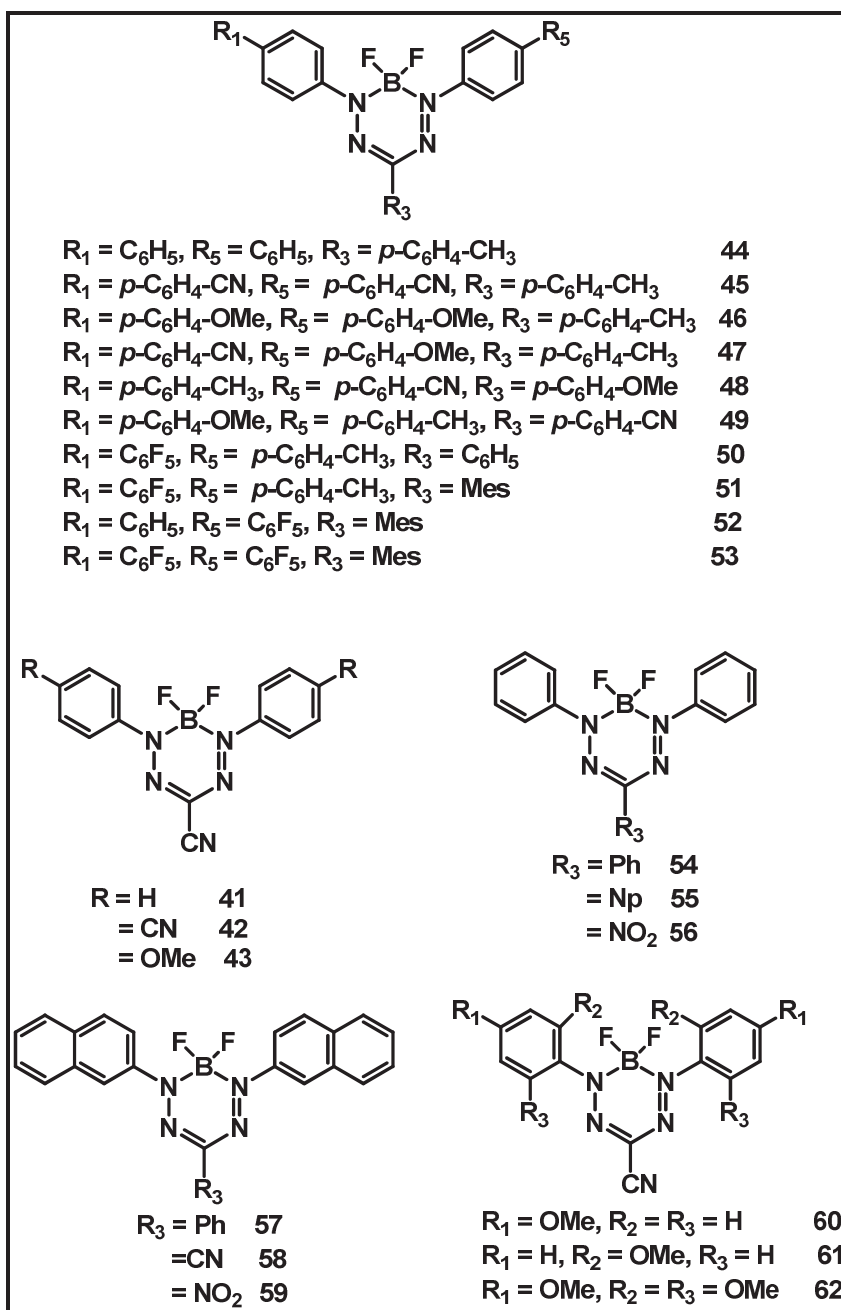


Figure 1.5: N,N- chelate tetra-coordinate boron complexes (41-62).

Recently Liu and co-workers synthesised a series of pyridyl enamido based boron complexes **63-66** with aggregation induced emission (AIE) as well as tunable substituent dependent emission and large Stokes shift in solution.⁴² Feng and co-workers developed triple boron-cored chromophores **67-70** by the complexation of 5,11,17-triazatrinaphthylene derivative ligands with boron (III) precursors like $BF_3 \cdot Et_2O$ or BPh_3 . These compounds exhibited the unique electronic properties

including large Stokes shift, tunable electrochemical behaviours, and low-lying LUMO energy levels.⁴³

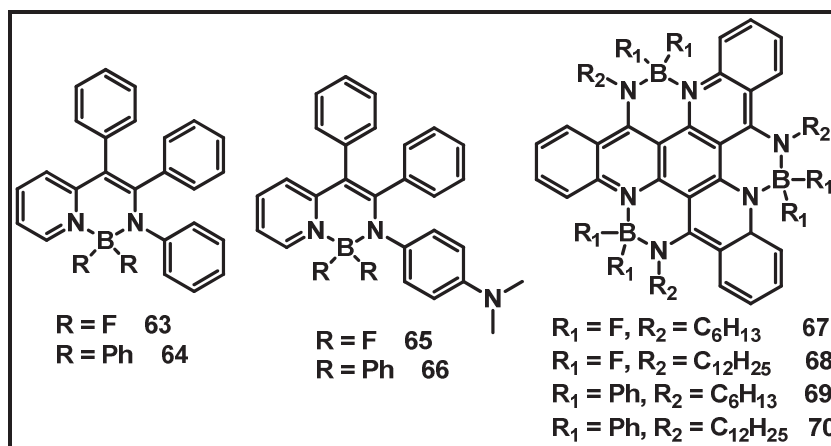


Figure 1.6: N,N- chelate tetra-coordinate boron complexes (**63-70**).

1.1.2.2 N,O- chelate compounds

Wang and co-workers reported a series of 8-hydroxyquinolinate (q) boron compounds **71-74** with the general formula of BR_2q , where $R =$ ethyl, phenyl, 1-naphthyl, and 2-naphthyl.⁴⁴ These boron compounds exhibited greenish blue emission with emission wave length of 495–500 nm and were also investigated in OLED as emitters and electron-transporting layers. In addition to this, they reported several 8-hydroxyquinolinate based linear and star-shaped polynuclear boron compounds **75-79**, to examine the effect of extended π -conjugation and the mutual influence of multiple boron centres. These compounds exhibited emission maxima ranged from 528 to 542 nm with increased thermal stability.⁴⁵ Later, Jäkle group reported a series of emission colour tunable boron compounds **80-86** by varying the substituents at the 5th position of the quinolate ligand. They observed that, electron withdrawing groups, blue shift the emission maxima relative to the nonsubstituted one, while electron donating groups red shift the emission maxima.⁴⁶ Wang and co-workers reported dinuclear ladder-type π -conjugated boron compounds **87-90**.⁴⁷ These compounds exhibited the emission maxima in the range from 584–604 nm, which were about 100

nm red shifted compared to the corresponding mononuclear boron compound **91**. They also observed that, these dinuclear ladder compounds exhibited high thermal stability and better performance in OLEDs over corresponding mononuclear boron compound.

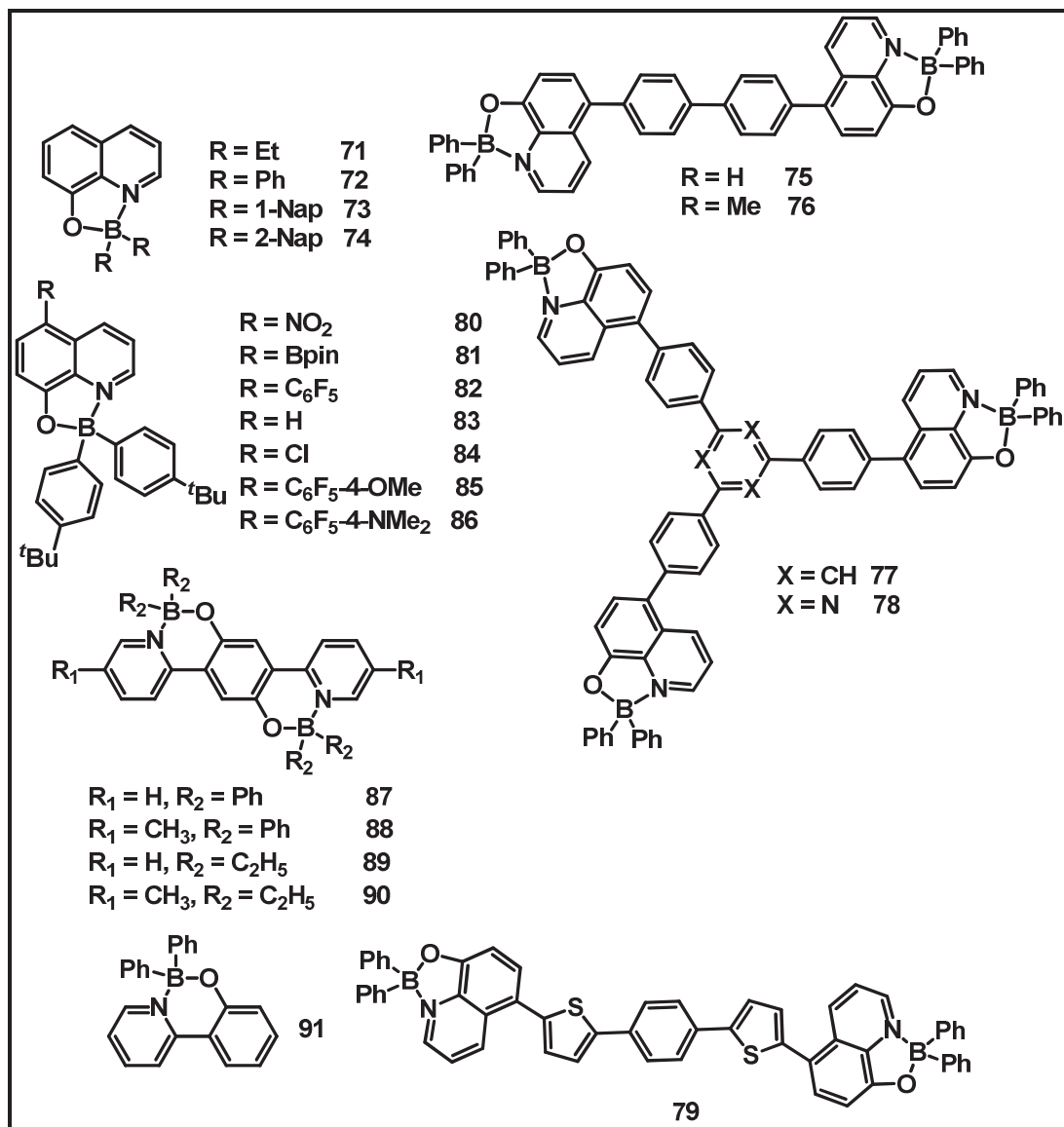


Figure 1.7: N,O- chelate tetra-coordinate boron complexes (**71-91**).

Ziessel, Ulrich, and co-workers reported a new type of boron complexes **92-98**, named boranils by complexation of anils (aniline-imines) with boron (III) precursors like BF₃.Et₂O or BPh₃. They found that, the photophysical properties of these compounds strongly dependent on the nature of *para* substituents on both the

phenol and imine sides of the compound.⁴⁸ Later they proved that these boranil dyes (**99**) can be utilized as a interesting candidates for bioconjugation to proteins such as bovine albumin serum (BSA) in biological media.⁴⁹ Recently Krishnan and co-workers reported thermally stable salicyldimine based diboron complexes (**100-102**) with emission maxima ranged from 460 to 494 nm.⁵⁰ Muthusubramanian reported bornil dyes **103** and **104** and explored their application as turn-on fluorescent probes for the detection of hydrogen peroxide.⁵¹

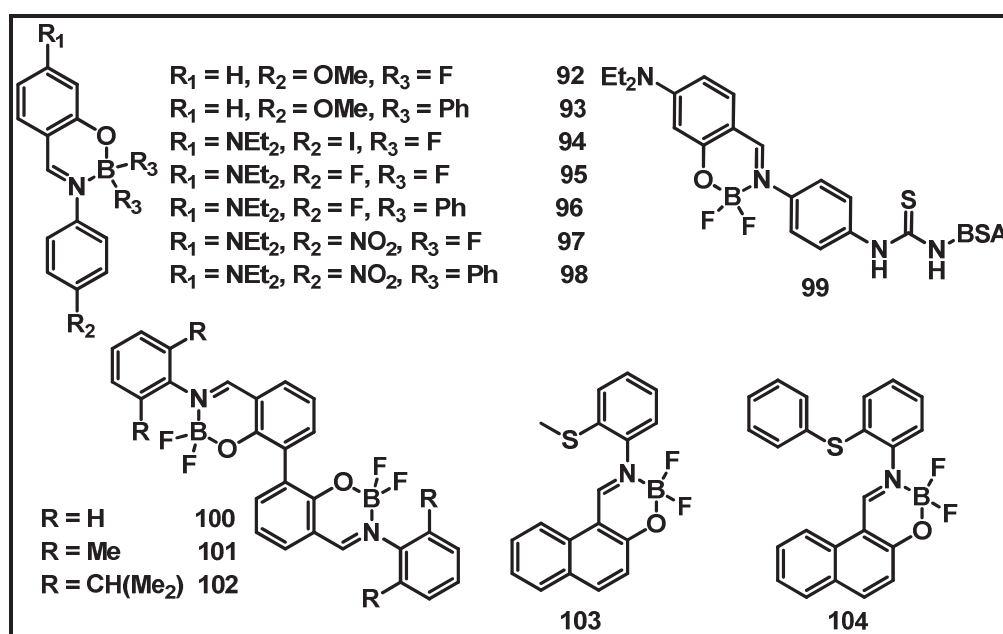


Figure 1.8: N,O- chelate tetra-coordinate boron complexes (**92-104**).

Yasuhiro Kubota, Masaki Matsui and co-workers reported pyrazine⁵² (**105-110**) or thiazole⁵³ (**111-114**) boron complexes bearing a β -ketoiminate ligands, which exhibits a large Stokes shifts, solid-state fluorescence and aggregation induced emission enhancement. Later, they reported solid state emissive, AIEE active pyrimidine mono and bisboron (**115-125**) complexes bearing a β -ketoiminate ligand. They also found that pyrimidine boron complexes bearing two phenyl groups on boron atom show more intense fluorescence than the corresponding BF_2

complexes.⁵⁴ Moreover D- π -A type pyrimidine diboron complexes **126-130** show solid state fluorescence in the NIR region.⁵⁵

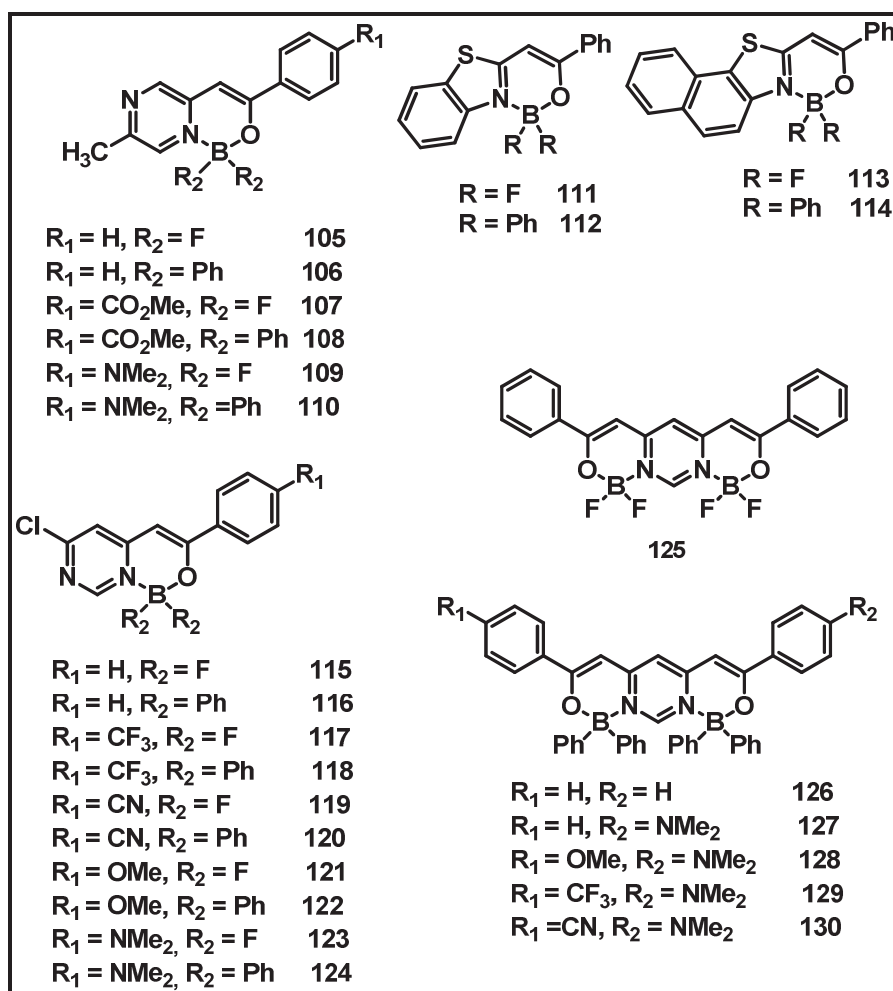


Figure 1.9: N,O- chelate tetra-coordinate boron complexes (**105-130**).

Lu and co-workers synthesised a series of carbazole⁵⁶ (**131** & **132**), triphenylamine⁵⁷ (**133**) and phenothiazine (**134-137**) functionalized β -iminoenolate boron complexes bearing a pyridine ligand and studied their mechanofluorochromic properties. Sun and co-workers synthesised quinoxaline- β -ketoiminate boron difluoride complexes **138-142** with strong luminescence both in solution and solid state. Moreover, these boron complexes exhibited reversible on-off solid state luminescence switching by acid/base fuming processes.⁵⁸ Very recently Lu and co-

workers reported non-traditional π -gelators based on β -iminoenolate and their difluoroboron complexes (**143-148**).⁵⁹

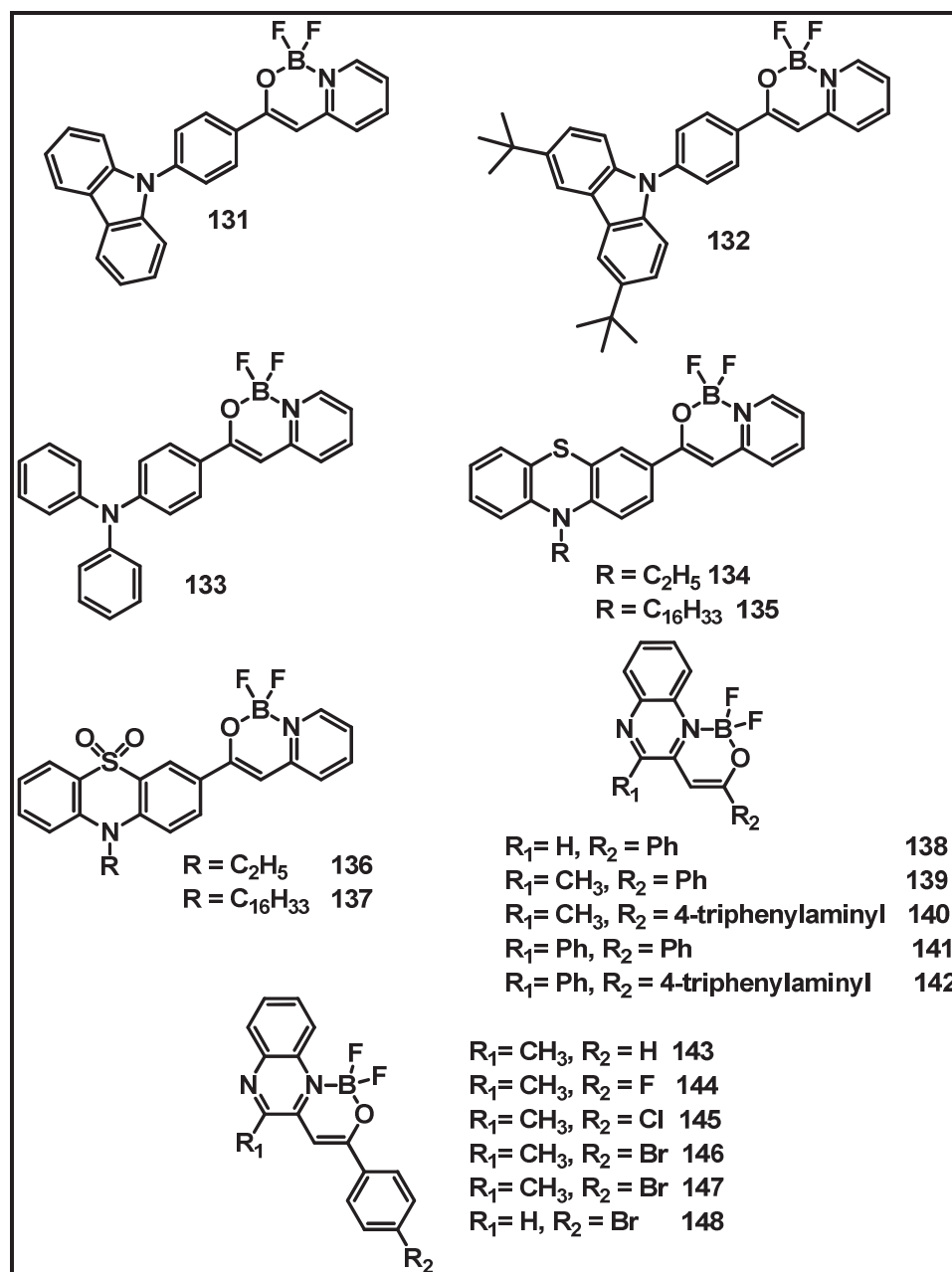


Figure 1.10: N,O- chelate tetra-coordinate boron complexes (**131-148**).

He and co-workers reported pyrimidine-based BF_2 complexes **149-150** with large Stokes shift, AIE effect, high solid-state luminescence and mechanochromic properties.⁶⁰ Later they synthesised the benzothiazole enolate ligand based boron complexes **151-154** with asymmetrical and propeller shaped structures, which

exhibited large Stokes shift in solution, AIE effect and intense solid-state emission.⁶¹

Zhao reported D- π -A type triphenylamine-functionalized thiazole based β -ketoiminate boron complexes (**155-158**).

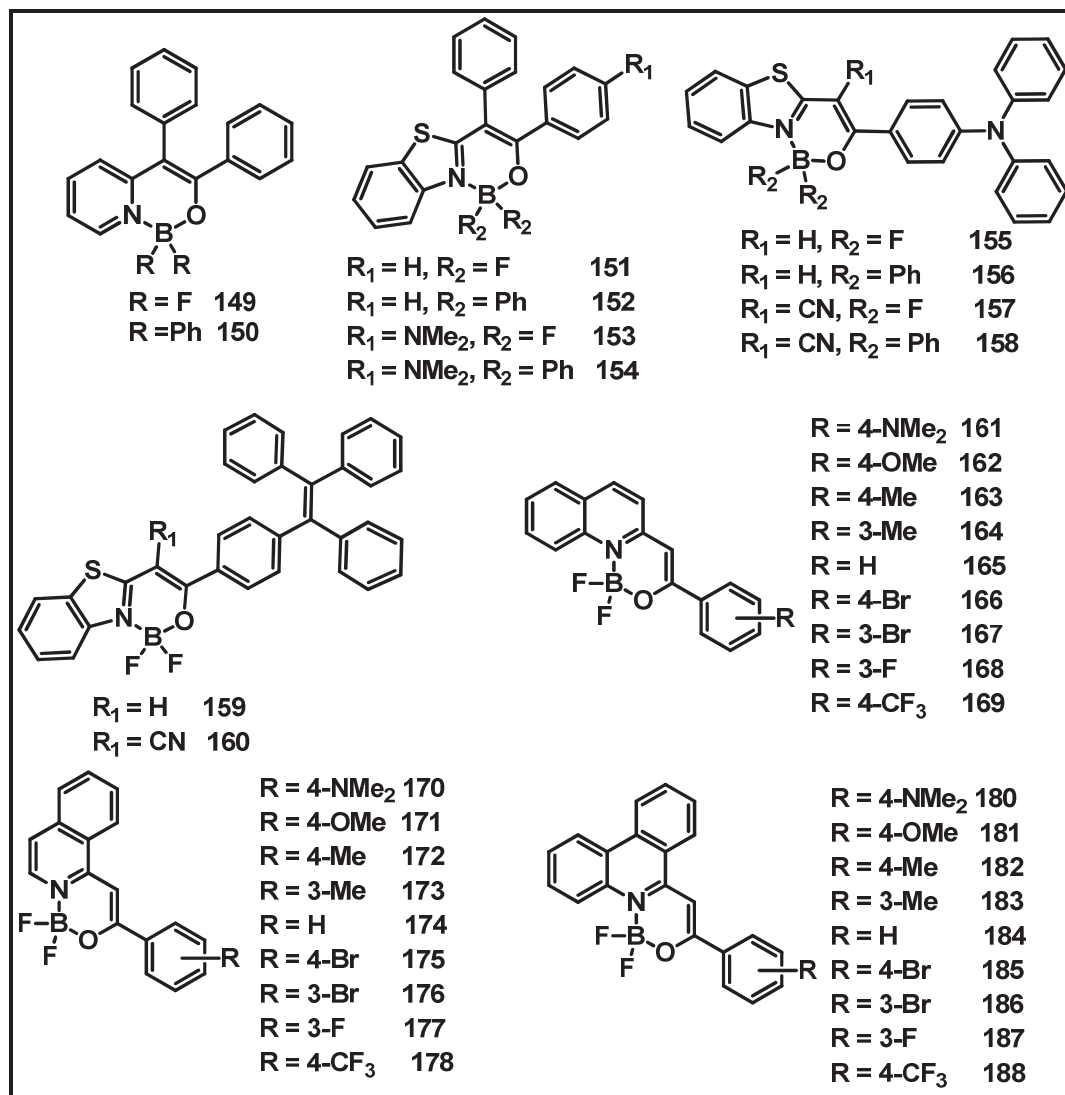


Figure 1.11: N,O- chelate tetra-coordinate boron complexes (**149-188**).

All these compounds exhibited strong intramolecular charge transition emission and strong cyano-dependent aggregation induced emission and mechanofluorochromic properties.⁶² Li and co-workers reported D- π -A type thiazole based β -ketoiminate boron complexes (**159-160**) connected with tetraphenylethene, which exhibited twisted intramolecular transition emission, strong AIE phenomenon and significant mechanofluorochromic properties.⁶³ Ośmiałowski and co-workers reported 2-

benzoylmethylenequinoline⁶⁴ (**161-169**), 1-benzoylmethyleneisoquinoline⁶⁵ (**170-178**), phenacylphenanthridine⁶⁶ (**180-188**) based boron complexes and studied the effect of substitution.

Kwak and Kim synthesized difluoroboron complexes based on 2-(2'-hydroxyphenyl)benzoxazole (**189**) and 2-(2'-hydroxyphenyl)benzothiazole ligands (**190**).⁶⁷ These boron complexes exhibited bright blue fluorescence with good thermal stability and high electron transport ability in OLEDs.

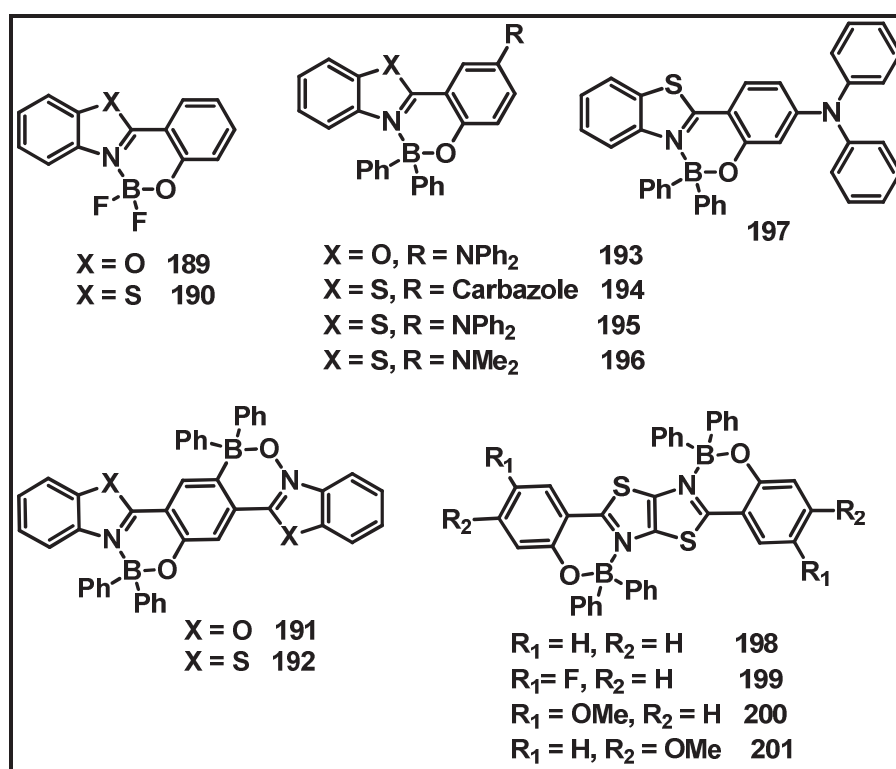


Figure 1.12: N,O- chelate tetra-coordinate boron complexes (**189-201**).

Zhang, Yue Wang and co-workers reported diboron containing fused complexes **191** and **192** which exhibits good thermal stability, high electron mobility, and intense solid state fluorescence and they also utilized them as a non doped red emitters in OLEDs.⁶⁸ Later they synthesised benzoxazole (**193**) and benzthiazole (**194-197**) boron complexes by introducing various amine groups. The emission colour of these boron complexes covered a wide range from deep blue to saturated red in both

solution and the solid state.⁶⁹ Lately, Zhang and co-workers synthesised a series of novel diboron containing π -conjugated ladders (**198-201**) from phenol substituted thiazolothiazole ligands and used them both as emitters and electron transporting materials in OLEDs. Due to the construction of diboron ladder type skeletons, these diboron complexes exhibited high thermal stability, high fluorescence quantum yields, and strong electron affinity.⁷⁰

Ziessel, Ulrich, and co-workers synthesised a series of boron complexes (**202-210**) based on electron donor/acceptor substituted 2-(2'-hydroxy phenyl)benzoxazole ligands. These boron complexes exhibited the emission wavelength ranging from 385 to 425 nm in dichloromethane.⁷¹ Later they synthesised the ethynyl extended regioisomers of difluoro or diphenyl borate complexes (**211-221**) and electron donating groups contained diphenyl borate complexes (**222-234**) based on 2-(2'-Hydroxyphenyl)benzoxazole.^{72,73} and they concluded that, the optical properties of these boron complexes highly depend on the electronic nature and position of substituents. Moreover, in all cases, as compared to BF_2 derivatives, the BPh_2 derivatives exhibited red shifted absorption and emission both in the solution and in the solid state. da Silva Ju'nior and co-workers synthesized the naphthoxazoles based boron complexes **225-226** and applied as superior and selective probes for endocytic pathway tracking in live cancer cells.⁷⁴

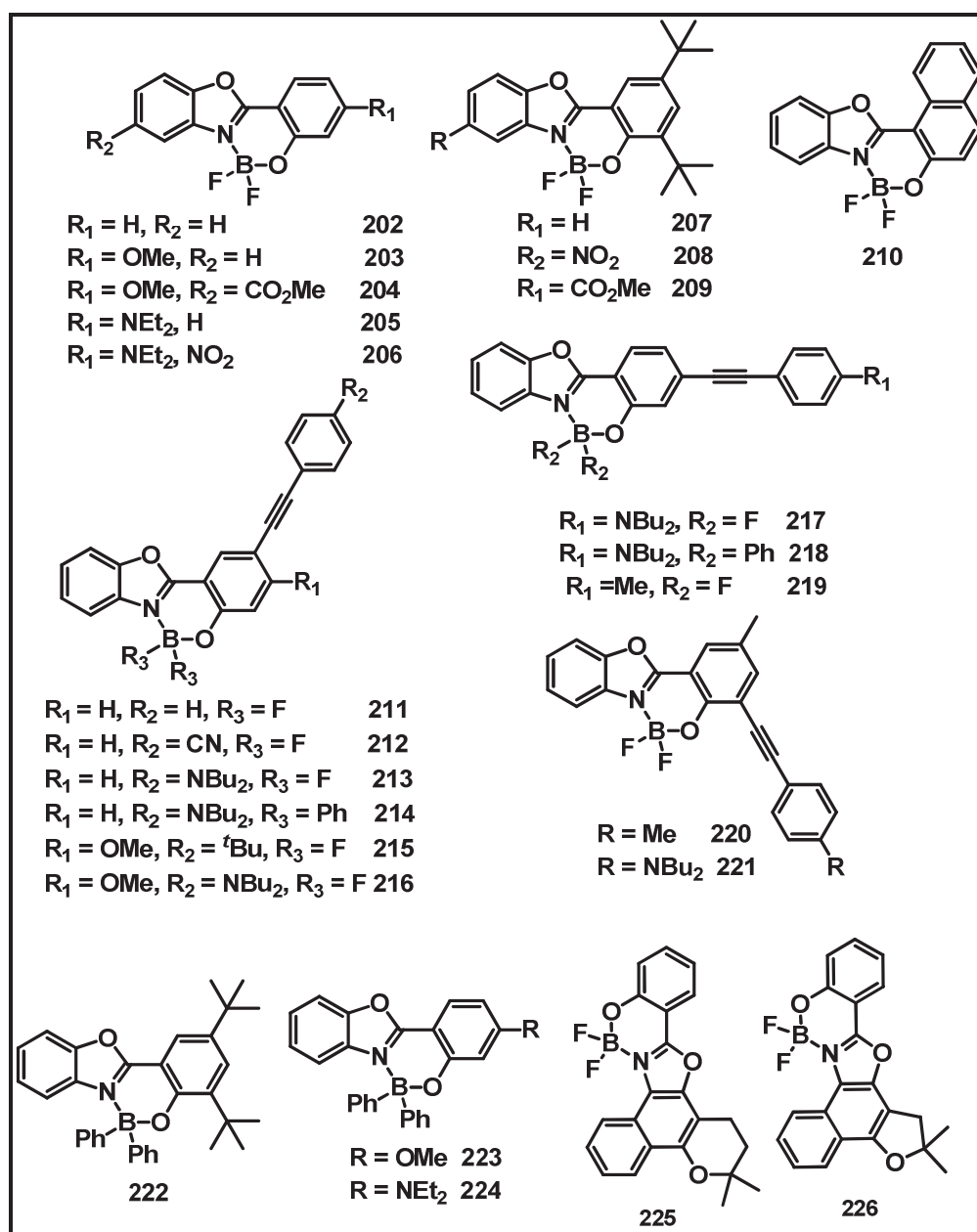


Figure 1.13: N,O- chelate tetra-coordinate boron complexes (202-226).

Ziessel, Ulrich, and co-workers reported a series of N-alkylated 2-(2'-hydroxyphenyl)benzimidazole (227-229) or N-arylated 9,10-phenanthroimidazole borate complexes (230-232). These complexes exhibited luminescence both in solution and solid state. The BODIPY substituted derivative (232) exhibited only unique emission of the BODIPY subunit when exciting at 360 nm due to quantitative excitonic energy transfer.⁷⁵ Zhang and co-workers synthesized boron complexes 233 and 234 from 2-(2'-hydroxyphenyl)benzimidazole ligand. Both compounds exhibited

high thermal stability, deep blue emission with good quantum yields and used as an emitter in OLEDs to generate efficient deep blue electroluminescence emission.⁷⁶

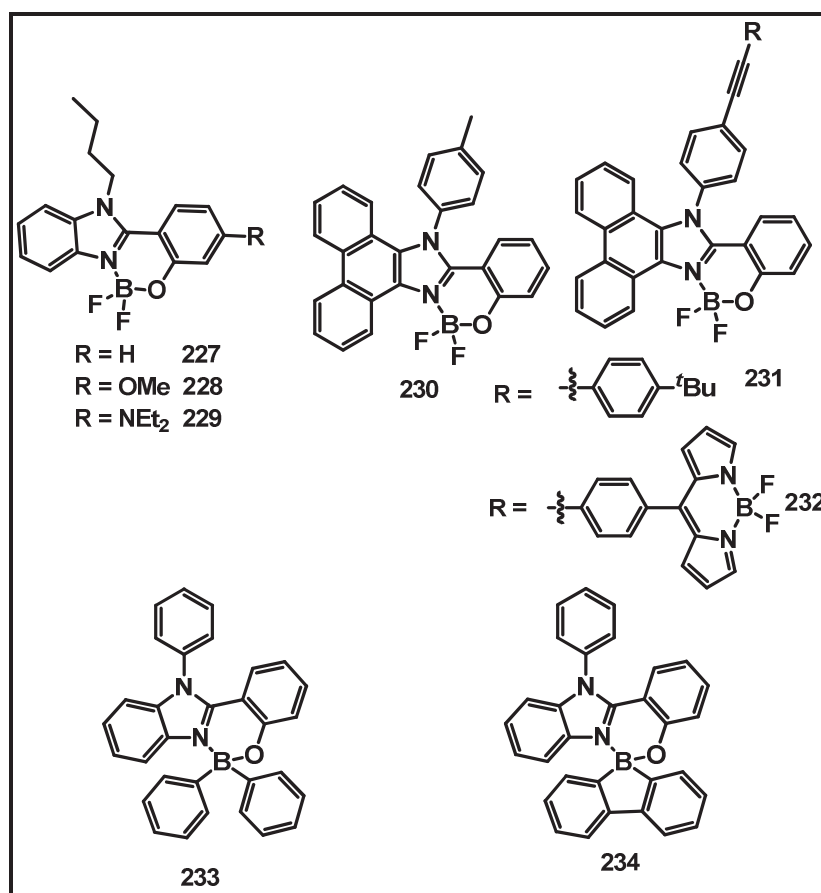


Figure 1.14: N,O- chelate tetra-coordinate boron complexes (227-234).

1.1.2.3 N,C- chelate boron compounds

Yamaguchi and co-workers reported the N,C- chelate boron compound **235** based on thienylthiazole ligand.⁷⁷ On the basis of the regioselective functionalization of **235**, three isomers of ladder type diboron compounds (**236-238**) were synthesized. These compounds exhibited high electron mobility due to the extended π -conjugation and the boron chelation. Later, Wakamiya and co-workers synthesized the boron complexes **239-240** via a coordination/cyclization protocol with $B(C_6F_5)_3$ in thiazolyl capped π -conjugated systems.⁷⁸ These diboron complexes showed high thermal stability and high electron affinity compared to their corresponding ligands.

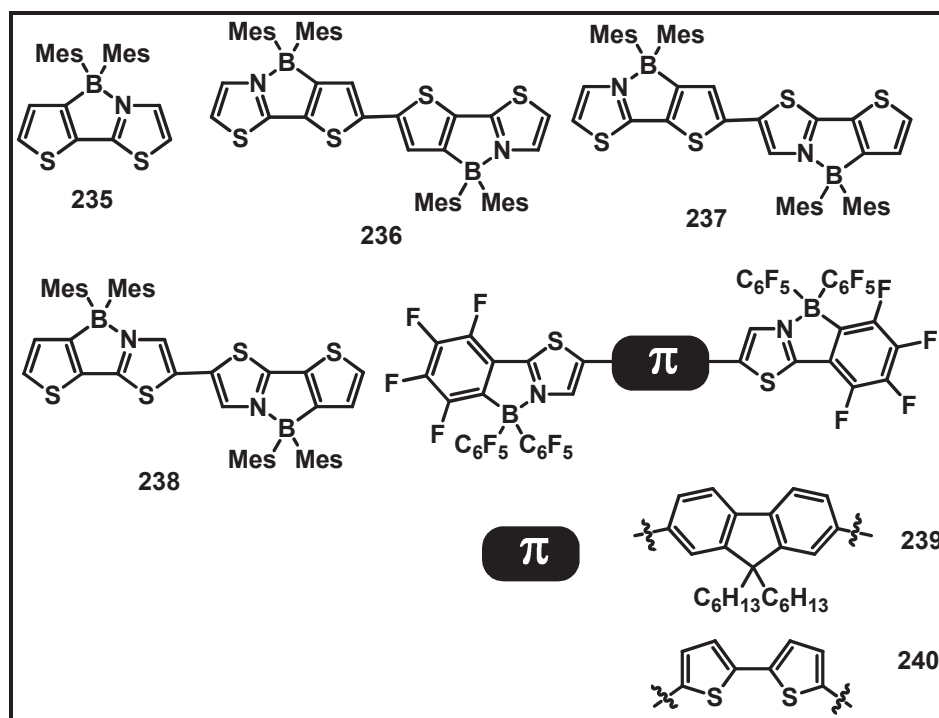


Figure 1.15: N,C- chelate tetra-coordinate boron compounds (**235-240**).

Zhang and co-workers reported a series of ladder type π -conjugated diboron complexes (**241-244**) by introducing electron-withdrawing/donating groups into the ladder skeleton or changing the aryl substituents on boron atoms.⁷⁹ Their studies revealed that, these diboron complexes exhibit high thermal stability, intense fluorescence, and strong electron affinity. Pischel and co-workers reported a series of highly fluorescent boron compounds (**245-250**) based on aryl isoquinoline skeleton with high chemical and photostability.⁸⁰ These compounds exhibited large Stokes shifts and good two-photon absorption owing to the intramolecular charge transitions and used in confocal fluorescence microscopy and bioimaging.

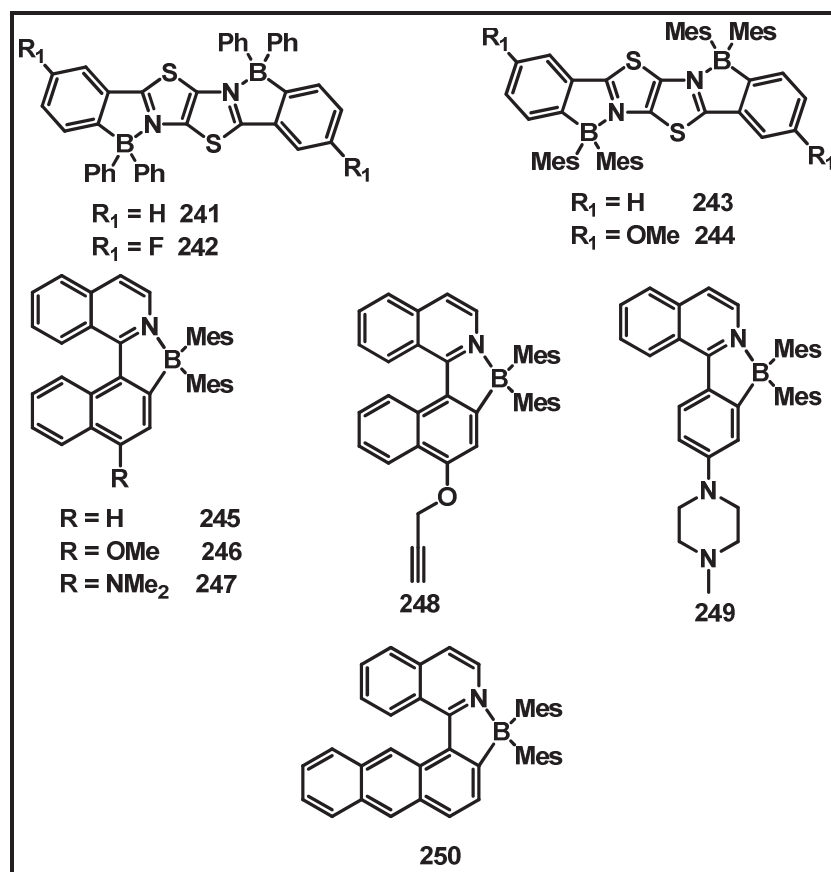


Figure 1.16: N,C- chelate tetra-coordinate boron compounds (241-250).

Wang and co-workers synthesized boron compound **251**, based on 2-phenyl pyridine ligand.⁸¹ Upon irradiation with ultraviolet light under nitrogen atmosphere, compound **251** was found to change colour rapidly from colourless to dark blue (**251 A**) and lose its fluorescence completely. This unusual photochromic behaviour is due to the facile and reversible C-C/C-B bond rearrangement. On exposure to light under air, the newly formed species (**251 A**) reacts rapidly with oxygen, eliminating the boron moiety from the chelate site and form **251B**.

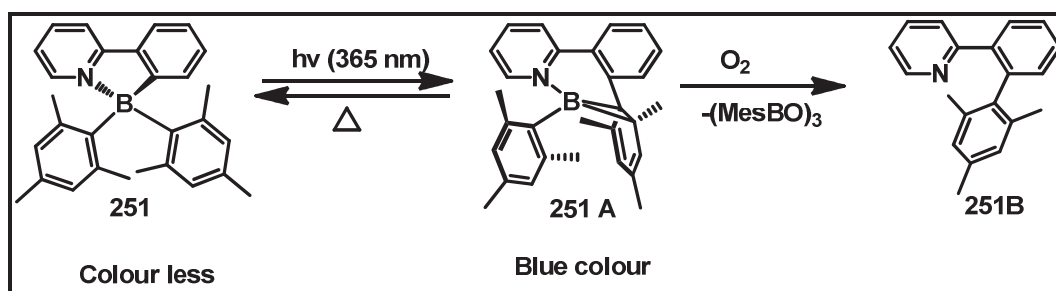


Figure 1.17: N,C- chelate tetra-coordinate boron compounds (251-251B).

In order to find the steric and electronic influence on photochromic switching, they synthesised a series of boron complexes **252** to **261** by varying the ligands and the aryl groups on boron centre.⁸² They found that compounds **252-259** exhibited photochromic switching process. Moreover compounds with electron donating groups such as SiMe₃ (**255**) accelerate the photochromic switching and the electron withdrawing carbonyl, fluoro groups on 2-phenyl pyridine chelate slow down the photochromic switching process. Compounds with phenyl or pentafluoro phenyl on boron centre (**260-261**) exhibited photochemical stability over compound with mesityl on boron centre, which indicates the necessity of mesityl groups for photoisomerization phenomenon of this class of compounds.

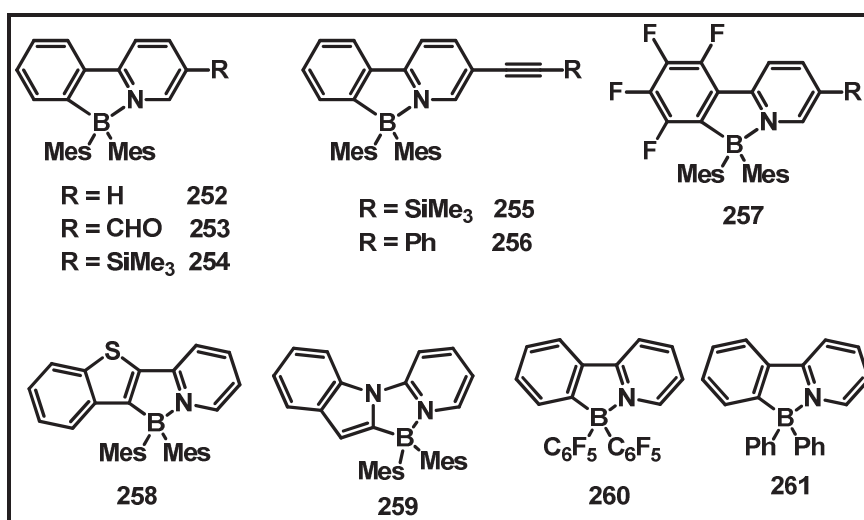


Figure 1.18: N,C- chelate tetra-coordinate boron compounds (**252-261**).

Later, they synthesized boron complexes (**262-265**) with extended π -conjugation using vinyl or acetylene spacer.⁸³ They found that, olefin-substituted compounds exhibit more photochemical stability over acetylene substituted compound (**263**). Upon exposure to UV light olefin-substituted compounds (**261**, **264**, **265**) undergo exclusively *cis* – *trans* isomerisation over its competitive photochromic switching process, thereby stabilizing the chromophore towards light.

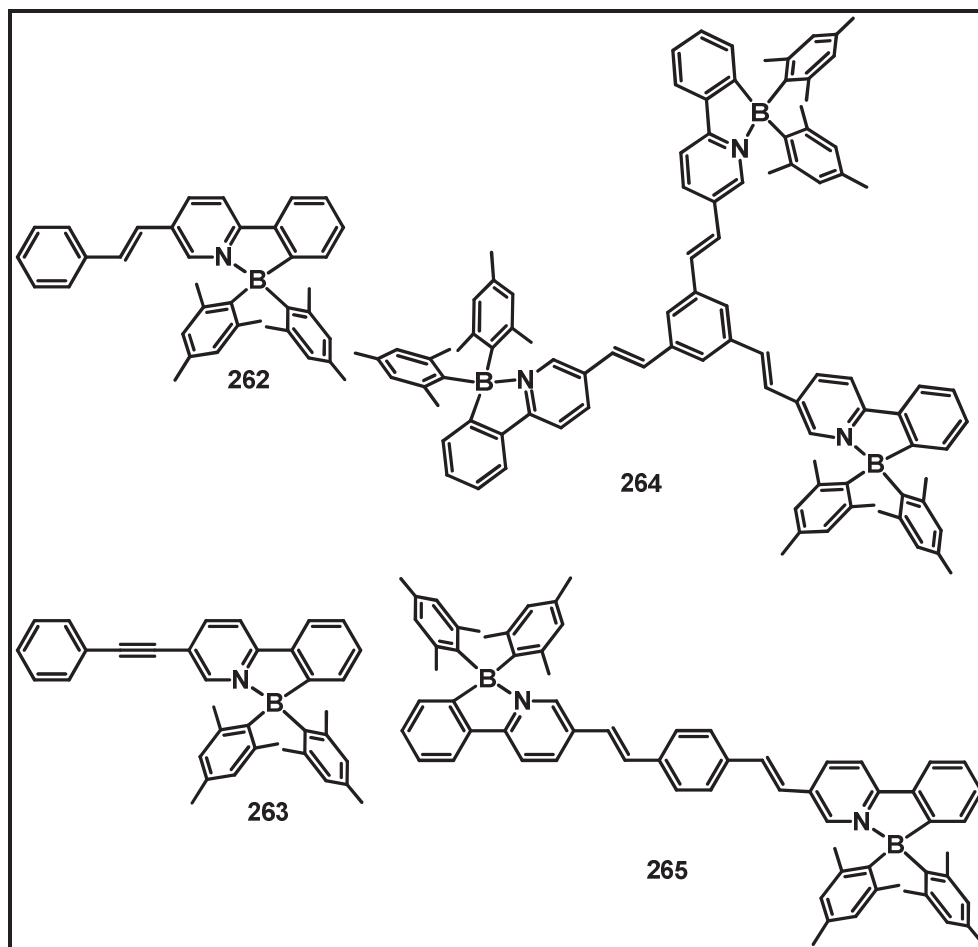


Figure 1.19: N,C- chelate tetra-coordinate boron compounds (262-265).

Azobenzene based N,C- chelate organoboron compounds (266-276) were reported by Kawashima and co-workers.^{84,85} These 2-borylazobenzenes showed yellow, green, orange, and red fluorescence and the colour of fluorescence highly depends on substituents on azobenzene. In order to prove the importance of pentafluorophenyl groups on fluorescence property, they have synthesized the compound **276** with *p*-fluorophenyl groups on the boron centre, which was found to be non emissive. They also synthesized 2,2'-diborylazobenzenes (277-280) with double N-B coordination.⁸⁶ These diboron compounds showed fluorescence emission with orange and red colours with fluorescence quantum yields (Φ_F) ranging from 0.26 to 0.73. The absorption and emission of diboryl compounds are red shifted compared to the corresponding monoboryl compounds. Moreover, they also synthesized a series

of boryl substituted N-arylimines (**281-288**) that showed blue or green fluorescence in hexane.

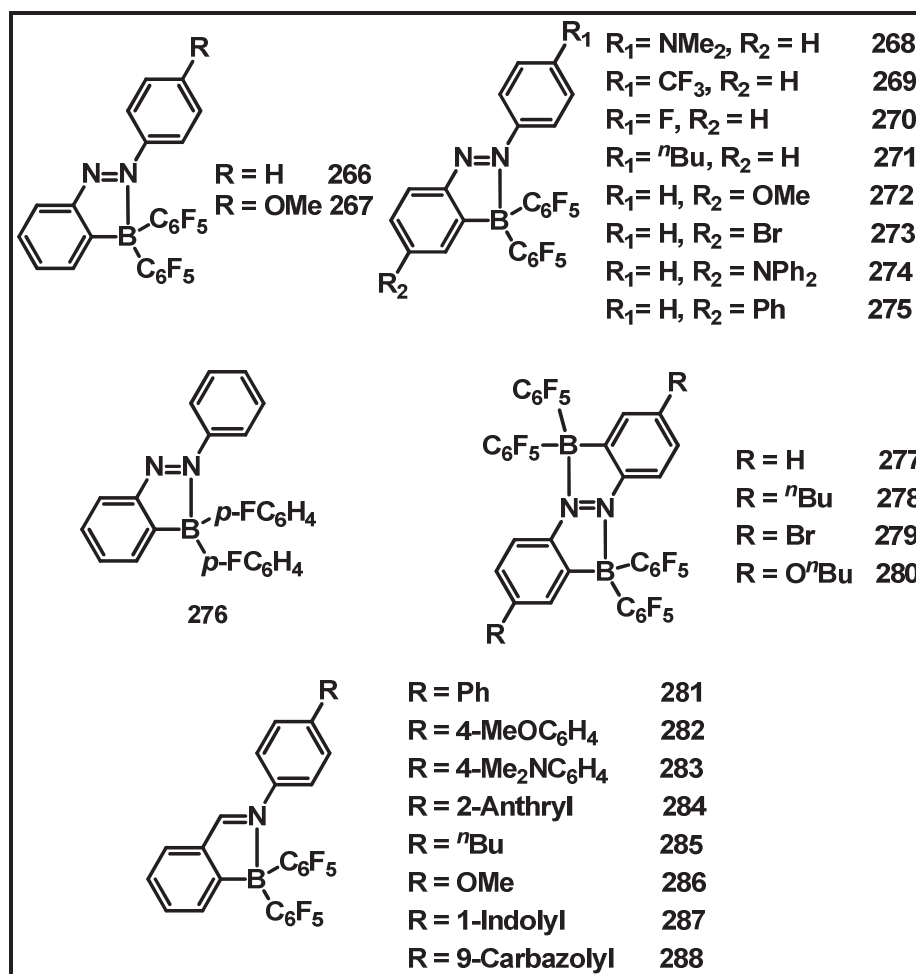


Figure 1.20: N,C- chelate tetra-coordinate boron compounds (266-288).

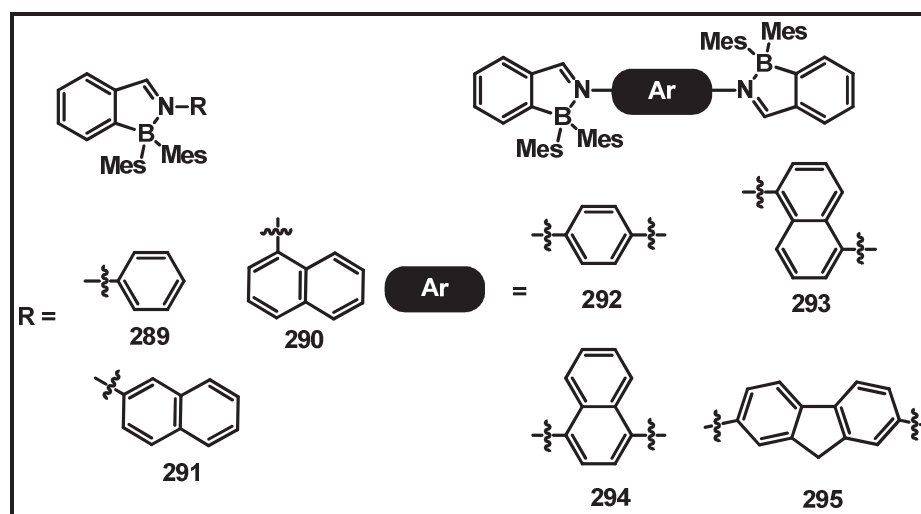


Figure 1.21: N,C- chelate tetra-coordinate boron compounds (289-295).

They also proved that, N-arylimine derivatives can act as fluorescent sensor for cyanide ion.⁸⁷ Wuertwein and co-workers reported a series of N-aryl-2-borylbenzaldimines (**289-291**) and their extended π -conjugated compounds with two 2-borylbenzaldimine (**292-295**) units as the terminating units.⁸⁸ They observed that, the dinuclear compounds with extended conjugation exhibited enhanced stability, large Stokes shifts and high electrochemical stability than the mononuclear compounds.

Murakami and co-workers first reported the electrophilic aromatic borylation strategy to prepare the N,C- chelate boron compounds in 2-aryl pyridine systems.⁸⁹ Later, this electrophilic aromatic borylation strategy has been utilized by Yam and co-workers to synthesize a series of diarylethene-containing N,C- chelate thienylpyridine-bis(alkynyl)borane compounds (**296-300**) and studied for their photochromic properties.⁹⁰

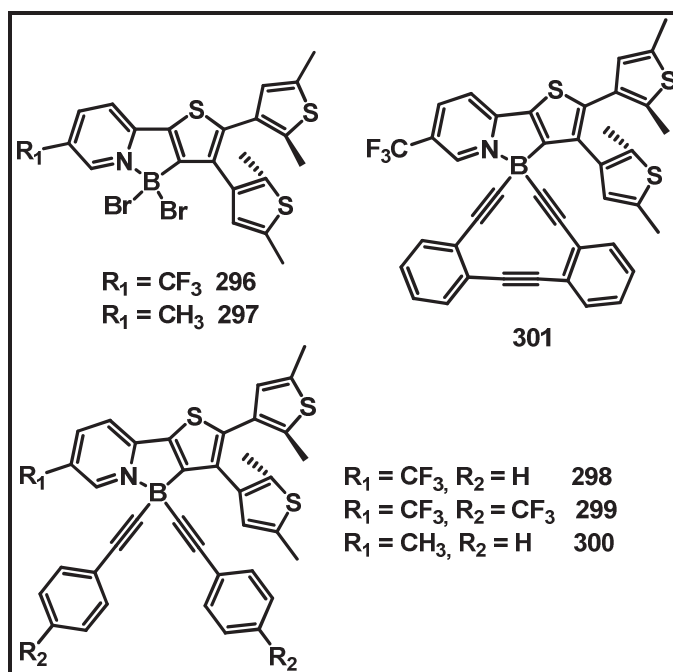


Figure 1.22: N,C- chelate tetra-coordinate boron compounds (**296-300**).

Qiu and co-workers synthesized tetraphenylethene containing N,C- chelate boron compounds **302** and **303**.⁹¹ These compounds exhibit aggregation induced

emission due to the presence of tetraphenylethene moiety and also shown good thermal stability with quantum yield near to unity. Later they synthesised boron compounds **304** and **305** which exhibit aggregation induced emission, high thermal stability with excellent solid state fluorescence quantum yields up to unity. These compounds were utilized as emitters in OLED and shown superior electroluminescent efficiencies over their corresponding ligands.⁹²

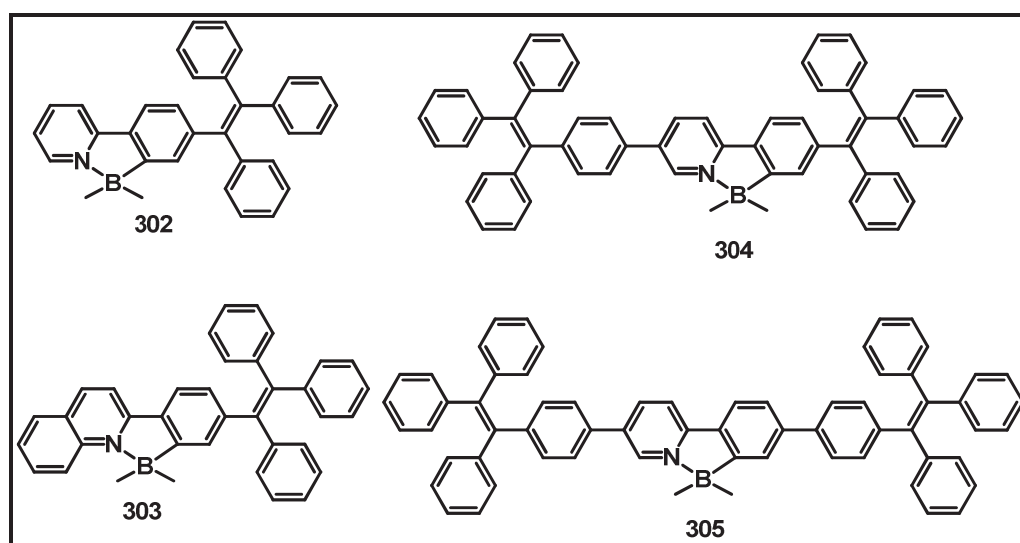


Figure 1.23: N,C- chelate tetra-coordinate boron compounds (**302-305**).

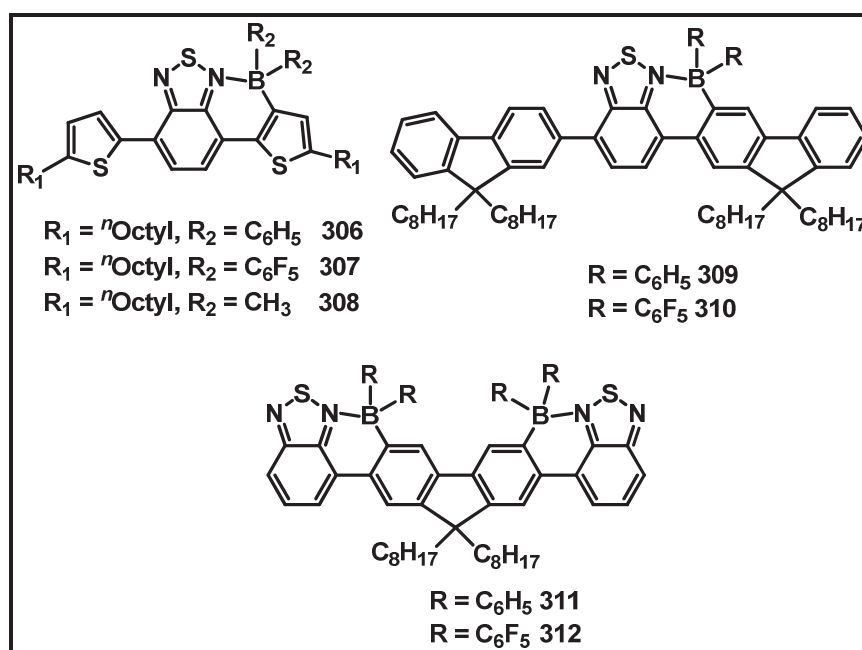


Figure 1.24: N,C- chelate tetra-coordinate boron compounds (**306-312**).

Ingleson, Turner and co-workers synthesized benzothiadiazole containing donor-acceptor materials by electrophilic borylation using BCl_3 . Compounds **306-308** are non emissive, however compound **309-312** exhibited emission maxima ranging from 636 to 730 nm with considerable Stokes shifts and excellent solid state quantum yields.⁹³ Later they extended their work to synthesize compounds **313** to **316** by Stille, Suzuki-Miyaura and Negishi cross coupling reactions of bromine functionalised borylated precursors.⁹⁴ All these complexes showed large Stokes shifts, low LUMO energies, small band gaps and fluorescence emission > 700 nm in methanol.

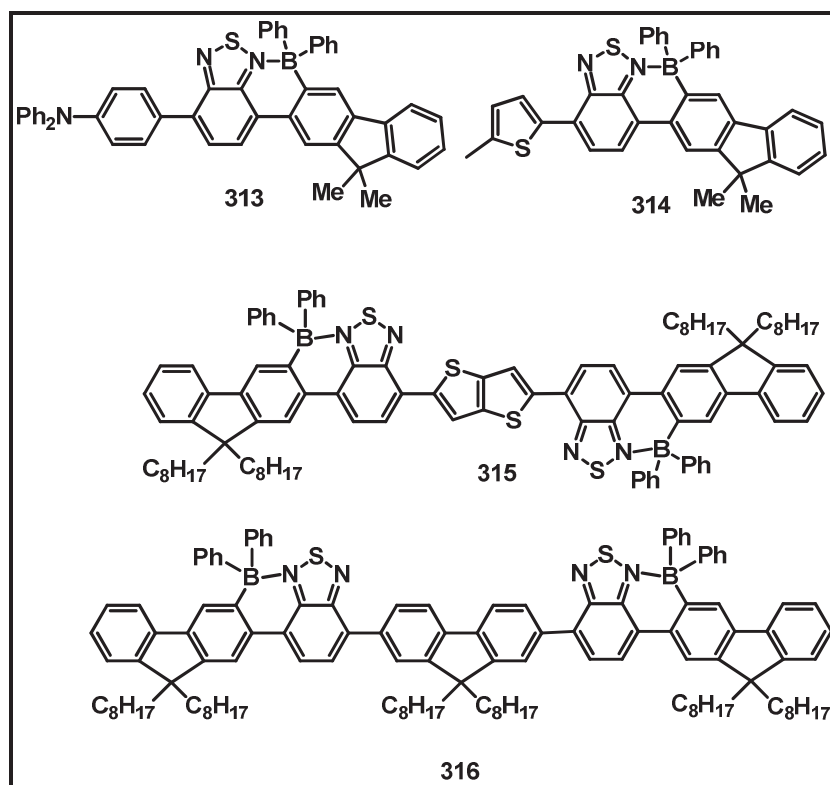


Figure 1.25: N,C- chelate tetra-coordinate boron compounds (**313-316**).

Patil and co-workers synthesized a series of boron compounds (**317-330**) based on 2-aryl quinoline ligands.⁹⁵ The tuning of emission colour was achieved by simply varying the substituents on either quinolines or the boron centre.

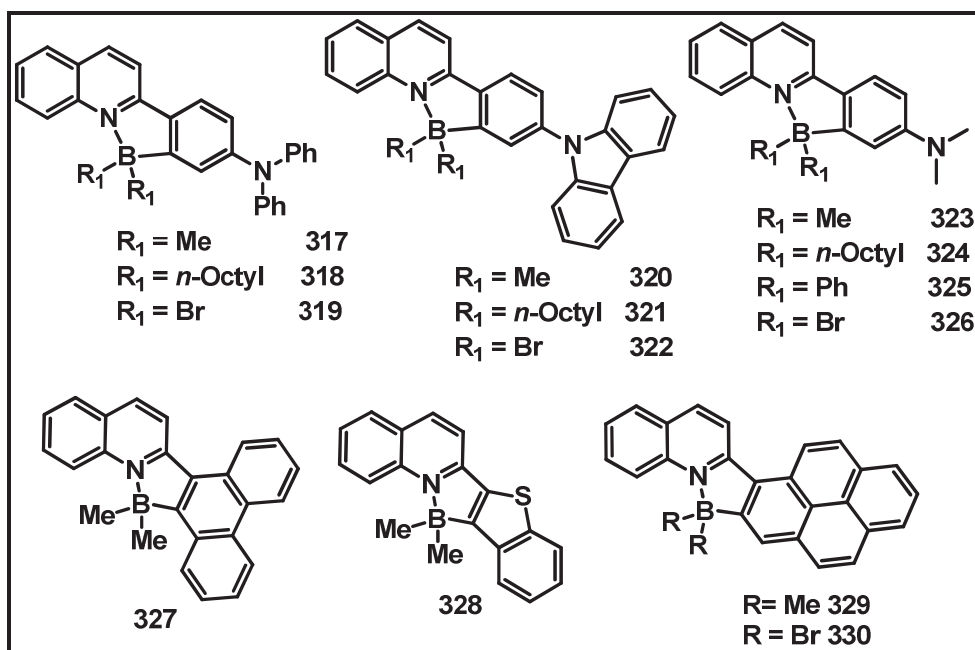


Figure 1.26: N,C- chelate tetra-coordinate boron compounds (317-330).

Yam and co-workers synthesized strongly emissive full color tunable rigid spiro fused boron compounds (331-338) by simply varying the substituents on pyridine ring and extending the π -conjugation on spiro frame work. Some of these compounds also employed as emitters in solution processed OLEDs.⁹⁶

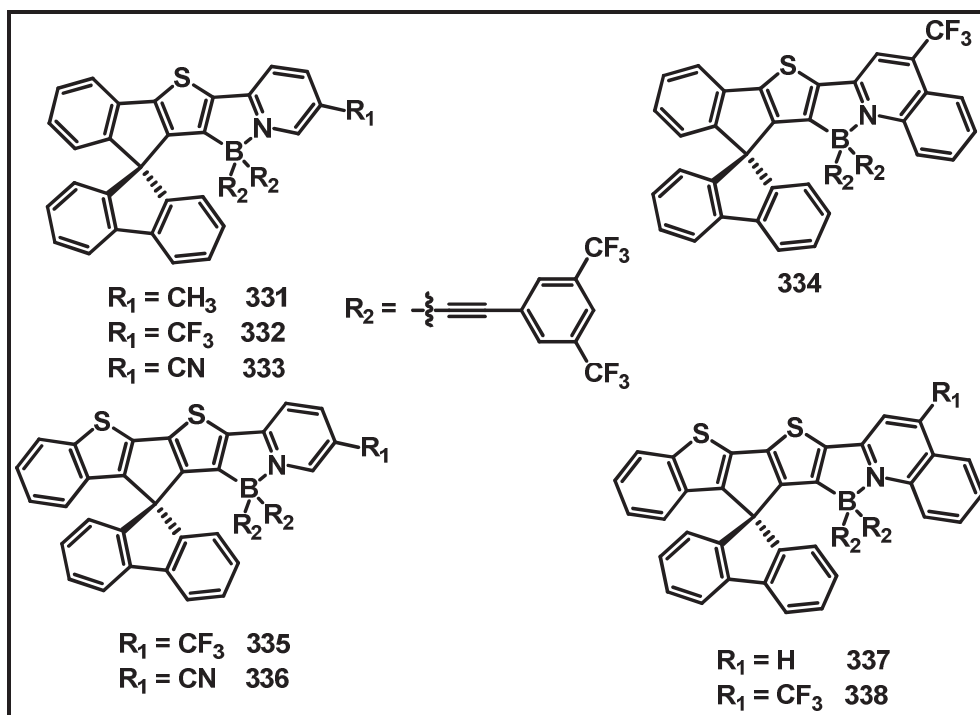


Figure 1.27: N,C- chelate tetra-coordinate boron compounds (331-338).

Jäkle and co-workers reported conjugated ladder type organoboron compounds (**339-340**) based on dipyriddyfluorene ligand.⁹⁷ These boron compounds showed strong blue emission with high quantum yields and underwent multistep reversible reduction and oxidation processes. Fang and co-workers reported two ladder type organoboron compounds (**341-342**) based on pyrazine derived donor-acceptor-donor precursors.⁹⁸ Because of electrophilic borylation, these compounds adopt rigid and coplanar conformations and also exhibited low lying LUMOs.

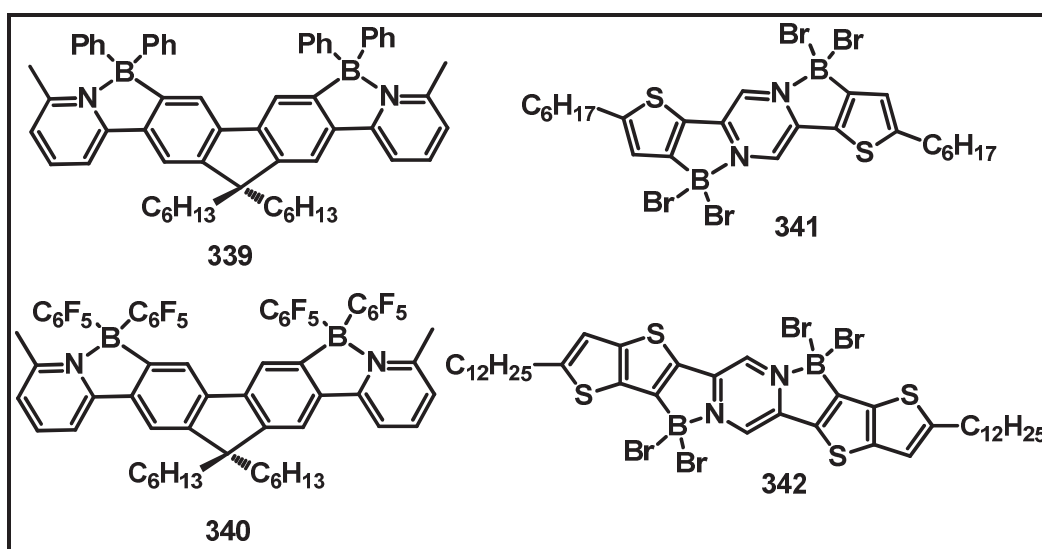


Figure 1.28: N,C- chelate tetra-coordinate boron compounds (**339-342**).

1.2 Aggregation induced emission.

In general, many conventional fluorophores are highly emissive in their dilute solutions; however, they are weakly emissive or even non-emissive in concentrated solutions or solid state. This phenomenon is known as aggregation caused quenching (ACQ). Typical fluorophores usually consist of planar aromatic rings which tend to pack as discs pile up due to strong π - π stacking interaction (Figure 1.28). This π - π stacking interaction leads to the formation of excimers and exciplexes that promotes the excited state to decay or relax back to the ground state *via* non radiative pathway, resulting in the emission quenching of the fluorophores.⁹⁹⁻¹⁰¹ This ACQ effect severely

limits the traditional fluorophores application in real world, because most of the luminophores are always used in the form of solids and aggregates. For example, for optoelectronics applications in organic light-emitting diodes (OLEDs) and organic field-effect transistors (OFETs), fluorophores are used as thin solid films and crystals.¹⁰² Besides this, ACQ is an obstacle when fluorophores are used as bioprobes and fluorescent sensors because they are often used in physiological buffers or aqueous media, where they tend to form aggregates, which leads to diminishment of emission of fluorophores. To eliminate or reduce this ACQ effect, numerous efforts including molecular design, physical aspects and engineering processes have been developed. For example, the introduction of branched chains, bulky cyclics, spiro kinks, encapsulation by amphiphilic surfactants and blending with polymers. All these approaches met with limited success and are often accompanied with severe side effects.

Tang and co-workers for the first time found that, aggregation played a constructive, instead of a destructive, role in the light-emitting process in a series of silole molecules.^{103,104} These molecules displayed faint emission when dissolved in solutions, but strong emission in their aggregate state and the phenomenon they coined as aggregation induced emission (AIE), which is exactly opposite to the ACQ effect. Hexaphenylsilole (HPS) is the first example among the AIE active silole compounds, from which the AIE phenomenon was unearthed. HPS is highly soluble in common organic solvent like acetonitrile, tetrahydrofuran (THF) and chloroform, slightly soluble in methanol, but completely insoluble in water. As shown in figure 1.29, HPS is non emissive when its was dissolved in acetonitrile solvent but its emission is turned on when the water fraction reaches to 80%, as a result of aggregation of the HPS molecules in the aqueous medium.

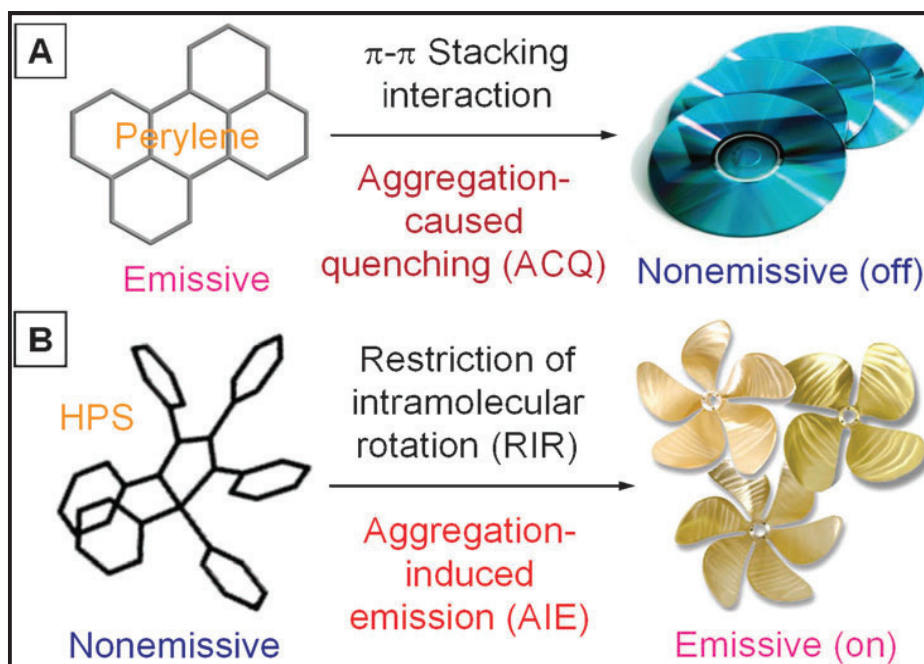


Figure 1.29: (A) Planar luminophoric molecules such as perylene tend to aggregate as discs pile up, due to the strong π - π stacking interactions between the aromatic rings, which commonly turns “off” light emission. (B) Non-planar luminogenic molecules such as hexaphenylsilole (HPS) behave oppositely, with their light emissions turned “on” by aggregate formation, due to the restriction of the intramolecular rotation (RIR) of the multiple phenyl rotors against the silole stator in the aggregate state [Adapted from ref.110].

HPS exhibited quantum yield as low as $\sim 0.20\%$ in acetonitrile, but the quantum yields rose to $\sim 56\%$ when volume fraction of water increased to 99%, which is ~ 255 -fold higher than that in the pure acetonitrile solution. By the experimental results and theoretical calculations, they proved that, the increased emission by aggregation is not due to conformational planarization, J-aggregate formation, and twisted intramolecular charge transfer (TICT). Based on systematic studies like viscosity effect, temperature effect, pressure effect they rationalized the “restriction of intramolecular rotation (RIR)” as the principal mechanism for the AIE effect. In the solutions at room temperature, the active intramolecular rotations of the peripheral phenyl rings around the axes of the single bonds linked to the central silole ring consumes the excited energy, leading to non-radiative decay, which renders the silole molecules nonemissive. The propeller like shapes of the silole molecules experience a

little π - π interaction in the solid state, hence the formation of excimer species can be ignored. The activated RIR process and the reduced chance of excimer formation synergistically make the silole molecules highly emissive in the solid state.

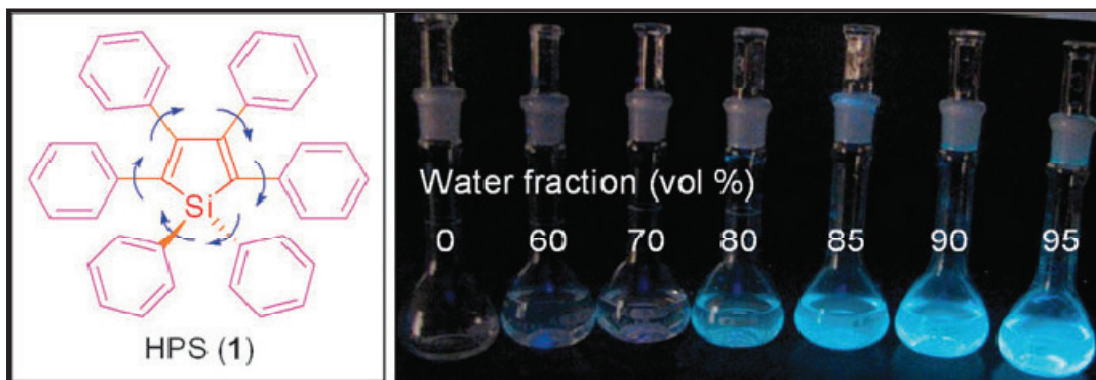


Figure 1.30: (Left) Chemical structure of HPS. (Right) HPS solutions in acetonitrile–water mixtures containing different volume fractions of water; photographs taken under illumination of a UV lamp [Adapted from Ref.109].

Another important AIE luminogen is tetraphenylethene¹⁰⁵ (TPE) in which central olefin statoris surrounded by four peripheral aromatic rotors (phenyl rings). The isolated TPE molecules in dilute solution are non emissive. In the excited state, the central olefinic double bond of TPE can be opened and thus generating two diphenylmethylene (DPM) units. The friction caused by their rotational or twisting motions against each other with the solvent molecules switch the photonic energy to thermal energy, leading to radiationless relaxation of the excitons. The cooperative effect of RIR and the highly twisted molecular conformation that reduce the intermolecular π - π stacking interactions makes the TPE molecules to highly emissive in solid state. By considering the principle of restriction of intramolecular motion, including rotation and vibration, many research groups have worked on to develop the interesting AIE and AIEE (aggregation induced enhanced emission) luminogens¹⁰⁶⁻¹¹⁰. Moreover, different types of AIE and AIEE luminogens and their derivatives have been used as bioprobes, stimuli responsive nanomaterials, chemosensors and active

layers in the construction of efficient organic light emitting diodes (Figure 1.30). The AIE and/or AIEE luminogens have great diversity in molecular structure: they can be pure hydrocarbons, heteroatom containing compounds, organometallic complexes, synthetic or natural polymers, or even unusual molecules without conventional chromophores.

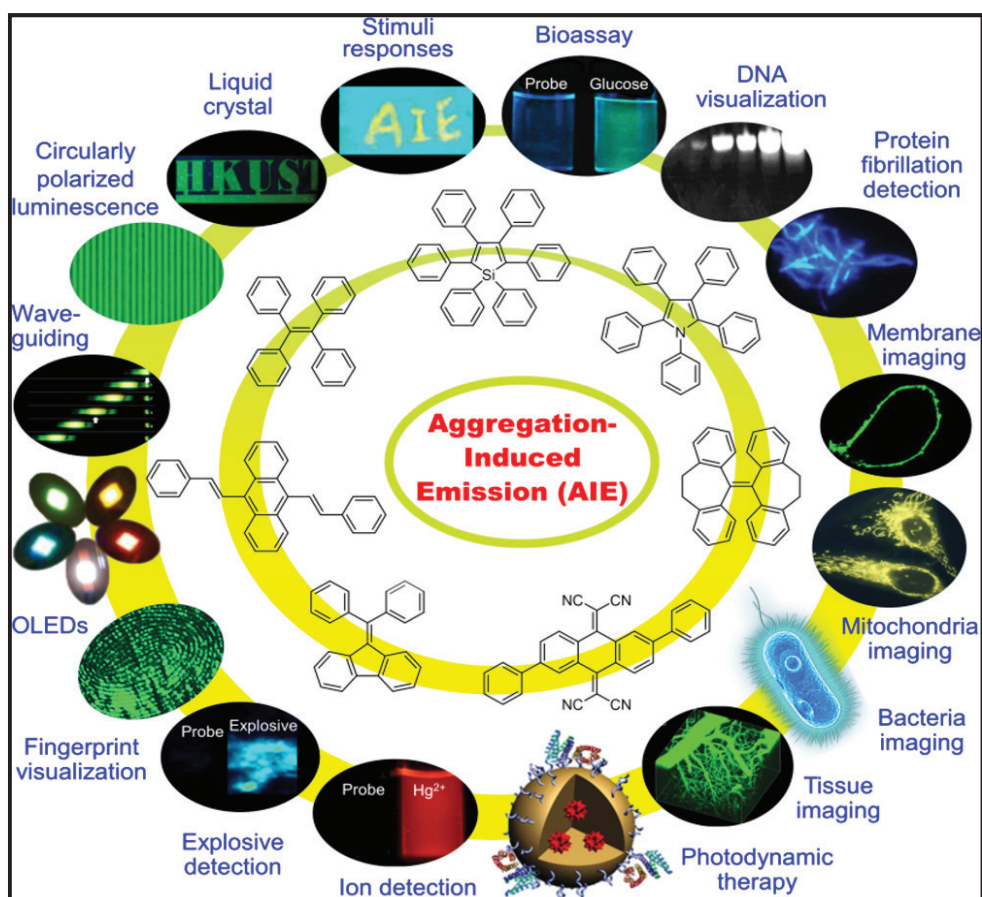


Figure 1.31: Typical examples of structural motifs of AIEgens and their technological applications [Adapted from ref.108].

The conventional fluorophores have been converted to AIEgen by means of (i) decorating ACQ fluorophores with AIEgens (Figure 1.31) (ii) replacing moieties of AIEgens with ACQ units (Figure 1.32) and (iii) creating new AIEgens from ACQ fluorophore (Figure 1.33).

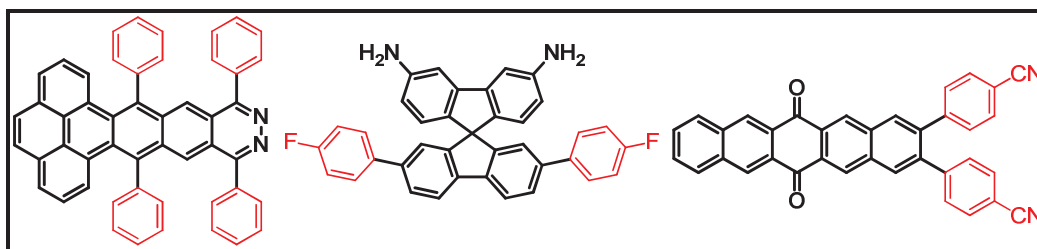


Figure 1.34: Examples of the transformation from ACQ to AIE by decorating ACQphores with aromatic rotors.

1.3 Scope of Thesis

From the brief introduction presented in the preceding sections on tri- and tetra- coordinate boron compounds and their potential applications in various fields like organic light emitting diodes (OLEDs), organic solid state lasers (OSLs), sensors, bioimages; the synthesis of tetra- coordinate boron compounds with rich photophysical properties are growing interest. The work described in this thesis focus on synthesis and study of pyrazole and imidazole based boron compounds. In addition to this, the present thesis also focuses on the synthesis and study of aggregation induced enhanced emission properties of tetra aryl pyrazole decorated polymers and phosphazene.

Chapter 2 outlines the synthesis, characterization, photophysical, and electrochemical properties of a series of tetraaryl imidazole boron complexes by varying the substituents at N-phenyl and para position of 2-phenol. All these compounds exhibit good thermal stability, moderate fluorescence quantum yields and interesting electrochemical properties. Moreover, N-phenyl substituted tetraaryl imidazole boron complexes were also used as electron transporting material in single layer organic light emitting devices.

In chapter 3, we described the synthesis of a series pyrazole based N,C-chelate boron compounds with different substituents at 4- position of N-phenyl. These compounds were characterized by multinuclear NMR spectroscopy and single crystal

X-ray diffraction analysis. All these compounds exhibit substituent dependent fluorescence emission. The second part of this chapter, describes the synthesis, characterization, photophysical and electrochemical properties of pyrazole based N,C-chelate dinuclear boron compounds with extended conjugation. All these compounds exhibit high thermal stability and good fluorescence quantum yields in solutions.

Chapter 4 deals with synthesis, characterization, photophysical and electrochemical properties of the phenanthrene imidazole based dinuclear boron compounds with different aromatic spacers. All these dinuclear compounds were characterized by various spectroscopic techniques and single crystal X-ray diffraction analysis. These compounds exhibit high thermal stability with fluorescence quantum yields reached nearer to unity.

Chapter 5 details the synthesis of tetra aryl pyrazole supported polymers and phosphazenes. The study of the photophysical properties of these polymers and phosphazenes in the aggregated and the non aggregated form reveals that they exhibits the aggregation induced emission enhancement (AIEE) phenomenon. Moreover, the aggregates of these polymers and phosphazenes were also used as a fluorescent probe for the explosive detection (picric acid).

1.4 References

- (1) Anthony, J. E.; Facchetti, A.; Heeney, M.; Marder, S. R.; Zhan, X. *Adv. Mater.* **2010**, *22*, 3876.
- (2) D'Andrade, B. W.; Forrest, S. R. *Adv. Mater.* **2004**, *16*, 1585.
- (3) Ashton, T. D.; Jolliffe, K. A.; Pfeffer, F. M. *Chem. Soc. Rev.* **2015**, *44*, 4547.
- (4) Figueira-Duarte, T. M.; Müllen, K. *Chem. Rev.* **2011**, *111*, 7260.
- (5) Mishra, A.; Bäuerle, P. *Angew. Chem. Int. Ed.* **2012**, *51*, 2020.
- (6) Jakle, F. *Coord. Chem. Rev.* **2006**, *250*, 1107.

-
- (7) Wade, C. R.; Broomsgrove, A. E. J.; Aldridge, S.; Gabbai, F. P. *Chem. Rev.***2010**, *110*, 3958.
 - (8) Hudson, Z. M.; Wang, S. *Acc. Chem. Res.***2009**, *42*, 1584.
 - (9) Entwistle, C. D.; Marder, T. B. *Chem. Mater.***2004**, *16*, 4574.
 - (10) Ji, L.; Griesbeck, S.; Marder, T. B. *Chem. Sci.***2017**.
 - (11) Wang, S. *Coord. Chem. Rev.***2001**, *215*, 79.
 - (12) Li, D.; Zhang, H.; Wang, Y. *Chem. Soc. Rev.***2013**, *42*, 8416.
 - (13) Tanaka, K.; Chujo, Y. *Npg Asia Mater***2015**, *7*, e223.
 - (14) Rao, Y.-L.; Wang, S. *Inorg. Chem.***2011**, *50*, 12263.
 - (15) Frath, D.; Massue, J.; Ulrich, G.; Ziessel, R. *Angew. Chem. Int. Ed. Engl.***2014**, *53*, 2290.
 - (16) Rao, Y.-L.; Amarne, H.; Wang, S. *Coord. Chem. Rev.***2012**, *256*, 759.
 - (17) Loudet, A.; Burgess, K. *Chem. Rev.***2007**, *107*, 4891.
 - (18) Ulrich, G.; Ziessel, R.; Harriman, A. *Angew. Chem. Int. Ed.***2008**, *47*, 1184.
 - (19) Ziessel, R.; Ulrich, G.; Harriman, A. *New J. Chem.***2007**, *31*, 496.
 - (20) Lakshmi, V.; Ravikanth, M. *J. Org. Chem.***2011**, *76*, 8466.
 - (21) Burghart, A.; Thoresen, L. H.; Chen, J.; Burgess, K.; Bergstrom, F.; Johansson, L. B. A. *Chem. Commun.***2000**, 2203.
 - (22) Ge, Y.; O'Shea, D. F. *Chem. Soc. Rev.***2016**, *45*, 3846.
 - (23) Zhang, D.; Wen, Y.; Xiao, Y.; Yu, G.; Liu, Y.; Qian, X. *Chem. Commun.***2008**, 4777.
 - (24) Liu, S.-F.; Wu, Q.; Schmider, H. L.; Aziz, H.; Hu, N.-X.; Popović, Z.; Wang, S. *J. Am. Chem. Soc.***2000**, *122*, 3671.
 - (25) Liang, F. S.; Cheng, Y. X.; Su, G. P.; Ma, D. G.; Wang, L. X.; Jing, X. B.; Wang, F. S. *Synth. Met.***2003**, *137*, 1109.

-
- (26) Liu, Q.; Mudadu, M. S.; Schmider, H.; Thummel, R.; Tao, Y.; Wang, S. *Organometallics***2002**, *21*, 4743.
- (27) Liddle, B. J.; Silva, R. M.; Morin, T. J.; Macedo, F. P.; Shukla, R.; Lindeman, S. V.; Gardinier, J. R. *J. Org. Chem***2007**, *72*, 5637.
- (28) Araneda, J. F.; Piers, W. E.; Heyne, B.; Parvez, M.; McDonald, R. *Angew. Chem. Int. Ed.***2011**, *50*, 12214.
- (29) Calhorda, M. J.; Suresh, D.; Gomes, P. T.; Di Paolo, R. E.; Macanita, A. L. *Dalton Trans.***2012**, *41*, 13210.
- (30) Suresh, D.; Lopes, P. S.; Ferreira, B.; Figueira, C. A.; Gomes, C. S. B.; Gomes, P. T.; Di Paolo, R. E.; Maçanita, A. L.; Duarte, M. T.; Charas, A.; Morgado, J.; Calhorda, M. J. *Chem. Eur. J.***2014**, *20*, 4126.
- (31) Suresh, D.; Gomes, C. S. B.; Lopes, P. S.; Figueira, C. A.; Ferreira, B.; Gomes, P. T.; Di Paolo, R. E.; Macanita, A. L.; Duarte, M. T.; Charas, A.; Morgado, J.; Vila-Vicosa, D.; Calhorda, M. J. *Chem. - Eur. J.***2015**, *21*, 9133.
- (32) Suresh, D.; Ferreira, B.; Lopes, P. S.; Gomes, C. S. B.; Krishnamoorthy, P.; Charas, A.; Vila-Vicosa, D.; Morgado, J.; Calhorda, M. J.; Macanita, A. L.; Gomes, P. T. *Dalton Trans.***2016**, *45*, 15603.
- (33) Barbon, S. M.; Reinkeluers, P. A.; Price, J. T.; Staroverov, V. N.; Gilroy, J. B. *Chem. Eur. J.***2014**, *20*, 11340.
- (34) Chang, M. C.; Chantzis, A.; Jacquemin, D.; Otten, E. *Dalton Trans.***2016**, *45*, 9477.
- (35) Barbon, S. M.; Price, J. T.; Reinkeluers, P. A.; Gilroy, J. B. *Inorg. Chem.***2014**, *53*, 10585.
- (36) Chang, M. C.; Otten, E. *Chem. Commun.***2014**, *50*, 7431.
- (37) Barbon, S. M.; Staroverov, V. N.; Gilroy, J. B. *J. Org. Chem.***2015**, *80*, 5226.
-

-
- (38) Hesari, M.; Barbon, S. M.; Staroverov, V. N.; Ding, Z.; Gilroy, J. B. *Chem. Commun.***2015**, *51*, 3766.
- (39) Maar, R. R.; Gilroy, J. B. *J. Mater. Chem. C***2016**, *4*, 6478.
- (40) Maar, R. R.; Barbon, S. M.; Sharma, N.; Groom, H.; Luyt, L. G.; Gilroy, J. B. *Chem. Eur. J.***2015**, *21*, 15589.
- (41) Novoa, S.; Paquette, J. A.; Barbon, S. M.; Maar, R. R.; Gilroy, J. B. *J. Mater. Chem. C***2016**, *4*, 3987.
- (42) Wang, X.; Wu, Y.; Liu, Q.; Li, Z.; Yan, H.; Ji, C.; Duan, J.; Liu, Z. *Chem. Commun.***2015**, *51*, 784.
- (43) Qiu, F.; Zhang, F.; Tang, R.; Fu, Y.; Wang, X.; Han, S.; Zhuang, X.; Feng, X. *Org. Lett.***2016**, *18*, 1398.
- (44) Wu, Q.; Esteghamatian, M.; Hu, N.-X.; Popovic, Z.; Enright, G.; Tao, Y.; D'Iorio, M.; Wang, S. *Chem. Mater.***1999**, *12*, 79.
- (45) Cui, Y.; Wang, S. *J. Org. Chem***2006**, *71*, 6485.
- (46) Qin, Y.; Kiburu, I.; Shah, S.; Jaekle, F. *Org. Lett.***2006**, *8*, 5227.
- (47) Zhang, Z.; Bi, H.; Zhang, Y.; Yao, D.; Gao, H.; Fan, Y.; Zhang, H.; Wang, Y.; Wang, Y.; Chen, Z.; Ma, D. *Inorg. Chem.***2009**, *48*, 7230.
- (48) Frath, D.; Azizi, S.; Ulrich, G.; Retailleau, P.; Ziessel, R. *Org. Lett.***2011**, *13*, 3414.
- (49) Frath, D.; Azizi, S.; Ulrich, G.; Ziessel, R. *Org. Lett.***2012**, *14*, 4774.
- (50) Dhanunjayarao, K.; Mukundam, V.; Ramesh, M.; Venkatasubbaiah, K. *Eur. J. Inorg. Chem.***2014**, 539.
- (51) Shanmugapriya, J.; Rajaguru, K.; Sivaraman, G.; Muthusubramanian, S.; Bhuvanesh, N. *RSC Adv.***2016**, *6*, 85838.
-

-
- (52) Kubota, Y.; Hara, H.; Tanaka, S.; Funabiki, K.; Matsui, M. *Org. Lett.***2011**, *13*, 6544.
- (53) Kubota, Y.; Tanaka, S.; Funabiki, K.; Matsui, M. *Org. Lett.***2012**, *14*, 4682.
- (54) Kubota, Y.; Ozaki, Y.; Funabiki, K.; Matsui, M. *J. Org. Chem.***2013**, *78*, 7058.
- (55) Kubota, Y.; Kasatani, K.; Niwa, T.; Sato, H.; Funabiki, K.; Matsui, M. *Chem. Eur. J.***2016**, *22*, 1816.
- (56) Zhang, Z.; Xue, P.; Gong, P.; Zhang, G.; Peng, J.; Lu, R. *J. Mater. Chem. C.***2014**, *2*, 9543.
- (57) Zhang, Z.; Wu, Z.; Sun, J.; Yao, B.; Xue, P.; Lu, R. *J. Mater. Chem. C.***2016**, *4*, 2854.
- (58) Liao, C.-W.; Rao M, R.; Sun, S.-S. *Chem. Commun.***2015**, *51*, 2656.
- (59) Wu, Z.; Sun, J.; Zhang, Z.; Yang, H.; Xue, P.; Lu, R. *Chem. Eur. J.***2017**, *23*, 1901.
- (60) Wu, Y.; Li, Z.; Liu, Q.; Wang, X.; Yan, H.; Gong, S.; Liu, Z.; He, W. *Org. Biomol. Chem.***2015**, *13*, 5775.
- (61) Gong, S.; Liu, Q.; Wang, X.; Xia, B.; Liu, Z.; He, W. *Dalton Trans.***2015**, *44*, 14063.
- (62) Zhou, L.; Xu, D.; Gao, H.; Han, A.; Yang, Y.; Zhang, C.; Liu, X.; Zhao, F. *RSC Adv.***2016**, *6*, 69560.
- (63) Gao, H.; Xu, D.; Liu, X.; Han, A.; Zhou, L.; Zhang, C.; Yang, Y.; Li, W. *RSC Adv.***2017**, *7*, 1348.
- (64) Zakrzewska, A.; Zaleśny, R.; Kolehmainen, E.; Ośmiałowski, B.; Jędrzejewska, B.; Ågren, H.; Pietrzak, M. *Dyes and Pigments***2013**, *99*, 957.
- (65) Ośmiałowski, B.; Zakrzewska, A.; Jędrzejewska, B.; Grabarz, A.; Zaleśny, R.; Bartkowiak, W.; Kolehmainen, E. *J. Org. Chem.***2015**, *80*, 2072.
-

-
- (66) Grabarz, A. M.; Jędrzejewska, B.; Zakrzewska, A.; Zaleśny, R.; Laurent, A. D.; Jacquemin, D.; Ośmiałowski, B. *J. Org. Chem.***2017**, *82*, 1529.
- (67) Kwak, M.-J.; Kim, Y.-M. *Bull. Korean Chem. Soc.***2009**, *30*, 2865.
- (68) Li, D.; Wang, K.; Huang, S.; Qu, S.; Liu, X.; Zhu, Q.; Zhang, H.; Wang, Y. *J. Mater. Chem.***2011**, *21*, 15298.
- (69) Li, D.; Zhang, H.; Wang, C.; Huang, S.; Guo, J.; Wang, Y. *J. Mater. Chem.***2012**, *22*, 4319.
- (70) Li, D.; Yuan, Y.; Bi, H.; Yao, D.; Zhao, X.; Tian, W.; Wang, Y.; Zhang, H. *Inorg. Chem.***2011**, *50*, 4825.
- (71) Massue, J.; Frath, D.; Ulrich, G.; Retailleau, P.; Ziessel, R. *Org. Lett.***2012**, *14*, 230.
- (72) Massue, J.; Frath, D.; Retailleau, P.; Ulrich, G.; Ziessel, R. *Chem. Eur. J.***2013**, *19*, 5375.
- (73) Massue, J.; Retailleau, P.; Ulrich, G.; Ziessel, R. *New J. Chem.***2013**, *37*, 1224.
- (74) Dias, G. G.; Rodrigues, B. L.; Resende, J. M.; Calado, H. D. R.; de Simone, C. A.; Silva, V. H. C.; Neto, B. A. D.; Goulart, M. O. F.; Ferreira, F. R.; Meira, A. S.; Pessoa, C.; Correa, J. R.; da Silva Junior, E. N. *Chem. Commun.***2015**, *51*, 9141.
- (75) Benelhadj, K.; Massue, J.; Retailleau, P.; Ulrich, G.; Ziessel, R. *Org. Lett.***2013**, *15*, 2918.
- (76) Zhang, Z.; Zhang, H.; Jiao, C.; Ye, K.; Zhang, H.; Zhang, J.; Wang, Y. *Inorg. Chem.***2015**, *54*, 2652.
- (77) Wakamiya, A.; Taniguchi, T.; Yamaguchi, S. *Angew. Chem. Int. Ed. Engl.***2006**, *45*, 3170.
-

-
- (78) Job, A.; Wakamiya, A.; Kehr, G.; Erker, G.; Yamaguchi, S. *Org. Lett.***2010**, *12*, 5470.
- (79) Li, D.; Zhang, Z.; Zhao, S.; Wang, Y.; Zhang, H. *Dalton Trans.***2011**, *40*, 1279.
- (80) Pais, V. F.; Alcaide, M. M.; Lopez-Rodriguez, R.; Collado, D.; Najera, F.; Perez-Inestrosa, E.; Alvarez, E.; Lassaletta, J. M.; Fernandez, R.; Ros, A.; Pischel, U. *Chem. - Eur. J.***2015**, *21*, 15369.
- (81) Rao, Y.-L.; Amarne, H.; Zhao, S.-B.; McCormick, T. M.; Martić, S.; Sun, Y.; Wang, R.-Y.; Wang, S. *J. Am. Chem. Soc.***2008**, *130*, 12898.
- (82) Amarne, H.; Baik, C.; Murphy, S. K.; Wang, S. *Chem. Eur. J.***2010**, *16*, 4750.
- (83) Baik, C.; Hudson, Z. M.; Amarne, H.; Wang, S. *J. Am. Chem. Soc.***2009**, *131*, 14549.
- (84) Yoshino, J.; Kano, N.; Kawashima, T. *Chem. Commun.***2007**, 559.
- (85) Yoshino, J.; Furuta, A.; Kambe, T.; Itoi, H.; Kano, N.; Kawashima, T.; Ito, Y.; Asashima, M. *Chem. Eur. J.***2010**, *16*, 5026.
- (86) Kano, N.; Furuta, A.; Kambe, T.; Yoshino, J.; Shibata, Y.; Kawashima, T.; Mizorogi, N.; Nagase, S. *Eur. J. Inorg. Chem.***2012**, *2012*, 1584.
- (87) Yoshino, J.; Kano, N.; Kawashima, T. *J. Org. Chem.***2009**, *74*, 7496.
- (88) Neue, B.; Froehlich, R.; Wibbeling, B.; Fukazawa, A.; Wakamiya, A.; Yamaguchi, S.; Wuerthwein, E.-U. *J. Org. Chem.***2012**, *77*, 2176.
- (89) Ishida, N.; Moriya, T.; Goya, T.; Murakami, M. *J. Org. Chem.***2010**, *75*, 8709.
- (90) Wong, H.-L.; Wong, W.-T.; Yam, V. W.-W. *Org. Lett.***2012**, *14*, 1862.
- (91) Zhao, Z.; Chang, Z.; He, B.; Chen, B.; Deng, C.; Lu, P.; Qiu, H.; Tang, B. Z. *Chem. Eur. J.***2013**, *19*, 11512.
-

-
- (92) He, B.; Chang, Z.; Jiang, Y.; Chen, B.; Lu, P.; Kwok, H. S.; Qin, A.; Zhao, Z.; Qiu, H. *Dyes Pigm.***2014**, *101*, 247.
- (93) Crossley, D. L.; Cade, I. A.; Clark, E. R.; Escande, A.; Humphries, M. J.; King, S. M.; Vitorica-Yrezabal, I.; Ingleson, M. J.; Turner, M. L. *Chem. Sci.***2015**, *6*, 5144.
- (94) Crossley, D. L.; Vitorica-Yrezabal, I.; Humphries, M. J.; Turner, M. L.; Ingleson, M. J. *Chem. Eur. J.***2016**, *22*, 12439.
- (95) Shaikh, A. C.; Ranade, D. S.; Thorat, S.; Maity, A.; Kulkarni, P. P.; Gonnade, R. G.; Munshi, P.; Patil, N. T. *Chem. Commun.***2015**, *51*, 16115.
- (96) Wong, B. Y.-W.; Wong, H.-L.; Wong, Y.-C.; Chan, M.-Y.; Yam, V. W.-W. *Chem. Eur. J.***2016**, *22*, 15095.
- (97) Yusuf, M.; Liu, K.; Guo, F.; Lalancette, R. A.; Jakle, F. *Dalton Trans.***2016**, *45*, 4580.
- (98) Zhu, C.; Guo, Z. H.; Mu, A. U.; Liu, Y.; Wheeler, S. E.; Fang, L. *J. Org. Chem.***2016**, *81*, 4347.
- (99) v. Büнау, G. *Berichte der Bunsengesellschaft für physikalische Chemie***1970**, *74*, 1294.
- (100) Thomas, S. W.; Joly, G. D.; Swager, T. M. *Chem. Rev.***2007**, *107*, 1339.
- (101) Zhang, X. H.; Chen, B. J.; Lin, X. Q.; Wong, O. Y.; Lee, C. S.; Kwong, H. L.; Lee, S. T.; Wu, S. K. *Chem. Mater.***2001**, *13*, 1565.
- (102) Chen, C.-T. *Chem. Mater.***2004**, *16*, 4389.
- (103) Tang, B. Z.; Zhan, X.; Yu, G.; Sze Lee, P. P.; Liu, Y.; Zhu, D. *J. Mater. Chem.***2001**, *11*, 2974.
- (104) Chen, J.; Law, C. C. W.; Lam, J. W. Y.; Dong, Y.; Lo, S. M. F.; Williams, I. D.; Zhu, D.; Tang, B. Z. *Chem. Mater.***2003**, *15*, 1535.
-

-
- (105) Zhao, Z.; Lam, J. W. Y.; Tang, B. Z. *J. Mater. Chem.***2012**, *22*, 23726.
- (106) Mei, J.; Hong, Y.; Lam, J. W. Y.; Qin, A.; Tang, Y.; Tang, B. Z. *Adv. Mater.***2014**, *26*, 5429.
- (107) Liang, J.; Tang, B. Z.; Liu, B. *Chem. Soc. Rev.***2015**, *44*, 2798.
- (108) Mei, J.; Leung, N. L. C.; Kwok, R. T. K.; Lam, J. W. Y.; Tang, B. Z. *Chem. Rev.***2015**, *115*, 11718.
- (109) Hong, Y.; Lam, J. W. Y.; Tang, B. Z. *Chem. Commun.***2009**, 4332.
- (110) Hong, Y.; Lam, J. W. Y.; Tang, B. Z. *Chem. Soc. Rev.***2011**, *40*, 5361.

CHAPTER 2A

Design, Synthesis, Photophysical and Electrochemical Properties of 2-(4,5-diphenyl-1-*p*-aryl-1H-imidazol-2-yl)phenol-based Boron Complexes

2A.1 Introduction	49
2A.2 Results and discussion	51
2A.2.1 Synthesis and characterization	51
2A.2.2 Photophysical studies	55
2A.2.3 Theoretical calculations	57
2A.2.4 Thermal studies	59
2A.2.5 Electrochemical studies	60
2A.2.6 Electroluminescent properties	61
2A.3 Conclusions	64
2A.4 Experimental section	64
2A.4.1 General information	64
2A.4.2 Synthetic procedure and spectral characterization	64
2A.5 References	71

2A.1 Introduction

Over the past decade, there has been a growing interest in the development of organic electronics for the applications in organic field effect transistors, organic light emitting diodes (OLEDs) and nonlinear optic materials.¹⁻³ Although organic materials have significant advantages over inorganic materials such as cost effectiveness, wide array of processing options and the ability to tune the photophysical properties using different synthetic approaches, but lack on long-term stability and performance. Intensive work in both academic and industry have been studied with a view to prepare conjugated frameworks of enhanced stability and performance. Incorporation of hetero atoms into the backbone of π -conjugated systems have turned out to be one of the widely used methods to tune the electronic structures thus produces desirable photophysical and electronic properties.^{4,5} In this regard, incorporation of main group elements into organic framework with extended conjugation have attracted much attention owing to their unusual optical and electronic properties.

Among various types of main group element-containing π -electron systems, tri⁶⁻⁹- and tetra-coordinated¹⁰⁻¹² boron compounds have received particular interest because of their applications in nonlinear optics, fluorescent sensors, organic light emitting diodes and biomolecular probes. Much effort has been devoted to the development of different types of tetra-coordinated boron compounds owing to their high stability towards air and moisture over tri-coordinated boron compounds. In particular, boron dipyrromethene¹³⁻¹⁵ (BODIPYs) dyes synthesized by the condensation of pyrrole, carbaldehyde and boron reagents have been used extensively as organic light emitting diodes, fluorescent imaging agents and sensors. Although BODIPYs exhibit strong fluorescence and high molar extinction coefficients, they suffer having small Stokes shift¹⁵ and weak solid-state emission. Efforts have been

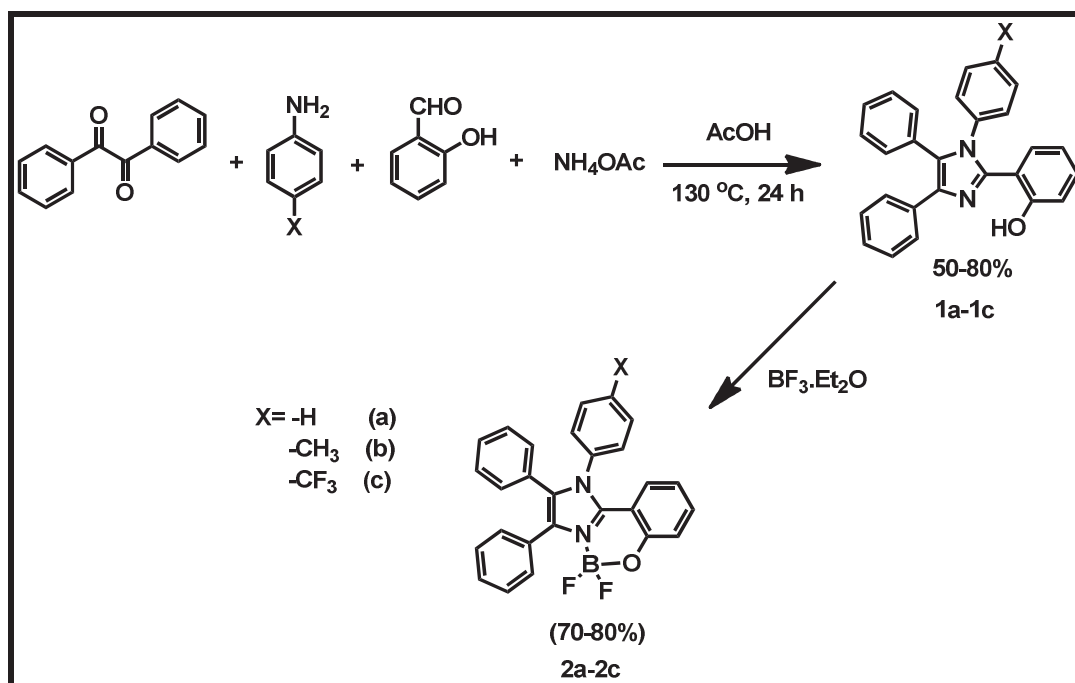
made to synthesise modified BODIPY fluorophores with pronounced Stokes shifts^{16,17} and better electroluminescent properties; however a distinct disadvantage of this approach is the assemblies made using this method are structurally complex and require multi-step organic synthesis.

Another strategy employed for the development of boron fluorophores with improved properties relies on principles of ligand design¹⁸⁻³⁰. Several examples of boron fluorophores with different architectures have been reported to intrinsically exhibit better photophysical properties not only in solution but also in the solid state. For example Massue *et al*^{31,32} reported a series of boron complexes based on 2-(2'-hydroxyphenyl)benzoxazole. Ahn and co-workers³³ reported the dramatic substituent effect of boron complexes based on 2-(benzothiazol-2-yl)phenols. Wagner and co-workers³⁴ reported aryl(hydro)boranes as versatile boron-containing π -electron materials. In pursuit of new ligand system, we noticed imidazoles are highly attractive synthons, especially tetraphenylimidazole based excited-state intramolecular proton-transfer (ESIPT) molecules that showed good electroluminescence, high thermal and morphological stability.^{35,36} Different synthetic approaches have been employed to modify the optical and charge transport properties of arylimidazoles.^{37,38} In an effort to tune the optical properties of imidazoles, Ziessel and co-workers introduced boron into the frame work of imidazoles through N,O-chelation.³⁸ In this chapter we describe the synthesis and characterizations of tetraarylimidazoles based boron complexes from simple starting materials and also present their photophysical, electrochemical and electroluminescent properties.

2A.2 Results and discussion

2A.2.1 Synthesis and characterization

The simple synthetic route adopted for the preparation of compound **2a-2c** is shown in Scheme 2A.1. The tetraarylimidazoles (**1a-1c**) were readily synthesized according to the literature-reported procedure³⁵ using commercially available reagents. The corresponding boron complexes **2a-2c** were synthesized by the complexation of tetraarylimidazoles (**1a-1c**) with $\text{BF}_3 \cdot \text{Et}_2\text{O}$ in the presence of diisopropylethylamine in more than 70% yield.



Scheme 2A.1: Synthetic route to the compounds **2a-2c**.

All three boron complexes were fully characterized using ^1H , ^{13}C , ^{11}B and ^{19}F NMR spectroscopy and high resolution mass spectrometry. The ^{11}B NMR spectra of complexes **2a-2c** show resonance around 1 ppm, which is characteristic of tetracoordinated boron and the ^{19}F chemical shifts appears around -139 ppm for the fluorine atoms attached to boron. A representative ^{11}B and ^{19}F NMR spectrum of compound **2c** is shown in Figure 2A.1 In ^{19}F NMR spectrum of compound **2c**, the signal resonates at -63.73 corresponds to CF_3 group while the signal resonates at

-138.29 corresponds to BF_2 .

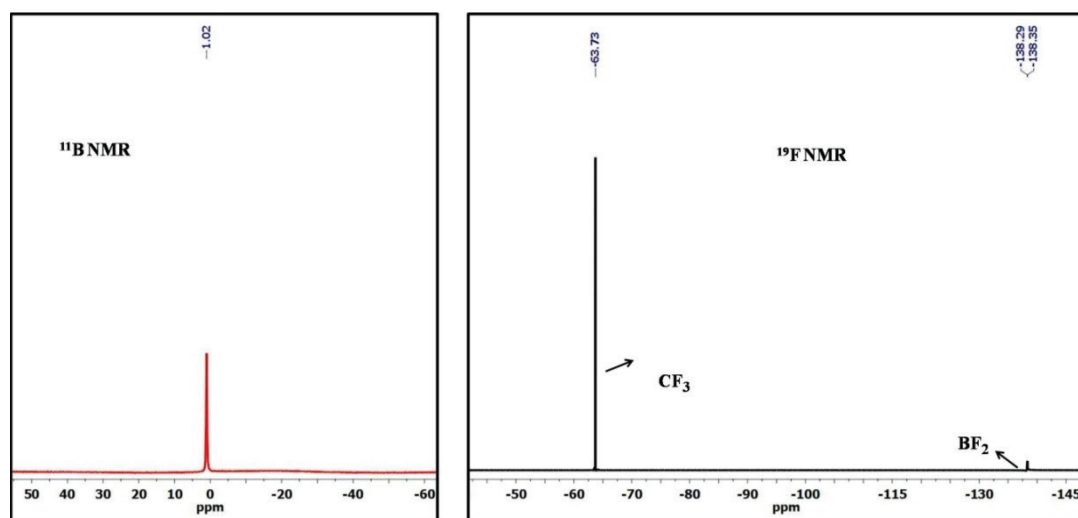


Figure 2A.1: ^{11}B and ^{19}F NMR spectrum of compound **2c**.

Single crystals of compounds **2a** and **2c** were grown and analysed using single crystal X-ray diffraction studies (Table 2A.2). Complexes **2a** and **2c** crystallizes in the triclinic $P-1$ space group and monoclinic $C2/c$ space group respectively. The molecular structure of **2a** and **2c** is shown in Figure 2A.2; selected bond lengths, bond angles pertaining to these complexes are summarized in Table 2A.1. In both structures (**2a** & **2c**) the boron atom assumes a distorted tetrahedral geometry. The B-N and B-O bond lengths in **2a** and **2c** are similar to those of the other literature reported boron complexes.³⁸ In both structures, the six-membered ring formed by the boron chelation takes a twisted conformation. The boron and oxygen atoms deviate from the imidazole plane by 0.06 Å and 0.66 Å in case of **2a** and 0.15 Å and 0.83 Å in case of **2c**. The dihedral angle between the imidazole and the phenolate is 19.46 ° (for **2a**) 22.13 ° (for **2c**) indicates that the π -system have distortion from the coplanar framework. The phenyl rings at the 1, 4 & 5-positions are severely twisted, the twist observed for **2a** is 70.34, 45.06 & 58.83 ° for **2c** is 64.17, 46.50 & 53.03 ° respectively (Figure 2A.3). This ring twist generate a propeller type conformation for the chromophores which helps in preventing the π - π stacking interactions. In general

the π - π stacking interactions are blamed for quenching of fluorescence in the solid state.

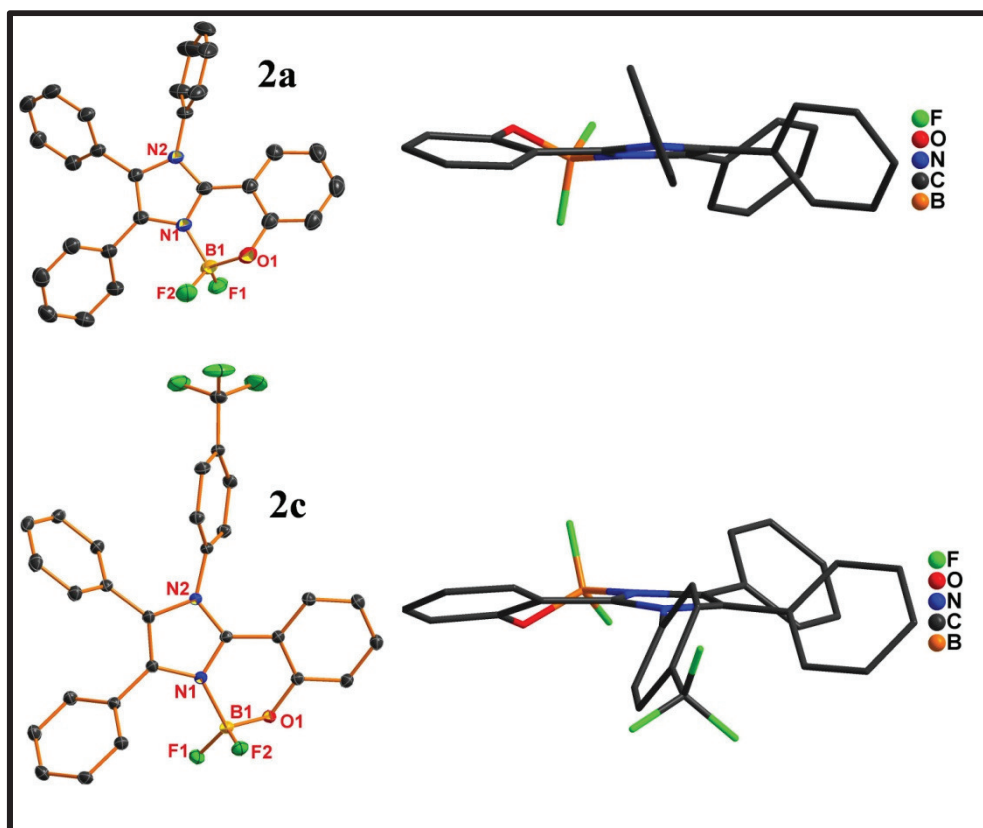


Figure 2A.2: Molecular structures of compounds **2a**, **2c** (left); Thermal ellipsoids are shown at 30% probability level for **2a** and 50% for **2c**. Side view of **2a**, **2c** (right). Co-crystallized solvent molecule and hydrogen atoms are omitted for clarity.

Table 2A.1: Comparison of some selected bond lengths [Å] and bond angles [deg] for compounds **2a** and **2c**.

Compound	2a	2c
B1-F1	1.383(2)	1.3751(13)
B1-F2	1.357(2)	1.3894(14)
B1-O1	1.455(3)	1.4585(14)
B1-N1	1.582(2)	1.5851(15)
F1-B1-F2	111.76(16)	111.58(9)
F1-B1-O1	110.55(16)	108.39(9)
F2-B1-O1	108.89(17)	111.09(9)
F1-B1-N1	107.49(15)	110.16(9)
F2-B1-N1	110.71(15)	108.13(9)
O1-B1-N1	107.35(14)	107.40(8)

Table 2A.2: Crystal data and structure refinement parameters for compounds **2a** and **2c**.

Crystal parameters	2a	2c
Empirical formula	C ₂₇ H ₁₉ BF ₂ N ₂ O	C ₅₈ H ₃₆ B ₂ F ₁₀ N ₅ O ₂
Formula weight	436.25	1046.54
Temperature/K	296(2)	100(2)
Crystal system	Triclinic	Monoclinic
Space group	<i>P</i> -1	<i>C</i> 2/ <i>c</i>
<i>a</i> /Å	10.2847(4)	31.603(4)
<i>b</i> /Å	10.8082(4)	8.6107(10)
<i>c</i> /Å	10.9755(4)	22.928(3)
α /°	85.101(3)	90
β /°	75.591(3)	129.760(11)
γ /°	67.342(2)	90
Volume/Å ³	1090.38(7)	4796.3(11)
<i>Z</i>	2	4
$\rho_{\text{calcd}}/\text{g cm}^{-3}$	1.329	1.449
$\mu(\text{MoK}\alpha) / \text{mm}^{-1}$	0.092	0.115
<i>F</i> (000)	452	2140
θ range for data collection/°	1.92 – 28.30	1.68 – 30.56
Index ranges	-12 ≤ <i>h</i> ≤ 13 -14 ≤ <i>k</i> ≤ 14 -14 ≤ <i>l</i> ≤ 14	-45 ≤ <i>h</i> ≤ 44 -12 ≤ <i>k</i> ≤ 12 -31 ≤ <i>l</i> ≤ 32
Reflns. collected	16890	39509
Independent reflns	5404 [<i>R</i> (int) = 0.0375]	7309 [<i>R</i> (int) = 0.0307]
Data/restraints/ Parameters	5404 / 0 / 299	7309 / 0 / 349
GOF on <i>F</i> ²	1.006	1.033
Final <i>R</i> indices [<i>I</i> > 2σ(<i>I</i>)]	<i>R</i> ₁ = 0.0465 <i>wR</i> ₂ = 0.1059	<i>R</i> ₁ = 0.0414 <i>wR</i> ₂ = 0.1122
<i>R</i> indices (all data)	<i>R</i> ₁ = 0.0945 <i>wR</i> ₂ = 0.1302	<i>R</i> ₁ = 0.0499 <i>wR</i> ₂ = 0.1187
Largest diff. peak /hole [e Å ⁻³]	0.200 and -0.142	0.607 and -0.316

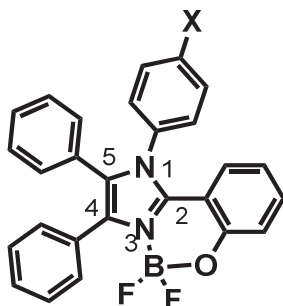


Figure 2A.3: Imidazole core numbering.

2A.2.2 Photophysical studies

The optical properties of boron complexes **2a-2c** were investigated by UV-Visible absorption and emission spectra in five different solvents of varying polarity. The resulting data are summarized in Table 2A.3. The UV-Visible absorption and emission spectra of these complexes in dichloromethane solution are shown in Figure 2A.4 & Table 2A.3. The absorption spectra of **2a-2c** in dichloromethane (Figure 2A.4) consist of two bands, the first band centered around 284 nm while the second band appeared at 325 nm ($\epsilon = 20\,500\text{ M}^{-1}\text{ cm}^{-1}$) for **2a**, 325 nm ($\epsilon = 21\,200\text{ M}^{-1}\text{ cm}^{-1}$) for **2b** and 328 nm ($\epsilon = 19\,100\text{ M}^{-1}\text{ cm}^{-1}$) for **2c**. The origin of this absorption was studied using theoretical calculation and will be described in the following section 2A.2.3. Emission spectra of complexes **2a-2c** were recorded by exciting their solutions at longer wavelength absorption maxima. In dichloromethane, these complexes exhibit intense blue emission (Figure 2A.5) with emission maxima centered at 378 for **2a**, 379 for **2b** and 387 for **2c**. All three complexes exhibited moderate emission quantum yields (Figure 2A.3) with larger Stokes shifts in comparison to typical BODIPYs systems. As compared to compound **2a** and **2b**, compound **2c** exhibits red shifted absorption and emission maxima, which can be attributed to the electron withdrawing nature of the- CF_3 substituent in complex **2c**. Both absorption and emission spectra of our boron complexes (**2a-2c**) were slightly affected with solvent polarity, which is quite a contrast result compared to the majority of BODIPY dyes.

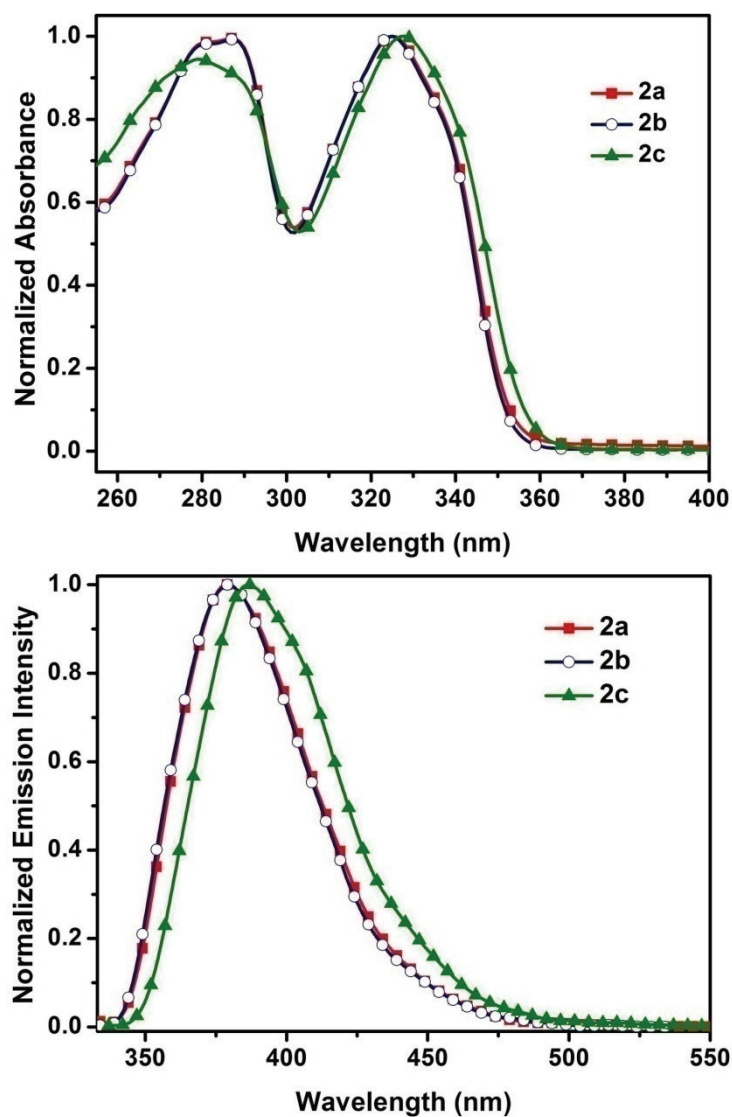


Figure 2A.4: (top) Normalized UV-Vis absorption & (bottom) Normalized fluorescence spectra of compounds **2a-2c** in dichloromethane (concentration = 4×10^{-5} M).

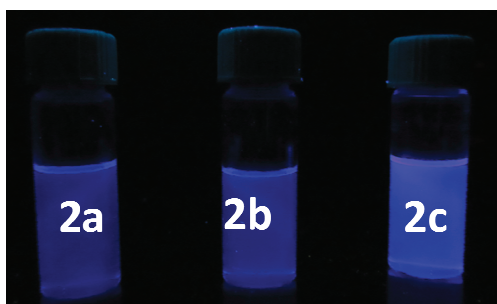


Figure 2A.5: The fluorescence photograph of compounds **2a-2c** in dichloromethane solution (wavelength of light is 365 nm).

Table 2A.3: Photophysical data of the imidazole boron compounds **2a-2c**.

Compound	solvent	λ_{\max}^a (nm)	ϵ_{\max} ($M^{-1}.cm^{-1} \times 10^3$)	$\lambda_{em}^{a,b}$ (nm)	$(\Phi)^{[c]}$
2a	Toluene	328	19.44	385	0.46
	THF	326	17.62	382	0.40
	CH ₂ Cl ₂	325	20.5	379	0.44
	CH ₃ CN	321	17.98	379	0.40
	DMF	323	18.78	382	0.45
2b	Toluene	328	17.94	384	0.40
	THF	326	16.63	382	0.58
	CH ₂ Cl ₂	325	21.2	379	0.45
	CH ₃ CN	321	16.64	379	0.44
	DMF	323	17.75	381	0.36
2c	Toluene	331	16.87	392	0.51
	THF	327	15.10	390	0.49
	CH ₂ Cl ₂	328	19.10	387	0.50
	CH ₃ CN	323	16.53	386	0.48
	DMF	325	18.08	388	0.39

^aLowest-energy absorption maximum (Concentration: 4×10^{-5} M). ^bExcited at the absorption maximum. ^c Fluorescence quantum yields were measured using quinine sulphate as the reference.

2A.2.3 Theoretical calculations

To gain further insight into the electronic structures of complexes **2a-2c**, we carried out density functional theory (DFT) calculations by the Gaussian 03 programmes using B3LYP/6-31G basis set. The pictorial diagrams of HOMOs and LUMOs and relevant energy for complexes **2a-2c** are shown in Figure 2A.6. In all three complexes the HOMOs are mainly contributed by the π -orbitals of the central imidazole, 2,4-phenyl and oxygen atom, whereas the LUMOs are consisting of π^* orbitals of the central imidazole, 1,2 & 5-phenyl moieties. An interesting observation is that the LUMO for **2c** is more effectively stabilized than the HOMO so that the gap between HOMO and LUMO gets smaller for **2c** (4.000 eV) compared to **2a** (4.245 eV) and **2b** (4.274 eV).

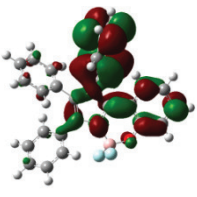
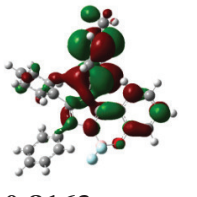
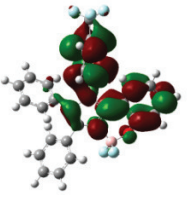
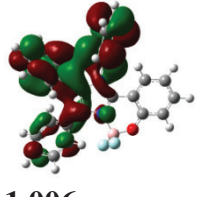
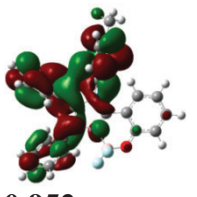
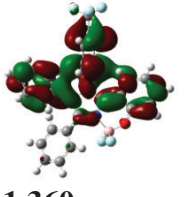
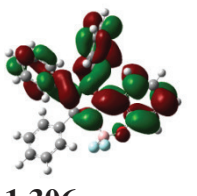
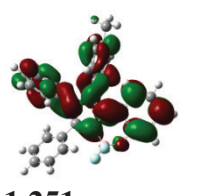
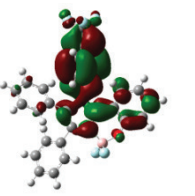
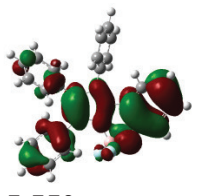
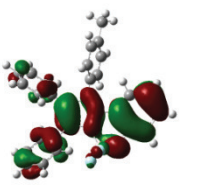
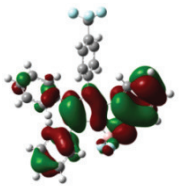
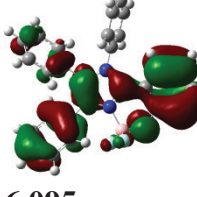
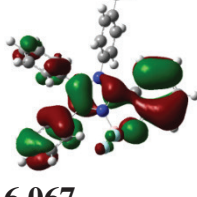
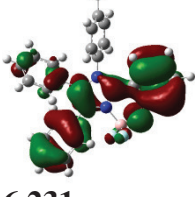
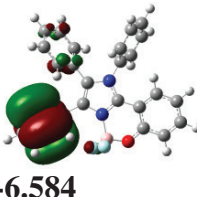
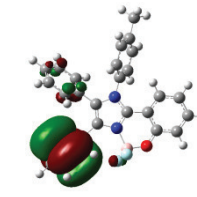
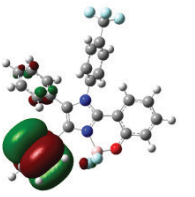
Compound	2a (eV)	2b (eV)	2c (eV)
LUMO+2	 -0.897	 -0.8163	 -1.224
LUMO+1	 -1.006	 -0.952	 -1.360
LUMO	 -1.306	 -1.251	 -1.714
HOMO	 -5.550	 -5.523	 -5.714
HOMO-1	 -6.095	 -6.067	 -6.231
HOMO-2	 -6.584	 -6.557	 -6.693

Figure 2A.6: Computed orbitals for compounds 2a-2c.

The electronic excitations for boron complexes **2a-2c** were calculated using TD-B3LYP/6-31-G (Table 2A.4). The calculated excitation values are comparable with the experimental results, especially the calculation perfectly reproduce the red shift for the complex **2c**.

Table 2A.4: Calculated electronic transitions for compound **2a-2c** from TD-DFT (B3LYP) calculations.

Compound	Transition	MO contributions	Energy gap eV (nm)	Oscillator strength/f
2a	$S_0 \rightarrow S_1$	HOMO→LUMO HOMO→LUMO+2	3.74 (331)	0.2743
	$S_0 \rightarrow S_2$	HOMO→LUMO+1 HOMO→LUMO+2	3.97 (312)	0.0544
	$S_0 \rightarrow S_3$	HOMO-1→LUMO HOMO→LUMO+1 HOMO→LUMO+2	4.09 (303)	0.0788
2b	$S_0 \rightarrow S_1$	HOMO→LUMO	3.76 (329)	0.3137
	$S_0 \rightarrow S_2$	HOMO→LUMO+1 HOMO→LUMO+2	4.00 (309)	0.0324
	$S_0 \rightarrow S_3$	HOMO-1→LUMO HOMO→LUMO+1 HOMO→LUMO+2	4.12 (300)	0.0683
2c	$S_0 \rightarrow S_1$	HOMO→LUMO	3.42 (362)	0.0654
	$S_0 \rightarrow S_2$	HOMO-1→LUMO HOMO→LUMO+1 HOMO→LUMO+2	3.80 (326)	0.0993
	$S_0 \rightarrow S_3$	HOMO-1→LUMO HOMO→LUMO+2	3.93 (315)	0.1243

2A.2.4 Thermal studies

The thermal properties of complexes **2a-2c** were investigated by thermogravimetric analysis (TGA) and differential scanning calorimetry (DSC) under a nitrogen atmosphere at a heating rate of 20 °C/min. All these boron complexes

exhibit good thermal stability (decomposition starts above 300 °C for **2a**&**2b**) (Figure 2A.7) with high melting points (> 270 °C).

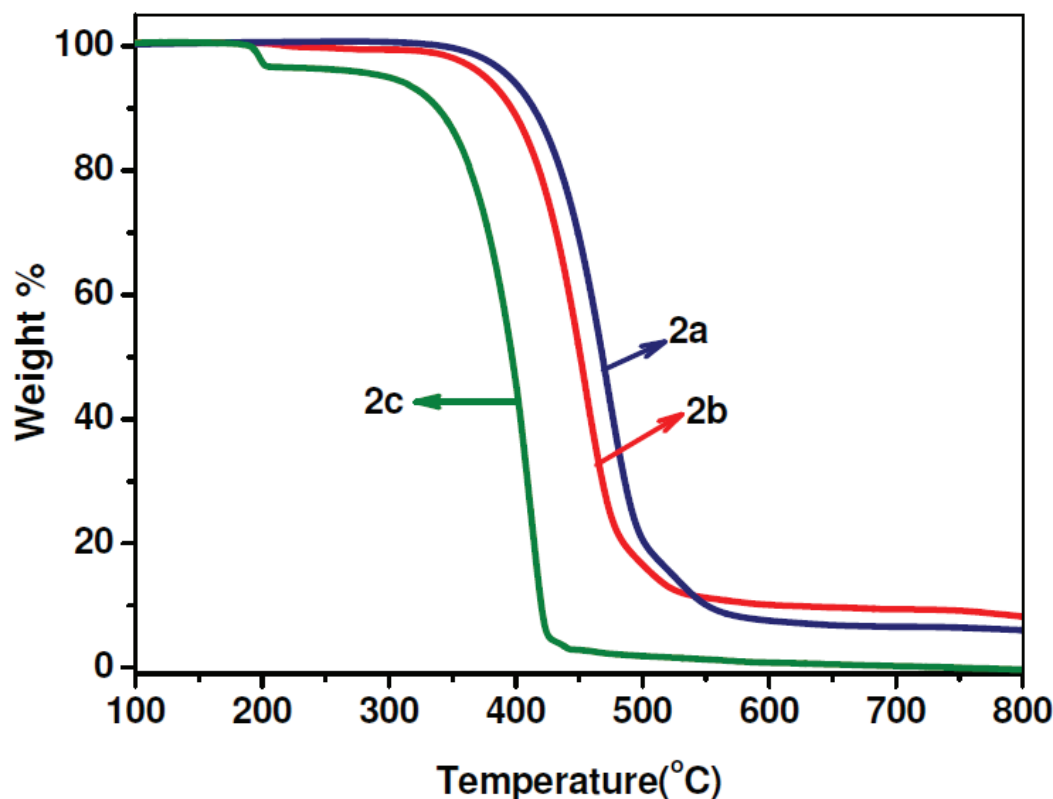


Figure 2A.7: TGA curves of **2a-2c** at a heating rate of 20 °C/min.

2A.2.5 Electrochemical studies

The electrochemical properties of complexes **2a-2c** were investigated by cyclic voltammetry in DMF solution using Bu_4NPF_6 as the electrolyte. Their cyclic voltammograms are shown in Figure 2A.8 and the relevant data are summarized in Table 2A.5. All three boron complexes exhibit one electron reduction. As compared to the reduction potential of boron complexes **2a** and **2b**, complex **2c** exhibits less reduction potential. The less reduction potential of **2c** can be attributed to electron withdrawing nature of $-\text{CF}_3$ moiety present in **2c**. The reduction potentials of our boron complexes (**2a-2c**) are comparable with those of the anilido-benzoxazole boron complexes reported by Lee and co-workers,³⁹ however notably highly negative than that of BODIPYs.⁴⁰

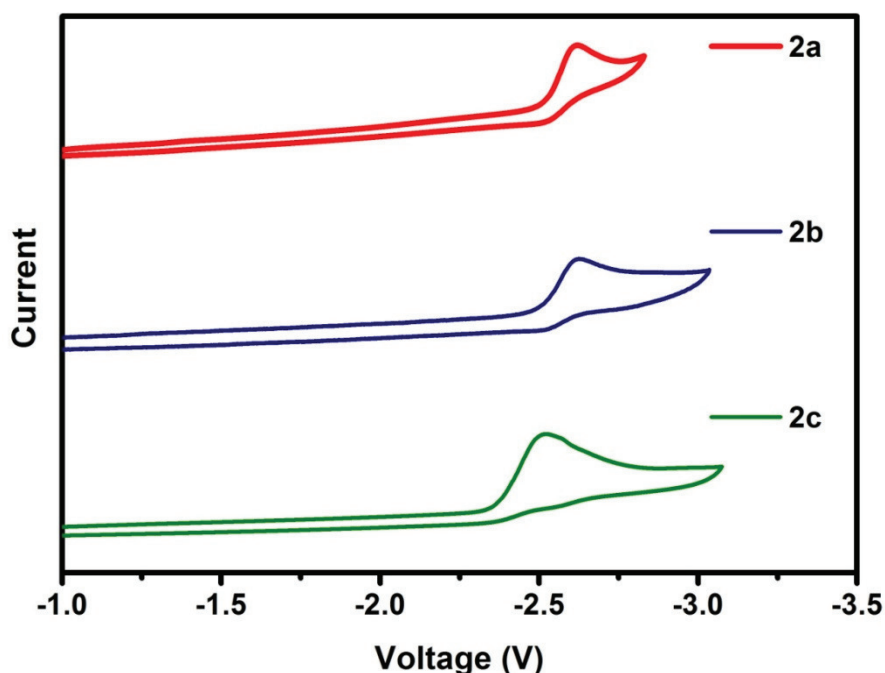


Figure 2A.8: Cyclic voltammograms of compounds **2a-2c** (vs. Ferrocene/Ferrocenium) with 0.1 M Bu₄NPF₆ in DMF as the supporting electrolyte (scan rate 100 mV/s)

Table 2A.5: Electrochemical data of compounds **2a-2c**.

Compound	Solvent	E _{pa} [#] (V)
2a	DMF	-2.62
2b	DMF	-2.59
2c	DMF	-2.43

E_{pa} = anodic peak potential

2A.2.5 Electroluminescent properties

To determine the electron transfer properties of the complexes (**2a-2c**) in polymer LEDs, we fabricated solution processed electrophosphorescent devices using a green phosphor, Ir(ppy)₃, as the dopant. Single layer devices with the configuration of ITO/PEDOT:PSS/PVK:Ir(ppy)₃ (8wt% - 16wt%): 2(40 wt%)/Mg/Ag were fabricated, where the ITO glass was used as a transparent anode; the conducting polymer poly(3,4-ethylenedioxythiophene):poly(styrenesulfonate) (PEDOT:PSS) was used as the hole-injection layer; poly(*N*-vinylcarbazole) (PVK) was used as the host

material; the electron-transporting material **2** was mixed into the host materials to promote electron transport in the emitting layer; $\text{Ir}(\text{ppy})_3$ with a concentration of 8 and 16 wt% was used as the emitter. Figure 2A.10 (a) shows the brightness-voltage (B - V) characteristics of the devices. According to the resulting characteristic curves, the turn-on voltages of **2a**, **2b**, and **2c** were 12.5 V, 23.5 V and 15 V, respectively (corresponding to 1 cd/m^2).

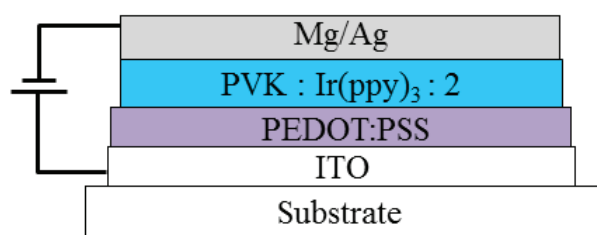


Figure 2A.9: Schematic illustration of EL device structure.

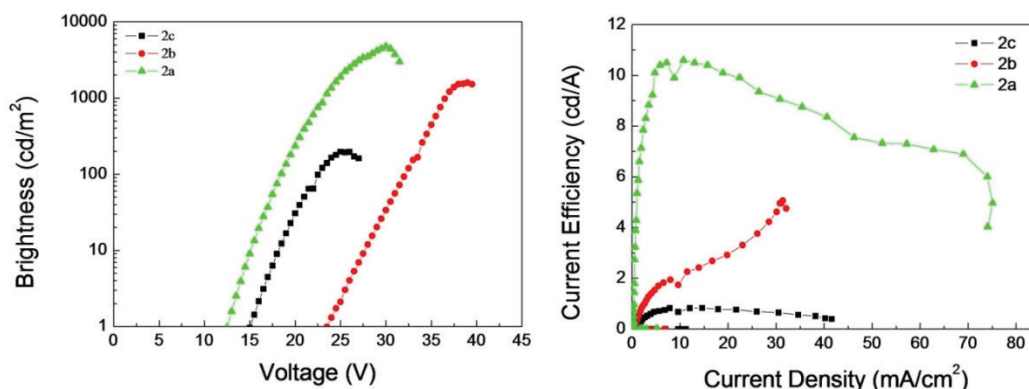


Figure 2A.10: EL characters of the device **2a-2c**. (left) brightness-voltage, (right) current efficiency-current density.

The maximum brightness obtained for **2a-2c** were 4760, 1600, and 200 cd/m^2 , respectively; and the highest current efficiency of 10.6, 5, and 0.8 cd/A respectively (Table 2A.6). The device characteristics suggest that the electron withdrawing groups (**2c**) are likely to prevent the current inject into the system and the electron donating group ($-\text{CH}_3$) of **2b** not only exhibits the poor efficiency but also reduces the brightness that attributed steric-hindrance to limit electron injection. To balance the hole and electron injection (compound **2a**), the amount of guest molecule ($\text{Ir}(\text{ppy})_3$)

was increased from 8 wt% to 16 wt%. The B - V curves of these two samples are summarized in Figure 2A.11 and Table 2A.7.

Table 2A.6: EL performances of the device **2a-2c**.

Device	Turn-on voltage at 1cd/m^2 (V)	Max. brightness (cd/m^2)	Efficiency ($\text{cd/A}/\text{voltage}(\text{v})$)
2a	12.5	4760	10.6
2b	23.5	1600	5
2c	15	200	0.8

The device with 16 wt% of guest molecule $\text{Ir}(\text{ppy})_3$ exhibits maximum brightness of 6450 cd/m^2 at 12.5 V, with maximum current efficiency ($\eta_{\text{c,max}}$) of 11.8 cd/A . The improved device performance may be attributed to the balanced recombination of holes and electrons.

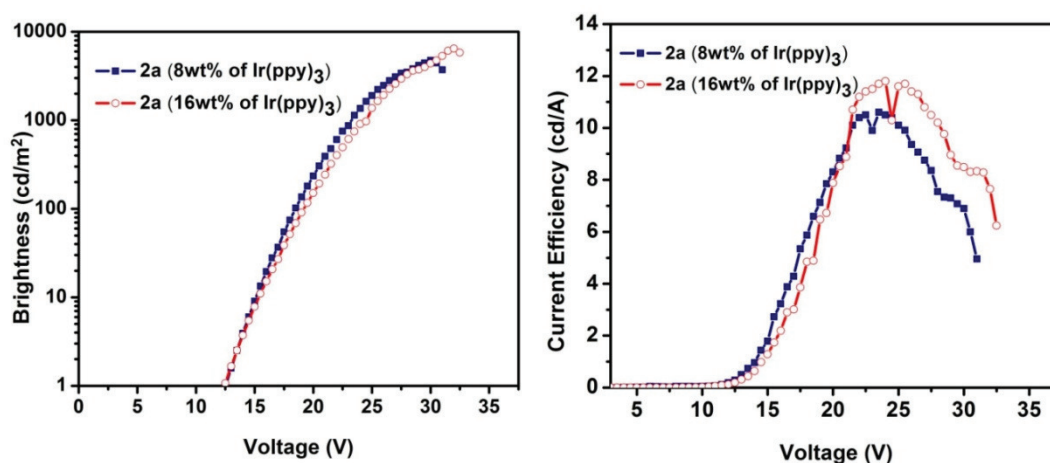


Figure 2A.11: EL performances of device **2a** that contain different ratio of guest. (left) brightness-voltage, (right) current efficiency-current density.

Table 2A.7: EL characters of the device **2a** that contain different ratio of guest.

Device	Turn-on voltage at 1cd/m^2 (V)	Max. brightness (cd/m^2)	Efficiency ($\text{cd/A}/\text{voltage}(\text{v})$)
2a (8 wt% of $\text{Ir}(\text{ppy})_3$)	12.5	4760	10.6
2a (16 wt% of $\text{Ir}(\text{ppy})_3$)	12.5	6450	11.8

2A.3 Conclusions

In summary, we have synthesized 2-(4,5-diphenyl-1-*p*-aryl-1H-imidazol-2-yl)phenol-based boron complexes (**2a-2c**) from the excited-state intramolecular, proton-transfer process celebrated tetraphenylimidazoles. We studied their photophysical, electrochemical and electroluminescence properties. All three new boron compounds showed intense blue emission in solution with good quantum yields and one electron electrochemical irreversible reduction. Furthermore these complexes also showed high thermal stability and also used as a electron-transporting material in single layer organic light emitting devices. With a doping concentration of 16 wt% (Ir(ppy)₃) boron complex **2a** exhibited a maximum brightness as high as 6450 cd/m² at 12.5V. We anticipate that our boron compounds have the potential to serve as electron-transporting material for further OLED applications.

2A.4 Experimental section

2A.4.1 General information

All reagents and starting materials were purchased from Sigma-Aldrich, Alfa-Aesar and Spectrochem chemical companies and used as received unless otherwise noted. Chlorinated solvents and acetonitrile were distilled from CaH₂. Tetrahydrofuran and toluene were distilled from Na/benzophenone prior to use. Tetraarylimidazoles (**1a-1c**) were prepared according to literature procedure.³⁵ All 400 MHz ¹H, 100 MHz ¹³C, 128 MHz ¹¹B, and 376 MHz ¹⁹F NMR spectra were recorded on a Bruker ARX 400 spectrometer operating at 400 MHz. All ¹H and ¹³C NMR spectra were referenced internally to solvent signals. ¹¹B NMR spectra were referenced externally to BF₃.Et₂O in CDCl₃ (δ = 0), ¹⁹F NMR spectra, to α,α,α-trifluorotoluene (0.05% in CDCl₃; δ = -63.73). All NMR spectra were recorded at ambient temperature. ESI mass spectra

were recorded on Bruker, microTOF-QII mass spectrometer. The absorbance spectra are recorded on a Perkin Elmer Lambda 750 UV–visible spectrometer. The fluorescence spectra are recorded on a Perkin Elmer LS-55 Fluorescence Spectrometer. The fluorescence spectra are corrected for the instrumental response. The quantum yield was calculated by measuring the integrated area under the emission curves and by using the following equation. $\Phi_{\text{sample}} = \Phi_{\text{standard}} \times (I_{\text{sample}}/I_{\text{standard}}) \times (\text{OD}_{\text{standard}}/\text{OD}_{\text{sample}}) \times (\eta_{\text{sample}}^2/\eta_{\text{standard}}^2)$ where, ‘ Φ ’ is the quantum yield, ‘I’ the integrated emission intensity, ‘OD’ the optical density at the excitation wavelength, and ‘ η ’ the refractive index of the solvent. The subscripts “standard” and “sample” refer to the fluorophore of reference and unknown respectively. In this case unknown is **2a-2c**, reference is quinine sulphate (quantum yield of quinine sulphate in 1 N H₂SO₄ is 0.55). Optically matched solutions with very similar optical densities of the “sample” and “standard” at a given absorbing wavelength were used for quantum yield calculations.

Elemental analyses were carried out by using a Thermo quest CE instrument model EA/110 CHNS-O elemental analyzer. Single-crystal X-ray diffraction data were collected on a Bruker APEX-II diffractometer equipped with an Oxford Instruments low-temperature attachment. The data were collected at 296 K (**2a**) and 100 K (**2c**) using, Mo-K α radiation (0.71073 Å). The structures were solved and refined with SHELX suite of programs. All non-hydrogen atoms were refined with anisotropic displacement coefficients. The H atoms were placed at calculated positions and were refined as riding atoms. DFT calculations were performed with the Gaussian03 program. The structures were optimized using 6-31G(d) (B3LYP) as the basis set. The input files were generated using X-ray data. Excitation data were determined using TD-DFT (B3LYP) calculations.

Cyclic voltammetry measurements were performed with a conventional three electrode cell using an electrochemical workstation (CH Instrument, Model: 1100A). The three-electrode system consisted of a Glassy carbon working electrode, a Pt wire as the secondary electrode, and a Ag wire as the reference electrode. The voltammograms were recorded with ca. 1.0×10^{-3} M solution in DMF containing Bu_4NPF_6 (0.1 M) as the supporting electrolyte. The scans were referenced after the addition of a small amount of ferrocene as the internal standard. Thermogravimetric analyses (TGA) were recorded on a PerkinElmer Pyris 6 TGA model in a nitrogen atmosphere at a heating rate of $20 \text{ }^\circ\text{C min}^{-1}$. Differential scanning calorimetric (DSC) analyses were recorded on a PerkinElmer Pyris 6 DSC model in a nitrogen atmosphere at a heating rate of $10 \text{ }^\circ\text{C min}^{-1}$. Electroluminescence properties were measured using a Minolta CS-100A instrument. The I - V and L - V characteristics of the devices were measured by integrating a Keithley 2400 source-meter as the voltage and current source and a Minolta CS100A instrument as the Luminance detector. All of the measurements and device fabrications were performed at room temperature in a dust-controlled environment.

Device Fabrication. The indium-tin oxide (ITO) glass plates were cleaned by sonication and rinsed in a series of solvents: the deionized water, Triton-100 water solution, deionized water, acetone, and then methanol. The solution composed of poly(ethylenedioxythiophene):poly(styrene sulfonic acid) (PEDOT:PSS) with Triton-100 (10:1 Vol.%) was spin-coated (5000 rpm, 60s) on top of the ITO substrates to form ca. 30 nm layer. The samples were then baked for 30 min at $130 \text{ }^\circ\text{C}$ under vacuum. Thin films of the emitting layer (EML) were made by spin casting the compounds dissolved in chloroform (10 mg/mL). These solutions were filtered using a membrane filter with the pore size of $0.45 \text{ } \mu\text{m}$. The thin film samples were then

thermally annealed in vacuum at 80 °C for 5 min. After cooling down to the room temperature, the substrate was transferred into a vacuum thermal evaporator. A 2 nm thick layer of Mg was deposited at a pressure below 2×10^{-6} torr through a mask. Another layer of 100 nm thick Ag was deposited as a protecting layer for Mg. The deposition rates for Mg and Ag cathodes were 1 and 4 Å/s, respectively, to form the active with an area of 0.126 cm². The thickness for each layer was measured by an Alpha step instrument.

2A.4.2 Synthetic procedure and spectral characterization

General procedure for the synthesis of tetraaryl imidazoles (1a-1c):

A mixture of benzil (1.0 equiv), substituted aniline (1.1 equiv), ammonium acetate (1.5 equiv, salicylaldehyde (1.0 equiv) and acetic acid was refluxed for 24 h. After the completion of the reaction, it was quenched by water and extracted with ethyl acetate (3 × 30 mL). The combined organic phases were washed with aqueous Na₂CO₃, water, brine and dried over Na₂SO₄. The solvent was removed under vacuum and the obtained solid was purified by silicagel column chromatography using *n*-hexane/EtOAc mixture as eluent.

2A.4.2.1 Synthesis of tetraaryl imidazole 1a

The quantities involved are as follows: Benzil (4.00 g, 19.02 mmol), aniline (1.90 g, 20.92 mmol), ammonium acetate (2.19 g, 28.54 mmol), salicylaldehyde (2.0 mL, 19.02 mmol) and acetic acid (20.00 mL). Yield: 4.40 g (80%). M.P: 238 °C. ¹H NMR (400 MHz, CDCl₃): δ = 6.49 (t, 1H, *J* = 8.0 Hz, ArH), 6.58 (d, 1H, *J* = 8.0 Hz, ArH), 7.11 (d, 1H, *J* = 8.2 Hz, ArH), 7.14 – 7.42 (m, 14H, ArH), 7.58 (d, 2H, *J* = 8.0 Hz, ArH) ppm. ¹³C NMR (100 MHz, CDCl₃): δ = 112.99, 117.88, 118.09, 126.33, 127.08, 128.60, 128.63, 128.74, 129.34, 129.70, 129.78, 130.20, 130.58, 131.44, 132.90, 135.05, 137.09, 144.97, 158.49

ppm. HR-MS (ESI): calcd. For $C_{27}H_{20}N_2O_1$ ($[M + H]^+$) : 389.1648, found : 389.1661.

2A.4.2.2 Synthesis of tetraaryl imidazole 1b

The quantities involved are as follows: Benzil (3.00 g, 14.27 mmol), *p*-toluidine (1.68 g, 15.69 mmol), ammonium acetate (1.64 g, 21.40 mmol), salicylaldehyde (1.52 mL, 14.27 mmol) and acetic acid (20.00 mL). Yield: 3.70 g (65%). M.P: 213 °C. 1H NMR (400 MHz, $CDCl_3$): δ = 2.39 (s, 3H, CH_3), 6.51 (t, 1H, J = 8.0 Hz, ArH), 6.62 (d, 1H, J = 8.2 Hz, ArH), 7.33 – 7.05 (m, 14H, ArH), 7.56 (d, 2H, J = 8.0 Hz, ArH). ^{13}C NMR (100 MHz, $CDCl_3$): δ = 21.39, 113.08, 117.89, 118.11, 126.40, 127.10, 127.22, 128.39, 128.42, 128.59, 129.85, 130.18, 130.33, 130.66, 131.46, 132.87, 134.38, 134.86, 139.40, 144.99, 158.48 ppm. HR-MS (ESI): calcd. for $C_{28}H_{22}N_2O_1$ ($[M + H]^+$) :403.1806, found : 403.1805.

2A.4.2.2 Synthesis of tetraaryl imidazole 1c

The quantities involved are as follows: Benzil (5.00 g, 23.78 mmol), 4-(trifluoromethyl)aniline (3.50 mL, 28.54 mmol), ammonium acetate (2.74g , 35.67 mmol), salicylaldehyde (2.50 mL, 23.78 mmol) and acetic acid (30.00 mL). Yield: 3.60 g (50%). M.P: 161 °C. 1H NMR (400 MHz, $CDCl_3$): δ = 6.45 (d, 2H, J = 4.2 Hz, ArH), 7.30 – 7.01 (m, 12H, ArH), 7.49 (d, 2H, J = 8.0 Hz, ArH), 7.56 (d, 1H, J = 8.2 Hz, ArH). ^{13}C NMR (100MHz, $CDCl_3$): 112.48, 118.07, 118.34, 119.48, 112.20, 124.91, 126.48, 126.80, 126.84, 127.15, 127.51, 128.50, 128.90, 129.05, 129.26, 130.30, 130.63, 130.87, 131.20, 131.39, 131.53, 131.86, 132.44, 135.59, 140.19, 144.95, 158.33 ppm. HR-MS (ESI): calcd. For $C_{28}H_{19}F_3N_2O_1$ ($[M + H]^+$) :457.1522, found :457.1571.

General procedure for the synthesis of imidazole boron difluoride complexes:

To a solution of imidazole (1 equiv) in anhydrous 1,2-dichloroethane under nitrogen, $\text{BF}_3 \cdot \text{Et}_2\text{O}$ (6 equiv) was added. After 5 minutes, diisopropylethylamine (DIEA) (6 equiv) was added and the resulting mixture stirred at 40 °C for 1 h. The crude solution was filtered through a column of basic Al_2O_3 , eluting with CH_2Cl_2 . The resulting solid was recrystallized using $\text{CH}_2\text{Cl}_2/n$ -hexane or CH_3CN to get pure product.

2A.4.2.1 Synthesis of boron difluoride complex 2a.

The quantities involved are as follows: Compound **1a** (2.00 g, 5.15 mmol), $\text{BF}_3 \cdot \text{Et}_2\text{O}$ (3.8 mL, 30.90 mmol) and diisopropylethylamine (5.34 mL, 30.90 mmol). Yield: 1.80 g (80%). mp: 301 °C. ^1H NMR (400 MHz, CDCl_3): δ = 6.44 (d, 1H, J = 8 Hz, ArH), 6.56 (t, 1H, J = 8 Hz, ArH), 6.93 (d, 2H, J = 8 Hz, ArH), 7.12-7.22 (m, 4H, ArH), 7.27-7.34 (m, 6H, ArH), 7.47-7.57 (m, 5H, ArH) ppm. ^{13}C NMR (100 MHz, CDCl_3): δ = 109.85, 119.15, 120.55, 124.87, 126.74, 128.24, 128.37, 128.44, 128.56, 129.01, 129.15, 130.47, 130.56, 130.75, 131.23, 132.42, 132.50, 133.13, 135.23, 156.81 ppm. ^{19}F NMR (376 MHz, CDCl_3): δ = -138.22 ppm. ^{11}B NMR (128 MHz, CDCl_3): δ = 1.17 (s) ppm. HR-MS (ESI): calcd. for $\text{C}_{27}\text{H}_{19}\text{B}_1\text{F}_2\text{N}_2\text{O}_1$ ($[\text{M}]^+$) : 436.1558, found : 436.1519. Elemental analysis calcd (%) for $\text{C}_{27}\text{H}_{19}\text{B}_1\text{F}_2\text{N}_2\text{O}_1$: C 74.33, H 4.39, N 6.42; found: C 74.20, H 4.28, N 6.29. IR (KBr): $\nu(\text{cm}^{-1})$ = 3056 (s), 1570 (m), 1503 (s), 1311 (m), 1266 (m), 1165 (m), 1150 (m), 1086 (m), 1053 (s), 921(m), 905 (s), 864 (m), 757 (m), 718 (m), 705 (m), 540 (m).

2A.4.2.2 Synthesis of boron difluoride complex 2b.

The quantities involved are as follows: Compound **1b** (1.50 g, 3.73 mmol), $\text{BF}_3 \cdot \text{Et}_2\text{O}$ (2.76 mL, 22.38 mmol) and diisopropylethylamine (3.87 mL, 22.38 mmol). Yield: 1.31 g (78%). mp: 274 °C. ^1H NMR (400 MHz, CDCl_3): δ = 2.44 (s, 1H, CH_3), 6.49 (d, 1H, J = 8 Hz, ArH), 6.58 (t, 1H, J = 8 Hz, ArH), 6.93 (d, 2H, J = 8 Hz, ArH), 7.12-7.24 (m, 6H, ArH), 7.28-7.33 (m, 6H, ArH), 7.50-7.53 (m, 2H, ArH). ^{13}C NMR (100 MHz, CDCl_3): δ = 21.40, 109.83, 118.99, 120.35, 124.79, 126.72, 128.09, 128.39, 128.82, 128.94, 130.44, 130.93, 131.11, 132.18, 132.43, 132.46, 132.91, 140.93, 141.38, 156.64 ppm. ^{19}F NMR (376 MHz, CDCl_3): δ = -138.24 ppm. ^{11}B NMR (128 MHz, CDCl_3): δ = 1.16 (s) ppm. HR-MS (ESI): calcd. for $\text{C}_{28}\text{H}_{21}\text{B}_1\text{F}_2\text{N}_2\text{O}_1$ ($[\text{M}]^+$) : 450.1714, found : 450.1687. Elemental analysis calcd (%) for $\text{C}_{28}\text{H}_{21}\text{B}_1\text{F}_2\text{N}_2\text{O}_1$: C 74.69, H 4.70, N 6.22; found: C 74.55, H 4.55, N 6.04. IR (KBr): $\nu(\text{cm}^{-1})$ = 3040 (m), 1610 (m), 1570 (m), 1497 (s), 1311 (m), 1267 (m), 1172 (m), 1051 (s), 904 (s), 855(m), 699 (m), 540 (m).

2A.4.2.3 Synthesis of boron difluoride complex 2c.

The quantities involved are as follows: Compound **1c** (1.60 g, 3.51 mmol), $\text{BF}_3 \cdot \text{Et}_2\text{O}$ (2.60 mL, 21.06 mmol) and diisopropylethylamine (3.64 mL, 21.06 mmol). Yield: 1.21 g (69%). mp: 288 °C. ^1H NMR (400 MHz, CDCl_3): δ = 6.42 (d, J = 8 Hz, 1H, ArH), 6.63 (t, J = 8 Hz, 1H, ArH), 6.94 (d, J = 8 Hz, 2H, ArH), 7.17-7.21 (t, J = 8 Hz, 3H, ArH), 7.27-7.37 (m, 5H, ArH), 7.45-7.52 (m, 4H, ArH), 7.77-7.79 (d, J = 8 Hz, 2H) ppm. ^{13}C NMR (100 MHz, CDCl_3): δ = 109.46, 119.34, 120.72, 121.92, 124.60, 126.23, 127.57, 127.61, 128.09, 128.24, 128.79, 129.13, 129.51, 130.45, 131.20, 132.33, 132.76, 132.97, 133.43, 138.34, 141.54, 156.85. ppm. ^{19}F NMR (376 MHz, CDCl_3): δ = -63.73 (s, CF_3), -138.30 (BF_2), ppm. ^{11}B NMR (128 MHz, CDCl_3): δ =

0.90 (s) ppm. HR-MS (ESI): calcd. for $C_{28}H_{18}B_1F_5N_2O_1$ ($[M]^+$): 504.1432, found : 504.1391. Elemental analysis calcd (%) for $C_{28}H_{18}B_1F_5N_2O_1$: C 66.69, H 3.60, N 5.56; found: C 66.53, H 3.48, N 5.50. IR (KBr): $\nu(\text{cm}^{-1}) = 3057$ (s), 1615 (m), 1575(m), 1502 (m), 1459(m), 1419 (m), 1386(m), 1323 (m), 1289 (m), 1266(s), 1154 (m), 907(m), 858 (m), 753 (m), 705 (m), 526 (m).

2A.5 References

- (1) Ostroverkhova, O. *Chem. Rev.***2016**, *116*, 13279.
- (2) Mishra, A.; Ma, C. Q.; Bäuerle, P. *Chem. Rev.***2009**, *109*, 1141.
- (3) Anthony, J. E. *Chem. Rev.***2006**, *106*, 5028.
- (4) Yamaguchi, S.; Fukazawa, A. *J. Synth. Org. Chem., Jpn.***2011**, *69*, 661.
- (5) Wu, B.; Yoshikai, N. *Organic & Biomolecular Chemistry***2016**, *14*, 5402.
- (6) Entwistle, C. D.; Marder, T. B. *Chem. Mater.***2004**, *16*, 4574.
- (7) Jäkle, F. *Coord. Chem. Rev.***2006**, *250*, 1107.
- (8) Wade, C. R.; Broomsgrove, A. E. J.; Aldridge, S.; Gabbai, F. P. *Chem. Rev.***2010**, *110*, 3958.
- (9) Ji, L.; Griesbeck, S.; Marder, T. B. *Chem. Sci.***2017**.
- (10) Li, D.; Zhang, H.; Wang, Y. *Chem. Soc. Rev.***2013**, *42*, 8416.
- (11) Rao, Y. L.; Wang, S. *Inorg. Chem.***2011**, *50*, 12263.
- (12) Frath, D.; Massue, J.; Ulrich, G.; Ziessel, R. *Angew. Chem. Int. Ed. Engl.***2014**, *53*, 2290.
- (13) Loudet, A.; Burgess, K. *Chem. Rev.***2007**, *107*, 4891.
- (14) Ulrich, G.; Ziessel, R.; Harriman, A. *Angew. Chem. Int. Ed.***2008**, *47*, 1184.
- (15) Ziessel, R.; Ulrich, G.; Harriman, A. *New J. Chem.***2007**, *31*, 496.
- (16) Lakshmi, V.; Ravikanth, M. *J. Org. Chem.***2011**, *76*, 8466.

- (17) Burghart, A.; Thoresen, L. H.; Chen, J.; Burgess, K.; Bergstrom, F.; Johansson, L. B. A. *Chem. Commun.***2000**, 2203.
- (18) Araneda, J. F.; Piers, W. E.; Heyne, B.; Parvez, M.; McDonald, R. *Angew. Chem. Int. Ed.***2011**, *50*, 12214.
- (19) Li, D.; Wang, K.; Huang, S.; Qu, S.; Liu, X.; Zhu, Q.; Zhang, H.; Wang, Y. *J. Mater. Chem.***2011**, *21*, 15298.
- (20) Liddle, B. J.; Silva, R. M.; Morin, T. J.; Macedo, F. P.; Shukla, R.; Lindeman, S. V.; Gardinier, J. R. *J. Org. Chem.***2007**, *72*, 5637.
- (21) Frath, D.; Azizi, S.; Ulrich, G.; Retailleau, P.; Ziesel, R. *Org. Lett.***2011**, *13*, 3414.
- (22) Qin, Y.; Kiburu, I.; Shah, S.; Jäkle, F. *Org. Lett.***2006**, *8*, 5227.
- (23) Suresh, D.; Gomes, C. S. B.; Gomes, P. T.; Di Paolo, R. E.; Macanita, A. L.; Calhorda, M. J.; Charas, A.; Morgado, J.; Teresa Duarte, M. *Dalton Trans.***2012**, *41*, 8502.
- (24) Maeda, C.; Todaka, T.; Ueda, T.; Ema, T. *Chem. - Eur. J.***2016**, *22*, 7508.
- (25) Qiu, F.; Zhang, F.; Tang, R.; Fu, Y.; Wang, X.; Han, S.; Zhuang, X.; Feng, X. *Org. Lett.***2016**, *18*, 1398.
- (26) Wang, X.; Wu, Y.; Liu, Q.; Li, Z.; Yan, H.; Ji, C.; Duan, J.; Liu, Z. *Chem. Commun.***2015**, *51*, 784.
- (27) Chang, M. C.; Chantzis, A.; Jacquemin, D.; Otten, E. *Dalton Trans.***2016**, *45*, 9477.
- (28) Zhang, P.; Liu, W.; Niu, G.; Xiao, H.; Wang, M.; Ge, J.; Wu, J.; Zhang, H.; Li, Y.; Wang, P. *J. Org. Chem.***2017**, *82*, 3456.
- (29) Grabarz, A. M.; Jędrzejewska, B.; Zakrzewska, A.; Zaleśny, R.; Laurent, A. D.; Jacquemin, D.; Ośmiałowski, B. *J. Org. Chem.***2017**, *82*, 1529.

- (30) Zhang, Z.; Wu, Z.; Sun, J.; Yao, B.; Xue, P.; Lu, R. *J. Mater. Chem. C*.**2016**, *4*, 2854.
- (31) Massue, J.; Frath, D.; Ulrich, G.; Retailleau, P.; Ziessel, R. *Org. Lett.***2012**, *14*, 230.
- (32) Massue, J.; Frath, D.; Retailleau, P.; Ulrich, G.; Ziessel, R. *Chem. Eur. J.***2013**, *19*, 5375.
- (33) Santra, M.; Moon, H.; Park, M. H.; Lee, T. W.; Kim, Y. K.; Ahn, K. H. *Chem. Eur. J.***2012**, *18*, 9886.
- (34) Lorbach, A.; Hübner, A.; Wagner, M. *Dalton Trans.***2012**, *41*, 6048.
- (35) Park, S.; Kwon, O. H.; Kim, S.; Park, S.; Choi, M. G.; Cha, M.; Park, S. Y.; Jang, D. J. *J. Am. Chem. Soc.***2005**, *127*, 10070.
- (36) Park, S.; Seo, J.; Kim, S. H.; Park, S. Y. *Adv. Funct. Mater.***2008**, *18*, 726.
- (37) Nayak, M. K. *J. Photochem. Photobiol., A*.**2012**, *241*, 26.
- (38) Benelhadj, K.; Massue, J.; Retailleau, P.; Ulrich, G.; Ziessel, R. *Org. Lett.***2013**, *15*, 2918.
- (39) Meesala, Y.; Kavala, V.; Chang, H.-C.; Kuo, T.-S.; Yao, C.-F.; Lee, W.-Z. *Dalton Trans.***2015**, *44*, 1120.
- (40) Nepomnyashchii, A. B.; Bard, A. J. *Acc. Chem. Res.***2012**, *45*, 1844.

CHAPTER 2B

Substituent variation at the *para*-position of 2-phenol of tetraaryl substituted imidazole boron difluoride complexes: Synthesis, characterization and photophysical properties

2B.1 Introduction	77
2B.2 Results and discussion	78
2B.2.1 Synthesis and characterization	78
2B.2.2 Single crystal X-ray analysis	80
2B.2.3 Photophysical studies	84
2B.2.4 Theoretical calculations	90
2B.2.5 Thermal studies	92
2B.2.6 Electrochemical studies	92
2B.3 Conclusions	93
2B.4 Experimental section	94
2B.4.1 General information	94
2B.4.2 Synthetic procedure and spectral characterization	96
2B.5 References	102

2B.1 Introduction

Fluorescent dyes based on pyridine, imidazole, pyrazine and oxadiazole have attracted interests owing to their applications in materials and biological chemistry. Among the different heterocycles, imidazoles and their derivatives have gained attraction primarily due to the fact that it is possible to use them in dye-sensitized solar cells, in the fabrication of light-emitting devices, as effective ambipolar materials and so on.¹⁻¹¹ Imidazoles containing 2-hydroxyphenyl exhibit excited state intramolecular proton transfer (ESIPT) processes. Taking advantage of these unique process new materials for optoelectronics, fluorescent probes and organic-light emitting diodes have been developed.¹²⁻²⁵ Tri- and tetra-coordinated boron fluorophores have been extensively studied for their potential application in various fields such as light-emitting diodes, non-linear optics, two-photon absorption and emission materials, fluoride and cyanide sensors.²⁶⁻⁴⁸ Complexation of boron with organic fluorophores results in new hybrid materials with different electronic and photophysical properties. In chapter 2A we describe the synthesis, photophysical and electrochemical properties of 2-(4,5-diphenyl-1-*p*-aryl-1H-imidazol-2-yl)phenol-based boron compounds⁴⁹ (Figure 2B.1 A). In an attempt to tune the photophysical properties of the imidazole complexes, we have attached different groups on the *para*-position of phenol (Figure 2B.1B). In this chapter we describe the substituent variation at the *para*-position of 2-phenol of tetraaryl substituted imidazole boron difluoride complexes and their photophysical and electrochemical properties.

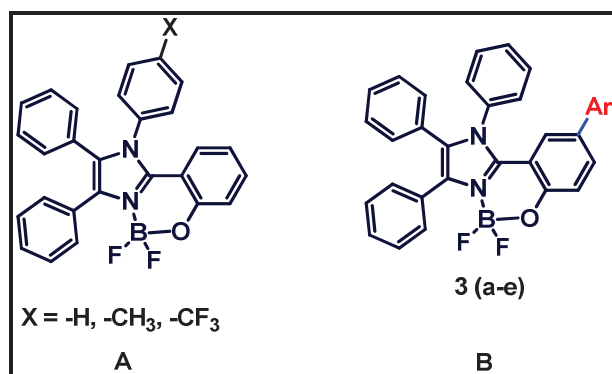
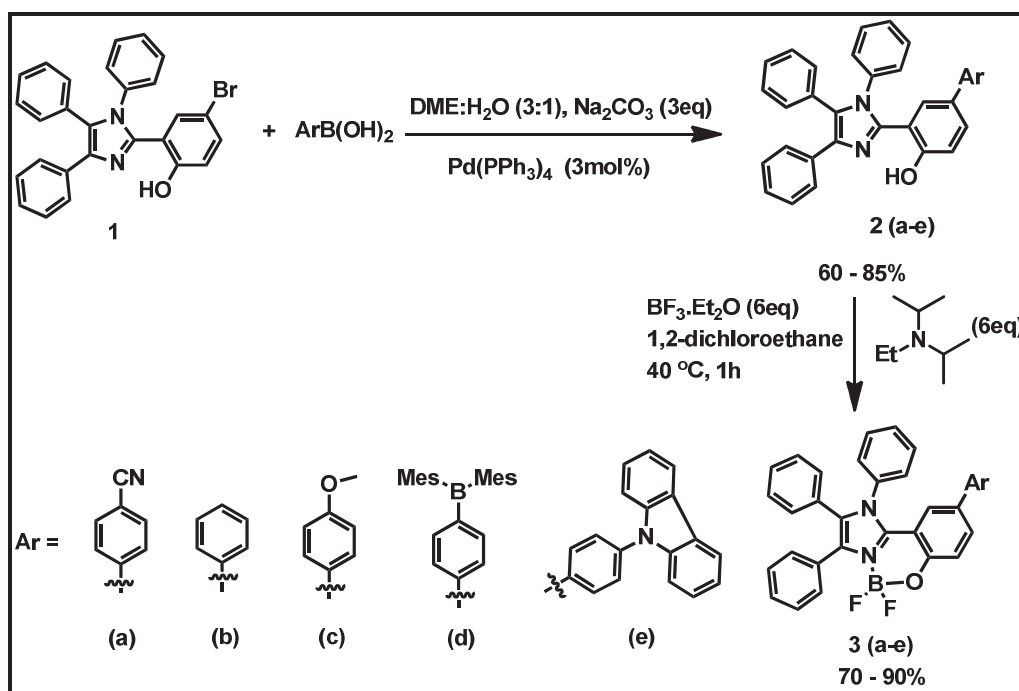


Figure 2B.1: Schematic representation of the skeleton of imidazole boron complexes.

2B.2 Results and discussion

2B.2.1 Synthesis and characterization

Scheme 2B.1 outlines the synthesis of imidazole boron complexes **3a-3e**.



Scheme 2B.1: Synthesis of imidazole boron complexes **3a-3e**.

The 4-bromo-2-(1,4,5-triphenyl-1H-imidazol-2-yl)phenol (**1**) was obtained in a one-step condensation reaction of benzil, 4-bromosalicylaldehyde, aniline with ammonium acetate in acetic acid at reflux in 80 % yield. Subsequent reaction of compound **1** with various arylboronic acids under Suzuki coupling reaction condition yielded the 2-

(1,4,5-triphenyl-1H-imidazol-2-yl)phenol derivatives with different substituents at the *para*-position of 2-phenol (**2a-2e**) in moderate yields.

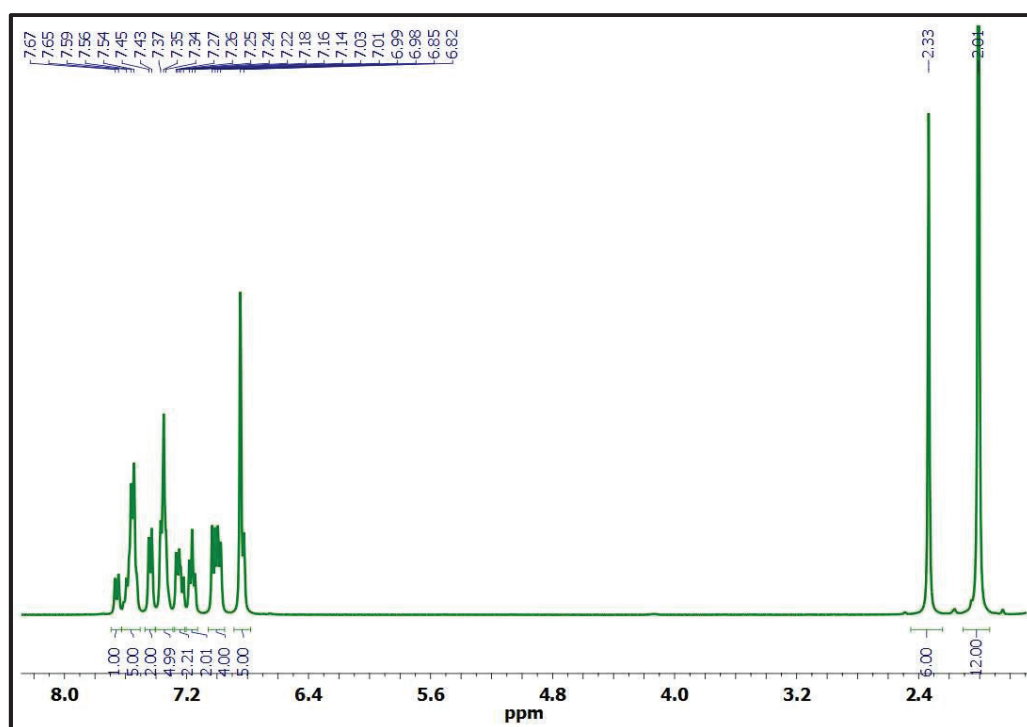


Figure 2B.2: ^1H NMR spectrum of compound **3d** recorded in CDCl_3 .

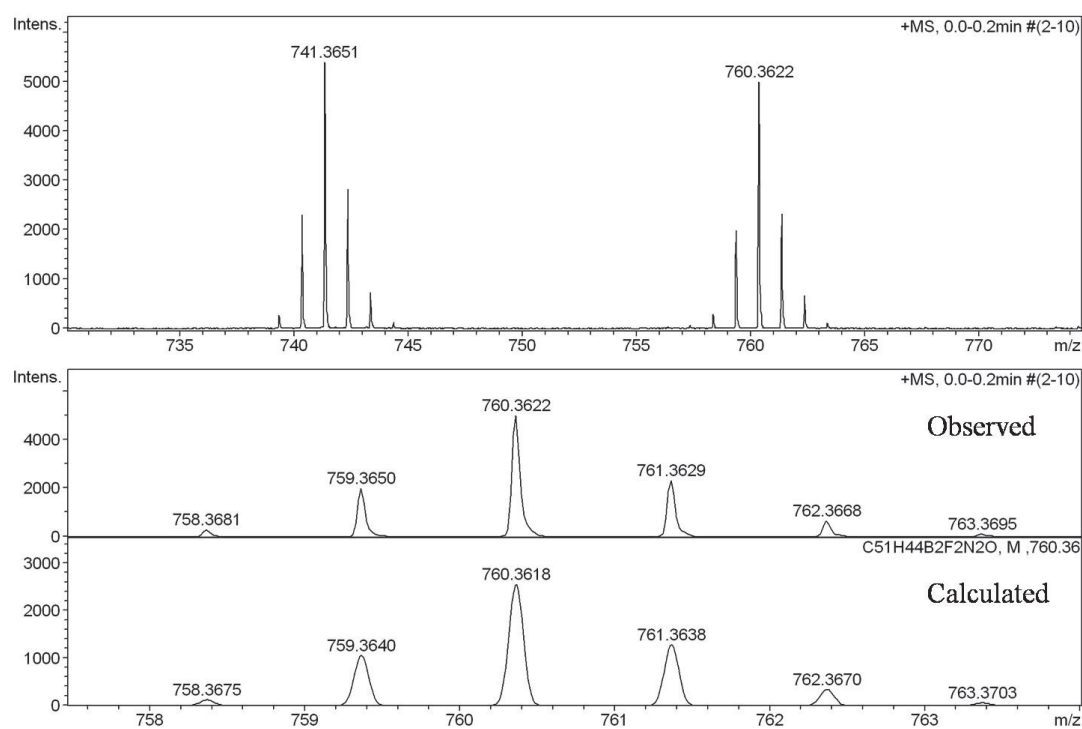


Figure 2B.3: HRMS of compound **3d**.

The treatment of compound **2a-2e** with excess amount of boron trifluoride etherate using diisopropylethylamine as a base in 1,2-dichloroethane at 40 °C resulted in imidazole boron complexes **3a-3e**, respectively in good yields. All imidazole-BF₂ complexes **3a-3e** were fully characterized by multinuclear (¹H, ¹³C, ¹¹B, ¹⁹F) NMR and high-resolution mass spectrometry (HRMS). The ¹¹B NMR spectra of complexes **3a-3e** show resonance around 1 ppm, which is characteristic of tetra-coordinated boron and the ¹⁹F chemical shifts appears around -139 ppm for the fluorine atoms attached to boron. A representative ¹H NMR spectrum and HRMS of compound **3d** is shown in Figure 2B.2 and 2B.3 respectively.

2B.2.2 Single crystal X-ray analysis

Single crystals of boron complexes **3a**, **3b**, **3d** and **3e** suitable for X-ray diffraction were grown by slow evaporation of respective dichloromethane/hexane solutions and determined by X-ray crystallography. The crystallographic data for **3a**, **3b**, **3d** and **3e** are given in Table 2B.3. Complexes **3a** and **3b** crystallized in monoclinic space group *P2₁/n*, whereas complexes **3d** and **3e** crystallized in monoclinic space groups *P2₁/c* and *C2/c* respectively. The molecular structures of **3a**, **3b**, **3d** and **3e** are shown in Figure 2B.4; selected bond lengths and bond angles are summarized Table 2B.1. The boron centre in all complexes is four coordinate and adopts a distorted tetrahedral geometry. Moreover, the six-membered ring constructed by the boron chelation takes a half chair conformation. In all compounds the boron atom deviates from the six-membered plane defined by C₃NOB (Nitrogen, boron, oxygen, C₂ carbon atoms and phenyl carbons directly attached to oxygen and C₂ carbon); the distance ranging from 0.002 to 0.37 Å (Table 2B.2). The B-N, B-F and B-O bond lengths and bond angles are comparable to other organoboron compounds reported in the literature.⁴⁹⁻⁵²

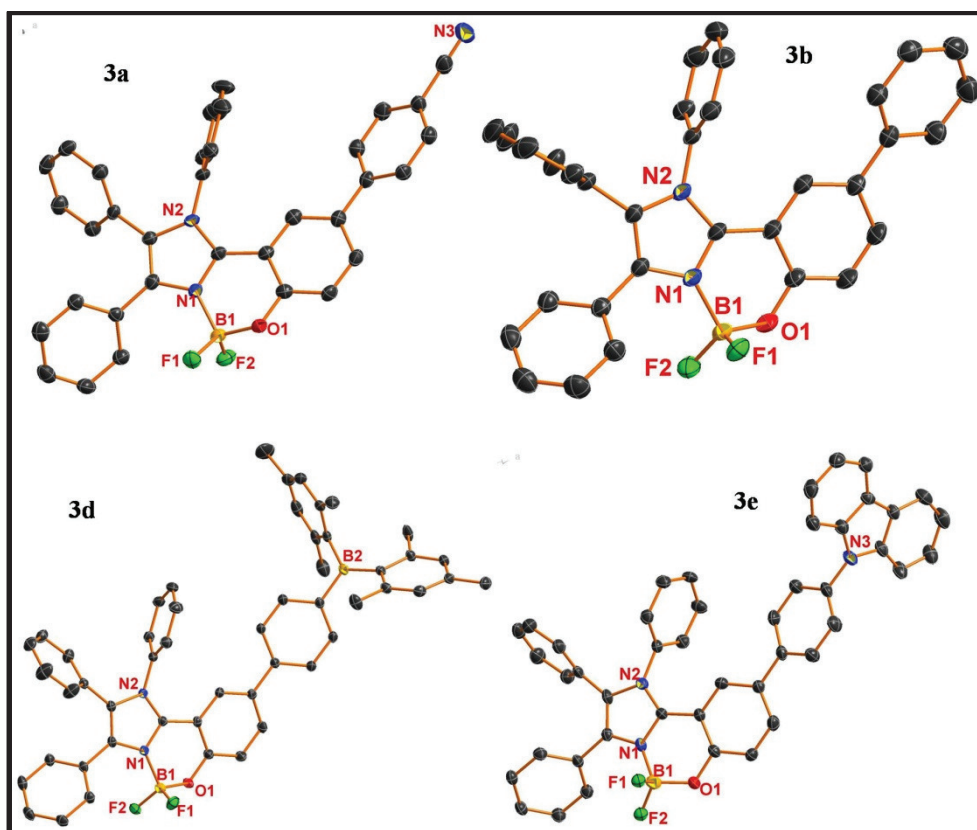
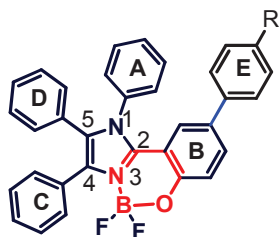


Figure 2B.4: Molecular structures of **3a**, **3b**, **3d** and **3e**. Hydrogen atoms and Co-crystallized solvent molecules are omitted for clarity. Thermal ellipsoids are shown at the 50% probability level for **3a**, **3d**, **3e** and 30% for **3b**.

Table 2B.1: Comparison of some selected bond lengths [Å] and bond angles [deg] for compounds **3a**, **3b**, **3d** and **3e**.

	3a	3b	3d	3e
B1-F1	1.370(5)	1.381(2)	1.384(3)	1.397(4)
B1-F2	1.389(4)	1.370(2)	1.376(3)	1.380(4)
B1-O1	1.448(5)	1.441(2)	1.445(4)	1.438(4)
B1-N1	1.576(5)	1.582(18)	1.589(3)	1.599(5)
F1-B1-F2	111.1(3)	110.95(15)	110.53(19)	109.6(3)
F1-B1-O1	109.1(3)	110.76(13)	111.22(19)	112.3(3)
F2-B1-O1	110.8(3)	109.03(14)	108.22(19)	108.9(3)
F1-B1-N1	110.4(3)	108.2(13)	108.59(18)	107.2(3)
F2-B1-N1	107.0(3)	109.48(12)	109.93(18)	111.4(3)
O1-B1-N1	108.5(3)	108.37(13)	108.32(17)	107.5(3)

Table 2B.2: Comparison of deviation of boron atom from C₃NBO plane [Å] and interplanar angles [deg] for compounds **3a**, **3b**, **3d** and **3e**.

	3a	3b	3d		3e	
			Molecule 1	Molecule 2	Molecule 1	Molecule 2
Deviation of B from C ₃ NBO plane (Å)	0.238	-0.236	0.237	-0.255	0.372	-0.002
Imidazole//plane B (°)	9.49	12.95	9.39	13.18	9.94	6.18
Imidazole //plane A (°)	70.76	88.35	82.42	79.46	77.32	83.34
Imidazole //plane D (°)	52.75	79.52	54.74	57.40	65.10	65.76
Imidazole //plane C (°)	43.52	38.74	49.22	67.80	51.17	74.64
Plane B//plane E (°)	29.95	23.19	24.39	20.42	23.53	24.10

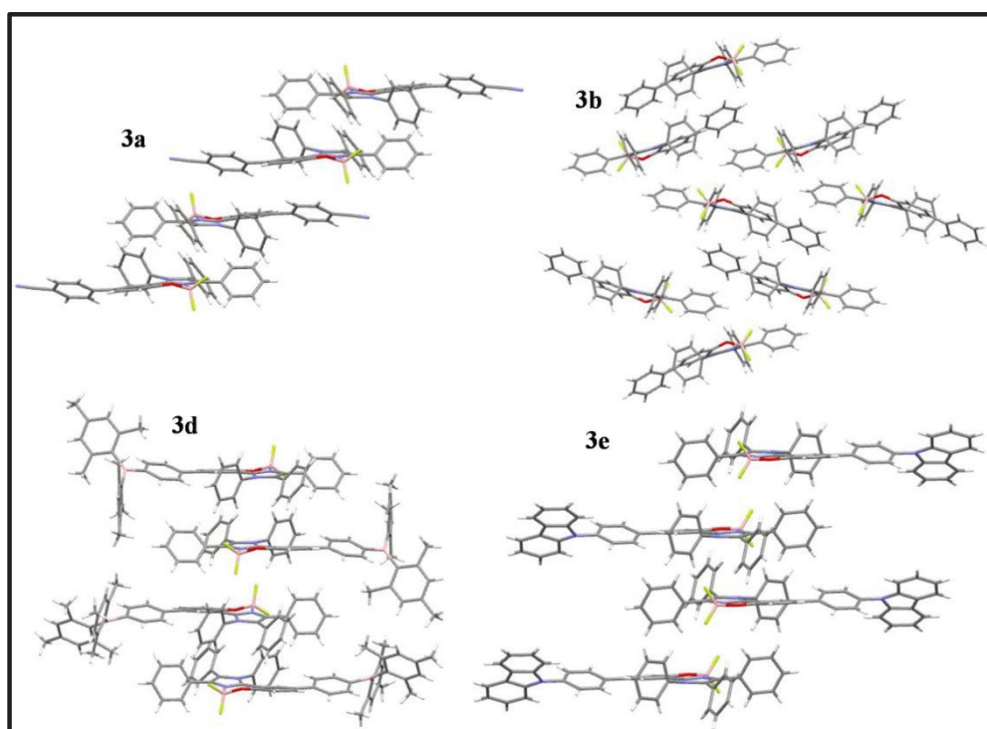
**Figure 2B.5.** Crystal-packing of **3a**, **3b**, **3d** and **3e**.

Table 2B.3: Crystal data and structure refinement parameters for compounds **3a**, **3b**, **3d** and **3e**.

Compound	3a	3b	3d	3e
Empirical formula	C ₃₄ H ₂₂ N ₃ OB F ₂	C ₃₃ H ₂₃ N ₂ OB F ₂	C ₅₂ H ₄₆ N ₂ OB ₂ F ₂ Cl ₂	C ₉₁ H ₆₂ N ₆ O ₂ B ₂ F ₄ Cl ₂
Formula weight	537.35	512.34	845.43	1439.98
Temperature/K	100	296.15	100.0	296.15
Crystal system	Monoclinic	Monoclinic	Monoclinic	Monoclinic
Space group	<i>P2₁/n</i>	<i>P2₁/n</i>	<i>P2₁/c</i>	<i>C2/c</i>
a/Å	13.4252(6)	10.9638(2)	16.1027(5)	48.841(3)
b/Å	11.5028(5)	12.5643(3)	38.6393(13)	9.7377(6)
c/Å	18.4940(9)	19.3445(5)	14.8231(5)	37.599(3)
α /°	90	90	90	90
β /°	105.659(3)	97.6660(10)	99.368(2)	127.547(8)
γ /°	90	90	90	90
Volume/Å ³	2750.0(2)	2640.94(10)	9099.9(5)	14178(2)
Z	4	4	8	8
ρ_{calcd} /g cm ⁻³	1.298	1.289	1.234	1.349
μ (MoK α)/mm ⁻¹	0.088	0.087	0.191	0.160
<i>F</i> (000)	1112.0	1064.0	3536.0	5968.0
2 θ range for data collection/°	4.216 to 51.566	6.826 to 61.044	2.978 to 52.11	2.21 to 51.572
Index ranges	-16 ≤ <i>h</i> ≤ 15, -14 ≤ <i>k</i> ≤ 14, -22 ≤ <i>l</i> ≤ 22	-14 ≤ <i>h</i> ≤ 15, -17 ≤ <i>k</i> ≤ 17, -27 ≤ <i>l</i> ≤ 27	-19 ≤ <i>h</i> ≤ 19, -47 ≤ <i>k</i> ≤ 47, -18 ≤ <i>l</i> ≤ 18	-59 ≤ <i>h</i> ≤ 58, -11 ≤ <i>k</i> ≤ 11, -45 ≤ <i>l</i> ≤ 46
Reflns. collected	31255	45581	101801	67633
Independent reflns	5248 [<i>R</i> _{int} = 0.1060, <i>R</i> _{sigma} = 0.0783]	7998 [<i>R</i> _{int} = 0.0566, <i>R</i> _{sigma} = 0.0406]	17908 [<i>R</i> _{int} = 0.0704, <i>R</i> _{sigma} = 0.0484]	13524 [<i>R</i> _{int} = 0.1013, <i>R</i> _{sigma} = 0.0986]
Data/restraints/ parameters	5248/0/370	7998/0/352	17908/0/1112	13524/0/965
GOF on <i>F</i> ²	1.139	1.007	1.074	1.009
Final <i>R</i> indices [<i>I</i> > 2 σ (<i>I</i>)]	<i>R</i> ₁ = 0.0690, <i>wR</i> ₂ = 0.1757	<i>R</i> ₁ = 0.0472, <i>wR</i> ₂ = 0.1092	<i>R</i> ₁ = 0.0552, <i>wR</i> ₂ = 0.1499	<i>R</i> ₁ = 0.0619, <i>wR</i> ₂ = 0.1469
<i>R</i> indices (all data)	<i>R</i> ₁ = 0.1129, <i>wR</i> ₂ = 0.2004	<i>R</i> ₁ = 0.1021, <i>wR</i> ₂ = 0.1324	<i>R</i> ₁ = 0.0811, <i>wR</i> ₂ = 0.1632	<i>R</i> ₁ = 0.1307, <i>wR</i> ₂ = 0.1842
Largest diff. peak /hole [e Å ⁻³]	0.34/-0.44	0.19/-0.20	0.92/-0.70	1.02/-0.58

The interplanar angle between the imidazole and the phenolate (Plane B) is 13.0 ° (for **3b**), 9.5 ° (**3a**), 9.4 ° & 13.2 ° (for **3d**) and 9.9 ° & 6.2 ° (for **3e**) which indicates that the imidazole and the phenolate skeleton is distorted. The interplanar angle between the imidazole and the phenyl rings (Plane A, C&D) at 1, 4 & 5 varies from 38.74 ° to

88.35 ° (Table 2B.2). The molecular packings of compound **3a**, **3b**, **3d** and **3e** are shown in Figure 2B.5.

2B.2.3 Photophysical studies

The photophysical properties of the boron complexes were investigated in five different solvents (Toluene, THF, CH₂Cl₂ and CH₃CN) of varying polarity by means of UV-Vis and fluorescence spectroscopy and the relevant data are summarized in Table 2B.4. A comparison of absorption and fluorescence spectra of the compounds **3a-3e** in dichloromethane is shown in Figure 2B.6. The absorption spectra of these complexes are comprised between 250-388 nm. Emission spectra were recorded by exciting at longer wavelength absorption maxima of these complexes in their respective solvents. Both absorption and emission profiles of compounds **3a-3e** were insensitive or little changes were observed by varying the solvent polarity. The emission and absorption maximum of compounds with electron donating groups or with greater extended degrees of π -conjugation exhibits slight red shift relative to that of compounds with electron withdrawing groups. Compounds **3a-3e** exhibited bright blue fluorescence (Figure 2B.7) with moderate quantum yields in dichloromethane solution where as the quantum yield of compound **3d** was high (Table 2B.4). In addition, all these compounds **3a-3e** also exhibit solid state emission with moderate quantum yields. Two emission bands were observed for compounds **3a-3d** and one broad emission band was observed for compound **3e** (Figure 2B.8). The higher energy band in **3a-3d** is similar to the band observed in solution which can be ascribed to the monomer emission. To determine the nature of emission observed for compounds **3a-3d** in the lower energy, we recorded emission spectra and powder XRD of the as prepared material, mechanically ground powder and fumed with dichloromethane samples.

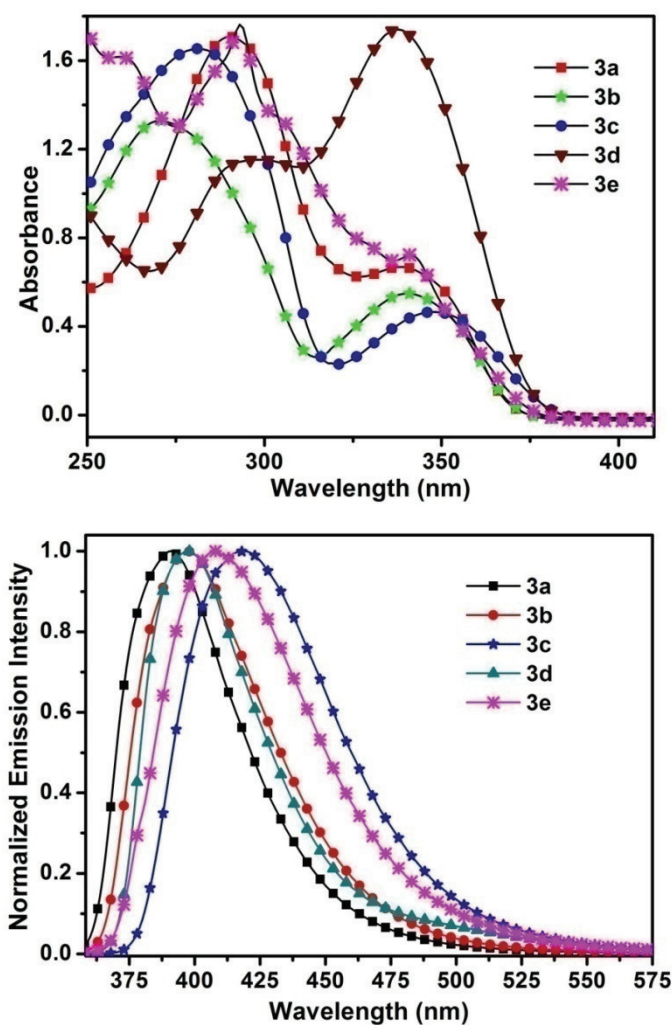


Figure 2B.6: (top) UV-Vis absorption spectra of **3a-3e** in CH₂Cl₂ (concentration = 4 × 10⁻⁵ M); (bottom) Normalized fluorescence spectra of **3a-3e** in CH₂Cl₂ (concentration = 4 × 10⁻⁵ M).

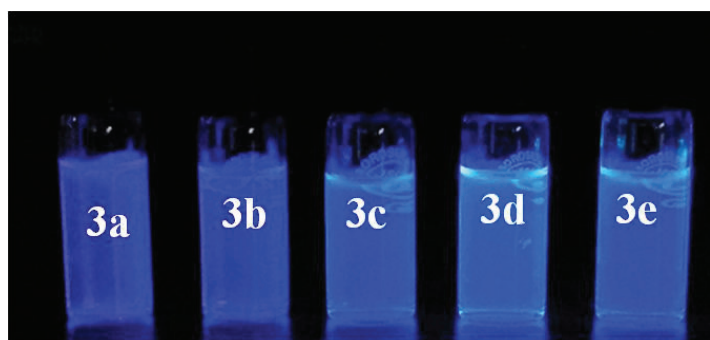


Figure 2B.7: The fluorescence photograph of compounds **3a-3e** in dichloromethane solution under UV excitation (λ_{ex} = 365 nm).

Table 2B.4: Photophysical data of the imidazole based boron compound **3a-3e**.

Compound	Solvent	$\lambda_{\text{abs}}^{\text{a}}/\text{nm}$ ($\epsilon_{\text{max}} \times 10^3/\text{M}^{-1} \text{cm}^{-1}$)	$\lambda_{\text{em}}^{\text{a,b}}/\text{nm}$	τ (ns)	$\Phi_{\text{F}}^{\text{c}}$
3a	Toluene	342 (13.7), 292 (30.9)	395	1.81	0.52
	THF	340 (16.0), 290 (39.3)	393	1.89	0.44
	CH ₂ Cl ₂	338 (16.7), 289 (42.7)	391	1.76	0.45
	CH ₃ CN	334 (16.2), 288 (42.3)	387	1.95	0.39
	Solid	360	398/461	0.59/4.61	0.39 ^d
3b	Toluene	343 (13.9), 283 (28.4)	400	1.60	0.29
	THF	341 (12.7), 272 (30.9)	398	1.66	0.27
	CH ₂ Cl ₂	340 (13.6), 269 (33.2)	397	1.58	0.26
	CH ₃ CN	336 (12.5), 268 (30.8)	395	1.74	0.30
	Solid	360	397/448	1.06/3.62	0.25 ^d
3c	Toluene	351 (09.5), 285 (29.4)	417	2.00	0.33
	THF	348 (10.4), 280 (35.5)	418	2.16	0.25
	CH ₂ Cl ₂	347 (11.7), 281 (41.3)	419	2.12	0.26
	CH ₃ CN	344 (10.5), 280 (0.37)	419	2.37	0.20
	Solid	381	420/475	1.43/3.43	0.17 ^d
3d	Toluene	342 (41.9), 295 (25.3)	400	1.83	0.76
	THF	341 (43.7), 293 (27.5)	399	1.69	0.64
	CH ₂ Cl ₂	337 (43.5), 294 (28.7)	397	1.88	0.63
	CH ₃ CN	336 (45.6), 295 (30.3)	407	1.87	0.71
	Solid	375	405/472	0.9/1.97	0.41 ^d
3e	Toluene	342 (18.0), 294 (41.7)	407	2.08	0.42
	THF	341 (19.5), 293 (47.1)	407	2.27	0.30
	CH ₂ Cl ₂	341 (18.0), 293 (44.0)	408	2.41	0.31
	CH ₃ CN	340 (20.3), 292 (48.9)	408	3.34	0.23
	Solid	376	423	2.11/3.1	0.21 ^d

^aLowest-energy absorption maximum (Concentrations in solutions were 4.00×10^{-5} M). ^b Excited at the longer wavelength absorption maximum. ^c Fluorescence quantum yields were measured using quinine sulphate as the reference. ^d Absolute solid state fluorescence quantum yields were measured by integrating sphere method.

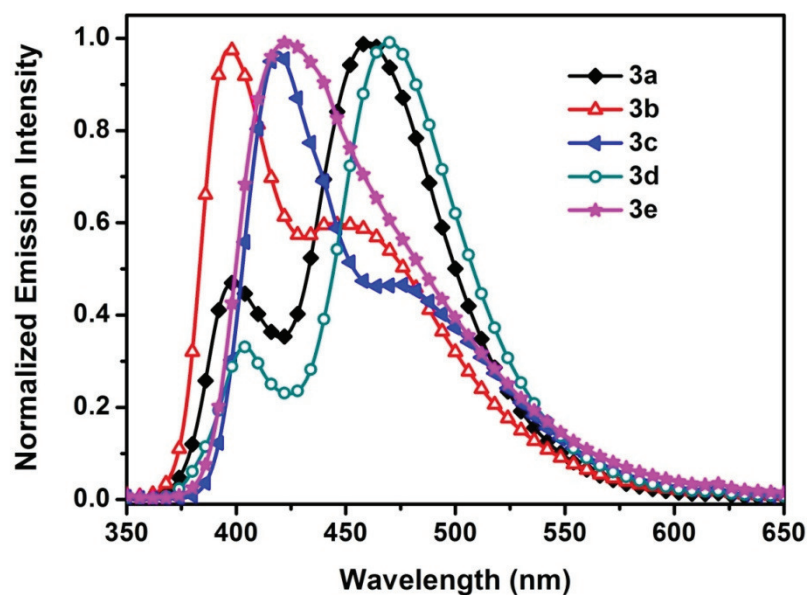


Figure 2B.8: Fluorescence spectra of 3a-3e in the solid state.

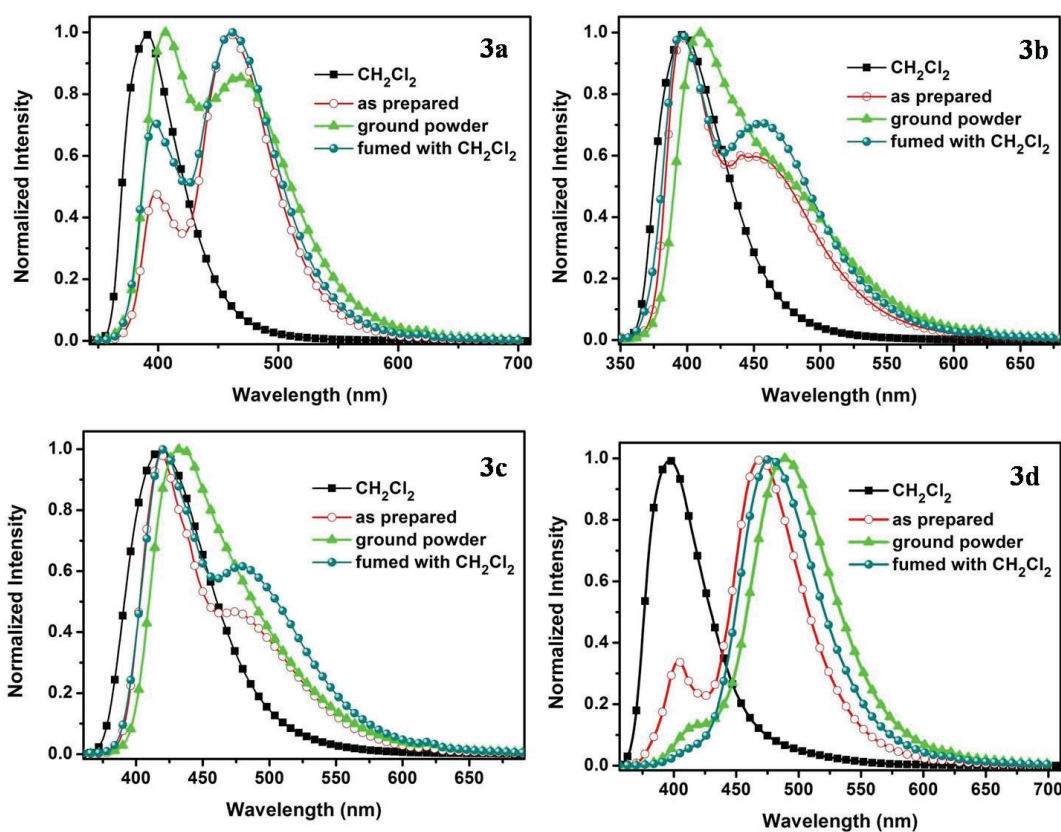


Figure 2B.9: Fluorescence spectra of compound 3a, 3b, 3c and 3c in different solid state ($\lambda_{\text{ex}} = 340 \text{ nm}$).

As shown in Figure 2B.9, compounds 3b and 3c exhibit only one broad emission band centred at 409 nm and 433 nm respectively for their ground powders. Upon

fuming with dichloromethane the lower energy band got recovered. Furthermore, we recorded powder XRD pattern of **3b** and **3c** of as prepared materials.

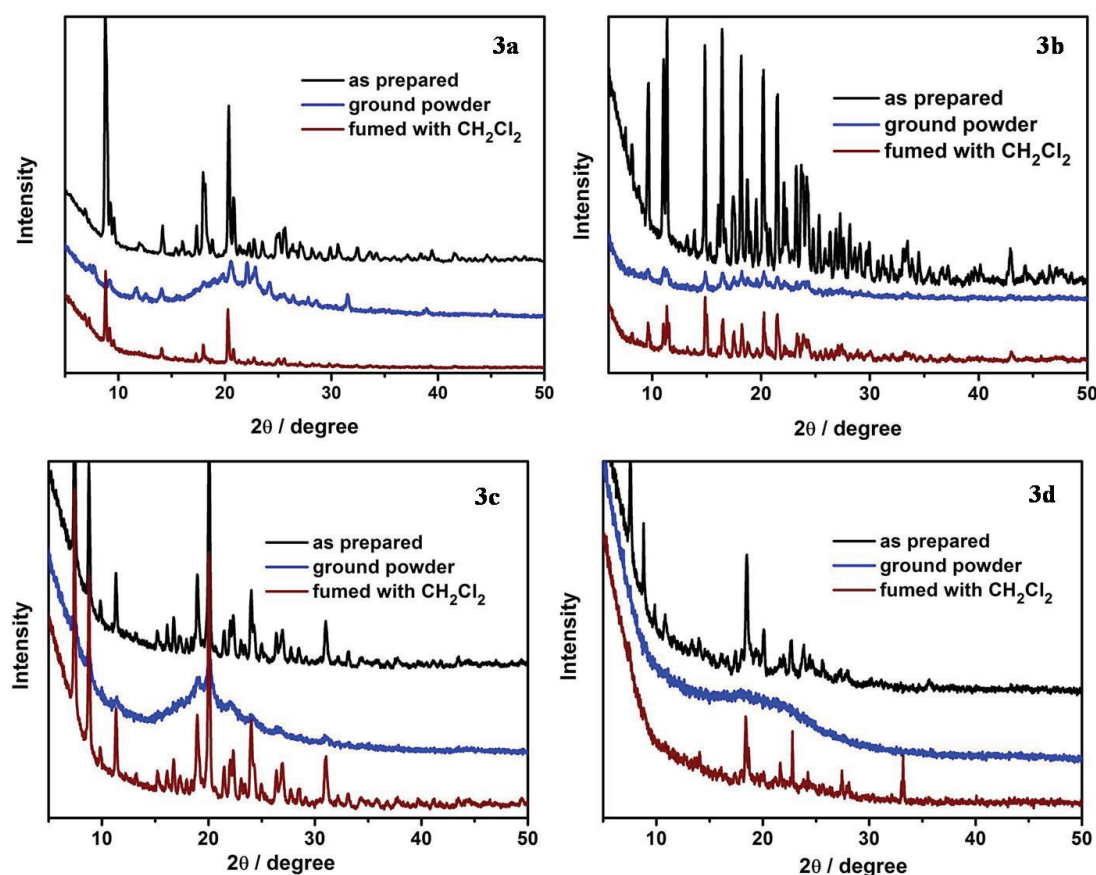


Figure 2B.10: X-ray diffraction patterns of different solids of compound **3a**, **3b**, **3c** and **3d**.

As shown in Figure 2B.10, the as prepared materials exhibit sharp diffraction peaks owing to the crystalline order present in the materials. When the as prepared materials were ground to powder, the diffraction peaks became weak or otherwise turned to amorphous. It should be noted that the XRD pattern was regained after fuming the samples with dichloromethane for 2 minutes. Moreover we also measured the fluorescence decay lifetimes of **3b** and **3c**. The as prepared material at 397 nm for **3b** and 420 nm for **3c** gave a life time of 1.06 ns and 1.43 ns respectively that is similar to the emission life time of 1.58 ns and 2.12 ns for **3b** and **3c** in dilute dichloromethane. However, the life time for the lower energy band at 448 nm for

3b band 475 nm for **3c** were comparatively longer (3.62 ns for **3b** and 3.43 ns for **3c**) and can be assigned to the emission of excimers. Hence, emission intensity at 448 nm and

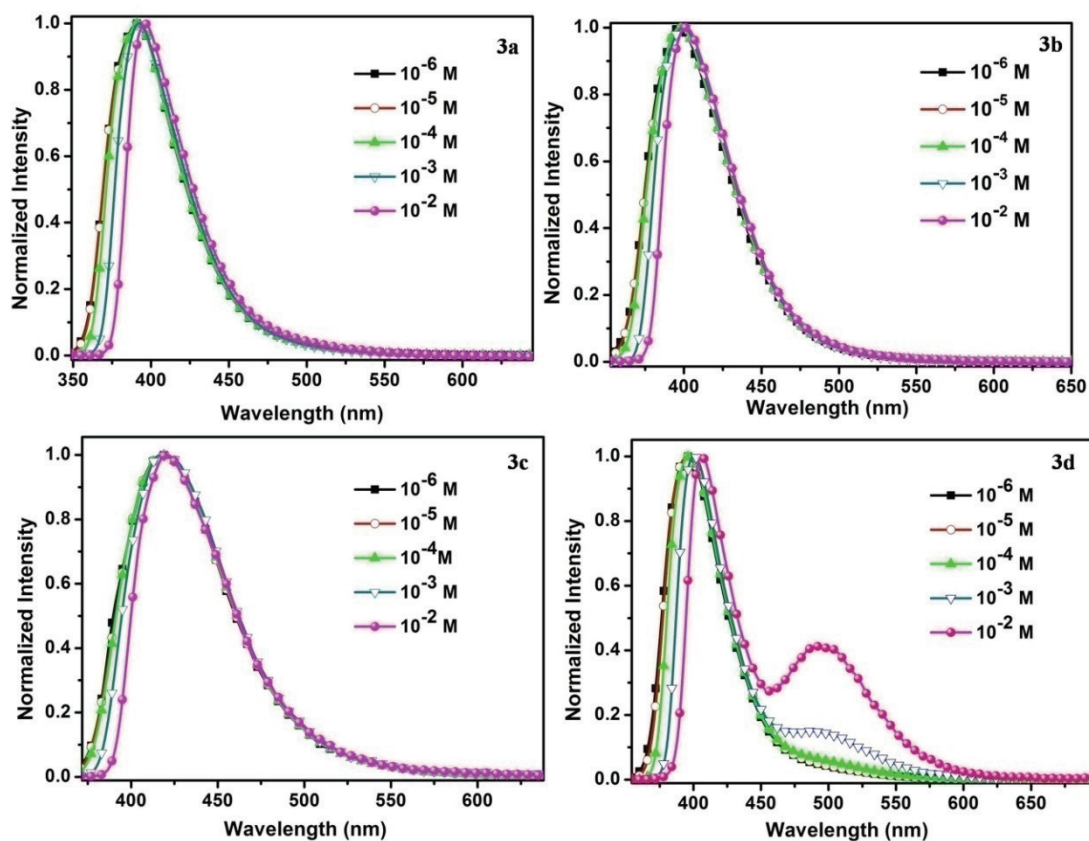


Figure 2B.11: Fluorescence spectra of compounds **3a**, **3b**, **3c** and **3d** recorded at various concentrations in tetrahydrofuran (THF) (excited at λ_{max}).

475 nm owing to the excimers decreased and only one broad emission band centred at 409 and 433 nm emerged in the ground powder and the phenomenon can be regained or reversed by fuming with dichloromethane. Although, similar morphology and molecular structure dependent solid state fluorescence properties were observed for compound **3a** the excimer formation is dominant over the monomer (Figure 2B.9). However, compound **3d** showed a slightly different phenomenon. The as prepared and grounded material of **3d** gave emission at lower energy irrespective of crystalline and amorphous state (Figure 2B.9). To verify the nature of the emission observed for compound **3d**, the fluorescence spectra of **3d** in THF with different concentrations

were measured. As shown in Figure 2B.11, the emission is dependent on the concentration; the low energy band intensity increases with increase in concentration. Moreover, compounds **3a**, **3b** and **3c** do not show any appreciable change in emission maxima with increase in concentration (Figure 2B.11). Thus in compounds **3a** and **3d**, the excimer emission is dominant and difficult to convert the same to monomer emission using mechanical grinding however in compound **3b** and **3c** the monomer emission is dominant. Use of mechanical force the excimer emission can be converted to the monomer emission in compounds **3b** and **3c**. However, in case of compound **3e** mostly monomer emission is prevalent in both solutions as well as in the solid state.

2B.2.4 Theoretical calculations

To further understand the electronic properties of the boron compounds **3a-3e**, we carried out density functional (DFT) calculations. As shown in Figure 2B.12, the HOMO of boron complexes **3a-3e** is mainly concentrated on biphenyl and imidazole core where as the LUMO is distributed on one of the phenyl rings of biphenyl and 1,5-phenyl rings in case of **3a**, **3b**, **3c** and **3e**, however in compound **3d** the LUMO is spread out over the biphenyl, boron and phenyl rings attached to boron atom. Compounds with electron withdrawing group on the *para*-position of biphenyl (**3a** & **3d**) show a significant decrease in the HOMO energy with respect to compound **3b**; whereas compound **3c** with electron donating group shows slight increase in the HOMO energy. The HOMO-LUMO gap in **3d** is lower than in **3b** due to lowering of LUMO level where as in **3c** increase in the HOMO-LUMO gap is realised. The former is possibly a result of overlap between the biphenyl π -system and the tri-coordinate boron centre.

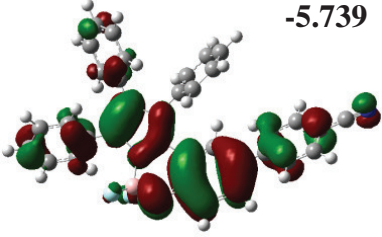
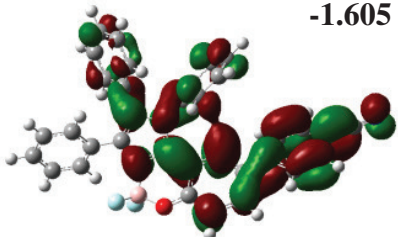
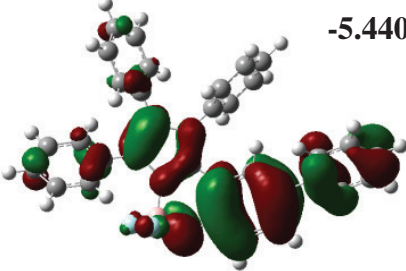
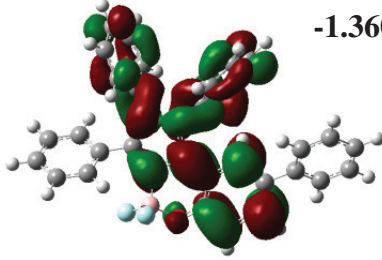
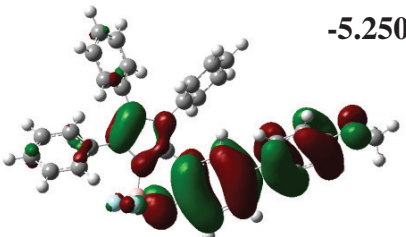
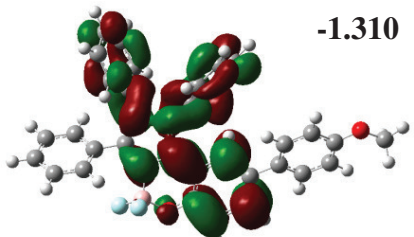
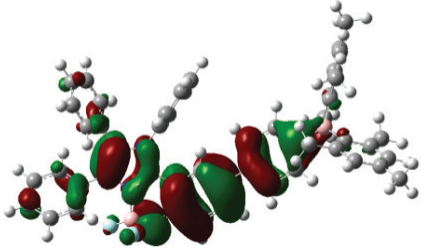
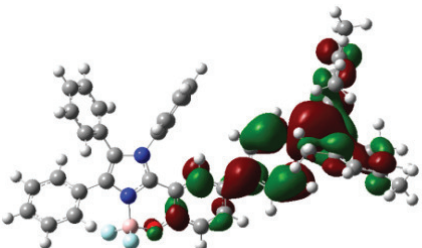
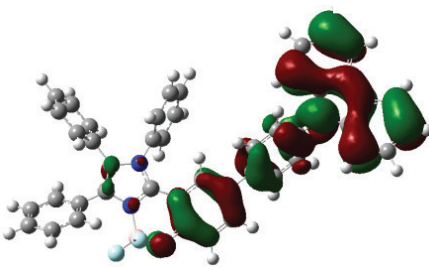
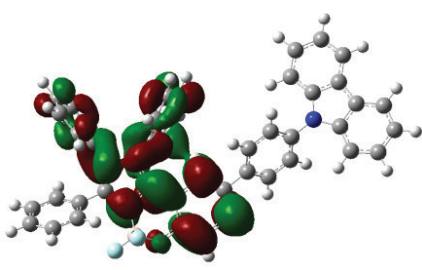
Compound	HOMO (eV)	LUMO (eV)
3a	 -5.739	 -1.605
3b	 -5.440	 -1.360
3c	 -5.250	 -1.310
3d	 -5.739	 -1.958
3e	 -5.576	 -1.714

Figure 2B.12: Computed orbitals for 3a-3e.

2B.2.5 Thermal studies

The thermal properties of complexes **3a-3e** were investigated by thermogravimetric analysis (TGA) under nitrogen atmosphere at a heating rate of 10 °C/min. The decomposition temperatures with 5% weight loss (Td5) for **3a-3e** are 389, 358, 413, 335 and 432 °C. All these compounds exhibit good thermal stability with high melting point (>278 °C).

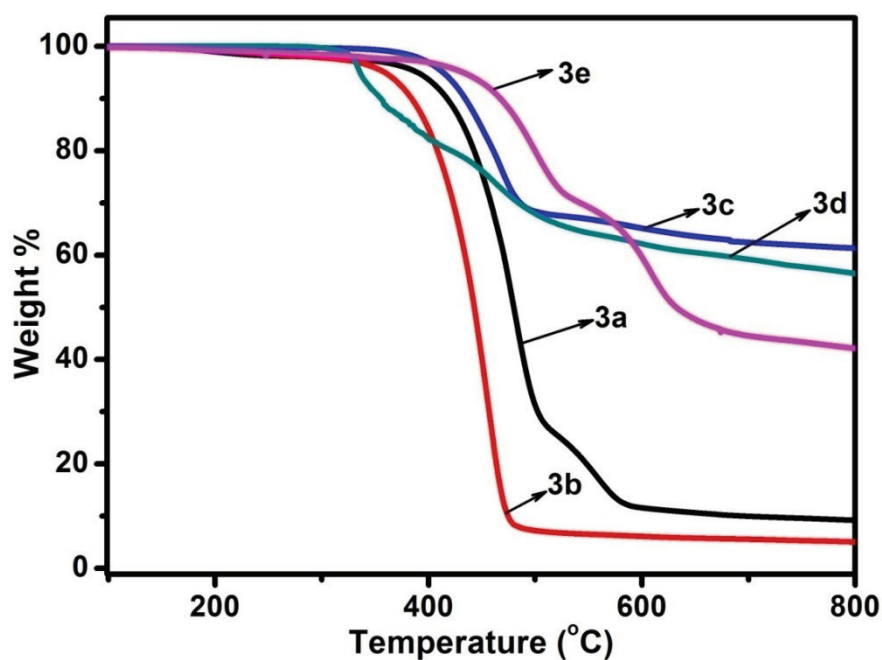


Figure 2B.13: TGA curves of **3a-3e** at heating rate of 10 °C /min.

2B.2.6 Electrochemical studies

The electrochemical properties of compounds **3a-3e** were examined by cyclic voltammetry at a scan rate of 100 mV/s using Bu_4NPF_6 as a supporting electrolyte in CH_3CN . The cyclic voltammograms of compounds **3a-3e** are shown in Figure 2B.14. Compounds **3b**, **3c** and **3e** exhibit one irreversible reduction whereas compounds **3a** and **3d** exhibit two reduction waves. The second reduction wave observed for **3a** is associated to the reduction of cyano group whereas in **3d** it is likely corresponds to the reduction of the tri-coordinated boron centre.

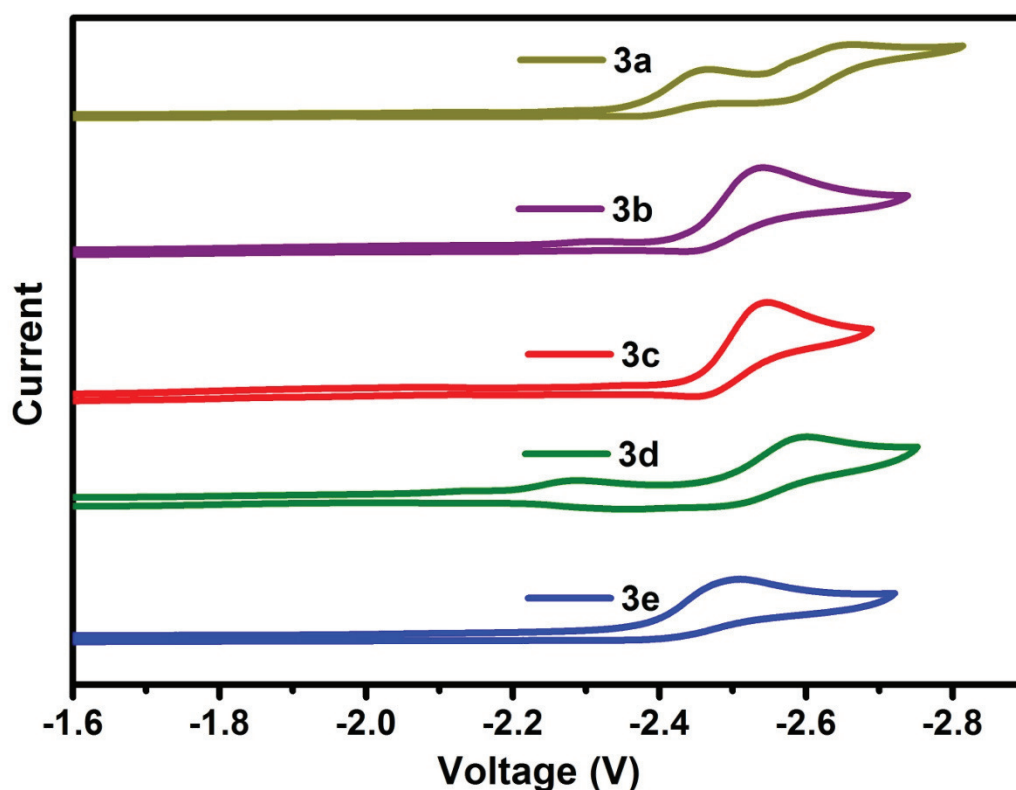


Figure 2B.14: Cyclic voltammograms of **3a**, **3b**, **3c**, **3d** and **3e** in CH₃CN (with 0.1 M ⁿBu₄NPF₆ supporting electrolyte; scan rate 100 mV/s). Referenced relative to Fc/Fc⁺ couple.

2B.3 Conclusions

In summary, we have synthesized five new biphenyl conjugated imidazole based boron complexes in three steps. All these imidazole based boron complexes were characterized by multinuclear NMR, high resolution HRMS and by X-ray diffraction in case of **3a**, **3b**, **3d** & **3e**. The photophysical properties of all these boron complexes were investigated in detail. Our new boron complexes displayed deep blue colour when excited at the absorption maxima. Furthermore, all the imidazole based boron complexes showed bright fluorescence in the solid state as well. However, as prepared material of compounds **3a-3d** showed two emission bands in the solid state. Upon grinding, the intensity of the lower energy emission of compounds **3a**, **3b** and **3c** reduced and the intensity at the higher energy increased. The emission decay curves in comparison with solution decay profile reveal that the emission at the lower

energy is due to excimer formation and the emission at the higher energy is owing to the monomers. Additionally the morphological changes were further analysed using powder XRD, the excimer formation is sensitive towards grinding and can be reversed by fuming with solvent.

2B.4 Experimental section

2B.4.1 General information

Reagents and starting materials were purchased from Alfa-Aesar, Sigma-Aldrich and Spectrochem chemical companies and used as received unless otherwise noted. Tetrahydrofuran and toluene were distilled from Na/benzophenone prior to use. Chlorinated solvents and acetonitrile were distilled from CaH₂. 4-Bromo-2-(1,4,5-triphenyl-1H-imidazol-2-yl)phenol, 4-(9H-carbazol-9-yl)phenylboronic acid and 4-(dimesitylboryl)phenylboronic acid were prepared according to literature procedures.⁵³⁻⁵⁶ All 400 MHz ¹H, 100 MHz ¹³C, 128 MHz ¹¹B, and 376 MHz ¹⁹F NMR spectra were recorded on a Bruker ARX 400 spectrometer operating at 400 MHz. All ¹H and ¹³C NMR spectra were referenced internally to solvent signals. ¹¹B NMR spectra were referenced externally to BF₃.Et₂O in CDCl₃ (δ= 0), ¹⁹F NMR spectra, to α,α,α-trifluorotoluene (0.05% in CDCl₃; δ = -63.73). ESI mass spectra were recorded on Bruker, microTOF-QII mass spectrometer. The absorbance spectra were recorded on a Perkin Elmer Lambda 750 UV–visible spectrometer. The fluorescence spectra are recorded on a Perkin Elmer LS-55 Fluorescence Spectrometer. The fluorescence spectra are corrected for the instrumental response. The quantum yield was calculated by measuring the integrated area under the emission curves and by using the following equation. $\Phi_{\text{sample}} = \Phi_{\text{standard}} \times (I_{\text{sample}}/I_{\text{standard}}) \times (\text{OD}_{\text{standard}}/\text{OD}_{\text{sample}}) \times (\eta_{\text{sample}}^2/\eta_{\text{standard}}^2)$ where, ‘Φ’ is the quantum yield, ‘I’ the integrated emission intensity, ‘OD’ the optical density at the

excitation wavelength, and ' η ' the refractive index of the solvent. The subscripts "standard" and "sample" refer to the fluorophore of reference and unknown respectively. In this case unknown is **3a-3e**, reference is quinine sulphate (quantum yield of quinine sulphate in 1 N H₂SO₄ is 0.55). Optically matched solutions with very similar optical densities of the "sample" and "standard" at a given absorbing wavelength were used for quantum yield calculations. Solid state emission spectra and absolute solid state quantum yields were recorded on Edinburg FLS spectrometer. Single-crystal X-ray diffraction data were collected on a Bruker APEX-II diffractometer equipped with an Oxford Instruments low-temperature attachment. The data were collected using, Mo-K α radiation (0.71073 Å). Using Olex2, the structures were solved with the ShelXS structure solution program using Direct Methods and refined with the ShelXL refinement package using Least Squares minimisation. The H atoms were placed at calculated positions and were refined as riding atoms. In compound **3d**, electron density resulting from one disordered solvent molecule was removed using OLEX solvent mask.

Cyclic voltammetry measurements were performed with a conventional three electrode cell using an electrochemical workstation (CH Instrument, Model: 1100A) The three-electrode system consisted of a Glassy carbon working electrode, a Pt wire as the secondary electrode, and a Ag wire as the reference electrode. The voltammograms were recorded with ca. 1.0×10^{-3} M solution in CH₃CN containing ⁿBu₄NPF₆ (0.1 M) as the supporting electrolyte. The scans were referenced after the addition of a small amount of ferrocene as the internal standard. DFT calculations were performed with the Gaussian09 program. The structures were optimized using 6-31G (d,p) (B3LYP) as the basis set. Frequency calculations confirmed the optimized structures to be local minimum structures. The input files were generated using X-ray

data for compounds **3a**, **3b**, **3d** and **3e**. Excitation data were determined using TD-DFT (B3LYP) calculations.

2B.4.2 Synthetic procedure and spectral characterization

2B.4.2.1 Synthesis of compound 1

Benzil (5.00 g, 23.78 mmol), 5-bromosalicylaldehyde (4.78 g, 23.78 mmol), ammonium acetate (1.83 g, 23.78 mmol), aniline (2.90 mL, 30.91 mmol) were taken in a 250 mL round bottom flask and 150 mL of glacial acetic acid was added. The reaction mixture was heated to reflux for 24 hours. After cooling to room temperature, 200 mL of dichloromethane and 200 mL of water were added, organic layer was separated and aqueous layer was extracted with dichloromethane (2 X 75 mL). The combined organic phase was washed with brine, dried over Na₂SO₄ and concentrated under vacuum. The obtained solid was purified through silica gel column chromatography using ethyl acetate and hexane as eluent. Yield: 8.89 g, (80%). mp: 198 °C. ¹H NMR (400 MHz, CDCl₃): δ = 7.58 (d, *J* = 6.9 Hz, 2H, ArH), 7.48 - 7.42 (m, 3H, ArH), 7.33 - 7.18 (m, 11H, ArH), 7.00 (d, *J* = 8 Hz, 1H, ArH), 6.64 (d, *J* = 1.9 Hz, 1H, ArH) ppm. ¹³C NMR (100 MHz, CDCl₃): δ = 157.48, 143.53, 136.30, 134.90, 132.98, 132.16, 131.36, 130.90, 129.90, 129.77, 129.20, 129.10, 128.88, 128.71, 128.52, 127.57, 127.20, 119.59, 114.27, 109.83. HR-MS (ESI): calcd. for C₂₇H₂₀Br₁N₂O₁ ([M + H]⁺): 467.0754, found : 467.0779.

General procedure for the synthesis of compounds (2a – 2e).

Degassed 1,2-dimethoxyethane and Pd(PPh₃)₄ (3 mol%) were added to compound **1** (1.0 equivalent) under inert atmosphere and stirred for 30 minutes at room temperature. Then appropriate arylboronic acid (1.3 equivalents) followed by freshly prepared, degassed solution of sodium carbonate (3.0 equivalents) in water was added and the mixture was heated at reflux for 16 hours. The solvent was removed from the

reaction mixture under reduced pressure and the residue was dissolved in dichloromethane and washed with water. The water fraction was extracted with dichloromethane. The combined organic fraction was washed with brine and dried over Na₂SO₄. The solvent was removed under reduced pressure. The obtained solid was purified through silica gel column chromatography using ethyl acetate and hexane as eluent.

2B.4.2.2 Synthesis of compound 2a

The quantities involved are as follows: Compound **1** (2.93 g, 6.28mmol), Pd(PPh₃)₄ (0.22 g, 3 mol%), arylboronic acid (1.20 g, 8.02 mmol), Na₂CO₃ (2.00 g, 18.84 mmol). Yield: 2.05 g, (67%). mp: 280 °C. ¹H NMR (400 MHz, CDCl₃): δ = 13.71 (brs, 1H, ArOH), 7.56 (d, *J* = 8 Hz, 2H, ArH), 7.51 - 7.42 (m, 6H, ArH), 7.28 - 7.15 (m, 12H, ArH), 7.05 (d, *J* = 8 Hz, 1H, ArH), 6.85 (s, 1H, ArH) ppm. ¹³C NMR (100 MHz, CDCl₃): δ = 159.38, 144.85, 144.46, 137.55, 135.53, 132.97, 132.42, 131.44, 130.89, 130.10, 129.63, 129.42, 128.99, 128.79, 128.71, 128.49, 128.44, 128.35, 127.35, 127.05, 126.50, 125.07, 119.14, 118.60, 113.49, 109.87 ppm. HR-MS (ESI): calcd. for C₃₄H₂₄N₃O₁ ([M +H]⁺) : 490.1914, found : 490.1909.

2B.4.2.3 Synthesis of compound 2b

The quantities involved are as follows: Compound **1** (1.00 g, 2.14 mmol), Pd(PPh₃)₄ (0.07 g, 3 mol%), arylboronic acid (0.34 g, 2.78 mmol), Na₂CO₃ (0.68 g, 6.42 mmol). Yield: 0.79 g, (80%). mp: 239 °C. ¹H NMR (400 MHz, CDCl₃): δ = 13.46 (brs, 1H, ArOH), 7.58 (d, *J* = 8 Hz, 2H, ArH), 7.48 - 7.43 (m, 4H, ArH), 7.31 - 7.15 (m, 14H, ArH), 7.00 (d, *J* = 7.1 Hz, 2H, ArH), 6.89 (d, *J* = 1.5 Hz, 1H, ArH) ppm. ¹³C NMR (100 MHz, CDCl₃): δ = 158.11, 144.93, 140.37, 137.51, 135.32, 133.01, 131.48, 130.68, 130.01, 129.79, 129.32, 128.96, 128.68, 128.65, 128.57, 128.46, 127.27,

127.10, 126.50, 126.20, 125.02, 118.22, 113.13 ppm. HR-MS (ESI): calcd. for $C_{33}H_{25}N_2O_1$ ($[M+H]^+$): 465.1961, found : 465.1987.

2B.4.2.4 Synthesis of compound 2c

The quantities involved are as follows: Compound **1** (2.50 g, 5.35 mmol), $Pd(PPh_3)_4$ (0.19 g, 3.0 mol%), arylboronic acid (1.05 g, 6.95 mmol), Na_2CO_3 (1.70 g, 16.05 mmol). Yield: 1.93 g, (73%). mp: 225 °C. 1H NMR (400 MHz, $CDCl_3$): δ = 7.60 (d, J = 4 Hz, 2H, ArH), 7.49 - 7.28 (m, 12H, ArH), 7.21 - 7.15 (m, 3H, ArH), 6.97 (d, J = 8 Hz, 2H, ArH), 6.89 (s, 1H, ArH), 6.81 (d, J = 8 Hz, 2H, ArH), 3.81 (s, 3H, OCH_3) ppm. ^{13}C NMR (100 MHz, $CDCl_3$): δ = 158.60, 157.38, 144.84, 137.17, 134.82, 132.97, 131.45, 130.64, 129.92, 129.49, 129.37, 128.85, 128.69, 128.51, 127.46, 127.26, 127.22, 125.00, 118.29, 114.01, 112.78, 55.39 ppm. HR-MS (ESI): calcd. for $C_{34}H_{27}N_2O_2$ ($[M+H]^+$): 495.2067, found : 495.2074.

2B.4.2.5 Synthesis of compound 2d

The quantities involved are as follows: Compound **1** (1.06 g, 2.28 mmol), $Pd(PPh_3)_4$ (0.79 g, 3 mol%), arylboronic acid (1.10 g, 2.97 mmol), Na_2CO_3 (0.72 g, 6.84 mmol). Yield: 1.05 g, (65%). mp: 254 °C. 1H NMR (400 MHz, $CDCl_3$): δ = 13.58 (brs, 1H, ArOH), 7.58 (d, J = 8 Hz, 2H, ArH), 7.53-7.50 (m, 1H, ArH), 7.44-7.40 (m, 5H, ArH), 7.30 - 7.15 (m, 11H, ArH), 7.00-6.96 (m, 3H, ArH), 6.84 (s, 4H, ArH), 2.34 (s, 6H, CH_3), 2.01 (s, 12H, CH_3) ppm. ^{13}C NMR (100 MHz, $CDCl_3$): δ = 158.72, 144.87, 143.60, 141.89, 140.95, 138.62, 137.41, 137.13, 135.43, 133.13, 131.46, 130.71, 129.99, 129.93, 129.83, 129.47, 128.88, 128.63, 128.44, 128.27, 127.22, 127.05, 125.43, 124.99, 118.27, 113.23, 23.58, 21.35 ppm. HR-MS (ESI): calcd. for $C_{51}H_{46}B_1N_2O_1$ ($[M+H]^+$): 713.3706, found : 713.3720.

2B.4.2.6 Synthesis of compound 2e

The quantities involved are as follows: Compound **1** (1.35 g, 2.90 mmol), Pd(PPh₃)₄ (0.10 g, 3 mol%), arylboronic acid (1.08 g, 3.77 mmol), Na₂CO₃ (0.92 g, 8.70 mmol). Yield: 1.37 g, (75%). mp: 240 °C. ¹H NMR (400 MHz, CDCl₃): δ = 8.15 (d, *J* = 4 Hz, 2H, ArH), 7.62 (d, *J* = 4 Hz, 2H, ArH), 7.51 - 7.38 (m, 10H, ArH), 7.32 - 7.24 (m, 13H, ArH), 7.22 - 7.15 (m, 4H) ppm. ¹³C NMR (100 MHz, CDCl₃): δ = 158.21, 144.67, 140.96, 139.40, 137.14, 136.11, 134.83, 131.44, 130.77, 129.99, 129.76, 129.40, 128.88, 128.71, 128.53, 127.52, 127.45, 127.21, 127.17, 126.01, 125.48, 123.46, 120.42, 120.02, 118.49, 112.96, 109.87 ppm. HR-MS (ESI): calcd. for C₄₅H₃₂N₃O₁([M + H]⁺): 630.2540, found : 630.2544.

General procedure for the synthesis of compounds (3a-3e)

To a solution of imidazole (Compound **2a-2e**) (1 equivalent) in anhydrous 1,2-dichloroethane under nitrogen, BF₃·Et₂O (6 equivalents) was added. After 5 minutes, N,N-diisopropylethylamine (DIPEA) (6 equivalents) was added and the resulting mixture was stirred at 40 °C for 1 h. The crude solution was filtered through a column of basic Al₂O₃ eluting with CH₂Cl₂. Solvent was removed under reduced pressure to obtain the product.

2B.4.2.7 Synthesis of compound 3a

The quantities involved are as follows: Compound **2a** (0.30 g, 0.61 mmol), BF₃·Et₂O (0.46 mL, 3.66 mmol) and N,N-diisopropylethylamine (0.63 mL, 3.66 mmol). Yield: 0.29 g, (87%). mp: 337 °C. ¹H NMR (400 MHz, CDCl₃): δ = 7.64 - 7.53 (m, 8H, ArH), 7.38 - 7.34 (m, 5H, ArH), 7.29 - 7.25 (m, 2H, ArH), 7.17 (t, *J* = 8 Hz, 2H, ArH), 7.10 (d, *J* = 8 Hz, 2H, ArH), 6.98 (d, *J* = 8 Hz, 2H, ArH), 6.71 (d, *J* = 4 Hz, 1H, ArH) ppm. ¹³C NMR (100 MHz, CDCl₃): δ = 157.33, 144.26, 140.89, 135.40, 132.60, 131.59, 131.21, 130.82, 130.79, 130.55, 129.58, 129.36, 129.18, 128.66, 128.51,

128.31, 128.18, 126.64, 126.42, 123.72, 121.28, 118.92, 110.51, 110.27 ppm. ^{19}F NMR (376 MHz, CDCl_3): $\delta = -137.62$ (BF_2) ppm. ^{11}B NMR (128 MHz, CDCl_3): $\delta = 0.96$ (s) ppm. HR-MS (ESI): calcd. for $\text{C}_{34}\text{H}_{22}\text{B}_1\text{F}_2\text{N}_3\text{O}_1$ ($[\text{M}]^+$) : 537.1824, found : 537.1860. IR (KBr): $\nu(\text{cm}^{-1}) = 3058$ (m), 2229 (m), 1620 (m), 1605 (m), 1526 (m), 1498 (s), 1457 (m), 1317 (m), 1155 (s), 1056 (s), 1036 (s), 913 (m), 835 (m), 710 (m), 697 (m), 557 (m).

2B.4.2.8 Synthesis of compound 3b

The quantities involved are as follows: Compound **2b** (0.30 g, 0.65 mmol), $\text{BF}_3 \cdot \text{Et}_2\text{O}$ (0.49 mL, 3.90 mmol) and *N,N*-diisopropylethylamine (0.67 mL, 3.90 mmol). Yield: 0.29 g, (88%). mp: 319 °C. ^1H NMR (400 MHz, CDCl_3): $\delta = 7.61 - 7.54$ (m, 6H, ArH), 7.36 - 7.33 (m, 5H, ArH), 7.28 - 7.22 (m, 5H, ArH), 7.16 (t, $J = 7.5$ Hz, 4H, ArH), 7.03 - 6.96 (m, 4H, ArH), 6.72 (d, $J = 2.1$ Hz, 2H, ArH) ppm. ^{13}C NMR (100 MHz, CDCl_3): $\delta = 156.29, 141.45, 139.83, 135.47, 132.54, 131.80, 131.78, 131.25, 130.70, 130.57, 129.22, 129.06, 128.75, 128.60, 128.50, 128.38, 128.27, 126.97, 126.66, 126.24, 123.38, 120.83, 109.91$ ppm. ^{19}F NMR (376 MHz, CDCl_3): $\delta = -137.97$ (BF_2) ppm. ^{11}B NMR (128 MHz, CDCl_3): $\delta = 0.98$ (s) ppm. HR-MS (ESI): calcd. for $\text{C}_{33}\text{H}_{23}\text{B}_1\text{F}_2\text{N}_2\text{O}_1\text{Na}$ ($[\text{M} + \text{Na}]^+$) : 535.1769, found : 535.1771. IR (KBr): $\nu(\text{cm}^{-1}) = 3058$ (m), 1617 (m), 1520 (s), 1497 (s), 1453 (m), 1311 (m), 1272 (m), 1088 (s), 1059 (s), 913 (m), 768 (m), 722 (m), 696 (m).

2B.4.2.9 Synthesis of compound 3c

The quantities involved are as follows: Compound **2c** (0.30 g, 0.61 mmol), $\text{BF}_3 \cdot \text{Et}_2\text{O}$ (0.45 mL, 3.66 mmol) and *N,N*-diisopropylethylamine (0.63 mL, 3.66 mmol). Yield: 0.30 g, (90%). mp: 278 °C. ^1H NMR (400 MHz, CDCl_3): $\delta = 7.63 - 7.51$ (m, 6H, ArH), 7.35 (d, $J = 8$ Hz, 5H, ArH), 7.26 - 7.21 (m, 2H, ArH), 7.16 (t, $J = 8$ Hz, 2H, ArH), 6.98 - 6.93 (m, 4H, ArH), 6.80 (d, $J = 8$ Hz, 2H, ArH), 6.65 (d, $J = 4$ Hz, 3H,

ArH), 3.79 (s, 3H, OCH₃) ppm. ¹³C NMR (100 MHz, CDCl₃): δ = 158.90, 155.79, 141.50, 135.48, 132.49, 132.44, 131.55, 131.41, 131.25, 130.67, 130.57, 129.20, 129.03, 128.58, 128.52, 128.42, 128.26, 127.28, 126.67, 122.86, 120.72, 114.17, 109.84, 55.43 ppm. ¹⁹F NMR (376 MHz, CDCl₃): δ = -137.37 (BF₂) ppm. ¹¹B NMR (128 MHz, CDCl₃): δ = 1.03 (s) ppm. HR-MS (ESI): calcd. for C₃₄H₂₆B₁F₂N₂O₂ ([M + H]⁺): 543.2056, found : 543.2072. IR (KBr): ν(cm⁻¹) = 3055 (m), 2839 (m), 1619 (m), 1609 (m), 1504 (s), 1454 (m), 1283 (s), 1250 (s), 1173 (m), 1054 (s), 1034 (s), 873 (m), 823 (s), 771 (m), 695 (m).

2B.4.2.10 Synthesis of compound 3d

The quantities involved are as follows: Compound **2d** (0.30 g, 0.42 mmol), BF₃·Et₂O (0.32 mL, 2.52 mmol) and N,N-diisopropylethylamine (0.44 mL, 2.52 mmol). Yield: 0.26 g, (84%). mp: 341 °C. ¹H NMR (400 MHz, CDCl₃): δ = 7.66 (d, *J* = 8 Hz, 1H, ArH), 7.59 – 7.54 (m, 5H, ArH), 7.44 (d, *J* = 8 Hz, 2H, ArH), 7.37 - 7.34 (m, 5H, ArH), 7.27 – 7.22 (m, 2H, ArH), 7.16 (t, *J* = 8 Hz, 2H, ArH), 7.03 - 6.98 (m, 4H, ArH), 6.82-6.85 (m, 5H, ArH), 2.33 (s, 6H, CH₃), 2.01 (s, 12H, CH₃) ppm. ¹³C NMR (100 MHz, CDCl₃): δ = 156.74, 144.06, 142.84, 141.79, 141.29, 140.95, 138.75, 137.19, 135.34, 132.62, 132.55, 131.82, 131.24, 131.08, 130.85, 130.69, 130.57, 129.22, 129.05, 128.58, 128.44, 128.30, 128.26, 126.61, 125.45, 123.45, 120.90, 109.97, 23.59, 21.36 ppm. ¹⁹F NMR (376 MHz, CDCl₃): δ = -137.73 (BF₂) ppm. ¹¹B NMR (128 MHz, CDCl₃): δ = 0.99 (s) ppm (only one ¹¹B signal observed may be due to dilute sample). HR-MS (ESI): calcd. for C₅₁H₄₄B₂F₂N₂O₁ ([M]⁺): 760.3618, found : 760.3622. IR (KBr): ν(cm⁻¹) = 3058 (m), 2918 (m), 1620 (m), 1598 (s), 1522 (s), 1421 (m), 1315 (m), 1154 (m), 1063 (s), 1038 (s), 918 (m), 848 (m), 820(m), 772 (m), 696 (m).

2B.4.2.11 Synthesis of compound 3e

The quantities involved are as follows: Compound **2e** (0.30 g, 0.48 mmol), $\text{BF}_3 \cdot \text{Et}_2\text{O}$ (0.36 mL, 2.88 mmol) and *N,N*-diisopropylethylamine (0.50 mL, 2.88 mmol). Yield: 0.27 g, (81%). mp: 316 °C. ^1H NMR (400 MHz, CDCl_3): δ = 8.17 (d, J = 8 Hz, 2H, ArH), 7.69 - 7.61 (m, 6H, ArH), 7.49 - 7.19 (m, 19H, ArH), 7.02 (d, J = 8 Hz, 2H, ArH), 6.84 (s, 1H, ArH) ppm. ^{13}C NMR (100 MHz, CDCl_3): δ = 156.52, 141.24, 140.87, 138.80, 136.54, 135.47, 132.67, 132.56, 131.57, 131.23, 130.75, 130.69, 130.56, 129.24, 129.05, 128.59, 128.53, 128.26, 127.44, 127.26, 126.55, 126.05, 123.51, 123.32, 120.98, 120.46, 120.13, 110.08, 109.82 ppm. ^{19}F NMR (376 MHz, CDCl_3): δ = -137.64 (BF_2) ppm. ^{11}B NMR (128 MHz, CDCl_3): δ = 1.07 (s) ppm. HR-MS (ESI): calcd. for $\text{C}_{45}\text{H}_{30}\text{BF}_2\text{N}_3\text{O}_1$ ($[\text{M}]^+$): 677.2452, found : 677.2459. IR (KBr): $\nu(\text{cm}^{-1})$ = 3054 (m), 1621 (m), 1505 (s), 1451 (s), 1314 (m), 1229 (m), 1152 (s), 1062 (s), 1038(m), 914 (m), 824 (m), 751 (m), 695 (m).

2B.5 References

- (1) Bellina, F.; Cauteruccio, S.; Monti, S.; Rossi, R. *Bioorg. Med. Chem. Lett.***2006**, *16*, 5757.
- (2) Coll, C.; Ros-Lis, J. V.; Martinez-Manez, R.; Marcos, M. D.; Sancenon, F.; Soto, J. *J. Mater. Chem.***2010**, *20*, 1442.
- (3) Shin, R. Y. C.; Kietzke, T.; Sudhakar, S.; Dodabalapur, A.; Chen, Z.-K.; Sellinger, A. *Chem. Mater.***2007**, *19*, 1892.
- (4) Chen, X.; Kang, S.; Kim, M. J.; Kim, J.; Kim, Y. S.; Kim, H.; Chi, B.; Kim, S.-J.; Lee, J. Y.; Yoon, J. *Angew. Chem., Int. Ed.***2010**, *49*, 1422.
- (5) Ge, Z.; Hayakawa, T.; Ando, S.; Ueda, M.; Akiike, T.; Miyamoto, H.; Kajita, T.; Kakimoto, M.-a. *Chem. Mater.***2008**, *20*, 2532.

-
- (6) Lai, M.-Y.; Chen, C.-H.; Huang, W.-S.; Lin, J. T.; Ke, T.-H.; Chen, L.-Y.; Tsai, M.-H.; Wu, C.-C. *Angew. Chem., Int. Ed.***2008**, *47*, 581.
- (7) Fang, Z.; Wang, S.; Zhao, L.; Xu, Z.; Ren, J.; Wang, X.; Yang, Q. *Mater. Chem. Phys.***2008**, *107*, 305.
- (8) Chen, C.-H.; Huang, W.-S.; Lai, M.-Y.; Tsao, W.-C.; Lin, J. T.; Wu, Y.-H.; Ke, T.-H.; Chen, L.-Y.; Wu, C.-C. *Adv. Funct. Mater.***2009**, *19*, 2661.
- (9) Fang, Z.; Wang, S.; Zhao, L.; Xu, Z.; Ren, J.; Wang, X.; Yang, Q. *Mater. Lett.***2007**, *61*, 4803.
- (10) Vlahakis, J. Z.; Hum, M.; Rahman, M. N.; Jia, Z.; Nakatsu, K.; Szarek, W. A. *Bioorg. Med. Chem.***2009**, *17*, 2461.
- (11) Bhandari, K.; Srinivas, N.; Marrapu, V. K.; Verma, A.; Srivastava, S.; Gupta, S. *Bioorg. Med. Chem. Lett.***2010**, *20*, 291.
- (12) Park, S.; Kwon, O.-H.; Kim, S.; Park, S.; Choi, M.-G.; Cha, M.; Park, S. Y.; Jang, D.-J. *J. Am. Chem. Soc.***2005**, *127*, 10070.
- (13) Lim, S.-J.; Seo, J.; Park, S. Y. *J. Am. Chem. Soc.***2006**, *128*, 14542.
- (14) Park, S.; Seo, J.; Kim, S. H.; Park, S. Y. *Adv. Funct. Mater.***2008**, *18*, 726.
- (15) Kim, C. H.; Park, J.; Seo, J.; Park, S. Y.; Joo, T. *J. Phys. Chem. A***2010**, *114*, 5618.
- (16) Kwon, J. E.; Park, S. Y. *Adv. Mater. (Weinheim, Ger.)***2011**, *23*, 3615.
- (17) Kim, S.; Chang, D. W.; Park, S. Y.; Kawai, H.; Nagamura, T. *Macromolecules***2002**, *35*, 2748.
- (18) Yang, Y.; Zhao, Q.; Feng, W.; Li, F. *Chem. Rev. (Washington, DC, U. S.)***2013**, *113*, 192.
- (19) Nayak, M. K. *J. Photochem. Photobiol., A***2012**, *241*, 26.
- (20) Chu, Q.; Medvetz, D. A.; Pang, Y. *Chem. Mater.***2007**, *19*, 6421.
-

-
- (21) Xu, Y.; Pang, Y. *Chem. Commun. (Cambridge, U. K.)***2010**, 46, 4070.
- (22) Xu, Z.; Xu, L.; Zhou, J.; Xu, Y.; Zhu, W.; Qian, X. *Chem. Commun.* **2012**, 48, 10871.
- (23) Hu, R.; Feng, J.; Hu, D.; Wang, S.; Li, S.; Li, Y.; Yang, G. *Angew. Chem., Int. Ed.***2010**, 49, 4915.
- (24) Dhanunjayarao, K.; Mukundam, V.; Venkatasubbaiah, K. *J. Mater. Chem. C*,**2014**, 2, 8599.
- (25) Dhanunjayarao, K.; Mukundam, V.; Venkatasubbaiah, K. *Sens. Actuators, B***2016**, 232, 175.
- (26) Ren, Y.; Jäkle, F. *Dalton Trans.***2016**, 45, 13996.
- (27) Jäkle, F. *Coord. Chem. Rev.***2006**, 250, 1107.
- (28) Entwistle, C. D.; Marder, T. B. *Chem. Mater.***2004**, 16, 4574.
- (29) Yuan, Z.; Collings, J. C.; Taylor, N. J.; Marder, T. B.; Jardin, C.; Halet, J.-F. *J. Solid State Chem.***2000**, 154, 5.
- (30) Lorbach, A.; Hubner, A.; Wagner, M. *Dalton Trans.***2012**, 41, 6048.
- (31) Entwistle, C. D.; Marder, T. B. *Angew. Chem., Int. Ed.***2002**, 41, 2927.
- (32) Heilmann, J. B.; Scheibitz, M.; Qin, Y.; Sundararaman, A.; Jäkle, F.; Kretz, T.; Bolte, M.; Lerner, H.-W.; Holthausen, M. C.; Wagner, M. *Angew. Chem., Int. Ed.***2006**, 45, 920.
- (33) Januszewski, E.; Bolte, M.; Lerner, H.-W.; Wagner, M. *Organometallics***2012**, 31, 8420.
- (34) Lorbach, A.; Bolte, M.; Li, H.; Lerner, H.-W.; Holthausen, M. C.; Jäkle, F.; Wagner, M. *Angew. Chem., Int. Ed.***2009**, 48, 4584.
- (35) Rao, Y.-L.; Amarne, H.; Wang, S. *Coord. Chem. Rev.***2012**, 256, 759.
- (36) Rao, Y.-L.; Wang, S. *Inorg. Chem.***2011**, 50, 12263.
-

-
- (37) Yamaguchi, S.; Wakamiya, A. *Pure Appl. Chem.***2006**, 78, 1413.
- (38) Yamaguchi, S.; Akiyama, S.; Tamao, K. *J. Am. Chem. Soc.***2001**, 123, 11372.
- (39) Wakamiya, A.; Taniguchi, T.; Yamaguchi, S. *Angew. Chem., Int. Ed.***2006**, 45, 3170.
- (40) Araneda, J. F.; Piers, W. E.; Heyne, B.; Parvez, M.; McDonald, R. *Angew. Chem., Int. Ed.***2011**, 50, 12214.
- (41) Jaska, C. A.; Emslie, D. J. H.; Bosdet, M. J. D.; Piers, W. E.; Sorensen, T. S.; Parvez, M. *J. Am. Chem. Soc.***2006**, 128, 10885.
- (42) Wade, C. R.; Broomsgrove, A. E. J.; Aldridge, S.; Gabbai, F. P. *Chem. Rev.***2010**, 110, 3958.
- (43) Wade, C. R.; Gabbai, F. P. *Inorg. Chem.***2010**, 49, 714.
- (44) Li, D.; Zhang, H.; Wang, Y. *Chem. Soc. Rev.***2013**, 42, 8416.
- (45) Dou, C.; Long, X.; Ding, Z.; Xie, Z.; Liu, J.; Wang, L. *Angew. Chem. Int. Ed.***2016**, 55, 1436.
- (46) Frath, D.; Massue, J.; Ulrich, G.; Ziesel, R. *Angew. Chem., Int. Ed.***2014**, 53, 2290.
- (47) Poverenov, E.; Zamoshchik, N.; Patra, A.; Ridelman, Y.; Bendikov, M. *J. Am. Chem. Soc.***2014**, 136, 5138.
- (48) Crossley, D. L.; Vitorica-Yrezabal, I.; Humphries, M. J.; Turner, M. L.; Ingleson, M. J. *Chem. Eur. J.***2016**, 22, 12439.
- (49) Mukundam, V.; Dhanunjayarao, K.; Chuang, C.-N.; Kang, D.-Y.; Leung, M.-k.; Hsieh, K.-H.; Venkatasubbaiah, K. *Dalton Trans.***2015**, 44, 10228.
- (50) Benelhadj, K.; Massue, J.; Retailleau, P.; Ulrich, G.; Ziesel, R. *Org. Lett.***2013**, 15, 2918.
-

-
- (51) Esparza-Ruiz, A.; Peña-Hueso, A.; Nöth, H.; Flores-Parra, A.; Contreras, R. *J. Organomet. Chem.* **2009**, *694*, 3814.
- (52) Dhanunjayarao, K.; Mukundam, V.; Ramesh, M.; Venkatasubbaiah, K. *Eur. J. Inorg. Chem.* **2014**, 539.
- (53) Park, S.; Kwon, O.-H.; Kim, S.; Park, S.; Choi, M.-G.; Cha, M.; Park, S. Y.; Jang, D.-J. *J. Am. Chem. Soc.* **2005**, *127*, 10070.
- (54) Jia, W.-L.; Bai, D.-R.; McCormick, T.; Liu, Q.-D.; Motala, M.; Wang, R.-Y.; Seward, C.; Tao, Y.; Wang, S. *Chem. Eur. J.* **2004**, *10*, 994.
- (55) Dhanunjayarao, K.; Mukundam, V.; Venkatasubbaiah, K. *J. Mater. Chem. C.* **2014**, *2*, 8599.
- (56) Zheng, Z.; Dong, Q.; Gou, L.; Su, J.-H.; Huang, J. *J. Mater. Chem. C.* **2014**, *2*, 9858.

CHAPTER 3A

Synthesis, photophysical and electrochemical properties of pyrazole based N,C- chelate mononuclear boron compounds

3A.1 Introduction	109
3A.2 Results and discussion	110
3A.2.1 Synthesis and characterization	110
3A.2.2 Photophysical studies	118
3A.2.3 Electrochemical studies	122
3A.3 Conclusions	123
3A.4 Experimental section	123
3A.4.1 General information	123
3A.4.2 Synthetic procedure and spectral characterization	124
3A.5 References	134

3A.1 Introduction

In the past two decades, tri¹⁻³ and tetra-coordinate⁴⁻⁷ organoboron compounds have received considerable attention owing to their use as new materials in different fields including organic field-effect transistors, sensor materials, biomolecular probes, organic light emitting diodes (OLEDs), and photovoltaics. The tetra-coordinate organoboron compounds are in general more stable compared to three-coordinate ones, which require bulky substituents to stabilize them. Recently, efforts have been devoted to the design and synthesis of tetracoordinate boron compounds with N,O-, N,N-, and, N,C-chromophores⁸⁻³⁰. Among them, boron dipyrromethene dyes³¹⁻³³ have been studied to a greater extent owing to their potential application in artificial light harvesters, fluorescent sensors, laser dyes, sensitizers for solar cells, and molecular photonic wires.

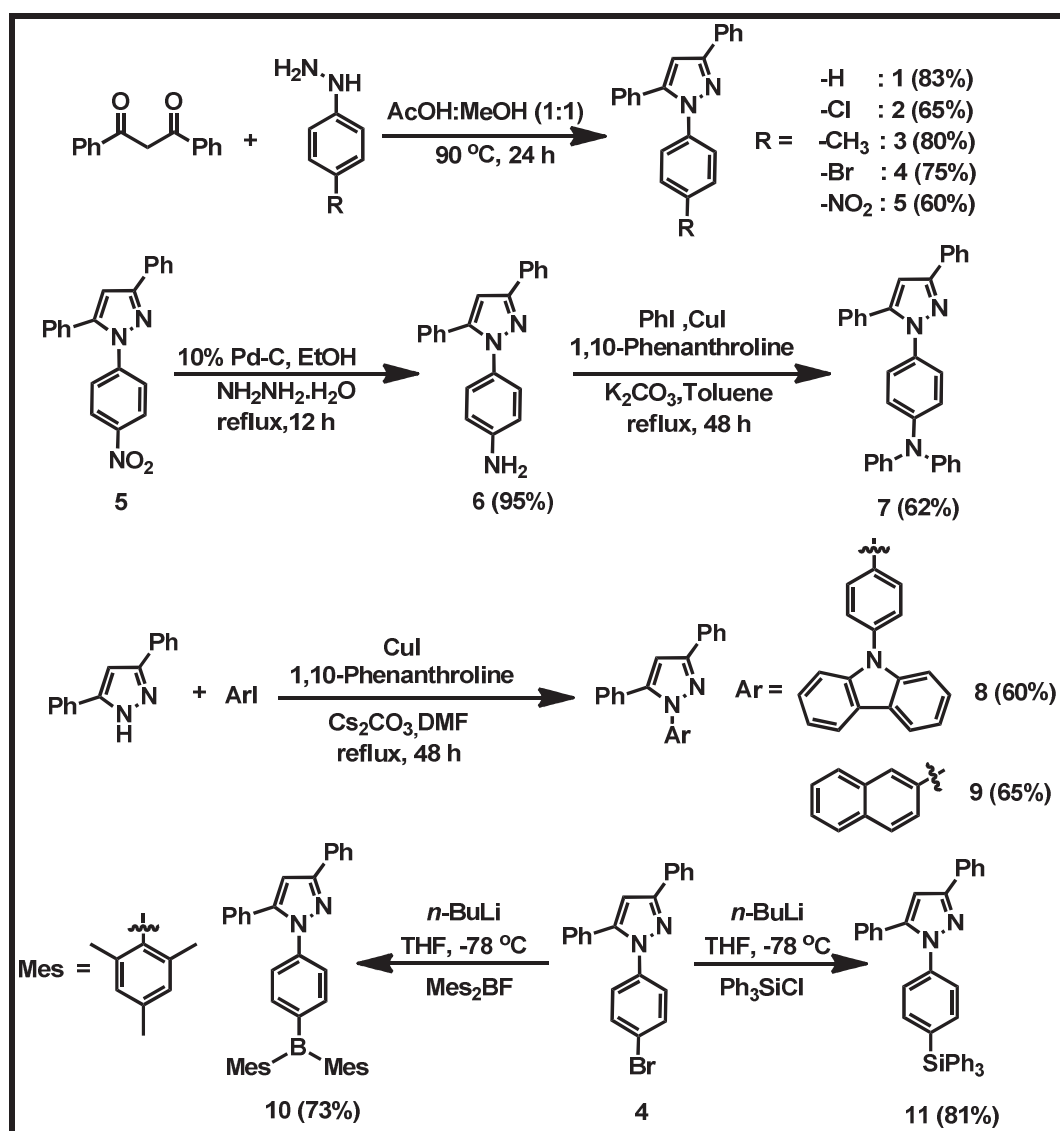
N,C- chelate tetra-coordinate boron compounds are emerging as useful subset of this family of fluorescent molecules due to their potential applications in areas ranging from OLEDs, biological imaging, lasing, to photochromic materials and molecular switches^{5,33-35}. Yamaguchi and co-workers reported the first example of N,C- chelate tetra-coordinate boron compounds with two bulky mesityl group on boron for thienylthiazole moiety^{36,37}. N,C- chelate tetra-coordinate boron compounds have most commonly been prepared by lithiation-borylation approaches,^{36,38,39} nucleophilic aromatic substitution⁴⁰, metal-catalyzed⁴¹ and metal-free electrophilic borylations⁴². The electrophilic aromatic borylation of phenylpyridines developed by Murakami and co-workers⁴³ have been utilized to develop various luminescent materials^{34,44}. A series of luminescent materials reported by Patil⁴⁵, Yam⁴⁶ showed tunable emission colours covering the entire visible spectrum. Qiu and co-workers^{47,48} reported tetraphenylethene (AIE active) based N,C- chelate boron compounds which

were used as emitters for OLEDs. In this chapter, we describe pyrazole based N,C-chelate boron compounds (**12-19**) synthesized by electrophillic aromatic borylation strategy and their photophysical, electrochemical properties.

3A.2 Results and discussion

3A.2.1 Synthesis and characterization

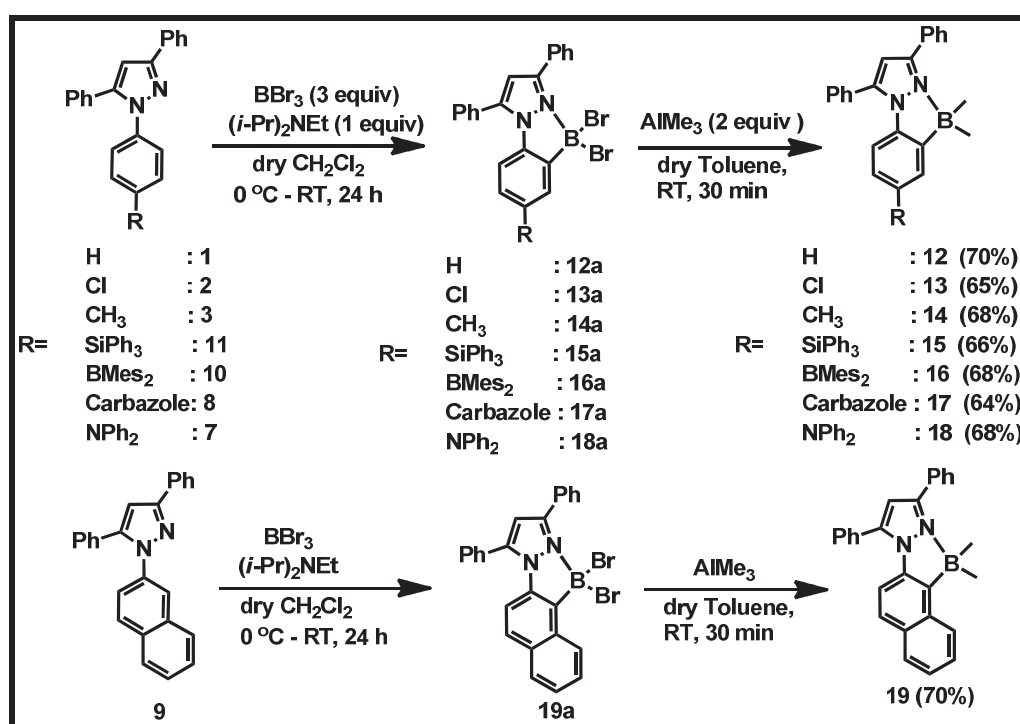
The synthetic route to various substituted triaryl pyrazoles is outlined in scheme 3A.1.



Scheme 3A.1: Synthesis of compounds 1-11.

Compounds **1-5** were synthesized by cyclocondensation of 1,3-diphenyl-1,3-propanedione with substituted hydrazines in acetic acid : methanol (1:1) under reflux

condition⁴⁹. Reduction of compound **5** using Pd/C and hydrazine monohydrate afforded the amino pyrazole **6** which was converted to pyrazole **7** as shown in scheme 3A.1. Compounds **8** and **9** were prepared from the reaction of 3,5-diphenyl-1H-pyrazole with corresponding aryl iodides under Cu catalysed Ullmann type reaction. The lithiated triphenyl pyrazole was prepared by the reaction of *n*-BuLi with compound **4**, which was quenched with chlorotriphenylsilane or fluorodimesitylborane to afford the pyrazoles **10** or **11** respectively.



Scheme 3A.2: Synthesis of compounds **12-19**.

Pyrazole based N,C- chelate dibromoborane compounds **12a-19a** were prepared from their corresponding pyrazole ligands through an electrophilic aromatic borylation reaction with BBr₃ under basic condition (*i*-Pr₂NEt). Without further purification, the pyrazole - dibromoborane complexes (**12a-19a**) were treated with trimethylaluminum (AlMe₃) to afford the desired products **12-19** in moderate yields (Scheme 3A.2). The crude products were purified by column chromatography over silica gel.

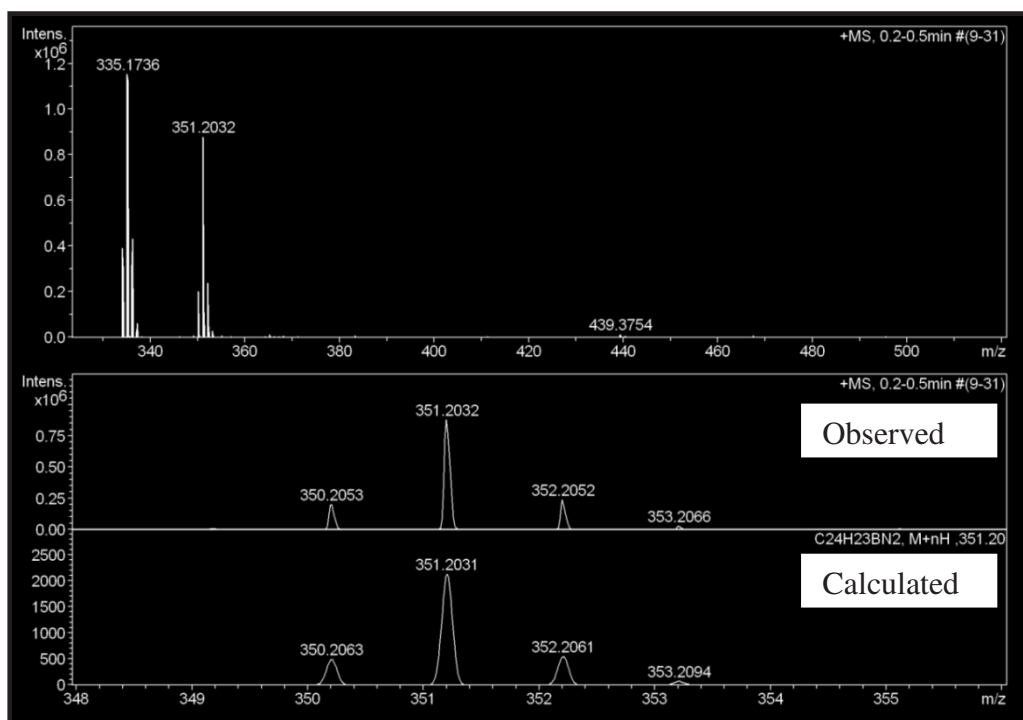


Figure 3A.1: HRMS spectrum of compound 14.

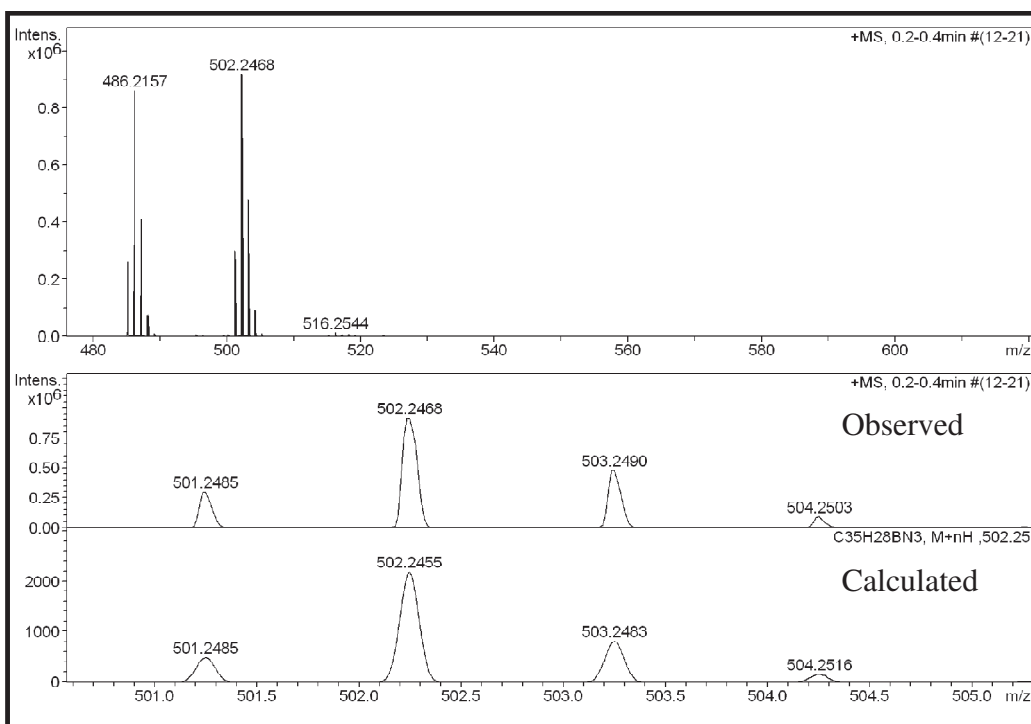


Figure 3A.2: HRMS spectrum of compound 17.

All these compounds were fully characterized by ¹H, ¹³C, ¹¹B NMR and high resolution mass spectrometry. All the boron compounds show characteristic [M+H]⁺ ions in HRMS mass spectrum. Representative HRMS spectra of compound 14&17 are

given in Figure 3A.1 and 3A.2. The ^{11}B NMR spectra of these complexes (**12-19**) show a broad resonance around 1 ppm, which is characteristic of tetra-coordinated boron. The ^1H NMR spectra of compounds **12-19** show resonance around 0.2 ppm which is readily assigned to $-\text{BMe}_2$. A representative ^1H and ^{11}B NMR spectrum for compound **19** is shown in Figure 3A.3 and Figure 3A.4 respectively.

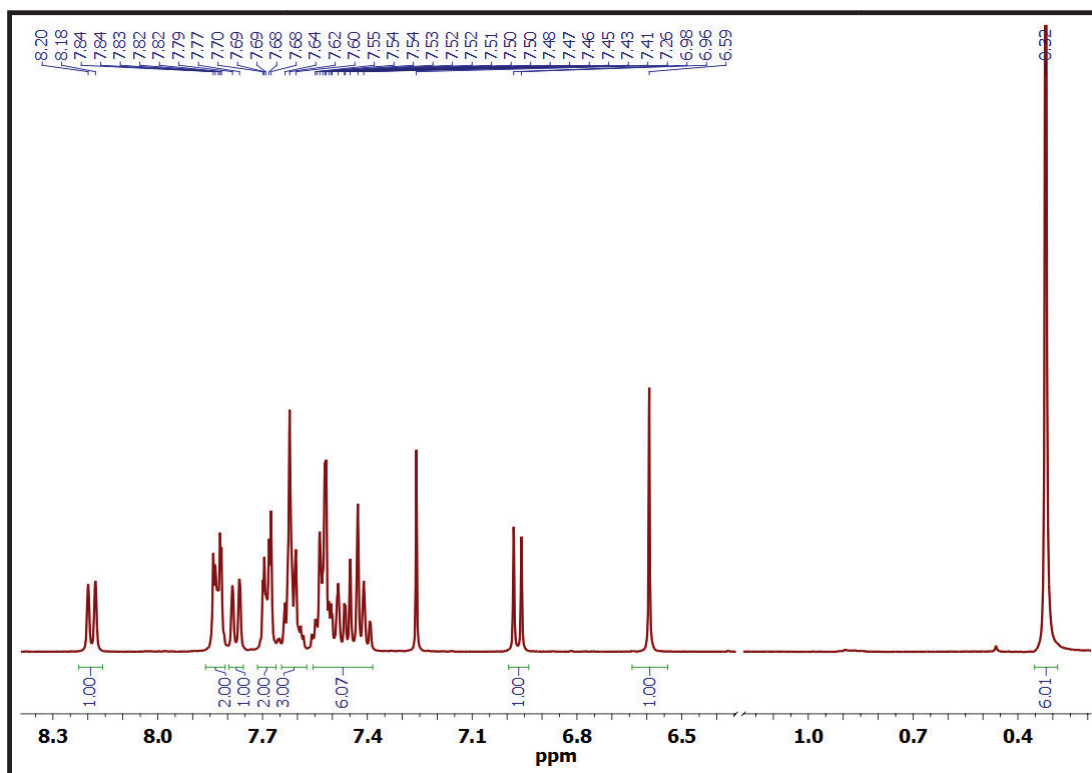


Figure 3A.3: ^1H NMR spectrum of compound **19** recorded in CDCl_3 .

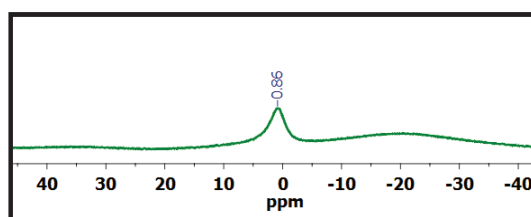


Figure 3A.4: ^{11}B NMR spectrum of compound **19** recorded in CDCl_3 .

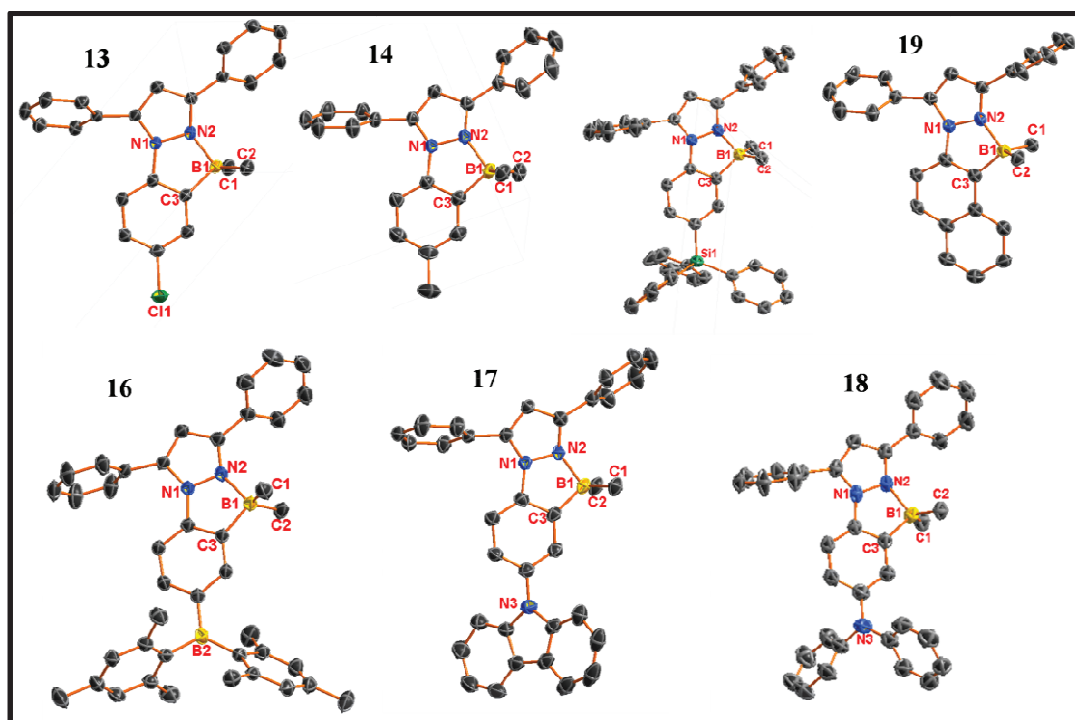


Figure 3A.5: Molecular structures of compound **13-19**. Hydrogen atoms have been omitted for clarity. Thermal ellipsoids are drawn at the 30% probability level.

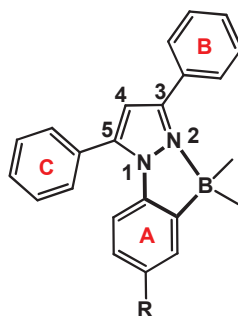
Table 3A.1: Comparison of selected bond lengths [\AA] and bond angles [deg] for compounds **13-19**.

Compound	13	14	15 (Molecule 1)	15 (Molecule 2)	16
B1-C1	1.616(2)	1.626(2)	1.611(3)	1.611(3)	1.606(3)
B1-C2	1.606(2)	1.608(2)	1.601(3)	1.613(3)	1.611(3)
B1-C3	1.609(2)	1.609(2)	1.611(3)	1.621(3)	1.613(3)
B1-N2	1.651(2)	1.6580(18)	1.670(3)	1.635(3)	1.654(2)
C1-B1-C2	115.24(14)	114.18(13)	113.63(18)	114.25(19)	115.23(18)
C1-B1-C3	109.54(13)	109.78(12)	112.33(18)	114.12(18)	114.15(16)
C2-B1-C3	114.76(14)	115.60(13)	113.50(18)	113.03(18)	111.95(17)
C1-B1-N2	110.51(13)	112.07(12)	112.83(17)	109.46(17)	107.69(16)
C2-B1-N2	110.36(13)	108.96(11)	108.45(17)	109.66(17)	110.95(15)
C3-B1-N2	94.55(11)	94.65(10)	94.59(15)	94.47(15)	94.91(13)

Compound	17	18	19 (Molecule 1)	19 (Molecule 2)
B1-C1	1.611(3)	1.611(4)	1.608(4)	1.614(4)
B1-C2	1.616(3)	1.608(4)	1.613(4)	1.615(4)
B1-C3	1.602(3)	1.605(4)	1.620(4)	1.624(4)
B1-N2	1.642(2)	1.672(4)	1.637(4)	1.626(4)
C1-B1-C2	113.25(16)	114.2(2)	114.1(3)	115.1(2)
C1-B1-C3	114.80(16)	110.9(2)	114.5(3)	113.8(2)
C2-B1-C3	112.05(15)	114.4(2)	114.2(2)	113.9(2)
C1-B1-N2	109.05(14)	111.2(2)	108.6(2)	108.9(2)
C2-B1-N2	111.69(15)	109.8(2)	114.2(2)	108.6(2)
C3-B1-N2	94.49(13)	94.79(18)	94.1(2)	94.3(2)

Single crystals of boron complexes **13-19** were grown from $\text{CH}_2\text{Cl}_2/\text{hexane}$ and analysed using single crystal X-ray diffraction studies. The molecular structures of compounds **13-19** are shown in Figure 3A.5; selected bond lengths and bond angles are summarized in Table 3A.1. Inter planar angles and crystal structure determination data for **13-19** are listed in Table 3A.2 and 3A.3 respectively.

Table 3A.2: Comparison of deviation of boron atom from $\text{C}_2\text{N}_2\text{B}$ plane [\AA] and inter planar angles [deg] for **13-19**.



	13	14	15 (Molecule 1)	15 (Molecule 2)	16
Deviation of B1 from $\text{C}_2\text{N}_2\text{B}$ Plane (\AA)	-0.0667	-0.0419	-0.0142	0.0056	-0.0218
Pyrazole//PlaneA	13.09(4)	11.037(51)	5.851(69)	1.492(71)	7.526(65)
Pyrazole//PlaneB	31.725(26)	36.567(57)	41.116(96)	85.735(93)	49.607(74)
Pyrazole//PlaneC	54.392(51)	62.446(53)	70.858(87)	84.071(11)	77.471(69)

	17	18	19 (Molecule 1)	19 (Molecule 2)
Deviation of B1 from $\text{C}_2\text{N}_2\text{B}$ Plane (\AA)	0.0236	-0.0288	-0.0072	-0.0083
Pyrazole//PlaneA	9.959(55)	3.182(102)	0.955(87)	0.994(95)
Pyrazole//PlaneB	57.371(71)	28.836(96)	84.904(115)	81.847(94)
Pyrazole//PlaneC	63.738(71)	80.239(98)	62.454(116)	56.414(12)

In all these compounds, the boron atom adopts a slightly distorted tetrahedral geometry and deviate from the five-membered plane defined by $\text{C}_2\text{N}_2\text{B}$ (pyrazole two nitrogen atoms, boron atom and phenyl carbons directly attached to boron and nitrogen); the distance ranging from 0.0072 to 0.0667 \AA (Table 3A.2). The B–N and B–C distances are in the typical range (Table 3A.1) and are consistent with values reported in literature for tetra- coordinated N,C- chelate boron complexes.^{45,47}

Table 3A.3.1: Crystal data and structure refinement parameters for compounds **13-16**.

Compound	13	14	15	16
Empirical formula	C ₂₃ H ₂₀ BClN ₂	C ₂₄ H ₂₃ N ₂ B	C ₄₁ H ₃₅ N ₂ BSi	C ₄₁ H ₄₂ B ₂ N ₂
Formula weight	370.67	350.25	594.61	584.39
Temperature/K	296.15	296.15	296.15	296.15
Crystal system	Monoclinic	Monoclinic	Triclinic	Triclinic
Space group	<i>P</i> 2 ₁ / <i>n</i>	<i>P</i> 2 ₁ / <i>n</i>	<i>P</i> -1	<i>P</i> -1
<i>a</i> /Å	7.0715(2)	11.9900(3)	10.4101(2)	11.3564(3)
<i>b</i> /Å	25.5143(9)	13.7454(4)	19.6137(4)	11.6102(3)
<i>c</i> /Å	11.0025(4)	12.7864(3)	19.7075(5)	15.7877(4)
α /°	90	90	117.9430(10)	73.720(2)
β /°	100.280(2)	109.2150(10)	93.9040(10)	70.414(2)
γ /°	90	90	104.2370(10)	62.8190(10)
Volume/Å ³	1953.25(11)	1989.90(9)	3365.68(13)	1724.38(8)
<i>Z</i>	4	4	4	2
ρ_{calcd} /g cm ⁻³	1.260	1.169	1.173	1.126
μ /mm ⁻¹	0.205	0.068	0.101	0.064
<i>F</i> (000)	776.0	744.0	1256.0	624.0
2 θ range for data collection/°	3.192 to 61.294	4.49 to 57.534	4.286 to 52.854	1.39 to 25.50
Index ranges	-10 ≤ <i>h</i> ≤ 9, -36 ≤ <i>k</i> ≤ 36, -15 ≤ <i>l</i> ≤ 15	-15 ≤ <i>h</i> ≤ 16, -16 ≤ <i>k</i> ≤ 18, -17 ≤ <i>l</i> ≤ 17	-13 ≤ <i>h</i> ≤ 11, -24 ≤ <i>k</i> ≤ 24, -24 ≤ <i>l</i> ≤ 24	-10 ≤ <i>h</i> ≤ 13, -14 ≤ <i>k</i> ≤ 14, -19 ≤ <i>l</i> ≤ 19
Reflns. collected	34519	31866	41489	24522
Independent reflns	5996 [<i>R</i> _{int} = 0.0537, <i>R</i> _{sigma} = 0.0422]	5136 [<i>R</i> _{int} = 0.0390, <i>R</i> _{sigma} = 0.0284]	13673 [<i>R</i> _{int} = 0.0442, <i>R</i> _{sigma} = 0.0534]	6413 <i>R</i> (int) = 0.0465]
Data/restraints/parameters	5996/0/246	5136/0/248	13673/0/815	6413 / 0 / 414
GOF on <i>F</i> ²	1.020	1.017	1.026	1.034
Final <i>R</i> indices [<i>I</i> > 2σ(<i>I</i>)]	<i>R</i> ₁ = 0.0499, <i>wR</i> ₂ = 0.1156	<i>R</i> ₁ = 0.0476, <i>wR</i> ₂ = 0.1195	<i>R</i> ₁ = 0.0503, <i>wR</i> ₂ = 0.1143	<i>R</i> ₁ = 0.0497, <i>wR</i> ₂ = 0.1393
<i>R</i> indices (all data)	<i>R</i> ₁ = 0.0901, <i>wR</i> ₂ = 0.1330	<i>R</i> ₁ = 0.0793, <i>wR</i> ₂ = 0.1376	<i>R</i> ₁ = 0.0935, <i>wR</i> ₂ = 0.1352	<i>R</i> ₁ = 0.0747, <i>wR</i> ₂ = 0.1660
Largest diff. peak and hole [e Å ⁻³]	0.20 and -0.34	0.19 and -0.17	0.21 and -0.21	0.207 and -0.197

The interplanar angle between the pyrazole and N-phenyl (Plane A or N-naphthyl in compound **19**) is 13.09 ° (for **13**), 11.037 ° (for **14**), 5.851 ° & 1.492 ° (for **15**), 7.52 ° (for **16**), 9.959 ° (for **17**), 3.182 ° (for **18**), and 0.955 ° & 0.944 ° (for **19**) which indicates pyrazole and N-phenyl skeleton have slight distortion, hence the groups

directly attached to the 4-position of N-phenyl show pronounced effect on photophysical properties. The interplanar angle between the pyrazole and the phenyl rings (Plane B & C) at 3 & 5 varies from 28.836 ° to 85.735 °.

Table 3A.3.2: Crystal data and structure refinement parameters for compounds **17-19**.

Crystal parameters	17	18	19
Empirical formula	C ₃₅ H ₂₈ BN ₃	C ₃₅ H ₃₀ N ₃ B	C ₂₇ H ₂₃ N ₂ B
Formula weight	501.41	503.43	386.28
Temperature/K	296.15	296.15	296.15
Crystal system	Monoclinic	Monoclinic	Triclinic
Space group	<i>P</i> -1	<i>P</i> 2 ₁	<i>P</i> -1
<i>a</i> /Å	9.3011(8)	9.7030(4)	8.8710(3)
<i>b</i> /Å	10.3000(9)	5.8707(2)	10.3279(4)
<i>c</i> /Å	15.9512(14)	25.2793(9)	24.3577(8)
α /°	82.043(5)	90	90.659(2)
β /°	88.324(6)	95.252(2)	94.834(2)
γ /°	65.375(5)	90	107.777(2)
Volume/Å ³	1375.1(2)	1433.95(9)	2115.88(13)
<i>Z</i>	2	2	4
ρ_{calcd} /g cm ⁻³	1.211	1.166	1.213
μ /mm ⁻¹	0.071	0.068	0.070
<i>F</i> (000)	528.0	532.0	816.0
2 θ range for data collection/°	2.58 to 61.162	6.716 to 52.232	4.144 to 51.986
Index ranges	-13 ≤ <i>h</i> ≤ 13, -14 ≤ <i>k</i> ≤ 14, -22 ≤ <i>l</i> ≤ 22	-11 ≤ <i>h</i> ≤ 11, -5 ≤ <i>k</i> ≤ 7, -31 ≤ <i>l</i> ≤ 31	-10 ≤ <i>h</i> ≤ 10, -12 ≤ <i>k</i> ≤ 11, -30 ≤ <i>l</i> ≤ 30
Reflns. Collected	23418	11245	27736
Independent reflns	8381 [<i>R</i> _{int} = 0.0548, <i>R</i> _{sigma} = 0.0642]	5089 [<i>R</i> _{int} = 0.0331, <i>R</i> _{sigma} = 0.0441]	8271 [<i>R</i> _{int} = 0.0622, <i>R</i> _{sigma} = 0.0628]
Data/restraints/ Parameters	8381/0/354	5089/1/356	8271/0/546
GOF on <i>F</i> ²	1.053	1.031	1.032
Final <i>R</i> indices [<i>I</i> > 2 σ (<i>I</i>)]	<i>R</i> ₁ = 0.0649, <i>wR</i> ₂ = 0.1697	<i>R</i> ₁ = 0.0425, <i>wR</i> ₂ = 0.0968	<i>R</i> ₁ = 0.0669, <i>wR</i> ₂ = 0.1620
<i>R</i> indices (all data)	<i>R</i> ₁ = 0.1337, <i>wR</i> ₂ = 0.2059	<i>R</i> ₁ = 0.0650, <i>wR</i> ₂ = 0.1080	<i>R</i> ₁ = 0.1113, <i>wR</i> ₂ = 0.1852
Largest diff. peak and hole [e Å ⁻³]	0.31 and -0.21	0.12 and -0.12	0.30 and -0.18

3A.2.2 Photophysical studies

The photophysical properties of the newly synthesized compounds were studied in four different solvents of varying polarity and the relevant data are summarized in Table 3A.4. A comparison of the UV-Vis absorption and fluorescence emission spectra of the boron complexes **12** - **19** recorded in dichloromethane is displayed in Figure 3A.6 and Figure 3A.8 respectively

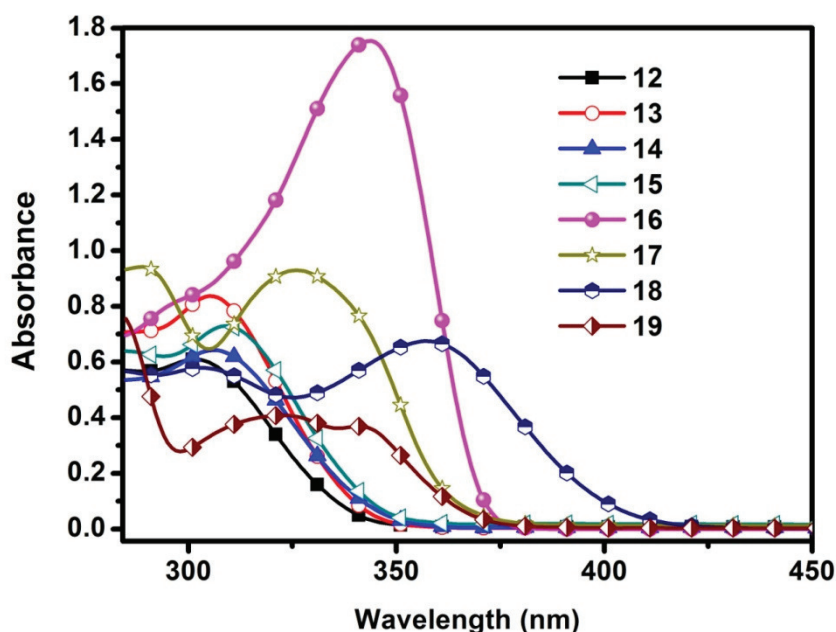


Figure 3A.6: Absorption spectra of **12-19** in dichloromethane (concentration: 4×10^{-5} M).

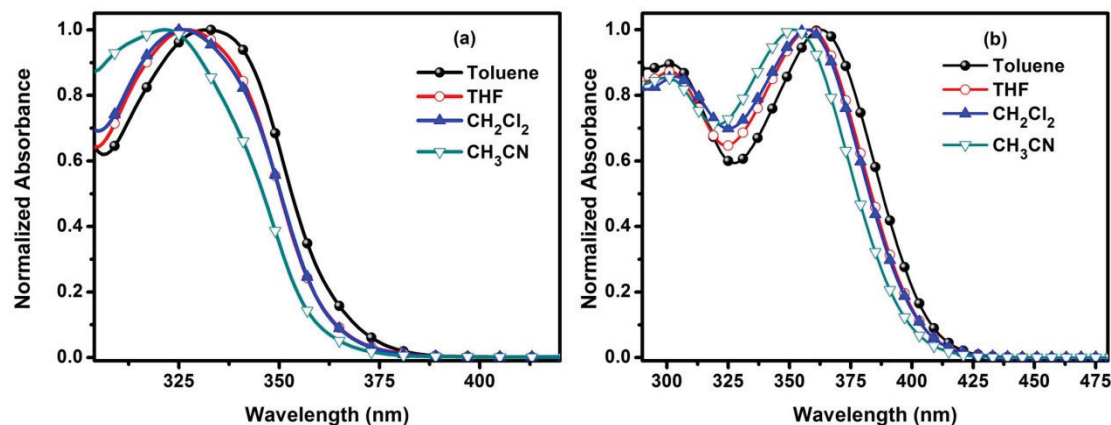


Figure 3A.7: Absorbance spectra of compounds **17** (a) and **18** (b) with increasing solvent polarity (concentration: 4×10^{-5} M).

Table 3A.4: Photophysical data of **12-19** in different solvents.

Compound	Solvent	λ_{\max}^a (nm)	ϵ_{\max} ($M^{-1} \text{ cm}^2 \times 10^3$)	$\lambda_{\text{em}}^{a,b}$ (nm)	Φ_F^c	Stokes shift (nm)
12	Toluene	304	20.3	422	0.03	118
	THF	302	20.5	422	0.02	120
	CH ₂ Cl ₂	302	15.2	422	0.01	120
	CH ₃ CN	299	18.5	425	N.D	126
13	Toluene	307	20.7	416	0.13	109
	THF	306	18.8	418	0.08	112
	CH ₂ Cl ₂	306	20.9	419	0.08	113
	CH ₃ CN	303	22.3	420	0.06	117
14	Toluene	309	14.4	434	0.16	125
	THF	308	15.6	438	0.14	130
	CH ₂ Cl ₂	306	16.0	440	0.13	134
	CH ₃ CN	305	16.1	443	0.13	138
15	Toluene	311	18.2	403	0.06	92
	THF	311	20.1	408	0.05	97
	CH ₂ Cl ₂	308	18.2	409	0.04	101
	CH ₃ CN	307	19.0	411	0.03	104
16	Toluene	344	35.4	395	0.23	51
	THF	344	39.3	392	0.30	48
	CH ₂ Cl ₂	344	43.8	393	0.28	49
	CH ₃ CN	342	39.07	390	0.27	48
17	Toluene	332	20.67	450	0.87	117
	THF	327	21.11	464	0.76	137
	CH ₂ Cl ₂	326	23.25	465	0.87	139
	CH ₃ CN	322	25.60	480	0.67	158
18	Toluene	363	19.26	504	0.57	141
	THF	358	20.95	526	0.42	168
	CH ₂ Cl ₂	357	16.88	533	0.43	176
	CH ₃ CN	352	17.07	559	0.15	207
19	Toluene	322	9.21	453	0.57	131
	THF	322	10.05	456	0.38	134
	CH ₂ Cl ₂	323	10.20	454	0.50	131
	CH ₃ CN	321	9.69	461	0.40	140

^a Lowest-energy absorption maximum (Concentration: 4.00×10^{-5} M). ^b Excited at the absorption maximum. ^c Absolute fluorescence quantum yields were measured using an integrating sphere. N.D = not detected.

Dichloromethane solutions of newly synthesized complexes **12-19** absorbs between 302-357 nm with molar extinction coefficients ranging from 10,200 to 43,850 $M^{-1} \text{ cm}^{-1}$. Interestingly compound **19** exhibit red shifted absorption ($\lambda_{\max} = 323$ nm) compared to compound **12** ($\lambda_{\max} = 302$ nm), due to increased conjugation.

Compounds **17** and **18** also show red shifted absorption bands due to electron donating nature of carbazole and $-\text{NPh}_2$ groups respectively. The λ_{max} of compound **16** shows a red shift compared to compound **12** with maximum molar extinction coefficient ($\epsilon = 43,850 \text{ M}^{-1} \text{ cm}^{-1}$). Most of these compounds do not show any solvatochromism except compound **17** & **18**. The absorption maxima got blue shifted with increasing solvent polarity (Figure 3A.7).

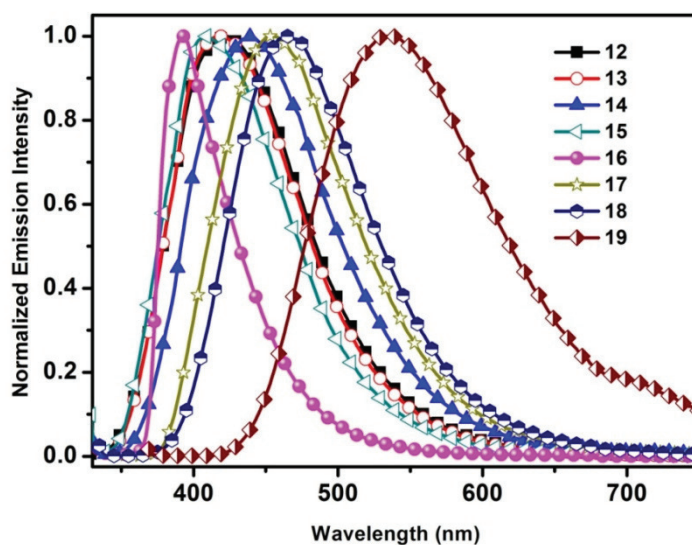


Figure 3A.8: A comparison of normalized fluorescence spectra of compounds **12-19** in dichloromethane (concentration: $4 \times 10^{-5} \text{ M}$).

The steady state fluorescence spectra of compounds **12-19** were recorded by exciting at their absorption maxima and the relevant data are summarized in Table 3A.4. The emission maxima of these compounds ranged from 393 to 533 nm in dichloromethane solution, suggesting that the substituents at 4-position of N-phenyl is indeed effective in tuning the emission maxima of this type of N,C- chelate organoboron compounds. As compared with emission maxima of compound **12**, compounds **13** and **15** have shown slightly blue shifted emission due to the presence of electron withdrawing chlorine and triphenylsilyl groups respectively. Compound **16** shows blue shifted emission ($\lambda_{\text{em}} = 393 \text{ nm}$) with smaller Stokes shift (49 nm) over compound **12** ($\lambda_{\text{em}} = 422 \text{ nm}$, Stokes shift 120 nm), which can be attributed to the

electron withdrawing nature of tri-coordinated boron present in compound **16**. Compared to all other pyrazole N,C- chelated boron compounds, compounds **17** and **18** exhibit highly red shifted emission due to the intramolecular charge transfer transitions from carbazole and -NPh₂ groups respectively. These charge transfer transitions are further supported by the positive solvatochromic emission of compound **17** and **18** with increase in solvent polarity (Figure 3A.9).

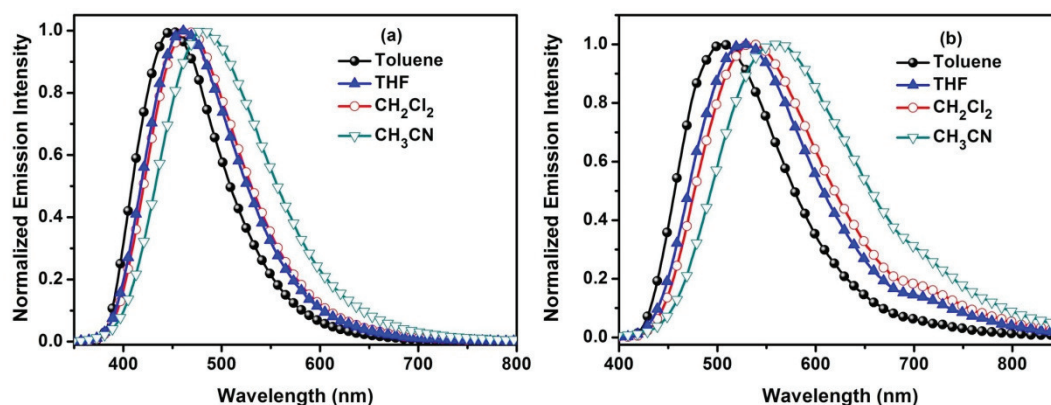


Figure 3A.9: Normalized fluorescence spectra of compounds **17** (a) and **18** (b) with increasing solvent polarity (concentration: 4×10^{-5} M).

The absolute fluorescence quantum yields in solutions were measured using an integrating sphere method. Compounds **12-15** are weakly fluorescent (Figure 3A.10) with quantum yields ranging from 0.01 to 0.16. However compounds **16-19** exhibit intense fluorescence (Figure 3A.10) with moderate to good quantum yields; highest quantum yield has been observed for carbazole substituted compound **16** ($\Phi_F = 0.87$).

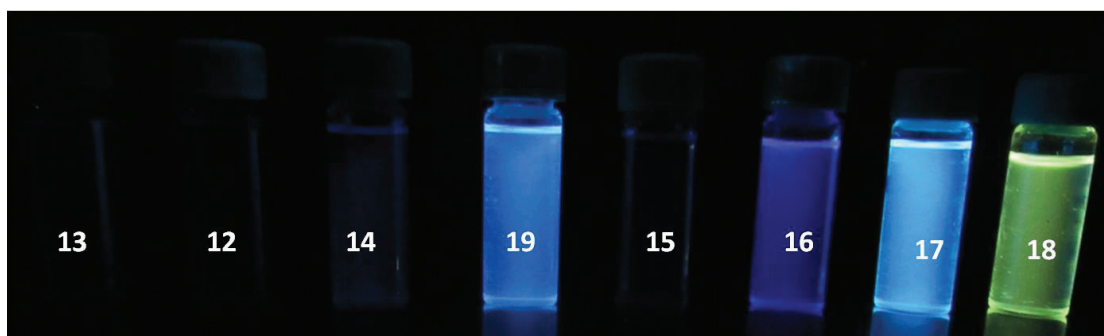


Figure 3A.10: The fluorescence photograph of compounds **12-19** in dichloromethane solution. Irradiation was performed with a UV lamp with a wavelength of 365 nm.

3A.2.3 Electrochemical studies.

The electrochemical properties of compounds **12-19** were studied by cyclic voltammetry at a scan rate of 100 mV/s using $n\text{Bu}_4\text{NPF}_6$ as a supporting electrolyte (0.1 M) in CH_3CN solution under nitrogen atmosphere and the data are summarized in Table 3A.5. The cyclic voltammograms of compounds **12-19** are shown in Figure 3A.11. All these compounds exhibit one irreversible reduction wave.

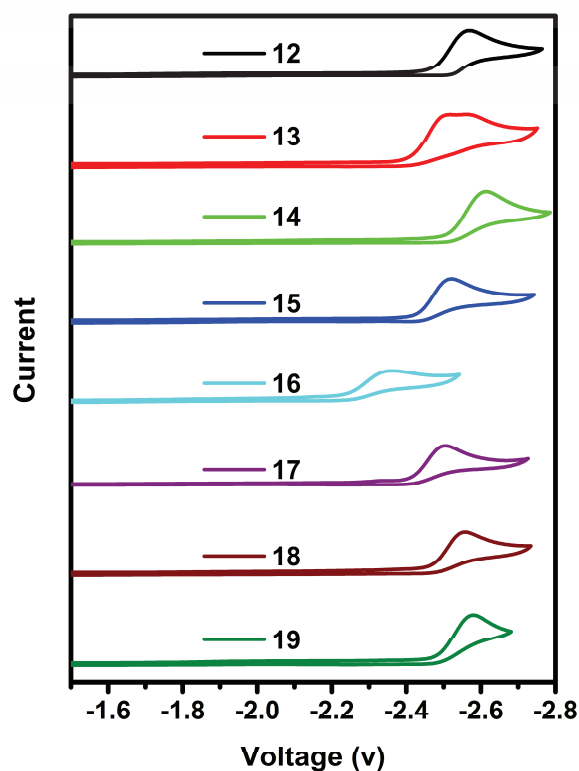


Figure 3A.11: Cyclic voltammograms of **12-19** recorded in CH_3CN containing 0.1M $n\text{Bu}_4\text{N}(\text{PF}_6)$ as supporting electrolyte; scan rate 100 mV/s. Referenced relative to Fc/Fc^+ couple.

Table 3A.5: Electrochemical data of **12-19**.

Compound	E _{pc}
12	-2.56
13	-2.54
14	-2.61
15	-2.52
16	-2.47
17	-2.50
18	-2.55
19	-2.58

3A.3 Conclusion

In conclusion, a series of pyrazole based N,C- chelate boron compounds (**12-19**) have been designed and synthesized by varying substituents at the 4-position of N-phenyl which helps in fine tuning the emission maxima of this class of compounds. Compounds **12-15** show weak fluorescence ranging from $\Phi_F = 0.01$ to 0.13. Moreover compounds **17&18** exhibit solvent dependent fluorescence due to charge transfer transitions from carbazole or $-NPh_2$ groups respectively. The electrochemical studies reveal that these compounds are electron deficient and exhibit one electron irreversible reduction process in cyclic voltammetry. All these properties indicate that these compounds could be useful in organic electronics and imaging applications.

3A.4 Experimental section

3A.4.1 General information

All reagents and starting materials were purchased from Sigma-Aldrich, Alfa Aesar and Spectrochem chemical companies and used as received unless otherwise noted. Tetrahydrofuran and toluene were distilled from Na/benzophenone prior to use. Dichloromethane, N,N-Dimethylformamide and acetonitrile were distilled from CaH_2 . 9-(4-Iodophenyl)-9H-carbazole,⁵⁰ dimesitylfluoroborane,⁵¹ 2-iodonaphthalene⁵² were synthesised by adopting the reported procedures. All 400 MHz 1H , 100 MHz ^{13}C and 128 MHz ^{11}B NMR spectra were recorded on a Bruker ARX 400 spectrometer operating at 400 MHz. All 1H and ^{13}C NMR spectra were referenced internally to solvent signals. ^{11}B NMR spectra were referenced externally to $BF_3 \cdot Et_2O$ in $CDCl_3$ ($\delta = 0$). ESI mass spectra were recorded using a Bruker microTOF-QII mass spectrometer. The absorbance spectra were recorded with a JASCO V-730 UV-Visible spectrometer and the fluorescence spectra were recorded using Edinburgh FS5 spectrofluorometer. Absolute fluorescence quantum yields of **12-19** in various

solvents were measured by integrating sphere technique using Edinburgh FS5 spectrofluorometer. Single-crystal X-ray diffraction data were collected on a Bruker APEX-II diffractometer equipped with an Oxford Instruments low-temperature attachment. The data were collected at 296.5 K using, Mo-K α radiation (0.71073 Å). SADABS absorption corrections were applied. The structures were solved and refined with SHELX suite of programs. All non-hydrogen atoms were refined with anisotropic displacement coefficients. The H atoms were placed at calculated positions and were refined as riding atoms.

3A.4.2 Synthetic procedure and spectral characterization of 1-19

General procedure for synthesis of compound 1-5

Substituted phenylhydrazine (1.1 equivalent) and 1,3-diphenylpropane-1,3-dione (1 equivalent) were dissolved in methanol / acetic acid (1:1) and heated to reflux for 24 h. The reaction mixture was cooled to room temperature and poured into water, extracted with ethyl acetate three times. The combined extracts were washed with saturated NaHCO₃ solution, distilled water, brine and dried over Na₂SO₄. The solvent was removed under reduced pressure and the resulting residue was purified by silica gel column chromatography using *n*-hexane / ethylacetate mixture as eluent.

3A.4.2.1. 1,3,5-Triphenyl-1H-pyrazole (1)

The quantities involved are as follows: 1,3-diphenylpropane-1,3-dione (6.00 g, 26.75 mmol), phenylhydrazine (2.89 mL, 29.43 mmol), methanol (30 mL), acetic acid (30 mL). Yield: 6.58 g, (83%). mp: 141 °C. ¹H NMR (400 MHz, CDCl₃): δ = 7.97 (d, *J* = 8 Hz, 2H, ArH), 7.47 – 7.29 (m, 13H, ArH), 6.85 (s, 1H, pyrazole-H) ppm. ¹³C NMR (100 MHz, CDCl₃): δ = 151.97, 144.41, 140.15, 133.07, 130.57, 128.92, 128.75, 128.69, 128.50, 128.32, 128.04, 127.44, 125.85, 125.31, 105.26. HR-MS (ESI): calcd. for C₂₁H₁₇N₂ ([M + H]⁺) : 297.1386, found : 297.1373.

3A.4.2. 2. 1-(4-Chlorophenyl)-3,5-diphenyl-1H-pyrazole (2)

The quantities involved are as follows: 1,3-diphenylpropane-1,3-dione (4.84 g, 21.59 mmol), 4-chlorophenylhydrazine hydrochloride (4.25 g, 23.74 mmol), methanol (25 mL), acetic acid (25 mL). Yield: 4.57 g, (65%). mp: 110 °C. ¹H NMR (400 MHz, CDCl₃): δ = 7.94 (d, *J* = 7.7 Hz, 2H, ArH), 7.45 (t, *J* = 7.5 Hz, 2H, ArH), 7.38 – 7.28 (m, 10H, ArH), 6.84 (s, 1H, pyrazole-H) ppm. ¹³C NMR (100 MHz, CDCl₃): δ = 152.32, 144.65, 138.61, 133.24, 132.76, 130.33, 129.20, 128.90, 128.84, 128.79, 128.74, 128.38, 126.48, 126.00, 105.71 ppm. HR-MS (ESI): calcd. for C₂₁H₁₆N₂Cl₁ ([M + H]⁺): 331.0997, found : 331.0981.

3A.4.2.3. 3,5-Diphenyl-1-(p-tolyl)-1H-pyrazole (3)

The quantities involved are as follows: 1,3-diphenylpropane-1,3-dione (4.00 g, 17.83 mmol), 4-methylphenylhydrazine hydrochloride (3.11 g, 19.62 mmol), methanol (25 mL), acetic acid (25 mL). Yield: 4.43 g, (80%). mp: 95 °C. ¹H NMR (400 MHz, CDCl₃): δ = 7.96 (d, *J* = 8 Hz, 2H, ArH), 7.45 (t, *J* = 8 Hz, 2H, ArH), 7.38 – 7.27 (m, 8H, ArH), 7.17 (d, *J* = 8 Hz, 2H, ArH), 6.84 (s, 1H, pyrazole-H) ppm. ¹³C NMR (100 MHz, CDCl₃): δ = 151.84, 144.39, 137.87, 137.42, 133.28, 130.80, 129.60, 128.83, 128.73, 128.54, 128.30, 128.01, 125.91, 125.27, 105.04, 21.21 ppm. HR-MS (ESI): calcd. for C₂₂H₁₉N₂ ([M + H]⁺): 311.1543, found : 311.1526.

3A.4.2.4. 1-(4-Bromophenyl)-3,5-diphenyl-1H-pyrazole (4)

The quantities involved are as follows: 1,3-diphenylpropane-1,3-dione (5.00 g, 22.30 mmol), 4-bromophenylhydrazine hydrochloride (5.48 g, 24.53 mmol), methanol (40 mL), acetic acid (40 mL). Yield: 6.27 g, (75%). mp: 137 °C. ¹H NMR (400 MHz, CDCl₃): δ = 7.99 (d, *J* = 7.5 Hz, 2H, ArH), 7.51 – 7.47 (m, 4H, ArH), 7.42 – 7.28 (m, 8H, ArH), 6.86 (s, 1H, pyrazole-H) ppm. ¹³C NMR (100 MHz, CDCl₃): δ = 152.42, 144.52, 139.27, 132.93, 132.12, 130.43, 128.89, 128.81, 128.78, 128.68, 128.29,

126.68, 125.94, 121.05, 105.79 ppm. HR-MS (ESI): calcd. for $C_{21}H_{16}N_2Br_1$ ($[M + H]^+$) : 375.0491, found : 375.0464.

3A.4.2.5. 1-(4-Nitrophenyl)-3,5-diphenyl-1H-pyrazole (5)

The quantities involved are as follows: 1,3-diphenylpropane-1,3-dione (7.98 g, 35.58 mmol), 4-nitrophenylhydrazine(6.00 g, 39.14 mmol), methanol (40 mL), acetic acid (40 mL). Yield: 7.28 g, (60%). mp: 125 °C. 1H NMR (400 MHz, $CDCl_3$): δ = 8.19 (d, J = 8 Hz, 2H, ArH), 7.93 (d, J = 8 Hz, 2H, ArH), 7.57 – 7.53 (m, 2H, ArH), 7.48 – 7.38(m, 6H, ArH), 7.33 – 7.30 (m, 2H, ArH), 6.87 (s, 1H, pyrazole-H) ppm. ^{13}C NMR (100 MHz, $CDCl_3$): δ = 153.43, 145.93, 145.08, 145.04, 132.42, 130.22, 129.25, 129.08, 128.97, 128.92, 128.74, 126.05, 124.62, 124.56, 107.34 ppm. HR-MS (ESI): calcd. for $C_{21}H_{16}N_3O_2$ ($[M + H]^+$) : 342.1237, found : 342.1200.

3A.4.2.6. 4-(3,5-diphenyl-1H-pyrazol-1-yl)aniline (6)

Compound **5** (4.00 g, 11.72 mmol), 10% Pd/C (0.15 g, 0.14 mmol) and hydrazine monohydrate (6.82 mL, 140.64 mmol) were mixed in ethanol (150 mL). The resulting mixture was heated to reflux for 6 hours under nitrogen atmosphere and then filtered through celite in hot condition. The filtrate was evaporated to dryness and the obtained residue was purified by silica gel column chromatography using dichloromethane and *n*-hexane as eluent. Yield: 3.46 g, (95%). mp: 160 °C. 1H NMR (400 MHz, $CDCl_3$): δ = 7.92 (d, J = 8 Hz, 2H, ArH), 7.45 – 7.31 (m, 8H, ArH), 7.14 (d, J = 8 Hz, 2H, ArH), 6.81 (s, 1H, pyrazole-H), 6.62 (d, J = 8.6 Hz, 2H, ArH), 3.74 (brs, 2H, Ar NH_2) ppm. ^{13}C NMR (100 MHz, $CDCl_3$): δ = 151.45, 146.09, 144.34, 133.39, 131.68, 130.82, 128.77, 128.72, 128.49, 128.15, 127.90, 126.89, 125.87, 115.14, 104.42 ppm. HR-MS (ESI): calcd. for $C_{21}H_{18}N_3$ ($[M + H]^+$) : 312.1495, found : 312.1472.

3A.4.2.7. 4-(3,5-Diphenyl-1H-pyrazol-1-yl)-N,N-diphenylaniline (7)

Compound **6** (3.00 g, 9.63 mmol), iodobenzene (2.69 mL, 24.08 mmol), potassium *tert*-butoxide (3.24 g, 28.9 mmol), CuI (0.055 g, 0.29 mmol), 1,10-phenanthroline (0.052 g, 0.29 mmol) were taken in 250 mL two necked round bottom flask, under nitrogen atmosphere and 75 mL of anhydrous degassed toluene was added. The reaction mixture was heated to reflux for 24 h. The reaction mixture was cooled to room temperature diluted with ethyl acetate and passed through silicagel. The solvent was removed under reduced pressure and the resultant residue was purified by silica gel column chromatography using ethylacetate and *n*-hexane as eluent. Yield: 3.12 g, (70%). mp: 189 °C. ¹H NMR (400 MHz, CDCl₃): δ = 7.94 (d, *J* = 8 Hz, 2H, ArH), 7.44 (t, *J* = 8 Hz, 2H, ArH), 7.36 – 7.22 (m, 12H, ArH), 7.13 – 7.03 (m, 8H, ArH), 6.83 (s, 1H, pyrazole-H) ppm. ¹³C NMR (100 MHz, CDCl₃): δ = 151.83, 147.53, 147.29, 144.43, 134.44, 133.22, 130.77, 129.47, 128.86, 128.75, 128.56, 128.39, 128.05, 126.34, 125.92, 124.75, 123.40, 123.36, 104.94 ppm. HR-MS (ESI): calcd. for C₃₃H₂₆N₃ ([M + H]⁺) : 464.2121, found : 464.2134.

3A.4.2.8. 9-(4-(3,5-Diphenyl-1H-pyrazol-1-yl)phenyl)-9H-carbazole (8)

3,5-Diphenyl-1H-pyrazole (1.79 g, 8.13 mmol), 9-(4-iodophenyl)-9H-carbazole (2.00 g, 5.42 mmol), CuI (0.31 g, 1.62 mmol), 1,10-phenanthroline (0.39 g, 2.17 mmol), Cs₂CO₃ (4.41 g, 13.55 mmol) were taken in 100 mL two necked round bottom flask under nitrogen atmosphere and 50 mL of anhydrous degassed DMF was added. The reaction mixture was heated to reflux for 24 h. The reaction mixture was cooled to room temperature, diluted with ethyl acetate and passed through silica gel. The solvent was removed under reduced pressure and the resultant residue was purified by silica gel column chromatography using ethylacetate and *n*-hexane as eluent. Yield: 1.50 g, (60%). mp: 140 °C. ¹H NMR (400 MHz, CDCl₃): δ = 8.16 (d, *J* = 8 Hz, 2H,

ArH), 7.99 (d, $J = 8.0$ Hz, 2H, ArH), 7.65 – 7.56 (m, 4H, ArH), 7.50 – 7.39 (m, 12H, ArH), 7.34 – 7.30 (m, 2H, ArH), 6.91 (s, 1H, pyrazole-H) ppm. ^{13}C NMR (100 MHz, CDCl_3): $\delta = 152.50, 144.73, 140.76, 139.04, 136.79, 132.98, 130.59, 128.99, 128.86, 128.82, 128.78, 128.34, 127.50, 126.63, 126.19, 125.99, 123.63, 120.51, 120.33, 109.78, 105.78$ ppm. HR-MS (ESI): calcd. for $\text{C}_{33}\text{H}_{24}\text{N}_3$ ($[\text{M} + \text{H}]^+$) : 462.1965, found : 462.1995.

3A.4.2.9. 1-(Naphthalen-2-yl)-3,5-diphenyl-1H-pyrazole (9)

Compound **9** was prepared by following a similar synthetic procedural that used for compound **8**. The quantities involved are as follows: 3,5-diphenyl-1H-pyrazole (2.62 g, 11.92 mmol), 2-iodonaphthalene (2.02 g, 7.95 mmol), CuI (0.45 g, 2.39 mmol), 1,10-phenanthroline (0.57 g, 3.18 mmol), Cs_2CO_3 (5.18 g, 15.9 mmol). Yield: 1.79 g, (65%). mp: 114 °C. ^1H NMR (400 MHz, CDCl_3): $\delta = 7.98$ (d, $J = 8$ Hz, 2H, ArH), 7.92 (d, $J = 1.7$ Hz, 1H, ArH), 7.86 – 7.77 (m, 3H, ArH), 7.52 – 7.45 (m, 5H, ArH), 7.39 – 7.21 (m, 6H, ArH), 6.89 (s, 1H, pyrazole-H) ppm. ^{13}C NMR (100 MHz, CDCl_3): $\delta = 152.27, 144.66, 137.76, 133.36, 133.18, 132.33, 130.69, 128.88, 128.79, 128.64, 128.46, 128.28, 128.15, 127.83, 126.76, 126.48, 125.97, 123.76, 123.48, 105.50$ ppm. HR-MS (ESI): calcd. for $\text{C}_{25}\text{H}_{19}\text{N}_2$ ($[\text{M} + \text{H}]^+$) : 347.1543, found : 347.1558

3A.4.2.10. 1-(4-(Dimesitylboryl)phenyl)-3,5-diphenyl-1H-pyrazole (10)

Compound **4** (4.41 g, 11.75 mmol) was dissolved in anhydrous THF (150 mL) under nitrogen atmosphere and the resulting solution was cooled to -78 °C with stirring. Then, *n*-BuLi (8.1 mL, 12.93 mmol, 1.6 M solution in hexane) was slowly added to the stirred solution over 20 min. After 1h, a solution of dimesitylfluoroborane (3.47 g, 12.93 mmol) in 35 mL of dry THF was added over 10 min. The reaction mixture was allowed to warm to room temperature and stirred for 24 h. Then, water was added to the reaction mixture and extracted with ethyl acetate. The combined extracts were

washed with brine and dried over anhydrous Na_2SO_4 . Solvent was removed under reduced pressure and the obtained residue was purified by silica gel column chromatography using ethyl acetate *n*-hexane as eluent. Yield: 4.67 g, (73%). mp: 195 °C. ^1H NMR (400 MHz, CDCl_3): δ = 8.02 (d, J = 7.5 Hz, 2H), 7.59 (d, J = 8.1 Hz, 2H), 7.50 (t, J = 7.5 Hz, 2H), 7.45 – 7.35 (m, 8H), 6.91 (s, 5H), 2.38 (s, 6H), 2.11 (s, 12H). ^{13}C NMR (100 MHz, CDCl_3): δ = 152.43, 144.86, 144.70, 142.79, 141.61, 140.87, 138.91, 137.13, 133.00, 130.66, 128.89, 128.75, 128.53, 128.49, 128.36, 128.21, 125.96, 124.64, 105.75, 23.55, 21.31. HR-MS (ESI): calcd. for $\text{C}_{39}\text{H}_{37}\text{B}_1\text{N}_2$ ($[\text{M} + \text{H}]^+$): 545.3129, found : 545.3138.

3A.4.2.11. 3,5-Diphenyl-1-(4-(triphenylsilyl)phenyl)-1H-pyrazole (11)

The quantities involved are as follows: Compound **4** (2.00 g, 5.33 mmol), *n*-BuLi (4 mL, 6.40 mmol, 1.6 M solution in hexane), chlorotriphenylsilane (1.88 g, 6.40 mmol). Yield: 2.39 g, (81%). mp: 193 °C. ^1H NMR (400 MHz, CDCl_3): δ = 7.94 (d, J = 8.0 Hz, 2H, ArH), 7.57 (d, J = 6.6 Hz, 8H, ArH), 7.47 – 7.34 (m, 19H, ArH), 6.84 (s, 1H, pyrazole-H) ppm. ^{13}C NMR (100MHz, CDCl_3): δ = 152.28, 144.56, 141.34, 137.11, 136.48, 133.95, 133.65, 133.07, 130.71, 129.84, 128.87, 128.75, 128.63, 128.49, 128.16, 128.06, 125.93, 124.45, 105.70 ppm. HR-MS (ESI): calcd. for $\text{C}_{39}\text{H}_{30}\text{N}_2\text{Si}$ ($[\text{M} + \text{H}]^+$): 555.2251 found : 555.2252.

General procedure for the synthesis of compounds 12-19

N - arylpyrazole (1 equiv) and (*i*-Pr) $_2$ NEt (1 equiv) were dissolved in anhydrous CH_2Cl_2 under nitrogen atmosphere at 0 °C then BBr_3 (3 equiv, 1.0 M in CH_2Cl_2) was added into the solution dropwise. The mixture was allowed to warm up and stirred for 24 h at room temperature. The reaction mixture was cooled to 0 °C, then saturated K_2CO_3 solution was added. The organic layer was separated and aqueous layer was extracted with CH_2Cl_2 (twice). The combined organic layers were washed with brine,

dried over Na₂SO₄ and concentrated. The resulting solid was washed with *n*-hexane, dried and proceed for next reaction without further purification. To a stirred solution of dibromo pyrazole-borane complex in toluene at room temperature was added AlMe₃ (2 equiv, 2 M in hexane). After being stirred at this temperature for 30 min, the reaction was quenched by adding water. The organic layer was separated and aqueous layer was extracted with CH₂Cl₂ (twice). The combined organic layers were washed with brine, dried over Na₂SO₄ and concentrated. The residue was purified by silica gel column chromatography using ethylacetate and *n*-hexane as eluent.

3A.4.2.12. 5,5-Dimethyl-1,3-diphenyl-5H-benzo[d]pyrazolo[1,2-a][1,2,3]diazaborol-4-ium-5-uide (12)

The quantities involved are as follows: Compound **1** (3.00 g, 10.12 mmol), (*i*-Pr)₂NEt (1.75 mL, 10.12 mmol), BBr₃ (1.0 M in CH₂Cl₂, 30.37 mL, 30.37 mmol), AlMe₃ (2 M in toluene, 10.12 mL, 20.24 mmol). Yield: 2.38 g, (70%). mp: 136 °C. ¹H NMR (400 MHz, CDCl₃): δ = 7.83 – 7.80 (m, 2H, ArH), 7.66 – 7.45 (m, 9H, ArH), 7.18 (t, *J* = 8 Hz, 1H, ArH), 6.93 (t, *J* = 8 Hz, 1H, ArH), 6.77 (d, *J* = 8 Hz, 1H, ArH), 6.58 (s, 1H, 4-pyrazole-H), 0.12 (s, 6H, BCH₃) ppm. ¹³C NMR (100 MHz, CDCl₃) δ = 148.47, 140.06, 138.45, 130.36, 129.78, 129.56, 129.14, 129.11, 128.92, 128.48, 126.73, 124.87, 111.87, 110.79, 9.26 (BCH₃) ppm. ¹¹B NMR (128 MHz, CDCl₃): δ = 0.68 (s) ppm. HR-MS (ESI): calcd for C₂₃H₂₂B₁N₂ ([M + H]⁺): 337.1875, found: 337.1865.

3A.4.2.13. 7-Chloro-5,5-dimethyl-1,3-diphenyl-5H-benzo[d]pyrazolo[1,2-a][1,2,3]diazaborol-4-ium-5-uide (13)

The quantities involved are as follows: Compound **2** (3.00 g, 9.07 mmol), (*i*-Pr)₂NEt (1.57 mL, 9.07 mmol), BBr₃ (1.0 M in CH₂Cl₂, 27.20 mL, 27.20 mmol), AlMe₃ (2 M in toluene, 9.07 mL, 18.13 mmol). Yield: 2.05 g, (65%). mp: 176 °C. ¹H NMR (400 MHz, CDCl₃): δ = 7.79 – 7.77 (m, 2H, ArH), 7.64 – 7.57 (m, 5H, ArH), 7.52 – 7.49

(m, 5H, ArH), 7.38 (d, $J = 2.0$ Hz, 1H, ArH), 6.88 (dd, $J = 8.5, 2.2$ Hz, 1H, ArH), 6.66 (d, $J = 8$ Hz, 1H, ArH), 6.58 (s, 1H, Pyrazole-H), 0.99 (s, 6H, BCH₃) ppm. ¹³C NMR (100 MHz, CDCl₃) $\delta = 156.26, 148.79, 140.19, 136.72, 132.68, 130.57, 129.72, 129.69, 129.47, 129.26, 129.08, 128.53, 128.51, 124.85, 112.92, 110.97, 9.06$ ppm. ¹¹B NMR (128 MHz, CDCl₃): $\delta = 0.14$ (s) ppm. HR-MS (ESI): calcd. for C₂₃H₂₁B₁N₂Cl₁ ([M + H]⁺): 371.1485, found : 371.1483.

3A.4.2.14. 5,5,7-Trimethyl-1,3-diphenyl-5H-benzo[d]pyrazolo[1,2-a][1,2,3]diazaborol-4-ium-5-uide (14)

The quantities involved are as follows: Compound **3** (3.00 g, 9.67 mmol), (*i*-Pr)₂NEt (1.68 mL, 9.67 mmol), BBr₃ (1.0 M in CH₂Cl₂, 29.01 mL, 29.01 mmol), AlMe₃ (2 M in toluene, 9.67 mL, 19.34 mmol). Yield: 2.30 g, (68%). mp: 184 °C. ¹H NMR (400 MHz, CDCl₃): $\delta = 7.83 - 7.82$ (m, 2H, ArH), 7.66 – 7.51 (m, 8H, ArH), 7.29 (s, 1H, ArH), 6.75 (d, $J = 8.0$ Hz, 2H, ArH), 6.69 – 6.67 (m, 1H, ArH), 6.58 (s, 1H, ArH), 2.36 (s, 3H, Ar-CH₃), 0.14 (s, 6H, BCH₃) ppm. ¹³C NMR (100 MHz, CDCl₃) $\delta = 156.43, 148.23, 139.67, 136.37, 136.35, 130.36, 130.28, 129.85, 129.75, 129.47, 129.09, 128.96, 128.45, 125.54, 111.62, 110.52, 21.40, 9.31$ (BCH₃) ppm. ¹¹B NMR (128 MHz, CDCl₃): $\delta = 0.29$ (s) ppm. HR-MS (ESI): calcd. for C₂₄H₂₄B₁N₂ ([M + H]⁺): 351.2031, found : 351.2032.

3A.4.2.15. 5,5-Dimethyl-1,3-diphenyl-7-(triphenylsilyl)-5H-benzo[d]pyrazolo[1,2-a][1,2,3]diazaborol-4-ium-5-uide (15)

The quantities involved are as follows: Compound **11** (1.75 g, 3.16 mmol), (*i*-Pr)₂NEt (0.54 mL, 3.16 mmol), BBr₃ (1.0 M in CH₂Cl₂, 9.48 mL, 9.48 mmol), AlMe₃ (2 M in toluene, 3.16 mL, 6.32 mmol). Yield: 1.24 g, (66%). mp: 212 °C. ¹H NMR (400 MHz, CDCl₃): $\delta = 7.85$ (dd, $J = 7.3, 1.6$ Hz, 2H, ArH), 7.81 (s, 1H, ArH), 7.67 – 7.52 (m, 14H, ArH), 7.47 – 7.38 (m, 9H, ArH), 7.13 (d, $J = 8$ Hz, 1H, ArH), 6.80 (d, $J = 8$ Hz,

1H, ArH), 6.62 (s, 1H, ArH), 0.15 (s, 6H, BCH₃) ppm. ¹³C NMR (101 MHz, CDCl₃) δ 155.05, 148.61, 140.39, 139.76, 138.00, 136.54, 135.12, 134.78, 133.49, 131.88, 130.38, 130.10, 129.74, 129.66, 129.61, 129.56, 129.12, 129.06, 128.81, 128.52, 127.99, 127.92, 9.26 (BCH₃) ppm. HR-MS (ESI): calcd for C₄₁H₃₆B₁N₂Si₁ ([M +H]⁺) 595.2743 found: 595.2717.

3A.4.2.16. 7-(Dimesitylboryl)-5,5-dimethyl-1,3-diphenyl-5H-benzo[d]pyrazolo[1,2-a][1,2,3]diazaborol-4-ium-5-uide (16)

The quantities involved are as follows: Compound **10** (2.30 g, 4.22 mmol), (*i*-Pr)₂NEt (0.73 mL, 4.22 mmol), BBr₃ (1.0 M in CH₂Cl₂, 12.67 mL, 12.67 mmol), AlMe₃ (2 M in toluene, 4.22 mL, 8.44 mmol). Yield: 1.68 g, (68%).mp: 267 °C. ¹H NMR (400 MHz, CDCl₃): δ = 7.83 – 7.81 (m, 2H, ArH), 7.70 – 7.64 (m, 3H, ArH), 7.58 – 7.50 (m, 6H, ArH), 7.09 (dd, *J* = 8.2, 1.2 Hz, 1H, ArH), 6.81 (s, 4H, ArH), 6.71 (d, *J* = 8.2 Hz, 1H, ArH), 6.61 (s, 1H, ArH), 2.31 (s, 6H, CH₃), 2.02 (s, 12H, CH₃), 0.09 (s, 6H, BCH₃) ppm. ¹³C NMR (100 MHz, CDCl₃): δ = 155.00, 148.87, 143.64, 142.19, 141.31, 140.92, 140.57, 138.92, 138.36, 134.41, 130.38, 129.84, 129.65, 129.62, 129.07, 128.80, 128.53, 128.19, 111.26, 111.07, 23.67, 21.34, 9.11 (BCH₃) ppm. ¹¹B NMR (128 MHz, CDCl₃): δ = 1.09 (s) ppm only one ¹¹B signal observed may be due to dilute sample. HR-MS (ESI): calcd for C₄₁H₄₃B₂N₂ ([M +H]⁺) 585.3620. found: 585.3592.

3A.4.2.17. 7-(9H-carbazol-9-yl)-5,5-dimethyl-1,3-diphenyl-5H-benzo[d]pyrazolo[1,2-a][1,2,3]diazaborol-4-ium-5-uide (17)

The quantities involved are as follows: Compound **8** (2.30 g, 4.98 mmol), (*i*-Pr)₂NEt (0.87 mL, 4.98 mmol), BBr₃ (1.0 M in CH₂Cl₂, 14.95 mL, 14.95 mmol), AlMe₃ (2 M in toluene, 4.98 mL, 9.96 mmol). Yield: 1.60 g, (64%).mp: 208 °C. ¹H NMR (400 MHz, CDCl₃): δ = 8.15 (d, *J* = 7.5 Hz, 2H, ArH), 7.86 (d, *J* = 5.2 Hz, 2H, ArH), 7.74

– 7.72 (m, 2H, ArH), 7.64 (s, 4H, ArH), 7.54 (d, $J = 6.3$ Hz, 3H, ArH), 7.47 – 7.40 (m, 4H, ArH), 7.30 – 7.27 (m, 2H, ArH), 7.14 – 7.12 (m, 1H, ArH), 6.97 (d, $J = 8$ Hz, 1H, ArH), 6.65 (s, 1H, ArH), 0.20 (s, 6H, BCH₃) ppm. ¹³C NMR (100 MHz, CDCl₃): $\delta = 158.94, 148.92, 141.07, 140.33, 137.13, 136.09, 130.60, 129.78, 129.74, 129.54, 129.31, 129.09, 128.65, 128.58, 128.18, 125.95, 123.42, 120.33, 119.83, 112.84, 110.99, 110.12, 9.23$ (BCH₃) ppm. ¹¹B NMR (128 MHz, CDCl₃): $\delta = 0.42$ (s) ppm. HR-MS (ESI): calcd. for C₃₅H₃₀B₁N₃ ([M +H]⁺) : 504.2612, found : 504.2627. HR-MS (ESI): calcd. for C₃₅H₂₉B₁N₃ ([M +H]⁺) : 502.2455, found : 502.2468.

3A.4.2.18. 7-(diphenylamino)-5,5-dimethyl-1,3-diphenyl-5H-benzo[d]pyrazolo[1,2-a][1,2,3]diazaborol-4-ium-5-uide (18)

The quantities involved are as follows: Compound **7** (2.00 g, 4.31 mmol), (*i*-Pr)₂NEt (0.75 mL, 4.31 mmol), BBr₃ (1.0 M in CH₂Cl₂, 12.94 mL, 12.94 mmol), AlMe₃ (2 M in toluene, 4.31 mL, 8.62 mmol). Yield: 1.34 g, (62%). mp: 205 °C. ¹H NMR (400 MHz, CDCl₃): $\delta = 7.81 - 7.78$ (m, 2H ArH), 7.65 – 7.63 (m, 2H, ArH), 7.56 – 7.48 (m, 6H, ArH), 7.24 – 7.20 (m, 5H, ArH), 7.09 – 7.07 (m, 4H, ArH), 6.99 – 6.95 m, 2H, ArH), 6.65 – 6.55 (m, 3H, ArH), 0.05 (s, 6H, BCH₃) ppm. ¹³C NMR (100 MHz, CDCl₃): $\delta = 157.99, 148.22, 148.18, 146.56, 139.43, 133.83, 130.29, 129.79, 129.48, 129.22, 129.09, 129.04, 128.89, 128.48, 125.37, 124.15, 122.50, 121.04, 112.55, 110.39, 9.22$ (BCH₃) ppm. ¹¹B NMR (128 MHz, CDCl₃): $\delta = 0.93$ (s) ppm. HR-MS (ESI): calcd. for C₃₅H₃₁B₁N₃ ([M +H]⁺) : 504.2612, found : 504.2627.

3A.4.2.19. 12,12-dimethyl-8,10-diphenyl-12H-naphtho[1,2-d]pyrazolo[1,2-a][1,2,3]diazaborol-11-ium-12-uide (19)

The quantities involved are as follows: Compound **9** (1.96 g, 5.66 mmol), (*i*-Pr)₂NEt (0.98 mL, 5.66 mmol), BBr₃ (1.0 M in CH₂Cl₂, 17.00 mL, 17.00 mmol), AlMe₃ (2 M in toluene, 5.66 mL, 11.32 mmol). Yield: 1.53 g, (70%). mp: 248 °C. H NMR (400

MHz, CDCl₃): δ = 8.19 (d, J = 8 Hz, 1H, ArH), 7.84 – 7.82 (m, 2H, ArH), 7.78 (d, J = 8.0 Hz, 1H, ArH), 7.70 – 7.68 (m, 2H, ArH), 7.64 – 7.58 (m, 3H, ArH), 7.55 – 7.48 (m, 3H, ArH), 7.48 – 7.39 (m, 3H, ArH), 6.97 (d, J = 8 Hz, 1H, ArH), 6.59 (s, 1H, ArH), 0.32 (s, 6H, BCH₃) ppm. ¹³C NMR (100 MHz, CDCl₃): δ = 148.37, 139.54, 134.84, 134.56, 132.41, 130.37, 129.93, 129.89, 129.55, 129.35, 129.16, 129.06, 128.60, 128.55, 128.48, 126.20, 125.89, 125.41, 112.03, 110.91, 9.39 (BCH₃) ppm. ¹¹B NMR (128 MHz, CDCl₃): δ = 0.68 (s) ppm. HR-MS (ESI): calcd for C₂₇H₂₄B₁N₂ ([M + H]⁺): 387.2032. found: 387.2034.

3A.5 References

- (1) Wade, C. R.; Broomsgrove, A. E. J.; Aldridge, S.; Gabbai, F. P. *Chem. Rev.***2010**, *110*, 3958.
- (2) Jakle, F. *Coord. Chem. Rev.***2006**, *250*, 1107.
- (3) Entwistle, C. D.; Marder, T. B. *Chem. Mater.***2004**, *16*, 4574.
- (4) Rao, Y.-L.; Amarne, H.; Wang, S. *Coord. Chem. Rev.***2012**, *256*, 759.
- (5) Rao, Y.-L.; Wang, S. *Inorg. Chem.***2011**, *50*, 12263.
- (6) Li, D.; Zhang, H.; Wang, Y. *Chem. Soc. Rev.***2013**, *42*, 8416.
- (7) Frath, D.; Massue, J.; Ulrich, G.; Ziessel, R. *Angew. Chem. Int. Ed. Engl.***2014**, *53*, 2290.
- (8) Frath, D.; Azizi, S.; Ulrich, G.; Retailleau, P.; Ziessel, R. *Org. Lett.***2011**, *13*, 3414.
- (9) Kubota, Y.; Tanaka, S.; Funabiki, K.; Matsui, M. *Org. Lett.***2012**, *14*, 4682.
- (10) Santra, M.; Moon, H.; Park, M.-H.; Lee, T.-W.; Kim, Y. K.; Ahn, K. H. *Chem. Eur. J.***2012**, *18*, 9886.
- (11) Benelhadj, K.; Massue, J.; Retailleau, P.; Ulrich, G.; Ziessel, R. *Org. Lett.***2013**, *15*, 2918.

- (12) Benelhadj, K.; Massue, J.; Retailleau, P.; Chibani, S.; Le Guennic, B.; Jacquemin, D.; Ziessel, R.; Ulrich, G. *Eur. J. Org. Chem.***2014**, 2014, 7156.
- (13) Gong, P.; Yang, H.; Sun, J.; Zhang, Z.; Sun, J.; Xue, P.; Lu, R. *J. Mater. Chem. C***2015**, 3, 10302.
- (14) Pais, V. F.; Ramirez-Lopez, P.; Romero-Arenas, A.; Collado, D.; Najera, F.; Perez-Inestrosa, E.; Fernandez, R.; Lassaletta, J. M.; Ros, A.; Pischel, U. *J. Org. Chem.***2016**, 81, 9605.
- (15) Wu, Z.; Sun, J.; Zhang, Z.; Yang, H.; Xue, P.; Lu, R. *Chem. Eur. J.***2017**, 23, 1901.
- (16) Quan, L.; Chen, Y.; Lv, X.-J.; Fu, W.-F. *Chem. Eur. J.***2012**, 18, 14599.
- (17) Chibani, S.; Le Guennic, B.; Charaf-Eddin, A.; Laurent, A. D.; Jacquemin, D. *Chem. Sci.***2013**, 4, 1950.
- (18) Li, W.; Lin, W.; Wang, J.; Guan, X. *Org. Lett.***2013**, 15, 1768.
- (19) Zhao, D.; Li, G.; Wu, D.; Qin, X.; Neuhaus, P.; Cheng, Y.; Yang, S.; Lu, Z.; Pu, X.; Long, C.; You, J. *Angew. Chem. Int. Ed.***2013**, 52, 13676.
- (20) Barbon, S. M.; Reinkeluers, P. A.; Price, J. T.; Staroverov, V. N.; Gilroy, J. B. *Chem. Eur. J.***2014**, 20, 11340.
- (21) Jiao, L.; Wu, Y.; Wang, S.; Hu, X.; Zhang, P.; Yu, C.; Cong, K.; Meng, Q.; Hao, E.; Vicente, M. G. H. *J. Org. Chem.***2014**, 79, 1830.
- (22) Yoshii, R.; Hirose, A.; Tanaka, K.; Chujo, Y. *J. Am. Chem. Soc.***2014**, 136, 18131.
- (23) Yu, C.; Jiao, L.; Zhang, P.; Feng, Z.; Cheng, C.; Wei, Y.; Mu, X.; Hao, E. *Org. Lett.***2014**, 16, 3048.
- (24) Liu, Q.; Wang, X.; Yan, H.; Wu, Y.; Li, Z.; Gong, S.; Liu, P.; Liu, Z. *J. Mater. Chem. C***2015**, 3, 2953.

- (25) Roubinet, B.; Massif, C.; Moreau, M.; Boschetti, F.; Ulrich, G.; Ziessel, R.; Renard, P.-Y.; Romieu, A. *Chem. - Eur. J.* **2015**, *21*, 14589.
- (26) Ge, Y.; O'Shea, D. F. *Chem. Soc. Rev.* **2016**, *45*, 3846.
- (27) Zhou, L.; Xu, D.; Gao, H.; Zhang, C.; Ni, F.; Zhao, W.; Cheng, D.; Liu, X.; Han, A. *J. Org. Chem.* **2016**, *81*, 7439.
- (28) Rao, Y.-L.; Amarne, H.; Zhao, S.-B.; McCormick, T. M.; Martić, S.; Sun, Y.; Wang, R.-Y.; Wang, S. *J. Am. Chem. Soc.* **2008**, *130*, 12898.
- (29) Amarne, H.; Baik, C.; Murphy, S. K.; Wang, S. *Chem. Eur. J.* **2010**, *16*, 4750.
- (30) Yoshino, J.; Kano, N.; Kawashima, T. *Dalton Trans.* **2013**, *42*, 15826.
- (31) Boens, N.; Leen, V.; Dehaen, W. *Chem. Soc. Rev.* **2012**, *41*, 1130.
- (32) Loudet, A.; Burgess, K. *Chem. Rev.* **2007**, *107*, 4891.
- (33) Ulrich, G.; Ziessel, R.; Harriman, A. *Angew. Chem. Int. Ed.* **2008**, *47*, 1184.
- (34) Wong, H.-L.; Wong, W.-T.; Yam, V. W.-W. *Org. Lett.* **2012**, *14*, 1862.
- (35) Rao, Y. L.; Amarne, H.; Lu, J. S.; Wang, S. *Dalton Trans.* **2013**, *42*, 638.
- (36) Wakamiya, A.; Taniguchi, T.; Yamaguchi, S. *Angew. Chem. Int. Ed. Engl.* **2006**, *45*, 3170.
- (37) Yoshino, J.; Kano, N.; Kawashima, T. *Chem. Commun.* **2007**, 559.
- (38) Rao, Y.-L.; Amarne, H.; Chen, L. D.; Brown, M. L.; Mosey, N. J.; Wang, S. *J. Am. Chem. Soc.* **2013**, *135*, 3407.
- (39) Murphy, S. K.; Baik, C.; Lu, J.-s.; Wang, S. *Org. Lett.* **2010**, *12*, 5266.
- (40) Job, A.; Wakamiya, A.; Kehr, G.; Erker, G.; Yamaguchi, S. *Org. Lett.* **2010**, *12*, 5470.
- (41) Ishida, N.; Narumi, M.; Murakami, M. *Helv. Chim. Acta.* **2012**, *95*, 2474.
- (42) Del Grosso, A.; Helm, M. D.; Solomon, S. A.; Caras-Quintero, D.; Ingleson, M. J. *Chem. Commun.* **2011**, *47*, 12459.

- (43) Ishida, N.; Moriya, T.; Goya, T.; Murakami, M. *J. Org. Chem.***2010**, *75*, 8709.
- (44) Baranov, M. S.; Solntsev, K. M.; Baleeva, N. S.; Mishin, A. S.; Lukyanov, S. A.; Lukyanov, K. A.; Yampolsky, I. V. *Chem. Eur. J.***2014**, *20*, 13234.
- (45) Shaikh, A. C.; Ranade, D. S.; Thorat, S.; Maity, A.; Kulkarni, P. P.; Gonnade, R. G.; Munshi, P.; Patil, N. T. *Chem. Commun.***2015**, *51*, 16115.
- (46) Wong, B. Y.-W.; Wong, H.-L.; Wong, Y.-C.; Chan, M.-Y.; Yam, V. W.-W. *Chem. Eur. J.***2016**, *22*, 15095.
- (47) Zhao, Z.; Chang, Z.; He, B.; Chen, B.; Deng, C.; Lu, P.; Qiu, H.; Tang, B. Z. *Chem. Eur. J.***2013**, *19*, 11512.
- (48) He, B.; Chang, Z.; Jiang, Y.; Chen, B.; Lu, P.; Kwok, H. S.; Qin, A.; Zhao, Z.; Qiu, H. *Dyes Pigm.***2014**, *101*, 247.
- (49) Mukherjee, S.; Salini, P. S.; Srinivasan, A.; Peruncheralathan, S. *Chem. Commun.***2015**, *51*, 17148.
- (50) Tian, Y.; Shi, W.; Luo, J.; Ma, F.; Mi, H.; Lei, Y. *J. Polym. Sci., Part A: Polym. Chem.***2013**, *51*, 3636.
- (51) Ito, A.; Kang, Y.; Saito, S.; Sakuda, E.; Kitamura, N. *Inorg. Chem.***2012**, *51*, 7722.
- (52) Minami, H.; Saito, T.; Wang, C.; Uchiyama, M. *Angew. Chem. Int. Ed.***2015**, *54*, 4665.

CHAPTER 3B

Synthesis, characterization, photophysical and electrochemical properties of pyrazole based N,C- chelate dinuclear boron compounds

3B.1 Introduction	141
3B.2 Results and discussion	142
3B.2.1 Synthesis and characterization	142
3B.2.2 Single crystal X-ray analysis	147
3B.2.3 Photophysical studies	152
3B.2.4 Thermal studies	156
3B.2.5 Electrochemical studies	157
3B.3 Conclusions	158
3B.4 Experimental section	158
3B.4.1 General information	158
3B.4.2 Synthetic procedure and spectral characterization	159
3B.5 References	166

3B.1 Introduction

Highly conjugated organic materials that can serve as electron transporting or accepting materials are of great interest due to their potential application in organic photovoltaics, organic light emitting diodes, field effect transistors and energy storage.¹ Tri- and tetra- coordinate boron compounds have attracted widespread attention in recent years owing to their interesting optical and electronic properties.²⁻⁸ Incorporation of tri- coordinated boron centres into conjugated π system leads to stabilization of the lowest unoccupied molecular orbitals (LUMO) through involvement of the empty p_z orbital on boron. The resultant materials show increased electron affinity. Compared to tri- coordinate boron compounds, tetra- coordinate boron compounds exhibit more stability owing to the coordination saturation of the boron centre. Moreover, four coordinate boron compounds with multiboron centres in their conjugated π -systems, exhibited strong luminescence, increased electron affinity and high thermal stability.⁹⁻²⁴

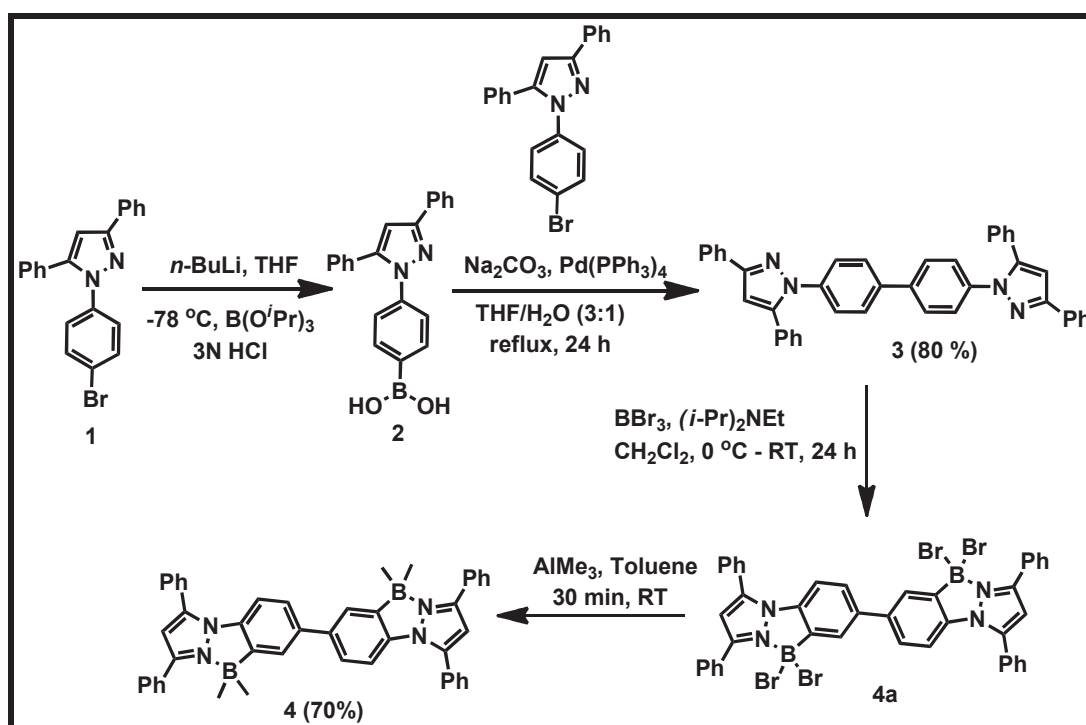
In 2006, Yamaguchi and co-workers reported the ladder type N,C- chelate diboron compounds featuring partial coplanarity and reduced band gap.¹⁰ Meanwhile, Kawashima and co-workers reported highly luminescent azobenzene or imine based N,C- chelate boron compound.²⁵⁻²⁷ Wang and co-workers reported several photochromic N,C- chelate boron compounds. The photochromic behaviour based on reversible structural changes through the formation or rupture of intramolecular C-C and C-B bond upon irradiation of light and heating.²⁸⁻³³ In 2010, Murakami and co-workers first reported the aromatic electrophilic borylation method to synthesize phenylpyridine boron complexes.³⁴ Since then, by following this methodology, several groups has synthesized the highly luminescent N,C- chelate boron

complexes.^{23,24,35-42} In this chapter, we describe the synthesis, photophysical, and electrochemical properties of pyrazole based N,C- chelate diboron compounds.

3B.2 Results and discussion

3B.2.1 Synthesis and characterization

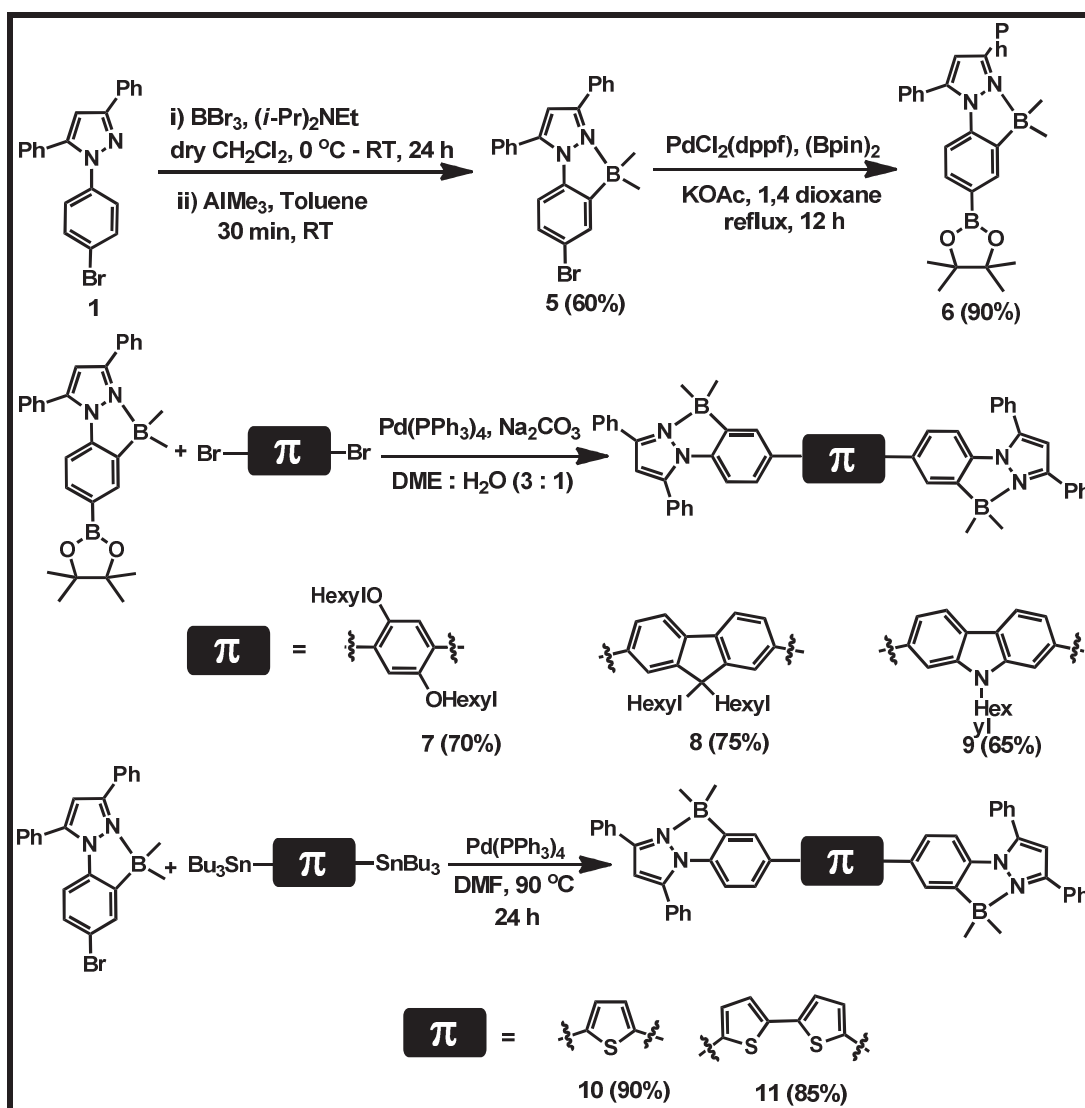
The synthetic routes to pyrazole based dinuclear N,C- chelate tetra-coordinate organoborons are illustrated in Scheme 3B.1 and 3B.2. 1-(4-Bromophenyl)-3,5-diphenyl-1H-pyrazole (**1**) was synthesized from commercially available starting materials 1,3-diphenyl-1,3-propanedione and 4-bromophenylhydrazine hydrochloride. Compound **1** was lithiated using *n*-BuLi, subsequent treatment with B(O^{*i*}Pr)₃ afforded (3,5-diphenyl-1H-pyrazol-1-yl)phenyl)boronic acid (**2**).



Scheme 3B.1: Synthesis of compound **4**.

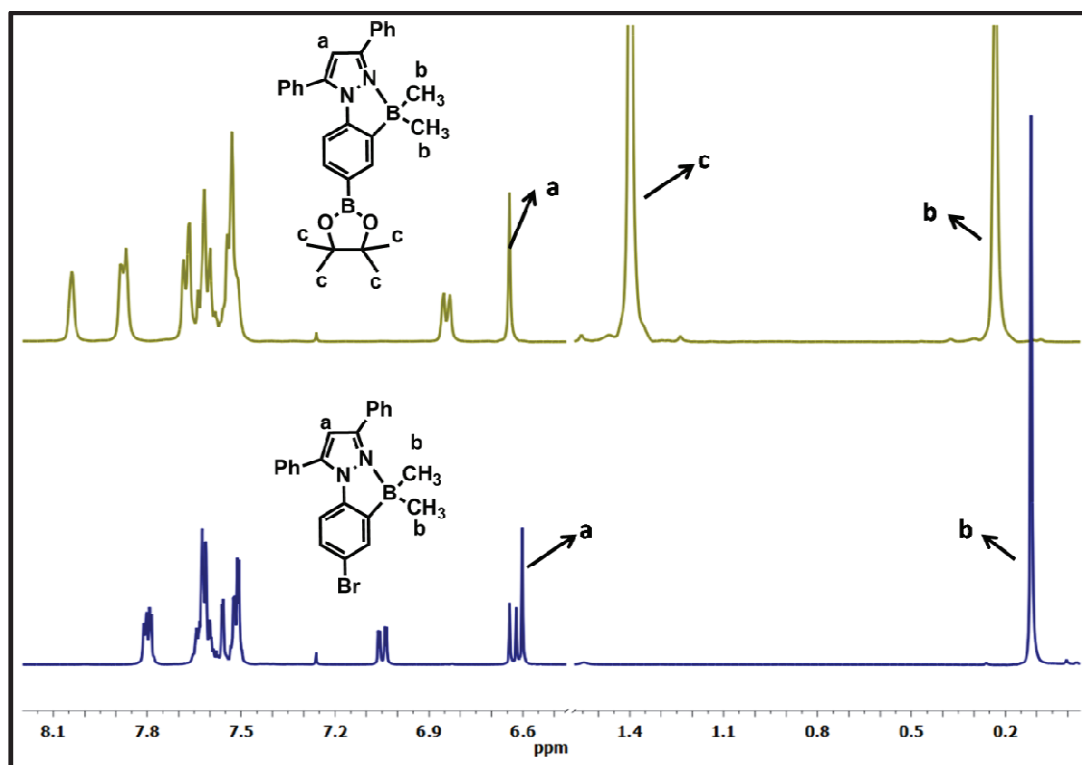
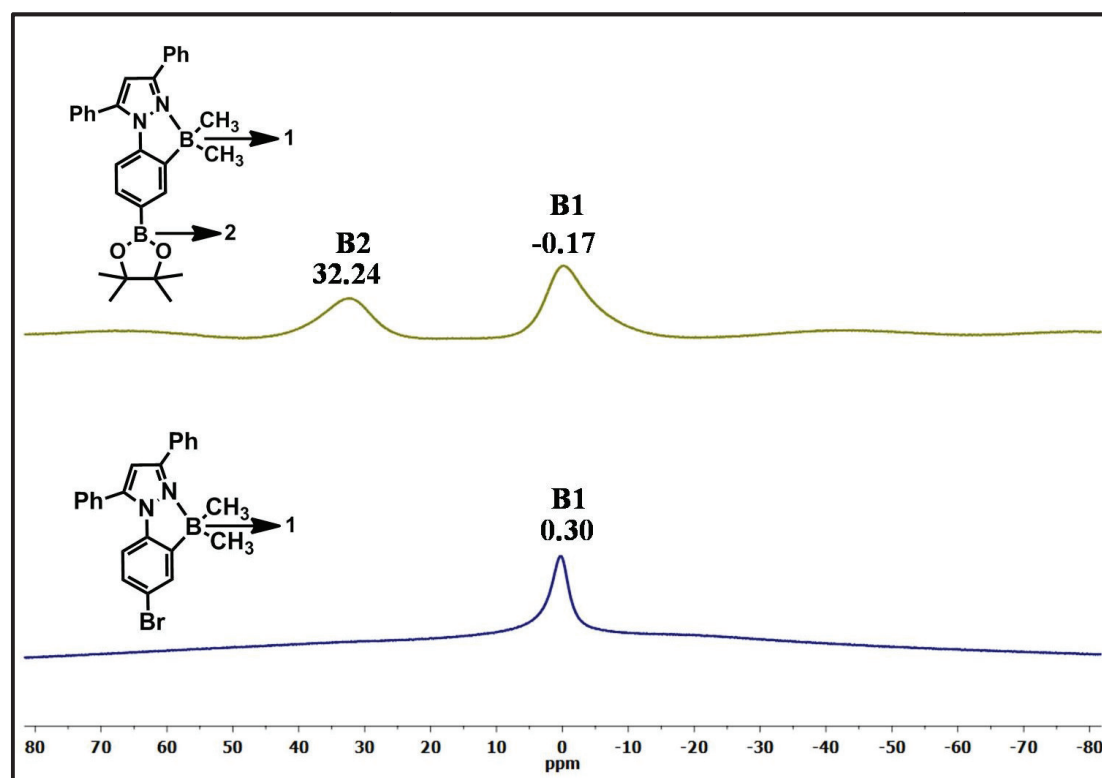
Compound **3** was synthesized using Suzuki coupling reaction between compound **1** and compound **2** under nitrogen atmosphere as shown in Scheme 3B.1. Reaction of compound **3** with BBr₃ in basic condition (*i*-Pr₂NEt) results dipyrazole-tetrabromodiborane complex (**4a**). Without further purification, dipyrazole-

tetrabromoborane complex (**4a**) was treated with trimethylaluminium (AlMe_3) to afford compound **4** in 70% yield.



Scheme 3B.2: Synthesis of compounds 7-11.

Compound **5** was prepared from compound **1**, by adopting a similar electrophilic aromatic borylation strategy that was used for the synthesis of compound **4**. The ^1H NMR spectrum of compound **5** shows a signal at 0.12 ppm corresponding to the methyl protons on the boron centre (Figure 3B.1). The ^{11}B NMR spectrum shows a broad singlet at 0.3 ppm which is characteristic of a tetra-coordinate boron centre (Figure 3B.2).

Figure 3B.1: ^1H NMR spectrum of compound 5 and 6.Figure 3B.2: ^{11}B NMR spectrum of compound 5 and 6.

The reaction of compound **5** with bis(pinacolato)diboron and catalytic amount of Pd(dppf)Cl₂ under Miyaura coupling condition afforded compound **6** in 90% yield. The ¹¹B NMR spectrum of compound **6** shows two peaks; the peak at -0.17 ppm corresponds to tetra-coordinate organoboron centre and the peak at 32.24 ppm correspond to boronate ester boron centre (Figure 3B.2).

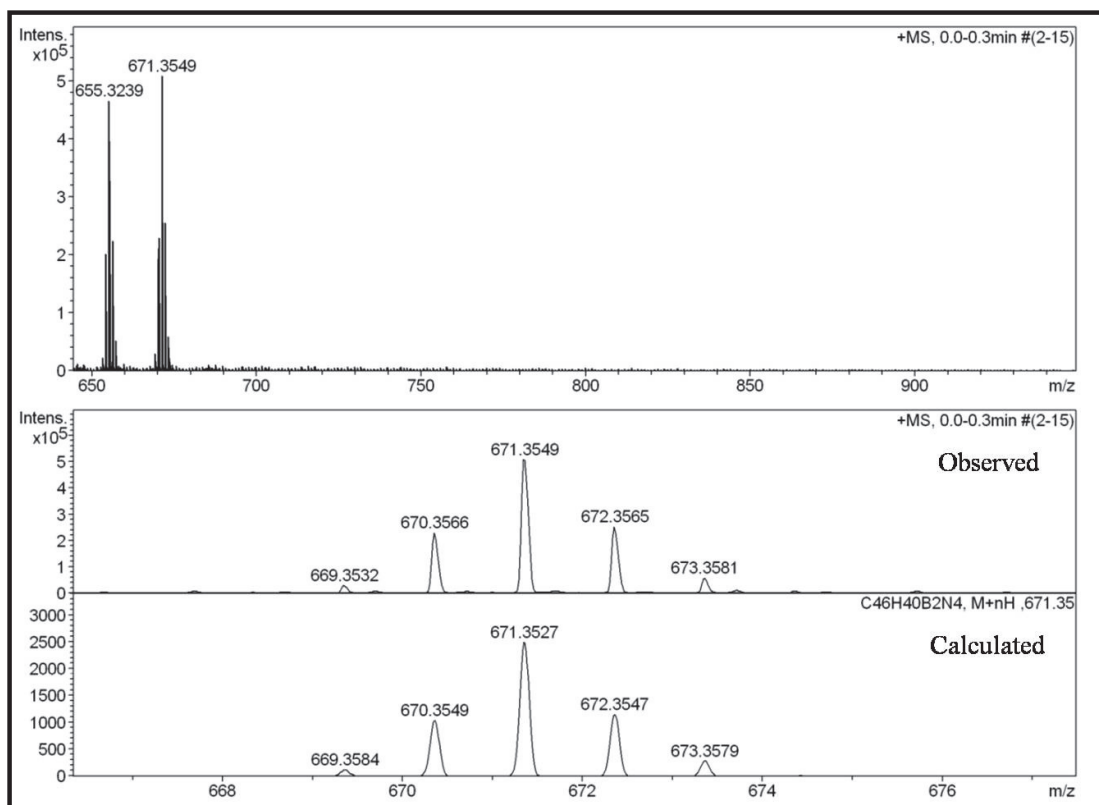


Figure 3B.3: HRMS spectrum of compound **4**.

Suzuki coupling between compound **6** and 1,4-dibromo-2,5-bis(hexyloxy)benzene (or) 2,7-dibromo-9,9-dihexyl-9H-fluorene (or) 2,7-dibromo-9-hexyl-9H-carbazole yielded compound **7** (or) **8**(or) **9** respectively. The reaction between compound **5** and 2,5-bis(tributylstannyl)thiophene (or) 5,5'-bis(tributylstannyl)-2,2'-bithiophene under Stille reaction condition afforded compounds **10**(or) **11** respectively (Scheme 3B.2). All the boron compounds (**4-11**) showed characteristic [M+H]⁺ or [M + Na]⁺ ions in HRMS spectra as shown in Figure 3B.3 for compound **4** and in Figure 3B.4 for compound **7** confirming the identities of

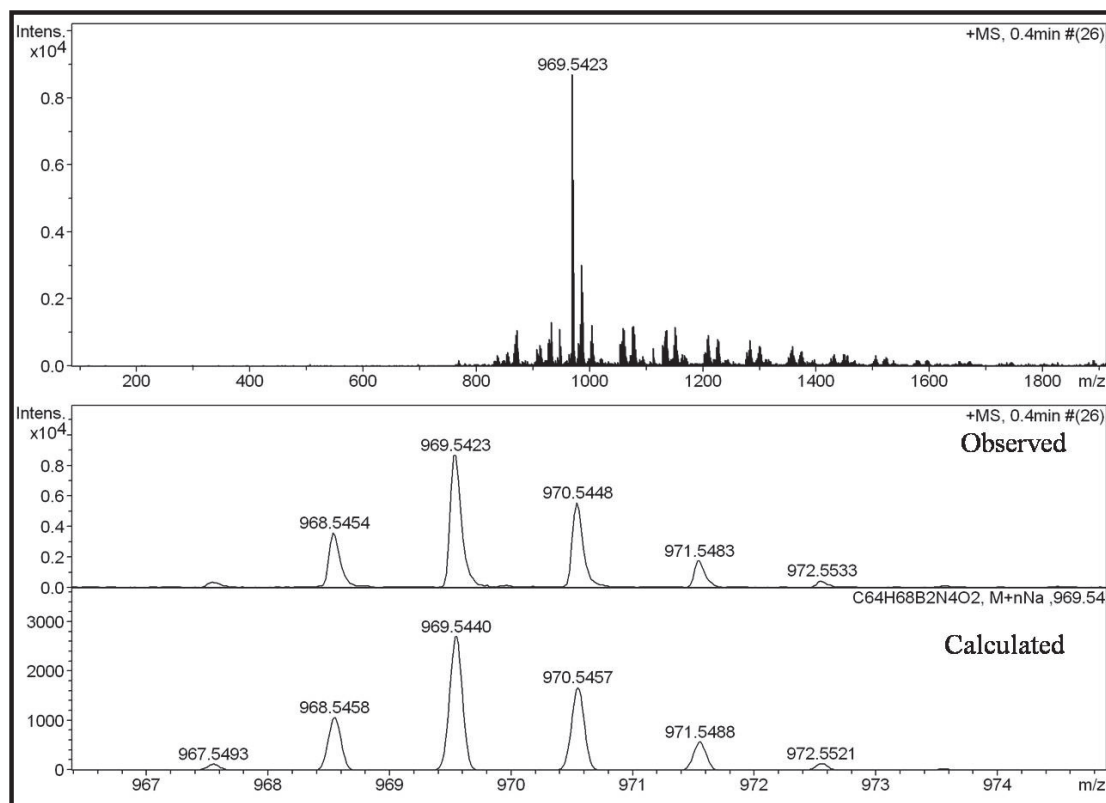
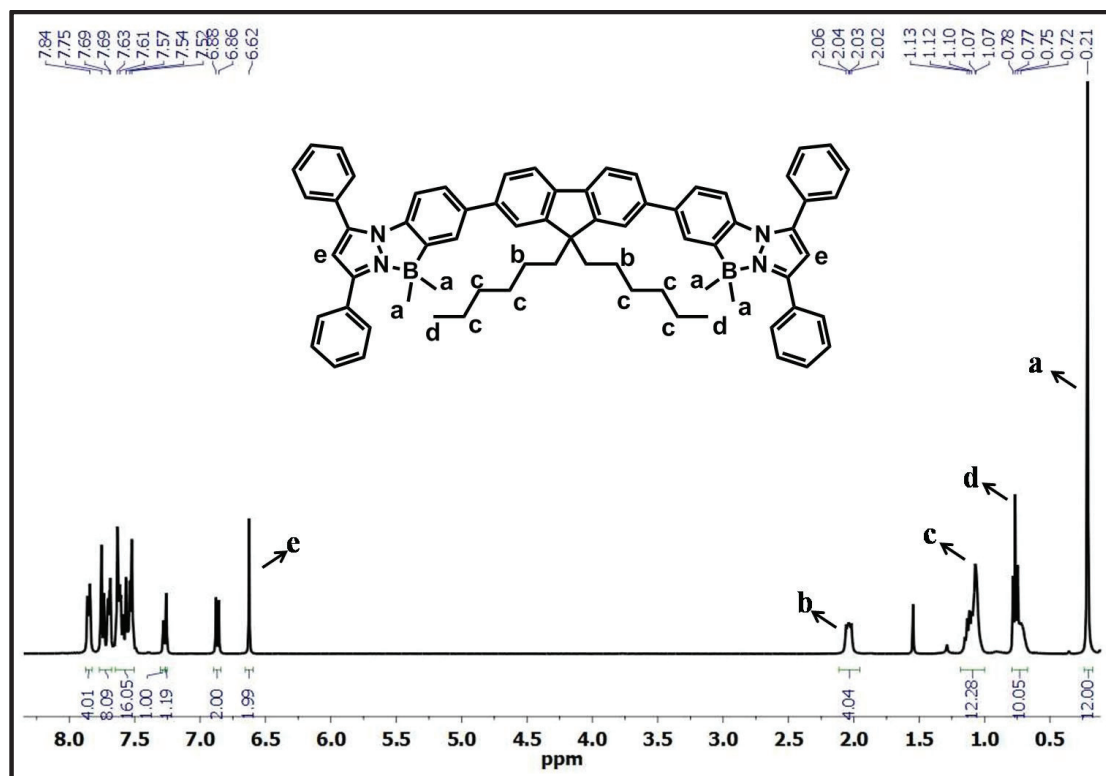


Figure 3B.4: HRMS spectrum of compound 7.

Figure 3B.5: ¹H NMR spectrum of compound 8 recorded in CDCl₃.

the compounds, these compounds were also characterised by ^1H , ^{13}C and ^{11}B NMR studies. A representative ^1H NMR spectrum of compound **8** is shown in Figure 3B.5, in which a signal appeared at 0.21 ppm corresponding to the methyl protons on the boron centres and a three set of protons appeared between 0.72 ppm to 2.06 ppm corresponding to the hexyl protons.

3B.2.2 Single crystal X-ray analysis

Compounds **4**, **8**, **10** and **11** were further characterized by X-ray diffraction analysis. Single crystals suitable for X-ray diffraction were grown by slow evaporation of $\text{CH}_2\text{Cl}_2/n$ -hexane mixture. Compounds **4**, **8**, **10** and **11** were crystallized in the monoclinic $P2_1/n$, triclinic $P-1$, triclinic $P-1$ and monoclinic $P2_1/c$ space groups respectively. The molecular structure of compound **4**, **8**, **10** and **11** are shown in Figure 3B.6; selected bond lengths and bond angles are summarized in Table 3B.1. Interplanar angles are listed in Table 3B.2 and crystallographic data for compound **4**, **8**, **10** and **11** are presented in Table 3B.3. In all these compounds the geometry around the boron centre is distorted tetrahedron. The boron atom deviates from the five-membered plane defined by $\text{C}_2\text{N}_2\text{B}$ (pyrazole two nitrogen atoms, boron atom and phenyl carbons directly attached to boron and nitrogen); the distance ranging from 0.016 to 0.076 Å (Table 3B.1). The B–N and B–C distances are in the typical range as observed in other literature reported compounds^{36,39} (Table 3B.1). The interplanar angle between the pyrazole (P1) and N-phenyl (Plane A) is 14.5 ° (for **4**), 6.35 ° (for **8**), 11.57 ° (for **10**), 10.17 ° (for **11**), whereas the interplanar angle between the pyrazole (P2) and its attached N-phenyl is 19.3 ° (for **8**), 7.35 ° (for **10**) (Table 3B.2), which indicates pyrazole and N-phenyl skeleton have slight distortion. Compounds **4** and **11** exhibited centre of inversion in their crystal structures which gives anti arrangement of two boron centres (B1 and B1*). The crystal structure of

compounds **8** and **10** are non centrosymmetric, in which both the boron centres (B1 and B2) are syn to each other.

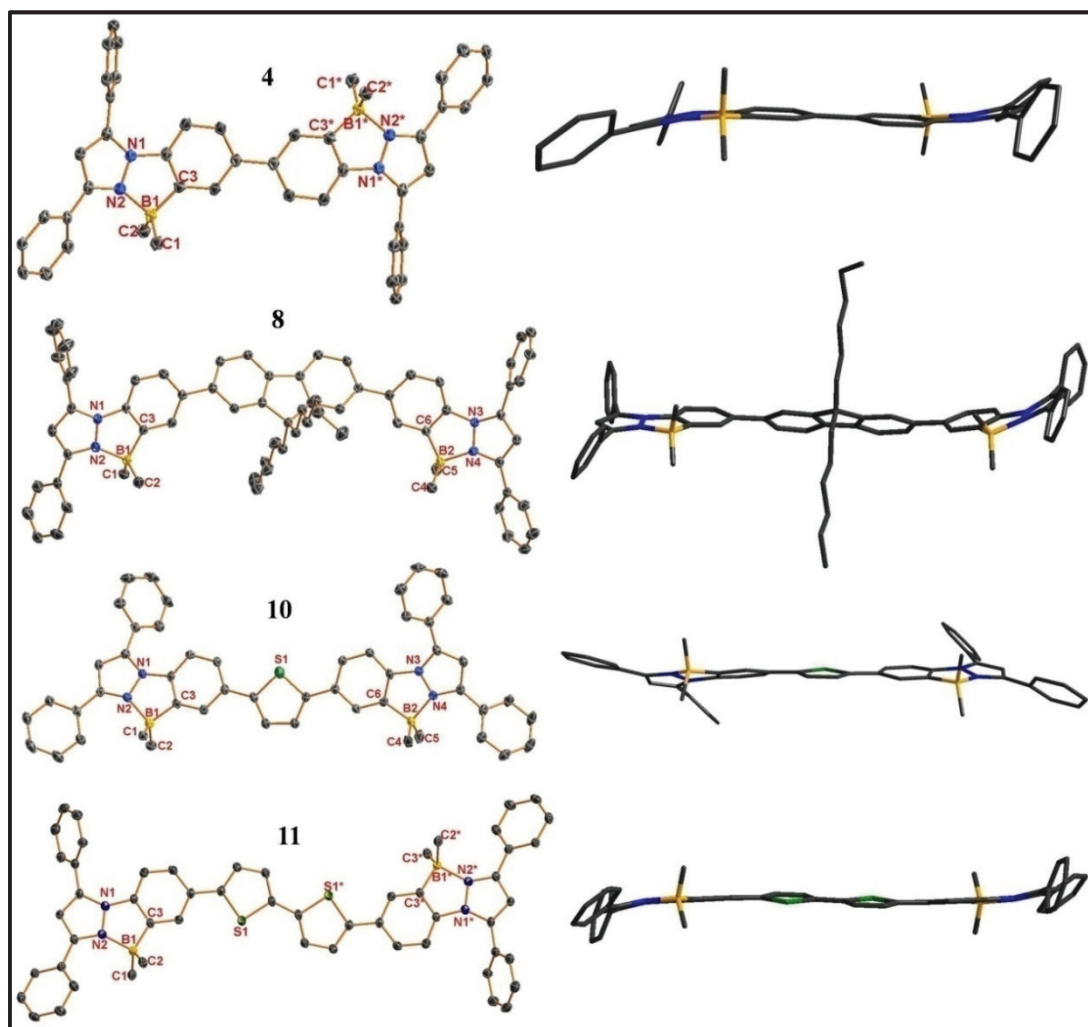


Figure 3B.6: Molecular structure of compound **4**, **8**, **10** and **11** (left), side view (right). Thermal ellipsoids are drawn at 30% probability level.

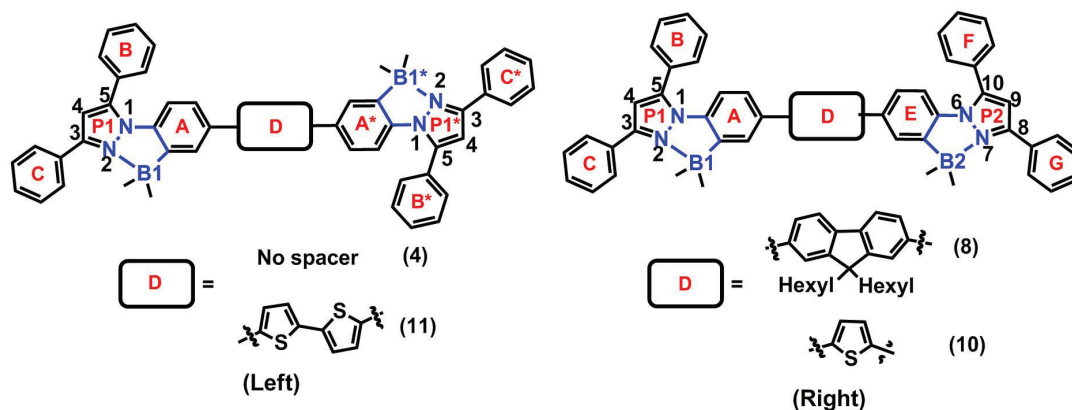
In compound **4**, the two N-phenyls attached to pyrazoles are coplanar (Figure 3B.6, side view of **4**) whereas in case of compound **11** the interplanar angle between N-phenyl (Plane A) and bithiophene spacer (Plane D) is 9.319° (Figure 3B.6, side view of **11**). The interplanar angle between N-phenyl (Plane A or Plane E) and π conjugated spacer (Plane D) is 34.107° & 36.410° (for **8**), 15.633° & 4.181° (for **10**). The interplanar angle between pyrazole and phenyl rings (Plane B, C, F & G) at 5,3,8 & 10 positions (Table 3B.2) varies from 13.439° to 84.205° ; these phenyl ring

twists could prevent the $\pi-\pi$ interactions in their solid state. In general $\pi-\pi$ interactions are responsible for fluorescence quenching in solid state which will be discussed in the next segment.

Table 3B.1: Comparison of selected bond lengths [\AA] and bond angles [deg] for compounds **4**, **8**, **10** and **11**.

Compound	4	8	10	11
B1-C1	1.612(6)	1.605(4)	1.614(5)	1.617(5)
B1-C2	1.625(5)	1.610(4)	1.618(5)	1.613(5)
B1-C3	1.604(6)	1.610(3)	1.606(5)	1.602(5)
B1-N2	1.654(5)	1.649(3)	1.671(5)	1.664(4)
C1-B1-C2	115.2(3)	113.7(2)	116.7(3)	113.6(3)
C1-B1-C3	114.6(3)	117.1(2)	110.3(3)	113.9(3)
C2-B1-C3	109.6(3)	110.3(2)	110.7(3)	111.9(3)
C1-B1-N2	109.7(3)	109.37(19)	112.8(3)	108.6(3)
C2-B1-N2	110.8(3)	110.2(2)	109.0(3)	112.7(3)
C3-B1-N2	95.1(3)	94.55(17)	95.2(2)	94.7(2)

Compound	8	10
B2-C4	1.612(4)	1.621(6)
B2-C5	1.616(3)	1.608(6)
B2-C6	1.608(3)	1.606(5)
B2-N4	1.649(3)	1.647(5)
C4-B2-C5	113.0(2)	116.1(4)
C4-B2-C6	115.2(2)	108.0(3)
C5-B2-C6	111.6(2)	114.8(3)
C4-B2-N4	109.18(19)	110.2(3)
C5-B2-N4	112.10(19)	114.8(3)
C6-B2-N4	94.35(16)	95.3(3)

Table 3B.2: Comparison of deviation of boron atom from C_2N_2B plane [\AA] and interplanar angles [deg] for compounds **4**, **8**, **10** and **11**.

	4	8	10	11
Deviation of B1 from C_2N_2B Plane (\AA)	-0.0766	-0.0356	0.0546	-0.0165
Pyrazole P1//Plane A	14.502(103)	6.353(84)	11.571(122)	10.172(90)
Pyrazole P1//Plane B	57.659(115)	84.205(82)	42.724(112)	62.86(10)
Pyrazole P1//Plane C	32.020(116)	60.999(88)	13.439(98)	29.87(105)
Plane A//Plane D		34.107(54)	15.633(91)	9.319(75)
Deviation of B2 from C_2N_2B Plane (\AA)		0.0553	-0.0468	
Pyrazole P2//Plane E		19.321(81)	7.351(104)	
Pyrazole P2//Plane F		60.295(75)	37.675(102)	
Pyrazole P2//Plane G		40.797(83)	37.305(125)	
Plane E P2//Plane D		36.410(58)	4.181(89)	

Table 3B.3: Crystal data and structure refinement parameters for compounds **4**, **8**, **10** and **11**.

Compound	4	8	9	10
Empirical formula	C ₄₆ H ₄₀ N ₄ B ₂	C ₇₁ H ₇₂ B ₂ N ₄	C ₅₀ H ₄₂ B ₂ N ₄ S	C ₅₄ H ₄₄ B ₂ N ₄ S ₂
Formula weight	670.44	1002.94	752.55	834.67
Temperature/K	100.00	100.00	100.00	100.00
Crystal system	Monoclinic	Triclinic	Triclinic	Monoclinic
Space group	<i>P</i> 2 ₁ / <i>n</i>	<i>P</i> -1	<i>P</i> -1	<i>P</i> 2 ₁ / <i>c</i>
<i>a</i> /Å	12.284(4)	13.4091(6)	11.5795(5)	7.0486(17)
<i>b</i> /Å	7.108(2)	14.0249(7)	12.0816(5)	15.859(4)
<i>c</i> /Å	21.887(9)	19.5464(13)	16.8101(11)	19.155(5)
α /°	90	109.303(4)	97.113(4)	90
β /°	105.717(7)	95.233(4)	100.900(4)	95.549(6)
γ /°	90	112.832(3)	117.414(3)	90
Volume/Å ³	1839.7(11)	3094.0(3)	1989.06(19)	2131.2(9)
<i>Z</i>	2	2	2	2
ρ_{calcd} /g cm ⁻³	1.210	1.077	1.257	1.301
μ /mm ⁻¹	0.070	0.062	0.123	0.169
<i>F</i> (000)	708.0	1072.0	792.0	876.0
2 θ range for data collection/°	3.464 to 50.88	2.282 to 51.444	2.542 to 52.3	3.34 to 50.938
Index ranges	-14 ≤ <i>h</i> ≤ 14, -4 ≤ <i>k</i> ≤ 8, -26 ≤ <i>l</i> ≤ 26	-16 ≤ <i>h</i> ≤ 16, -16 ≤ <i>k</i> ≤ 17, -23 ≤ <i>l</i> ≤ 23	-14 ≤ <i>h</i> ≤ 14, -14 ≤ <i>k</i> ≤ 14, -20 ≤ <i>l</i> ≤ 20	-7 ≤ <i>h</i> ≤ 8, -19 ≤ <i>k</i> ≤ 19, -23 ≤ <i>l</i> ≤ 23
Reflns. collected	9945	38403	24253	27851
Independent reflns	3380 [<i>R</i> _{int} = 0.0800, <i>R</i> _{sigma} = 0.1002]	11760 [<i>R</i> _{int} = 0.0744, <i>R</i> _{sigma} = 0.0881]	7866 [<i>R</i> _{int} = 0.0550, <i>R</i> _{sigma} = 0.0628]	3937 [<i>R</i> _{int} = 0.1428, <i>R</i> _{sigma} = 0.1165]
Data/restraints/parameters	3380/0/237	11760/27/713	7866/0/519	3937/0/283
GOF on <i>F</i> ²	1.029	0.940	1.064	0.978
Final <i>R</i> indices [<i>I</i> > 2 σ (<i>I</i>)]	<i>R</i> ₁ = 0.0770, <i>wR</i> ₂ = 0.1886	<i>R</i> ₁ = 0.0569, <i>wR</i> ₂ = 0.1477	<i>R</i> ₁ = 0.0665, <i>wR</i> ₂ = 0.1697	<i>R</i> ₁ = 0.0559, <i>wR</i> ₂ = 0.1223
<i>R</i> indices (all data)	<i>R</i> ₁ = 0.1389, <i>wR</i> ₂ = 0.2299	<i>R</i> ₁ = 0.1060, <i>wR</i> ₂ = 0.1669	<i>R</i> ₁ = 0.0894, <i>wR</i> ₂ = 0.1819	<i>R</i> ₁ = 0.1252, <i>wR</i> ₂ = 0.1524
Largest diff. peak and hole [e Å ⁻³]	0.39 and -0.31	0.28 and -0.28	0.41 and -0.28	0.30 and -0.24

3B.2.3 Photophysical Studies

All boron compounds showed limited solubility in non polar and protic solvents; hence, the photophysical studies were performed in CH₂Cl₂, DMF and THF. The photophysical data of **4** and **7-11** in solution of various solvents are presented in Table 3B.4 and their normalized absorption and emission spectra recorded in dichloromethane are displayed in Figure 3B.7 and 3B.8 respectively. All these compounds exhibit slight red shift in absorption with increasing solvent polarity and display similar optical features such as a broad, unstructured band. The maximum wavelength of these compounds comprised between 337 and 399 nm (Figure 3B.7). The molar absorption coefficients of compounds **4** and **7-11** are in the range of 54550 to 110940 M⁻¹·cm⁻¹ in CH₂Cl₂. The absence of structuration of the absorption bands is presumably related to free rotations occurring in solution. Absorption maxima of all these dinuclear boron compounds were tuned by altering the π-conjugated spacer. The compounds **7-11** exhibit red shifted absorption than compound **4** owing to the increased π-conjugation length. Compounds **10** and **11** exhibit longer wavelength absorption maxima as compared to compounds **4** and **7-9**, which can be attributed to the better conjugation occurring in thienyl systems. The steady state fluorescence spectra of compounds **4** and **7-11** were recorded by exciting at their absorption maxima and the relevant data are summarised in Table 3B.4. Compounds **4** and **7-9** exhibited red shifted emission with increase of solvents polarity; however, emission maxima of compounds **10** and **11** are slightly affected with solvent polarity. As compared with emission maxima of compound **4**, compounds **8** and **9** have shown blue shifted emission and compounds **7**, **10** and **11** have shown red shifted emission. The quantum yields of these N,C- chelate pyrazole dimers ranges from 0.32 (for **11**) to 0.94 (for **9**) in dichloromethane. Compounds **8** and **9** exhibit highest quantum yields

compared to compound **1** due to the presence of extended π -conjugated fluorenyl and carbazolyl spacers respectively.

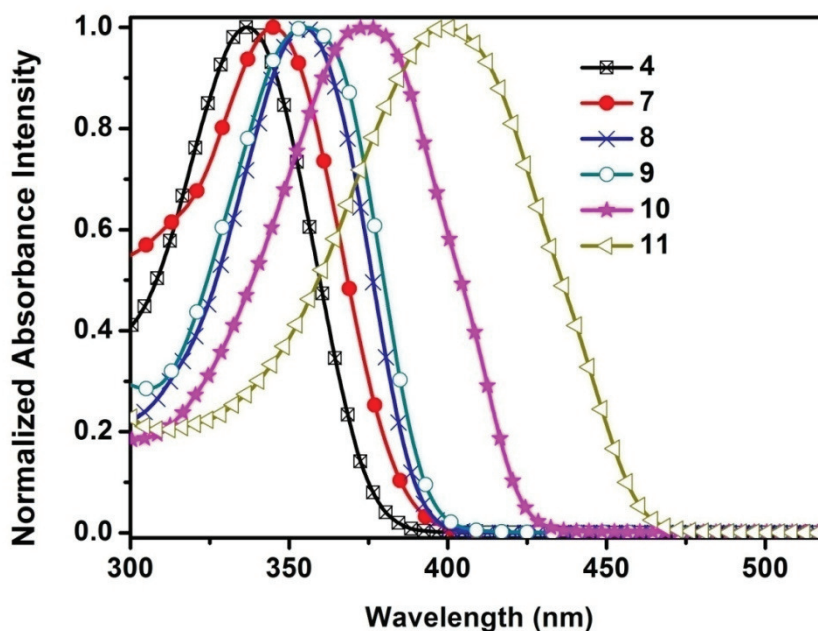


Figure 3B.7: Comparison of normalized absorption spectra of **4** and **7-11** in dichloromethane (concentration: 1×10^{-5} M).

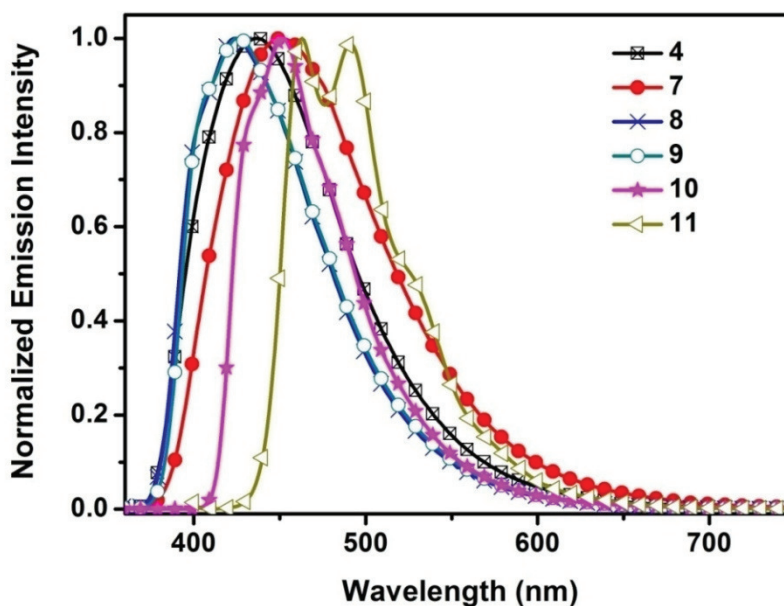


Figure 3B.8: Comparison of normalized emission spectra of **4** and **7-11** in dichloromethane (concentration: 1×10^{-5} M).

As compared to compounds **4**, **7-9**, the thienyl systems containing compounds **10** and **11** exhibit less fluorescence quantum yields, which may be attributable to the presence of sulphur atom in the thienyl systems, enhancing intersystem crossing rate.

The Stokes shifts of these compounds range from 69 nm (for **8**) to 130 nm (for **7**) and which are highly depend on the solvent polarity.

Table 3B.4: Photophysical properties of **4** and **7-11** in various solvents at 298 K.

Compound	Solvent	λ_{\max}^a (nm)	ϵ_{\max} ($M^{-1} \text{ cm}^{-1} \times 10^3$)	$\lambda_{\text{em}}^{a,b}$ (nm)	Φ_F^c	Stokes shift (nm)	τ
4	THF	339	51.96	435	0.67	96	2.20
	CH ₂ Cl ₂	337	49.29	437	0.78	100	2.29
	DMF	340	43.79	444	0.83	104	2.55
	Solid			417	0.80		
7	THF	345	43.09	448	0.70	103	2.57
	CH ₂ Cl ₂	345	54.55	451	0.71	106	2.85
	DMF	348	45.84	478	0.65	130	2.20
	Solid			435	0.30		
8	THF	355	121.24	424	0.80	69	1.54
	CH ₂ Cl ₂	354	110.94	424	0.94	70	1.62
	DMF	358	119.48	433	0.83	75	1.88
	Solid			414	0.35		
9	THF	357	100.49	428	0.93	71	1.67
	CH ₂ Cl ₂	355	87.23	426	0.83	71	2.18
	DMF	360	93.72	446	0.87	86	1.66
	Solid			431	0.38		
10	THF	374	61.61	452	0.56	78	0.91
	CH ₂ Cl ₂	374	81.57	452	0.48	78	0.88
	DMF	379	70.28	455	0.52	76	1.07
	Solid			481	0.18		
11	THF	399	42.20	490	0.34	91	0.51
	CH ₂ Cl ₂	399	62.26	491	0.32	92	0.49
	DMF	407	58.46	493	0.37	86	0.50
	Solid			577	0.23		

^a Absorption maximum (Concentration: 1×10^{-5} M). ^b Excited at the absorption maximum. ^c Absolute fluorescence quantum yields were measured using an integrating sphere.

Compounds **4** and **7-9** exhibit increase in Stokes shifts with the increase of solvent polarity, whereas compounds **10** and **11** exhibit decrease in Stokes shifts with increase of solvent polarity.

All the boron compounds also exhibit bright solid state fluorescence (Figure 3B.9 & 3B.10) with quantum yields ranging from 0.18 to 0.80. Compounds **4**, **7** and **8**

showed blue shifted emission in the solid state in comparison to the emission in dichloromethane solution. The solid state emission of compound **9** is not much changed, however compounds **10** and **11** showed red shifted emission in comparison to their emission in solution state. The solid state quantum yields of these compounds **4** and **7-11** are lower as compared to the quantum yield of the compounds in the solution state, which can be attributed to the increased intermolecular interactions in the solid state.

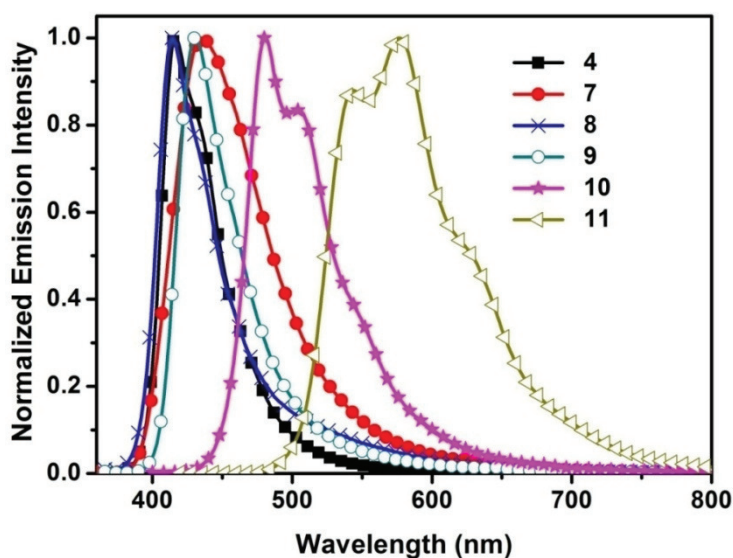


Figure 3B.9: A comparison of normalized emission spectra of **4** and **7-11** in solid state.

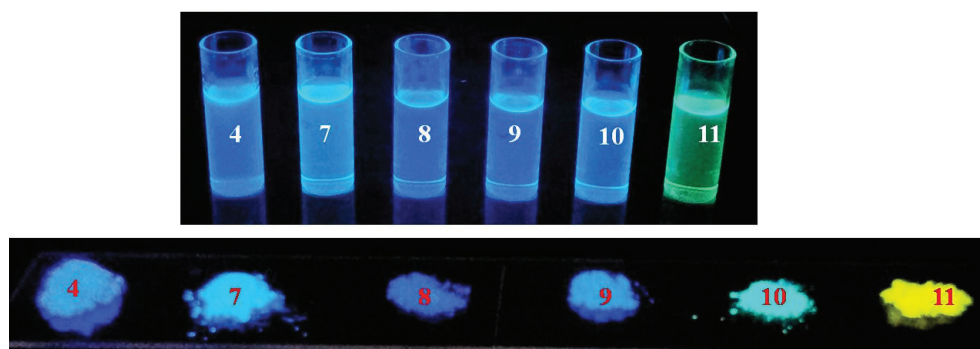


Figure 3B.10: The fluorescence photographs of compound **4** and **7-11** in dichloromethane solution (top) and in solid state (bottom). Irradiation was performed with a UV lamp with a wavelength of 365 nm.

3B.2.4. Thermal Studies:

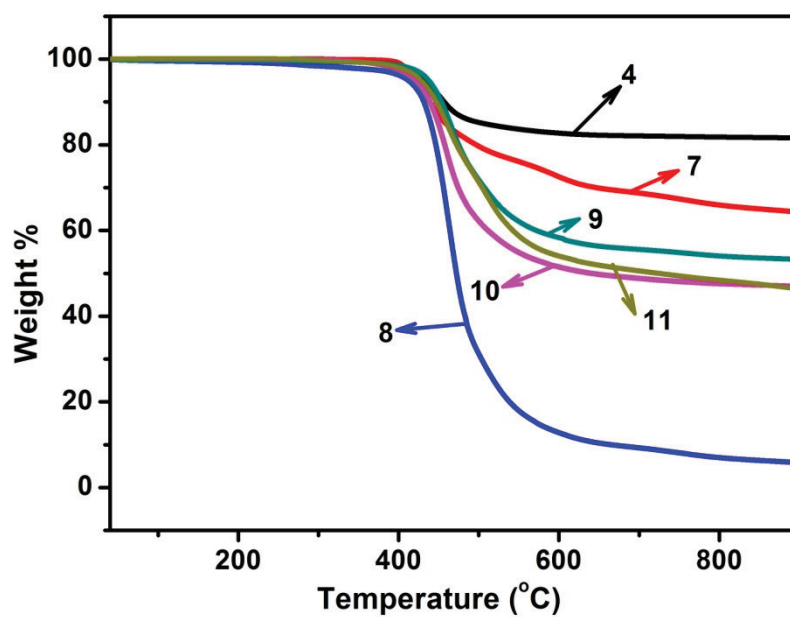


Figure 3B.11: TGA curves of 4 and 7-11 at a heating rate of 10 °C/min.

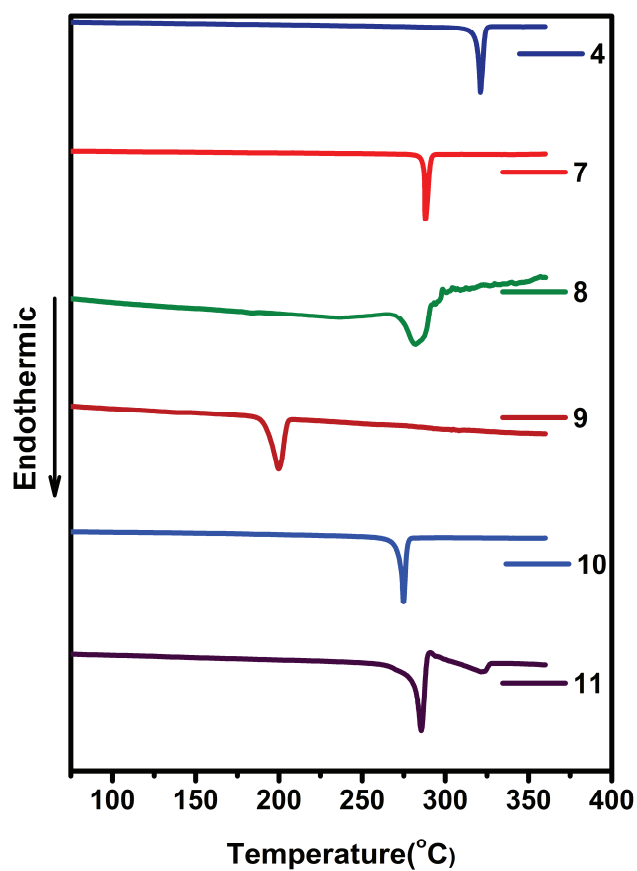


Figure 3B.12: DSC curves of 4 and 7-11 at heating rate of 10 °C/min.

Thermal properties of the dinuclear N,C- chelate organoboron compounds (**4** and **7-11**) were characterized by thermogravimetric analysis(TGA) (Figure 3B.11) and differential scanning calorimetry (DSC) under nitrogen atmosphere at the heating rate of $10\text{ }^{\circ}\text{C min}^{-1}$. The melting points of **4** and **7-11** were measured using DSC. As depicted in Figure 3B.12 the decomposition temperatures (T_{d5}) (corresponds to 5% weight loss) of compounds **4** and **7-11** are 434, 422, 412, 435, 421 and 427 respectively. Compounds **7-9** have shown low melting point and decomposition temperature over **4**. TGA and DSC analysis reveal that these compounds exhibit high thermal stability.

3B.2.5 Electrochemical Studies

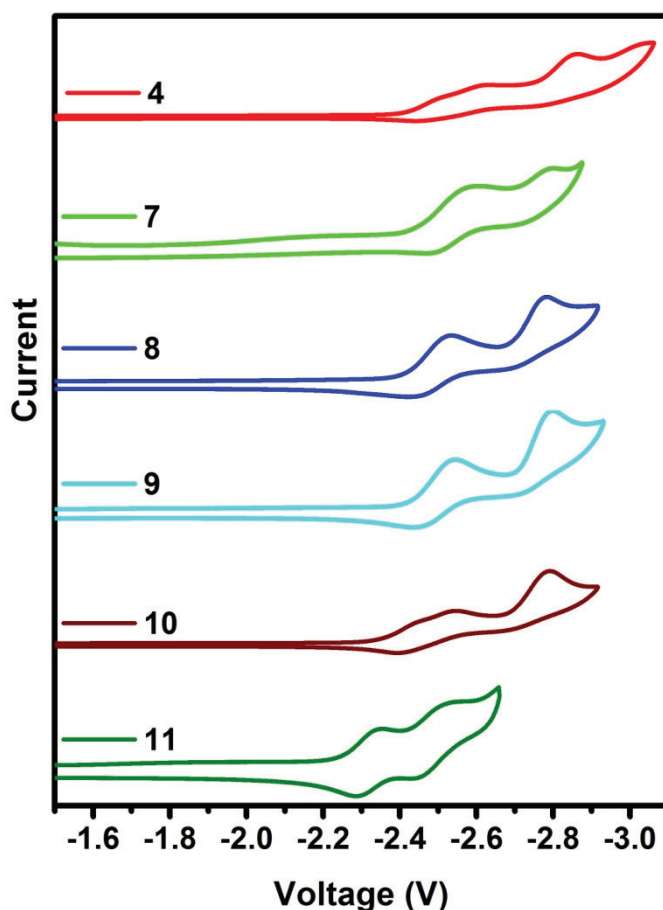


Figure 3B.13: Cyclic voltammograms of **4**, **7-11** recorded in DMF containing 0.1M $\text{Bu}_4\text{N}(\text{PF}_6)$ as supporting electrolyte; scan rate 100 mV/s . Referenced relative to Fc/Fc^+ couple.

The electrochemical properties of pyrazole based dinuclear boron compounds **4** and **7-11** were studied by cyclic voltammetry at a scan rate of 100 mV/s using $n\text{Bu}_4\text{NPF}_6$ as a supporting electrolyte (0.1 M) in DMF solution under nitrogen atmosphere. The cyclic voltammograms of compounds **4** and **7-11** are shown in Figure 3B.13. Compounds **4** and **7-10** displayed two quasi-reversible reduction peaks whereas compound **11** displayed two reversible reduction peaks. Compound **11** exhibited less negative reduction potentials as compared the compounds **4** and **7-10**.

3B.3 Conclusions

In conclusion, we have synthesized a series of pyrazole based dinuclear compounds (**4** and **7-11**) with different π -conjugation lengths by varying the π -conjugation spacer. The absorbance and emission maxima of these compounds greatly depend on π -conjugation spacer. These compounds exhibited fluorescence emission both in solution and solid state. Furthermore these compounds exhibited high thermal stability. The electrochemical and photophysical properties, suggesting the possibility of these diboron compounds as emitters and/or electron transporting materials in OLEDs.

3B.4 Experimental Section

3B.4.1. General Information

All reagents and starting materials were purchased from Sigma-Aldrich, Alfa Aesar and Spectrochem chemical companies and used as received unless otherwise noted. Tetrahydrofuran and toluene were distilled from Na/benzophenone prior to use. Dichloromethane, N,N-dimethylformamide and acetonitrile were distilled from CaH_2 . 2,7-Dibromo-9,9-dihexyl-9H-fluorene, 1,4-Dibromo-2,5-bis(hexyloxy)benzene, 2,7-dibromo-9-hexyl-9H-carbazole, 2,5-bis(tributylstannyl)thiophene and 5,5'-bis(tributylstannyl)-2,2'-bithiophene were prepared by following literature reported

methods.⁴³⁻⁴⁶ All 400 MHz ¹H, 100 MHz ¹³C and 128 MHz ¹¹B NMR spectra were recorded on a Bruker ARX 400 spectrometer operating at 400 MHz. All ¹H and ¹³C NMR spectra were referenced internally to solvent signals. ¹¹B NMR spectra were referenced externally to BF₃·Et₂O in CDCl₃ (δ = 0). ESI mass spectra were recorded using a Bruker microTOF-QII mass spectrometer. The absorbance spectra were recorded with a JASCO V-730 UV-Visible spectrometer. The fluorescence spectra were recorded using Edinburgh FS5 spectrofluorometer. Absolute fluorescence quantum yields of compounds **4** and **7-11** in solution and solid state were measured by integrating sphere method using Edinburgh FS5 spectrofluorometer.

Single-crystal X-ray diffraction data were collected on a Bruker APEX-II diffractometer equipped with an Oxford Instruments low-temperature attachment. The data were collected at 100 K using Mo-Kα radiation (0.71073 Å). SADABS absorption corrections were applied. The structures were solved and refined with SHELX suite of programs. All non-hydrogen atoms were refined with anisotropic displacement coefficients. The H atoms were placed at calculated positions and were refined as riding atoms.

3B.4.2 Synthetic procedure and spectral characterization

3B.4.2.1 Synthesis of compound 1

4-Bromophenylhydrazine hydrochloride (5.48 g, 24.53 mmol), and 1,3-diphenylpropane-1,3-dione (5.00 g, 22.30 mmol) were dissolved in 40 mL of methanol and 40 mL of acetic acid. The reaction mixture was heated to reflux for 24h and then poured into distilled water, extracted with ethyl acetate. The combined organic layers were washed with saturated NaHCO₃ solution, distilled water and brine then dried over Na₂SO₄. The solvent was removed under vacuum and the resulting residue was purified by silica gel column chromatography using ethyl acetate and *n*-

hexane as eluent. Yield: 6.27 g, (75%). mp: 137 °C. ^1H NMR (400 MHz, CDCl_3): δ = 7.99 (d, J = 7.5 Hz, 2H), 7.51 – 7.47 (m, 4H), 7.42 – 7.28 (m, 8H), 6.86 (s, 1H) ppm. ^{13}C NMR (100 MHz, CDCl_3): δ = 152.27, 144.36, 139.14, 132.83, 131.98, 130.30, 128.76, 128.72, 128.66, 128.55, 128.18, 126.54, 125.83, 120.92, 105.70 ppm. HR-MS (ESI): calcd. for $\text{C}_{21}\text{H}_{16}\text{N}_2\text{Br}_1$ ($[\text{M} + \text{H}]^+$) : 375.0491, found : 375.0464.

3B.4.2.2 Synthesis of compound 2

n-BuLi (7.00 mL, 11.19 mmol, 1.6 M in hexane) was added dropwise to a solution of compound **1** (3.50 g, 9.32 mmol) at -78 °C in anhydrous THF under nitrogen atmosphere. After being stirred at the same temperature for 0.5 h, $\text{B}(\text{O}^i\text{Pr})_3$ (11.19 mmol, 2.58 mL) was added dropwise *via* syringe. The reaction mixture was warmed to room temperature and stirred over night. 3 N HCl (75 mL) was added to the reaction mixture, stirred for 1 h and extracted with ethyl acetate. The combined organic layers were washed with brine, dried over Na_2SO_4 and concentrated. The resultant compound was washed with hot *n*-hexane and diethyl ether to yield compound **2** as a white powder.

3B.4.2.3 Synthesis of compound 3

Degassed THF: H_2O (60 mL: 20 mL) was added to compound **1** (3.30 g, 8.82 mmol), compound **2** (3.30 g, 9.70 mmol), Na_2CO_3 (4.69 g, 44.1 mmol), $\text{Pd}(\text{PPh}_3)_4$ (305 mg, 0.264 mmol) under nitrogen atmosphere. The reaction mixture was heated to reflux for 24 h. The reaction mixture was cooled to room temperature then distilled water was added to the reaction mixture and extracted with ethyl acetate (3×25 mL). The combined organic layers were washed with brine solution, dried over Na_2SO_4 and concentrated. The residue was purified by silica gel column chromatography using *n*-hexane/ethyl acetate mixture as eluent. Yield: 4.16 g, (80%). mp: 280 °C. ^1H NMR (400 MHz, CDCl_3): δ = 7.97 – 7.92 (m, 4H), 7.61 – 7.54 (m, 2H), 7.47 – 7.43 (m,

8H), 7.38 – 7.33 (m, 12H), 6.85 (s, 2H) ppm. ^{13}C NMR (100 MHz, CDCl_3): δ = 152.28, 144.54, 139.68, 139.10, 133.12, 130.73, 128.96, 128.81, 128.73, 128.56, 128.21, 127.56, 125.97, 125.55, 105.64 ppm. HR-MS (ESI): calcd. for $\text{C}_{42}\text{H}_{31}\text{N}_4$ ($[\text{M} + \text{H}]^+$): 591.2543, found : 591.2514.

3B.4.2.4 Synthesis of compound 4

To a stirred solution of compound **3** (1.5 g, 2.54 mmol) and N,N-diisopropylethylamine (*i*-Pr₂NEt) (0.88 mL, 5.08 mmol) in 100 mL of CH_2Cl_2 at 0 °C was added BBr_3 (1.0 M in dichloromethane, 15.23 mL, 15.23 mmol) under nitrogen. After being stirred at room temperature for 24 h, saturated K_2CO_3 aqueous solution was added to the reaction mixture and extracted with CH_2Cl_2 (3 × 30 mL). The combined organic layers were washed with water, dried over MgSO_4 and concentrated under vacuum to afford the crude product. Under nitrogen atmosphere AlMe_3 (2.0 M in toluene, 5.08 mL, 10.16 mmol) was added to the crude product in CH_2Cl_2 and toluene (50 mL : 50 mL) at room temperature. After being stirred at this temperature for 0.5 h, the reaction was quenched by adding water and extracted with CH_2Cl_2 (3 × 30 mL). The combined organic layers were washed with water and brine, dried over Na_2SO_4 and concentrated under reduced pressure. The resultant residue was purified by silica gel column chromatography using *n*-hexane/dichloromethane mixture as eluent. Yield: 1.70 g, (70 %). mp: 321 °C. ^1H NMR (400 MHz, CDCl_3): δ = 7.83 – 7.80 (m, 4H), 7.67 – 7.64 (m, 6H), 7.61 – 7.56 (m, 6H), 7.53 – 7.49 (m, 6H), 7.18 (dd, J = 8, 1.6 Hz, 2H), 6.79 (d, J = 8 Hz, 2H), 6.59 (s, 2H), 0.13 (s, 12H) ppm. ^{13}C NMR (100 MHz, CDCl_3): δ = 156.73, 148.53, 139.97, 139.91, 137.70, 130.37, 129.78, 129.75, 129.54, 129.15, 129.09, 128.86, 128.48, 111.96, 110.73, 9.34 ppm. ^{11}B NMR (128 MHz, CDCl_3): δ = 0.87 (s) ppm. HR-MS (ESI): calcd. for $\text{C}_{46}\text{H}_{41}\text{B}_2\text{N}_4$ ($[\text{M} + \text{H}]^+$): 671.3527, found : 671.3549.

3B.4.2.5 Synthesis of compound 5

Compound **5** was prepared following a procedure similar to that used for compound **4**. The quantities involved are as follows: compound **1** (10.00 g, 26.65 mmol), N,N-diisopropylethylamine (*i*-Pr₂NEt) (4.62 mL, 26.65 mmol), BBr₃ (1.0 M in dichloromethane, 79.95 mL, 79.95 mmol) and Me₃Al (1.0 M in toluene, 53.3 mL, 53.3 mmol). Yield: 6.63 g, (60 %). mp: 188 °C. ¹H NMR (400 MHz, CDCl₃): δ = 7.81 – 7.79 (m, 2H), 7.64 – 7.50 (m, 9H), 7.05 (dd, *J* = 8.5, 2.1 Hz, 1H), 6.63 (d, *J* = 8.5 Hz, 1H), 6.60 (s, 1H), 0.12 (s, 6H) ppm. ¹³C NMR (100 MHz, CDCl₃): δ = 159.40, 148.76, 140.27, 137.15, 132.67, 130.57, 129.72, 129.64, 129.42, 129.25, 129.05, 128.52, 128.44, 127.71, 121.15, 113.35, 111.02, 9.10 ppm. ¹¹B NMR (128 MHz, CDCl₃): δ = 0.30 ppm. HR-MS (ESI): calcd. for C₂₃H₂₁B₁Br₁N₂ ([M + H]⁺): 415.0980, found : 415.1013.

3B.4.2.6 Synthesis of compound 6

Degassed 1,4-dioxane was added to compound **5** (5.00 g, 12.04 mmol), potassium acetate (3.54 g, 36.12 mmol), bis(pinacolato)diboron (3.36 g, 13.24 mmol), Pd(dppf)Cl₂ (264 mg, 0.361 mmol) under nitrogen atmosphere in a 250 mL round bottom flask fitted with reflux condenser. After being stirred at 100 °C temperature for 12 h, the reaction mixture was poured into water, extracted with CH₂Cl₂. The combined organic layers were washed with brine solution, dried over Na₂SO₄ and concentrated. The residue was purified by silica gel column chromatography using *n*-hexane/ethyl acetate mixture as eluent. Yield: 5.00 g, (90 %). mp: 217 °C. ¹H NMR (400 MHz, CDCl₃): δ = 8.04 (s, 1H), 7.91 – 7.84 (m, 2H), 7.68 – 7.51 (m, 9H), 6.84 (d, *J* = 8.1 Hz, 1H), 6.64 (s, 1H), 1.40 (s, 12H), 0.23 (s, 6H) ppm. ¹³C NMR (100 MHz, CDCl₃): δ = 154.85, 148.68, 140.67, 140.31, 136.38, 132.04, 130.36, 129.64, 129.56, 129.03, 128.66, 128.42, 126.88, 111.16, 110.93, 83.64, 24.97, 9.28 ppm. ¹¹B

NMR (128 MHz, CDCl₃): δ = 32.24 (s), -0.17 (s) ppm. HR-MS (ESI): calcd. for C₂₉H₃₂B₂N₂O₂ ([M + H]⁺): 463.2733, found : 463.2733.

3B.4.2.7 Synthesis of compound 7

1,4-Dibromo-2,5-bis(hexyloxy)benzene (656 mg, 1.50 mmol) and Pd(PPh₃)₄ (104 mg, 0.09 mmol) were dissolved in 75 mL of degassed 1,2-dimethoxyethane under N₂ at room temperature. After being stirred at this temperature for 30 min, compound **6** (1.53 g, 3.30 mmol) and freshly prepared degassed solution of Na₂CO₃ (954 mg, 9.00 mmol) in water were added. The reaction mixture was heated to reflux for 18 h and cooled to room temperature. Distilled water was added to the reaction mixture and extracted with CH₂Cl₂. The combined organic layers were washed with brine solution, dried over Na₂SO₄ and concentrated. The residue was purified by silica gel column chromatography using *n*-hexane/dichloromethane mixture as eluent. Yield: 1.00 g, (70%). mp: 288 °C. ¹H NMR (400 MHz, CDCl₃): δ = 7.84 – 7.82 (m, 4H), 7.69 – 7.66 (m, 6H), 7.62 – 7.57 (m, 6H), 7.54 – 7.49 (m, 6H), 7.16 (dd, *J* = 8, 1.7 Hz, 2H), 6.97 (s, 2H), 6.80 (d, *J* = 8 Hz, 2H), 6.59 (s, 2H), 3.88 (t, *J* = 8 Hz, 4H), 1.70 – 1.63 (m, 4H), 1.39 – 1.32 (m, 4H), 1.28 – 1.22 (m, 8H), 0.84 (t, *J* = 8 Hz, 6H), 0.15 (s, 12H) ppm. ¹³C NMR (100 MHz, CDCl₃): δ = 155.67, 150.46, 148.46, 139.96, 137.43, 136.88, 131.04, 130.94, 130.34, 129.82, 129.53, 129.13, 129.10, 128.98, 128.49, 126.29, 116.43, 111.31, 110.70, 69.76, 31.65, 29.50, 25.96, 22.69, 14.19, 9.31 ppm. ¹¹B NMR (128 MHz, CDCl₃): δ = -0.63 (s) ppm. HR-MS (ESI): calcd. for C₆₄H₆₈B₂N₄O₂Na₁ ([M + Na]⁺): 969.5400, found : 969.5423.

3B.4.2.8 Synthesis of compound 8

Compound **8** was prepared following a procedure similar to that used for compound **7**. The quantities involved are as follows: 2,7-dibromo-9,9-dihexyl-9H-fluorene (0.49 g, 0.1 mmol) and Pd(PPh₃)₄ (68 mg, 0.06 mol%), compound **6**(1.00 g, 2.17 mmol),

Na₂CO₃(0.63 g, 5.94 mmol). Yield: 0.70 g, (70%). mp: 282 °C. ¹H NMR (400 MHz, CDCl₃): δ = 7.85 (dd, *J* = 7.5, 1.8 Hz, 2H), 7.75 – 7.69 (m, 8H), 7.63 – 7.51 (m, 16H), 7.28 (d, *J* = 1.7 Hz, 1H), 7.26 (s, 1H), 6.87 (d, *J* = 8 Hz, 2H), 6.62 (s, 2H), 2.06 – 2.02 (m, 4H), 1.12 – 1.07 (m, 12H), 0.78 – 0.75 (m, 10H), 0.21 (s, 12H) ppm. ¹³C NMR (100 MHz, CDCl₃): δ = 156.93, 151.67, 148.63, 140.35, 140.16, 140.04, 140.01, 137.79, 130.42, 129.81, 129.74, 129.60, 129.19, 129.12, 128.89, 128.52, 128.31, 126.18, 124.20, 121.64, 119.91, 112.09, 110.82, 55.37, 40.63, 31.60, 29.83, 23.90, 22.71, 14.14, 9.40 ppm. ¹¹B NMR (128 MHz, CDCl₃): δ = -2.60 (s) ppm. HR-MS (ESI): calcd. for C₇₁H₇₂B₂N₄K₁ ([M + K]⁺): 1041.5596, found : 1041.5568.

3B.4.2.9 Synthesis of compound 9

Compound **9** was prepared following a procedure similar to that used for compound **7**. The quantities involved are as follows: 2,7-Dibromo-9-hexyl-9H-carbazole (0.48 g, 1.17 mmol), compound **6** (1.19 g, 2.58 mmol), Na₂CO₃ (746 mg, 7.03 mmol), Pd(PPh₃)₄ (81 mg, 0.07 mmol). Yield: 0.70 g, (65%). mp: 199 °C. ¹H NMR (400 MHz, CDCl₃): δ = 8.13 (d, *J* = 8 Hz, 2H), 7.88 – 7.82 (m, 6H), 7.72 – 7.70 (m, 4H), 7.64 – 7.60 (m, 8H), 7.55 – 7.49(m, 8H), 7.33 (dd, *J* = 8.4, 1.8 Hz, 2H), 6.90 (d, *J* = 8.4 Hz, 2H), 6.63 (s, 2H), 4.39 (t, *J* = 8 Hz, 2H), 1.97 – 1.90 (m, 2H), 1.48 - 1.42 (m, 2H), 1.38 – 1.30 (m, 4H), 0.89 (t, *J* = 8 Hz, 3H), 0.23 (s, 12H) ppm. ¹³C NMR (100 MHz, CDCl₃): δ = 156.87, 148.53, 141.51, 140.63, 139.95, 139.39, 137.69, 130.32, 129.72, 129.65, 129.50, 129.10, 129.02, 128.80, 128.74, 128.42, 124.47, 121.81, 120.43, 118.85, 112.00, 110.73, 107.24, 43.06, 31.62, 29.02, 27.01, 22.60, 14.09, 9.32 ppm. ¹¹B NMR (128 MHz, CDCl₃): δ = -1.18 (s) ppm. HR-MS (ESI): calcd. for C₆₄H₅₉B₂N₅Na₁ ([M + Na]⁺): 942.4868, found : 942.4865

3B.4.2.10 Synthesis of compound 10

Degassed DMF (80 mL) was added to 2,5-bis(tributylstannyl)thiophene (1.10 g, 1.66 mmol), compound **5** (1.51 g, 3.65 mmol) and Pd(PPh₃)₄ (115 mg, 0.099 mmol) under nitrogen atmosphere in a round bottom flask. After being stirred at 120 °C for 12 h, the reaction mixture was poured into water and extracted with CH₂Cl₂. The combined organic layers were washed with brine solution, dried over Na₂SO₄ and concentrated. The residue was purified by silica gel column chromatography using *n*-hexane/dichloromethane mixture as eluent. Yield: 1.12 g, (90%). mp: 274 °C. ¹H NMR (400 MHz, CDCl₃): δ = 7.82 – 7.80 (m, 4H), 7.68 – 7.64 (m, 6H), 7.62 – 7.58 (m, 6H), 7.51 – 7.49 (m, 6H), 7.24 (s, 2H), 7.19 (dd, *J* = 8.4, 1.2 Hz, 2H), 6.75 (d, *J* = 8 Hz, 2H), 6.59 (s, 2H), 0.13 (s, 12H) ppm. ¹³C NMR (100 MHz, CDCl₃): δ = 157.09, 148.62, 143.82, 139.97, 137.77, 132.78, 130.42, 129.72, 129.62, 129.59, 129.17, 129.06, 128.69, 128.49, 126.73, 123.87, 122.59, 112.16, 110.84, 9.32 ppm. ¹¹B NMR (128 MHz, CDCl₃): δ = 1.78 (s) ppm. HR-MS (ESI): calcd. for C₅₀H₄₃B₂N₄S₁ ([M + H]⁺): 753.3405, found : 753.3452.

3B.4.2.1 Synthesis of compound 11

Compound **11** was prepared following a procedure similar to that used for compound **10**. The quantities involved are as follows: 5,5'-Bis(tributylstannyl)-2,2'-bithiophene (1.27 g, 1.71 mmol), compound **5** (1.56 g, 3.76 mmol), Pd(PPh₃)₄ (118 mg, 0.102 mmol). Yield: 1.21 g, (85%). mp: 285 °C. ¹H NMR (400 MHz, CDCl₃): δ = 7.82 – 7.80 (m, 4H), 7.66 – 7.58 (m, 13H), 7.51 – 7.50 (m, 6H), 7.19 – 7.12 (m, 5H), 6.75 (d, *J* = 8 Hz, 2H), 6.59 (s, 2H), 0.13 (s, 12H) ppm. ¹³C NMR (100 MHz, CDCl₃): δ = 157.21, 148.71, 143.63, 140.03, 137.93, 136.66, 132.45, 130.48, 129.79, 129.65, 129.22, 129.11, 128.75, 128.53, 126.79, 124.44, 123.71, 122.68, 112.21, 110.91, 9.27 ppm. HR-MS (ESI): calcd. for C₅₄H₄₄B₂N₄S₂Na₁ ([M + Na]⁺): 857.3103, found : 857.3136.

3B.5 References

- (1) Anthony, J. E.; Facchetti, A.; Heeney, M.; Marder, S. R.; Zhan, X. *Adv. Mater.***2010**, *22*, 3876.
- (2) Entwistle, C. D.; Marder, T. B. *Chem. Mater.***2004**, *16*, 4574.
- (3) Jakle, F. *Coord. Chem. Rev.***2006**, *250*, 1107.
- (4) Jäkle, F. *Chem. Rev.***2010**, *110*, 3985.
- (5) Rao, Y.-L.; Wang, S. *Inorg. Chem.***2011**, *50*, 12263.
- (6) Li, D.; Zhang, H.; Wang, Y. *Chem. Soc. Rev.***2013**, *42*, 8416.
- (7) Frath, D.; Massue, J.; Ulrich, G.; Ziessel, R. *Angew. Chem. Int. Ed. Engl.***2014**, *53*, 2290.
- (8) Ji, L.; Griesbeck, S.; Marder, T. B. *Chem. Sci.***2017**.
- (9) Cui, Y.; Wang, S. *J. Org. Chem.***2006**, *71*, 6485.
- (10) Wakamiya, A.; Taniguchi, T.; Yamaguchi, S. *Angew. Chem. Int. Ed. Engl.***2006**, *45*, 3170.
- (11) Zhang, Z.; Bi, H.; Zhang, Y.; Yao, D.; Gao, H.; Fan, Y.; Zhang, H.; Wang, Y.; Wang, Y.; Chen, Z.; Ma, D. *Inorg. Chem.***2009**, *48*, 7230.
- (12) Job, A.; Wakamiya, A.; Kehr, G.; Erker, G.; Yamaguchi, S. *Org. Lett.***2010**, *12*, 5470.
- (13) Li, D.; Zhang, Z.; Zhao, S.; Wang, Y.; Zhang, H. *Dalton Trans.***2011**, *40*, 1279.
- (14) Li, D.; Wang, K.; Huang, S.; Qu, S.; Liu, X.; Zhu, Q.; Zhang, H.; Wang, Y. *J. Mater. Chem.***2011**, *21*, 15298.
- (15) Li, D.; Yuan, Y.; Bi, H.; Yao, D.; Zhao, X.; Tian, W.; Wang, Y.; Zhang, H. *Inorg. Chem.***2011**, *50*, 4825.

- (16) Neue, B.; Froehlich, R.; Wibbeling, B.; Fukazawa, A.; Wakamiya, A.; Yamaguchi, S.; Wuerthwein, E.-U. *J. Org. Chem.* **2012**, *77*, 2176.
- (17) Kubota, Y.; Ozaki, Y.; Funabiki, K.; Matsui, M. *J. Org. Chem.* **2013**, *78*, 7058.
- (18) Shimizu, S.; Iino, T.; Saeki, A.; Seki, S.; Kobayashi, N. *Chem. Eur. J.* **2015**, *21*, 2893.
- (19) Suresh, D.; Gomes, C. S. B.; Lopes, P. S.; Figueira, C. A.; Ferreira, B.; Gomes, P. T.; Di Paolo, R. E.; Macanita, A. L.; Duarte, M. T.; Charas, A.; Morgado, J.; Vila-Vicosa, D.; Calhorda, M. J. *Chem. Eur. J.* **2015**, *21*, 9133.
- (20) Frath, D.; Benelhadj, K.; Munch, M.; Massue, J.; Ulrich, G. *J. Org. Chem.* **2016**, *81*, 9658.
- (21) Grandl, M.; Sun, Y.; Pammer, F. *Chem. Eur. J.* **2016**, *22*, 3976.
- (22) Nakamura, T.; Furukawa, S.; Nakamura, E. *Chem. Asian J.* **2016**, *11*, 2016.
- (23) Yusuf, M.; Liu, K.; Guo, F.; Lalancette, R. A.; Jakle, F. *Dalton Trans.* **2016**, *45*, 4580.
- (24) Schraff, S.; Sun, Y.; Pammer, F. *J. Mater. Chem. C.* **2017**, *5*, 1730.
- (25) Yoshino, J.; Kano, N.; Kawashima, T. *Dalton Trans.* **2013**, *42*, 15826.
- (26) Yoshino, J.; Kano, N.; Kawashima, T. *Chem. Commun.* **2007**, 559.
- (27) Yoshino, J.; Kano, N.; Kawashima, T. *J. Org. Chem.* **2009**, *74*, 7496.
- (28) Rao, Y.-L.; Amarne, H.; Zhao, S.-B.; McCormick, T. M.; Martić, S.; Sun, Y.; Wang, R.-Y.; Wang, S. *J. Am. Chem. Soc.* **2008**, *130*, 12898.
- (29) Yang, D.-T.; Mellerup, S. K.; Peng, J.-B.; Wang, X.; Li, Q.-S.; Wang, S. *J. Am. Chem. Soc.* **2016**, *138*, 11513.
- (30) Mellerup, S. K.; Rao, Y.-L.; Amarne, H.; Wang, S. *Org. Lett.* **2016**, *18*, 4436.
- (31) Rao, Y.-L.; Hoerl, C.; Braunschweig, H.; Wang, S. *Angew. Chem., Int. Ed.* **2014**, *53*, 9086.

- (32) Rao, Y.-L.; Amarne, H.; Chen, L. D.; Brown, M. L.; Mosey, N. J.; Wang, S. J. *Am. Chem. Soc.***2013**, *135*, 3407.
- (33) Rao, Y.-L.; Amarne, H.; Wang, S. *Coord. Chem. Rev.***2012**, *256*, 759.
- (34) Ishida, N.; Moriya, T.; Goya, T.; Murakami, M. *J. Org. Chem***2010**, *75*, 8709.
- (35) Zhu, C.; Guo, Z. H.; Mu, A. U.; Liu, Y.; Wheeler, S. E.; Fang, L. *J. Org. Chem.***2016**, *81*, 4347.
- (36) Zhao, Z.; Chang, Z.; He, B.; Chen, B.; Deng, C.; Lu, P.; Qiu, H.; Tang, B. Z. *Chem. Eur. J.***2013**, *19*, 11512.
- (37) Wong, H.-L.; Wong, W.-T.; Yam, V. W.-W. *Org. Lett.***2012**, *14*, 1862.
- (38) Wong, B. Y.-W.; Wong, H.-L.; Wong, Y.-C.; Chan, M.-Y.; Yam, V. W.-W. *Chem. Eur. J.***2016**, *22*, 15095.
- (39) Shaikh, A. C.; Ranade, D. S.; Thorat, S.; Maity, A.; Kulkarni, P. P.; Gonnade, R. G.; Munshi, P.; Patil, N. T. *Chem. Commun.***2015**, *51*, 16115.
- (40) He, B.; Chang, Z.; Jiang, Y.; Chen, B.; Lu, P.; Kwok, H. S.; Qin, A.; Zhao, Z.; Qiu, H. *Dyes Pigm.***2014**, *101*, 247.
- (41) Crossley, D. L.; Vitorica-Yrezabal, I.; Humphries, M. J.; Turner, M. L.; Ingleson, M. J. *Chem. Eur. J.***2016**, *22*, 12439.
- (42) Crossley, D. L.; Cade, I. A.; Clark, E. R.; Escande, A.; Humphries, M. J.; King, S. M.; Vitorica-Yrezabal, I.; Ingleson, M. J.; Turner, M. L. *Chem. Sci.***2015**, *6*, 5144.
- (43) Pal, B.; Yen, W.-C.; Yang, J.-S.; Su, W.-F. *Macromolecules***2007**, *40*, 8189.
- (44) Rice, N. A.; Adronov, A. *Macromolecules***2013**, *46*, 3850.
- (45) Guo, X.; Watson, M. D. *Org. Lett.***2008**, *10*, 5333.
- (46) Norris, B. N.; Zhang, S.; Campbell, C. M.; Auletta, J. T.; Calvo-Marzal, P.; Hutchison, G. R.; Meyer, T. Y. *Macromolecules***2013**, *46*, 1384.

CHAPTER 4

Phenanthrene imidazole based N,C- chelate diboron complexes: Synthesis, characterization and photophysical properties

4.1 Introduction	173
4.2 Results and discussion	174
4.2.1 Synthesis and characterization	174
4.2.2 Single crystal X-ray analysis	177
4.2.3 Photophysical studies	182
4.2.4 Thermal studies	185
4.2.5 Electrochemical studies	186
4.3 Conclusions	187
4.4 Experimental section	187
4.4.1 General information	187
4.4.2 Synthetic procedure and spectral characterization	188
4.5 References	196

4.1 Introduction

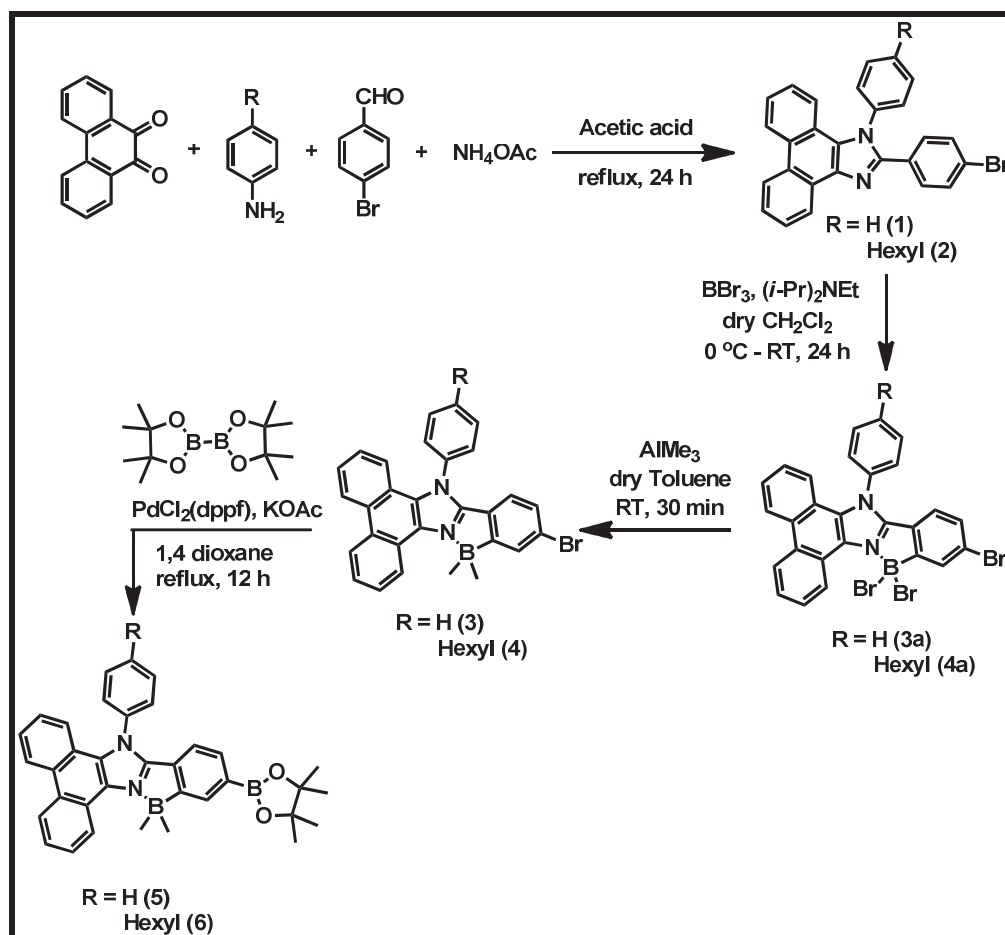
Organic fluorescent materials have gained great interest on account of their potential applications in OLEDs, organic light emitting field effect transistors and fluorescent sensors.¹⁻⁴ Tetra-coordinate boron compounds are a family of efficient luminescent materials and several classes of tetra-coordinate boron chromophores, including N,O-, N,N- and N,C- chelate π -systems have been designed and synthesized.⁵⁻⁸ N,C- chelate boron compounds with intramolecular B–N donor-acceptor bond has gained interest owing to their potential applications in organic electronics, fluorescent sensors, bio-imaging, development of near infrared materials, photochromic materials and molecular switches.^{5,6,8-11}

Several examples mononuclear and di or multi nuclear N,C- chelate boron compounds have been developed by the groups of Yamaguchi^{12,13} and Wang^{5,8,14-18}. Kawashima and co-workers reported the azobenzene and aromatic aldimines based N,C- chelate boron compounds.^{10,19,20} Zhang and co-workers synthesized a series of N,C- chelate boron compounds based on substituted diphenyl thiazolothiazole ligand.²¹ Pischel and co-workers reported a series of highly fluorescent N,C- chelate boron compounds based on aryl isoquinoline skeleton.¹¹ Recently N,C- chelate boron polymers have been used as a electron acceptors for all polymer solar cell devices.^{22,23} After development of electrophilic aromatic borylation method by Murakami²⁴ and co-workers in phenylpyridine system; several groups are actively involved in the synthesis of N,C- chelate boron compounds with different ligand systems.^{9,25-33} In chapter 3B we describe the N,C- chelate dinuclear boron compounds based on pyrazole. In this chapter, we describe the synthesis, characterization, photophysical and electrochemical properties of phenanthrene imidazole based N,C- chelate dinuclear boron compounds.

4.2 Results and discussion

4.2.1 Synthesis and characterization

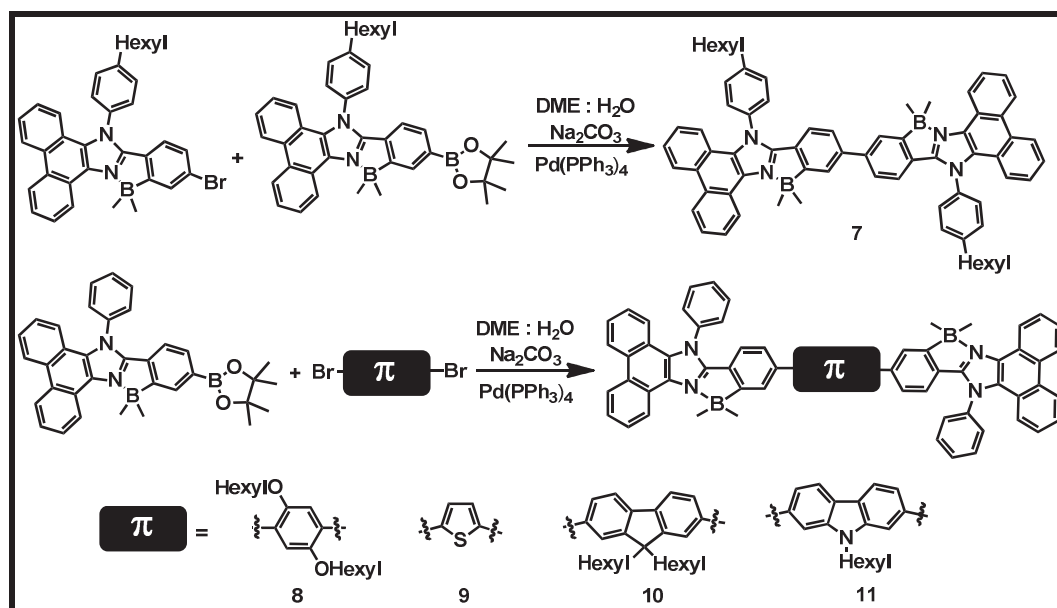
The synthetic pathways that we employed to obtain the target compounds are shown in Scheme 4.1 and Scheme 4.2.



Scheme 4.1: Synthesis of compounds **5** and **6**.

The starting materials **1** and **2** were synthesised in good yields by a four component reaction involving commercially available substances 9,10-phenanthrenequinone, 4-bromobenzaldehyde, aniline (for **1**) or 4-hexylaniline (for **2**), and ammonium acetate in glacial acetic acid by modifying the literature procedure.³⁴ Compounds **1** and **2** were subjected to electrophilic aromatic borylation reaction with BBr_3 in the presence of *N,N*-diisopropyl-*N*-ethylamine ($i\text{-Pr}_2\text{NEt}$) to afford imidazole-dibromoborane complexes (**3a**, **4a**). Without further purification the phenanthrene

imidazole-dibromo borane complexes (**3a**, **4a**) were treated with trimethylaluminium (AlMe_3) to afford the desired products **3** and **4** in moderate yields.



Scheme 4.2: Synthesis of compounds **7-11**.

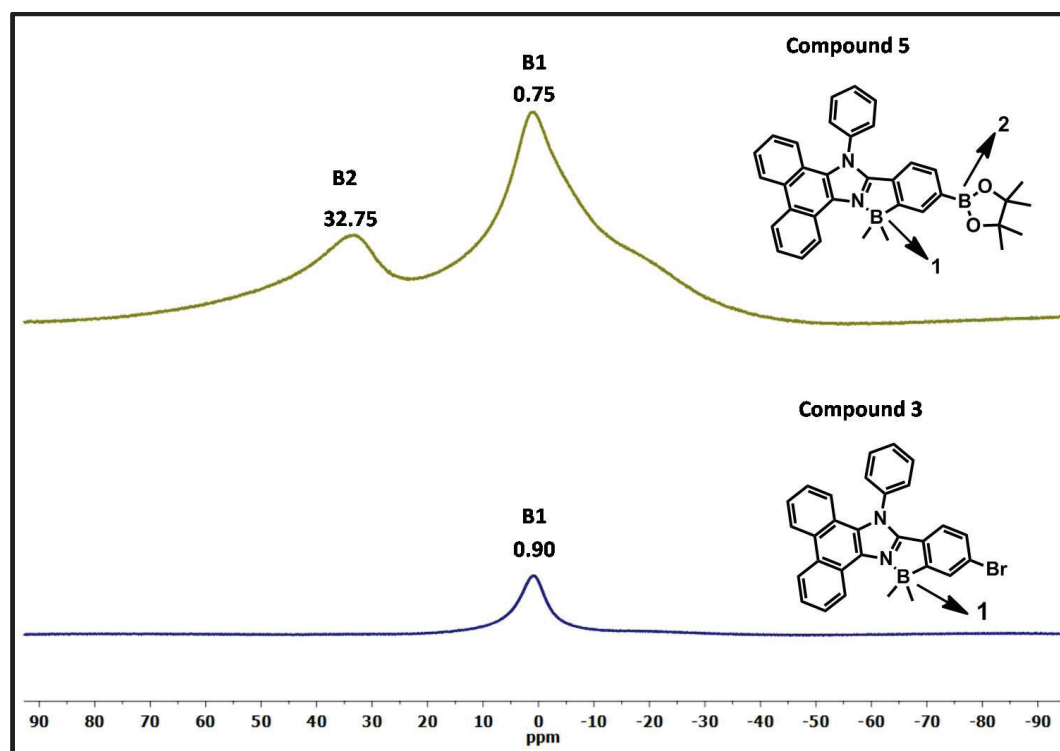


Figure 4.1: ^{11}B NMR of compounds **3** and **5**.

The reaction of compound **3** or **4** with bis(pinacolato)diboron and catalytic amount of $\text{Pd}(\text{dppf})\text{Cl}_2$ under Miyaura coupling condition afforded compounds **5** and **6**

respectively in 85% for **5** , 90% for **6** . The ^{11}B NMR spectrum of compound **5** shows two peaks; the peak at 0.75 ppm corresponds to a tetra- coordinate boron centre and the peak at 32.75 ppm corresponds to boronate ester boron centre (Figure 4.1). Compound **7** was synthesized using Suzuki coupling between compound **4** and compound **6**.

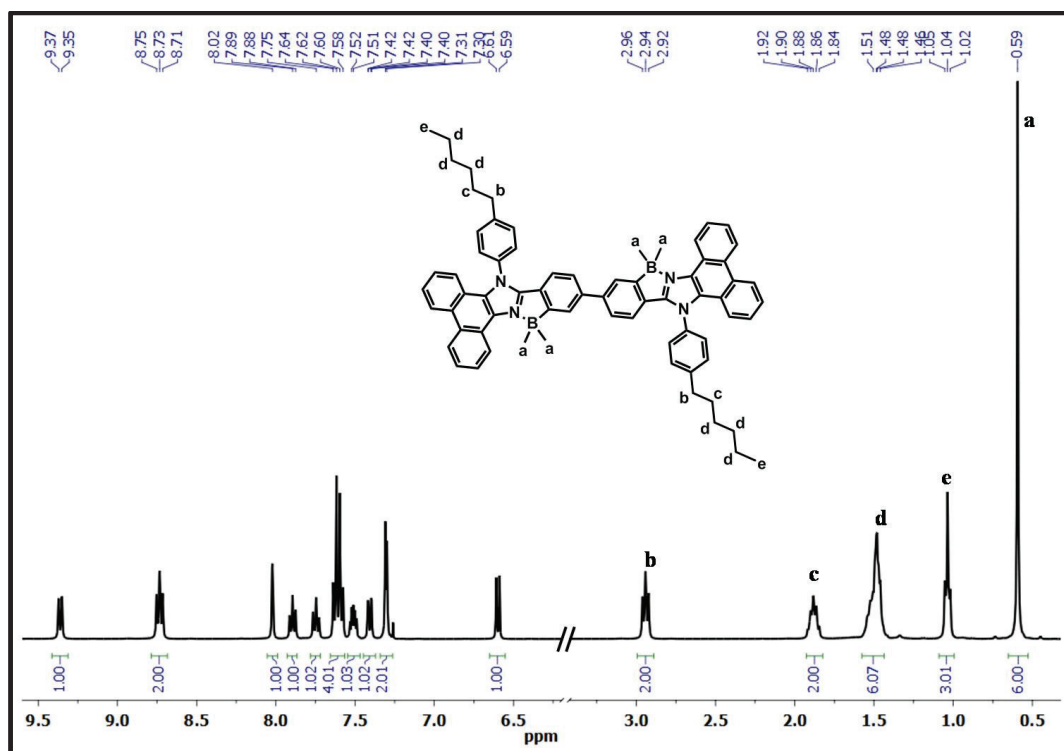


Figure 4.2: ^1H NMR spectrum of compound **7**.

The Suzuki coupling between compound **5** and 1,4-dibromo-2,5-bis(hexyloxy)benzene (or) 2,5-dibromothiophene (or) 2,7-dibromo-9,9-dihexyl-9H-fluorene (or) 2,7-dibromo-9-hexyl-9H-carbazole afforded compound **8** (or) **9** (or) **10** (or) **11** respectively in moderate yields. All the compounds were purified by silica gel column chromatography and characterized by ^1H , ^{13}C , ^{11}B NMR and HRMS. In ^1H NMR spectra, the signal resonate at 0.59 (for **7**), 0.52 (for **8**), 0.49 (for **9**), 0.61 (for **10**), 0.54 (for **11**) corresponding to the methyl protons on boron centre. A representative ^1H NMR for **7** and HRMS for **8** were shown in Figure 4.2 and Figure 4.3 respectively.

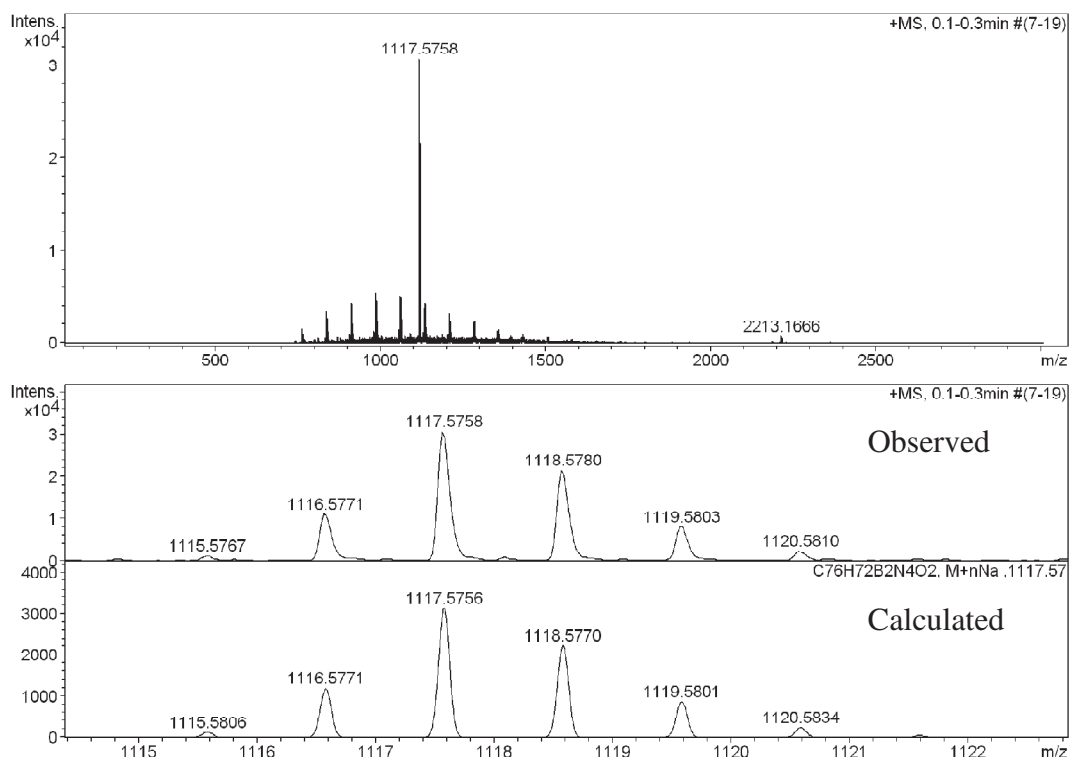


Figure 4.3: HRMS of compound 8.

4.2.2. Single crystal X-ray analysis

Single crystals of compounds **7**, **8**, **9** and **10** suitable for X-ray diffraction were obtained from slow evaporation of respective solutions in CH₂Cl₂/hexane mixture. Compounds **7**, **8**, **9** and **10** were crystallized in the monoclinic *C2/c*, monoclinic *C2/c*, triclinic *P-1* and triclinic *P-1* space groups respectively. The molecular structures of compounds **7**, **8**, **9** and **10** are shown in Figure 4.4; selected bond lengths and bond angles are summarized in Table 4.1. Interplanar angles are listed in Table 4.2 and crystallographic data for compounds **7-10** are presented in Table 4.3. In all the compounds, the boron center is tetra-coordinate and adopts a typical distorted tetrahedral geometry. The boron atom deviates from the five-membered plane defined by C₃NB (Imidazole N2, C2 and phenyl carbons directly attached boron, C2); the distance ranging from 0.0017 Å to 0.0390 Å (Table 4.2). The B–N and B–C distances

are in the typical range and are consistent with other literature reported N,C- chelate tetra-coordinate boron complexes^{26,29} (Table 4.1).

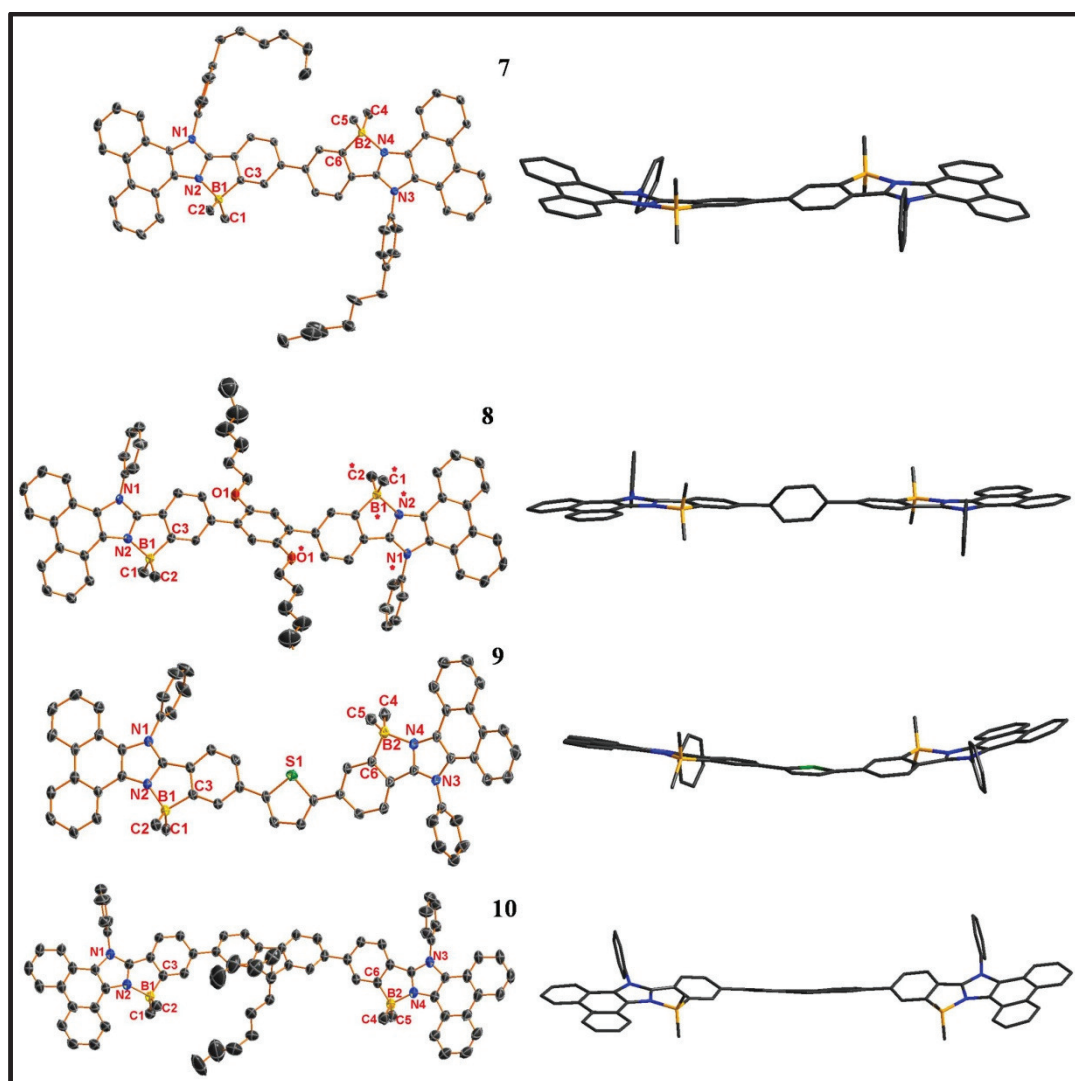


Figure 4.4: Molecular structure of compound **7**, **8**, **9** and **10** (left); side view (right). Thermal ellipsoids are drawn at 30% probability level.

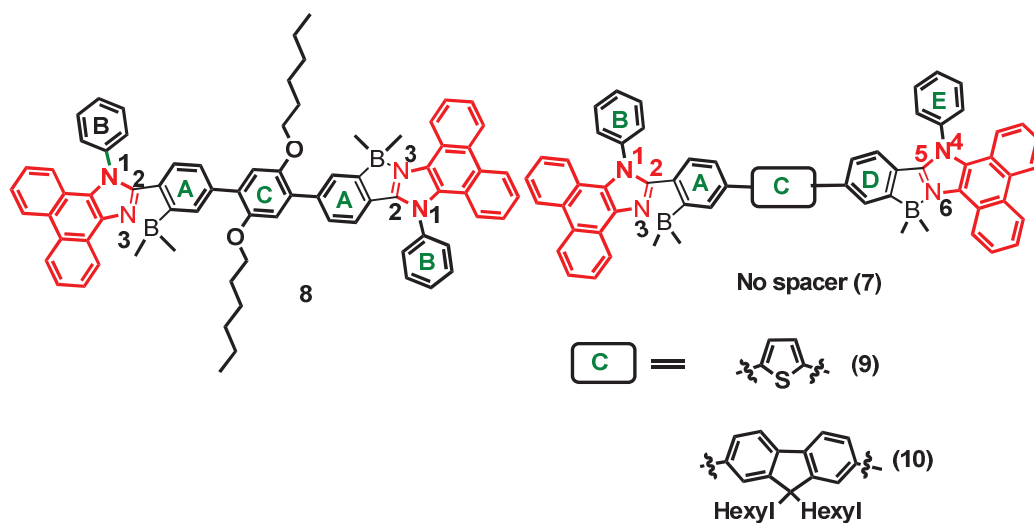
The inter-planar angle between the imidazole and 2-phenyl (Plane A) is 18.346° (for **7**) 8.193° (for **8**) 2.226° (for **9**), 8.379° (for **10**) whereas the inter-planar angle between the imidazole and 5-phenyl (Plane D) is 11.473° (for **7**), 17.031° (for **9**), 6.470° (for **10**); which indicate imidazoles and phenyl groups at 2 or 5 positions (Plane A or B) have distortion. Compound **7** exhibit crystallographic inversion centre in which both boron centres are anti to each other whereas compounds **8**, **9** and **10** have crystallized in non-centrosymmetric system and have anti conformation of boron

centres in compounds **8** & **9** and syn conformation of boron centres in compound **10**. In compound **7** both imidazole moieties (Plane A//Plane D) were twisted by 18.830°. The interplanar angle between 2-phenyl (Plane A) or 5-phenyl (Plane D) and π spacer (Plane C) is 52.909° (for **8**), 5.451° & 12.100° (for **9**), 28.696° & 38.543° (for **10**) which indicates that thiophene spacer in compound **9** is nearly planar with its attached imidazole moieties, whereas 1,4-bis(hexyloxy)benzene spacer in compound **8** and fluorenyl spacer in compound **10** are twisted with their attached imidazole moieties (side views in Figure 4.4).

Table 4.1: Comparison of selected bond lengths [Å] and bond angles [deg] for compounds **7-10**.

Compound	7	8	9	10
B1-C1	1.604(4)	1.623(6)	1.620(5)	1.604(6)
B1-C2	1.616(4)	1.605(6)	1.632(5)	1.610(5)
B1-C3	1.622(3)	1.621(5)	1.617(5)	1.606(5)
B1-N2	1.656(3)	1.661(5)	1.645(4)	1.653(4)
C1-B1-C2	116.7(2)	115.6(3)	115.3(3)	114.9(3)
C1-B1-C3	111.1(2)	111.8(3)	111.8(3)	112.6(3)
C2-B1-C3	111.1(2)	112.4(3)	111.6(3)	110.8(3)
C1-B1-N2	112.3(2)	110.0(3)	109.5(3)	111.0(3)
C2-B1-N2	108.52(19)	110.0(3)	111.4(3)	110.8(3)
C3-B1-N2	94.97(16)	95.1(3)	95.5(3)	114.9(3)

Compound	7	9	10
B2-C4	1.615(4)	1.601(5)	1.610(5)
B2-C5	1.606(4)	1.627(5)	1.609(5)
B2-C6	1.612(3)	1.620(5)	1.611(5)
B2-N4	1.657(3)	1.664(4)	1.654(4)
C4-B2-C5	113.8(2)	116.3(3)	114.7(3)
C4-B2-C6	110.34(19)	110.2(3)	112.1(3)
C5-B2-C6	112.47(19)	112.8(3)	112.4(3)
C4-B2-N4	112.5(2)	113.4(3)	108.8(3)
C5-B2-N4	111.23(18)	107.1(3)	111.8(3)
C6-B2-N4	95.05(16)	95.0(2)	95.3(2)

Table 4.2: Comparison of deviation of boron atom from C_3NB plane [\AA] and interplanar angles [deg] for compounds **7-10**.

Compound	7	8	9	10
Deviation of B1 from C_3NB Plane (\AA)	0.0017	0.0220	0.0390	0.0059
Imidazole //Plane A	18.346(47)	8.193(91)	2.226(61)	8.379(70)
Imidazole //Plane B	83.251(45)	83.477(95)	86.927(101)	81.636(126)
Plane A//Plane C		52.909(113)	5.451(85)	28.696(85)
Deviation of B2 from C_3NB Plane (\AA)	-0.0243		-0.0159	-0.0144
Imidazole //Plane D	11.473(46)		17.031(68)	6.470(82)
Imidazole //Plane E	85.155(68)		86.765(80)	83.413(117)
Plane D//Plane C			12.100(79)	38.543(82)
Plane A//Plane D	18.830(63)			

Table 4.3: Crystal data and structure refinement parameters for compounds **7**, **8**, **9** & **10**.

Compound	7	8	9	10
Empirical formula	C ₇₀ H ₆₈ B ₂ N ₄	C ₇₈ H ₇₄ B ₂ Cl ₆ N ₄ O ₂	C ₆₂ H ₄₆ B ₂ N ₄ S	C ₈₃ H ₇₆ B ₂ N ₄
Formula weight	986.90	1333.73	900.71	1151.09
Temperature/K	100.00	296.15	296.15	296.15
Crystal system	Monoclinic	Monoclinic	Triclinic	Triclinic
Space group	C2/c	C2/c	<i>P</i> -1	<i>P</i> -1
<i>a</i> /Å	16.7657(16)	24.990(2)	10.0256(8)	15.4087(5)
<i>b</i> /Å	17.7131(16)	18.4811(17)	11.0728(11)	16.2830(6)
<i>c</i> /Å	38.891(3)	17.3011(17)	23.605(2)	16.8471(8)
α /°	90	90	82.719(5)	103.453(4)
β /°	95.378(7)	108.166(6)	81.300(5)	115.561(4)
γ /°	90	90	78.268(6)	105.550(3)
Volume/Å ³	11498.7(18)	7592.2(12)	2523.7(4)	3365.7(3)
<i>Z</i>	8	4	2	2
ρ_{calcd} /g cm ⁻³	1.140	1.167	1.185	1.136
μ /mm ⁻¹	0.065	0.272	0.108	0.492
<i>F</i> (000)	4208.0	2792.0	944.0	1224.0
2 θ range for data collection/°	3.352 to 56.956	2.792 to 50.874	1.754 to 50.812	8.688 to 136.476
Index ranges	-22 ≤ <i>h</i> ≤ 22, -23 ≤ <i>k</i> ≤ 23, -52 ≤ <i>l</i> ≤ 0	-30 ≤ <i>h</i> ≤ 30, -22 ≤ <i>k</i> ≤ 22, -20 ≤ <i>l</i> ≤ 20	-12 ≤ <i>h</i> ≤ 11, -13 ≤ <i>k</i> ≤ 13, -28 ≤ <i>l</i> ≤ 28	-18 ≤ <i>h</i> ≤ 18, -19 ≤ <i>k</i> ≤ 16, -20 ≤ <i>l</i> ≤ 17
Reflns. collected	28794	46270	24254	33325
Independent reflns	14456 [<i>R</i> _{int} = 0.0593, <i>R</i> _{sigma} = 0.0809]	7001 [<i>R</i> _{int} = 0.1419, <i>R</i> _{sigma} = 0.0947]	9227 [<i>R</i> _{int} = 0.0722, <i>R</i> _{sigma} = 0.1251]	12279 [<i>R</i> _{int} = 0.0367, <i>R</i> _{sigma} = 0.0428]
Data/restraints/parameters	14456/0/691	7001/55/456	9227/0/626	12279/102/976
GOF on <i>F</i> ²	1.107	0.933	0.896	1.031
Final <i>R</i> indices [<i>I</i> > 2 σ (<i>I</i>)]	<i>R</i> ₁ = 0.0731, <i>wR</i> ₂ = 0.2060	<i>R</i> ₁ = 0.0764, <i>wR</i> ₂ = 0.1972	<i>R</i> ₁ = 0.0614, <i>wR</i> ₂ = 0.1345	<i>R</i> ₁ = 0.0830, <i>wR</i> ₂ = 0.2417
<i>R</i> indices (all data)	<i>R</i> ₁ = 0.1209, <i>wR</i> ₂ = 0.2287	<i>R</i> ₁ = 0.1665, <i>wR</i> ₂ = 0.2331	<i>R</i> ₁ = 0.1535, <i>wR</i> ₂ = 0.1577	<i>R</i> ₁ = 0.1181, <i>wR</i> ₂ = 0.2715
Largest diff. peak/hole [e Å ⁻³]	0.96/-0.61	0.35/-0.34	0.23/-0.28	0.42/-0.39

4.2.3. Photophysical Studies

Compounds **7-11** were insoluble in non polar and protic solvents; hence, the UV-Vis absorption and emission properties were performed in CH₂Cl₂, DMF and THF solvents and relevant data are summarized in Table 4.4. The normalized UV-Vis absorption and fluorescence spectra of compounds **7-11** in dichloromethane are displayed in Figure 4.5 and Figure 4.6 respectively.

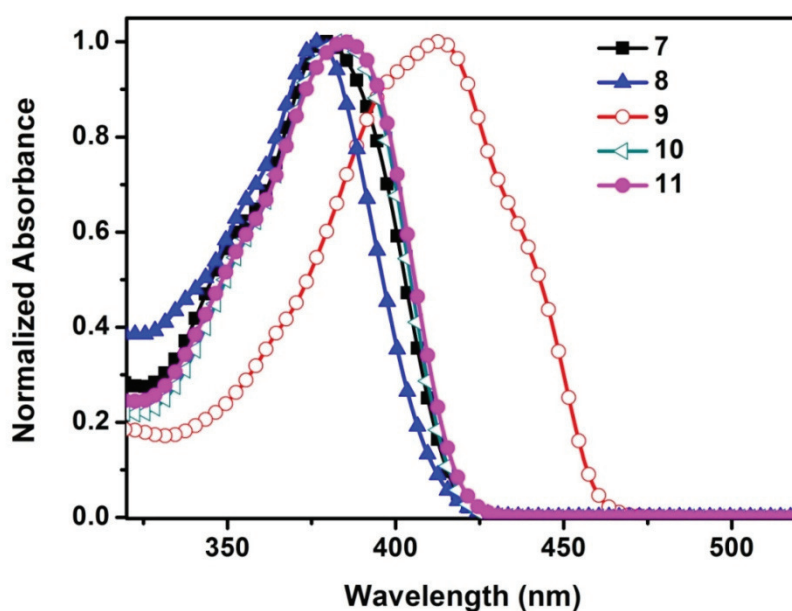


Figure 4.5: Comparison of normalized absorption spectra of **7-11** in dichloromethane (concentration: 1×10^{-5} M).

The absorption spectra of compounds **7-11** are less sensitive towards solvent polarity, which indicates that the interaction of these compounds with the solvents in the ground state is less significant. Absorption maxima of these compounds comprised between 377 - 413 nm with molar absorption coefficients ranging from 56010 to 75400 M⁻¹ cm⁻¹ in dichloromethane solution. The absorption of compound **9** was red shifted compared to other compounds which is attributed to the better conjugation nature of thiophene (Figure 4.4).

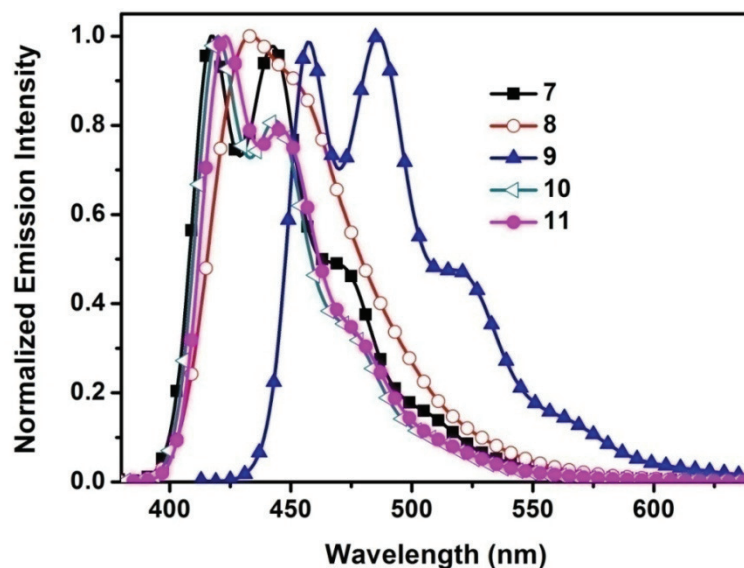


Figure 4.6: Comparison of normalized emission spectra of **7-11** in dichloromethane (concentration: 1×10^{-5} M).

Table 4.4: Photophysical properties of **7-11** in various solvents and in solid state.

Compound	Solvent	λ_{\max}^a (nm)	ϵ_{\max} ($M^{-1}cm^{-1} \times 10^3$)	$\lambda_{em}^{a,b}$ (nm)	Φ_F^c	Stokes shift (nm)
7	THF	378	58.02	415	0.93	37
	CH ₂ Cl ₂	379	58.02	418	0.98	39
	DMF	380	56.25	444	0.90	39
	Solid			483	0.20	
8	THF	376	68.53	431	0.89	55
	CH ₂ Cl ₂	377	56.01	434	0.87	57
	DMF	378	69.55	437	0.90	59
	Solid			446	0.51	
9	THF	413	76.47	484	0.59	71
	CH ₂ Cl ₂	413	57.91	486	0.65	73
	DMF	415	74.44	487	0.59	72
	Solid			507	0.32	
10	THF	382	122.55	419	0.92	37
	CH ₂ Cl ₂	383	75.40	420	0.98	37
	DMF	384	98.64	422	0.99	38
	Solid			451	0.33	
11	THF	385	151.12	422	0.98	37
	CH ₂ Cl ₂	385	74.59	423	0.98	38
	DMF	386	110.32	425	0.99	39
	Solid			467	0.30	

^a Absorption maximum (Concentration: 1×10^{-5} M). ^b Excited at the absorption maximum. ^c Fluorescence quantum yields were measured using quinine sulphate as the reference.

The steady state fluorescence spectra of compounds **7-11** were recorded by exciting at their absorption maxima and the relevant data are summarised in Table 4.4. The emission maxima of these compounds ranged from 418 to 486 nm in CH₂Cl₂ and slightly affected with solvent polarity. Compounds **9-11** exhibit red shifted emission maxima over compound **7** due to increase in conjugation. All these compounds exhibit good fluorescent quantum yields ranging from 0.59 to 0.99.

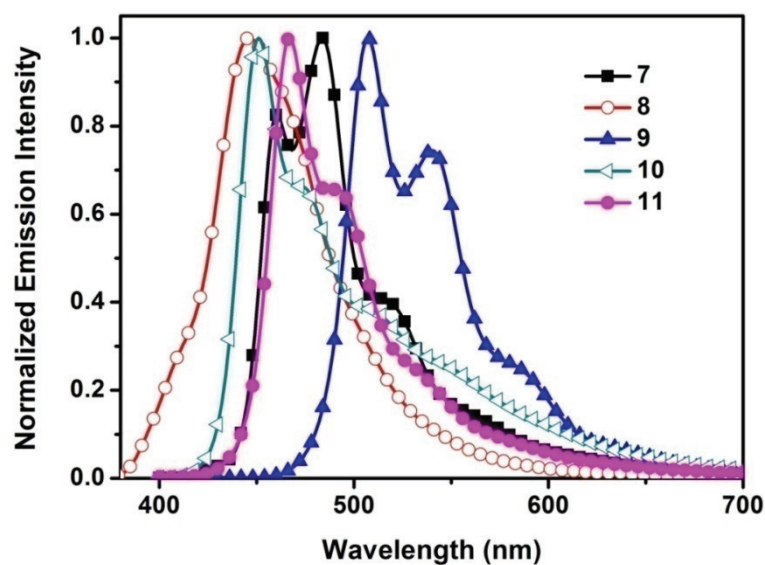


Figure 4.7: Comparison of normalized emission spectra of **7-11** in solid state.

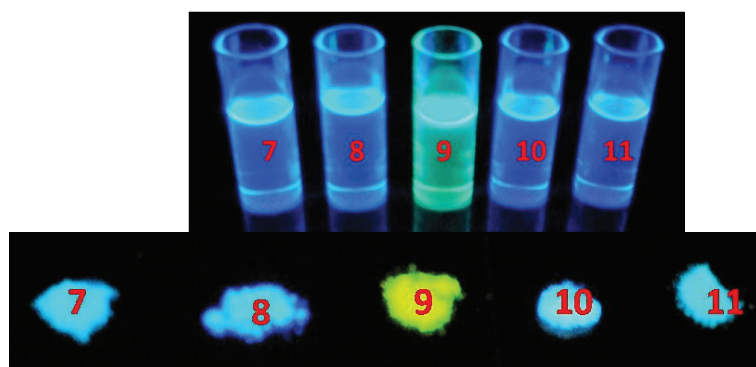


Figure 4.8: The fluorescence photograph of compounds **7-11** in dichloromethane solution (top) and in solid state (bottom). Irradiation was performed with a UV lamp of a wavelength of 365 nm.

As compared to compound **7**, **8**, **10** and **11**, compound **9** exhibits lower fluorescence quantum yield, which may be attributable to the presence of the heavier sulphur atom

in the thiophene ring, enhancing the intersystem crossing rate.³⁵ The Stokes shifts of these compounds observed in the range from 37 nm (for **10**) to 73 nm (for **9**). Compounds **7-11** also exhibit bright solid state emission (Figure 4.8) with red shifted emission maxima in comparison to their emission in solution state. These compounds exhibit solid state quantum yields ranged from 0.20 to 0.55, which are significantly lower than their solution state quantum yields. The observed red shifted emissions and lower quantum yields in solid state might be because of increased intermolecular interactions in the solid state.

4.2.4 Thermal Studies

Thermal properties of these dinuclear N,C- chelate organoboron compounds (**7-11**) were investigated by thermogravimetric analysis (TGA) and differential scanning calorimetry (DSC) under nitrogen atmosphere at the heating rate of 10 °C min⁻¹.

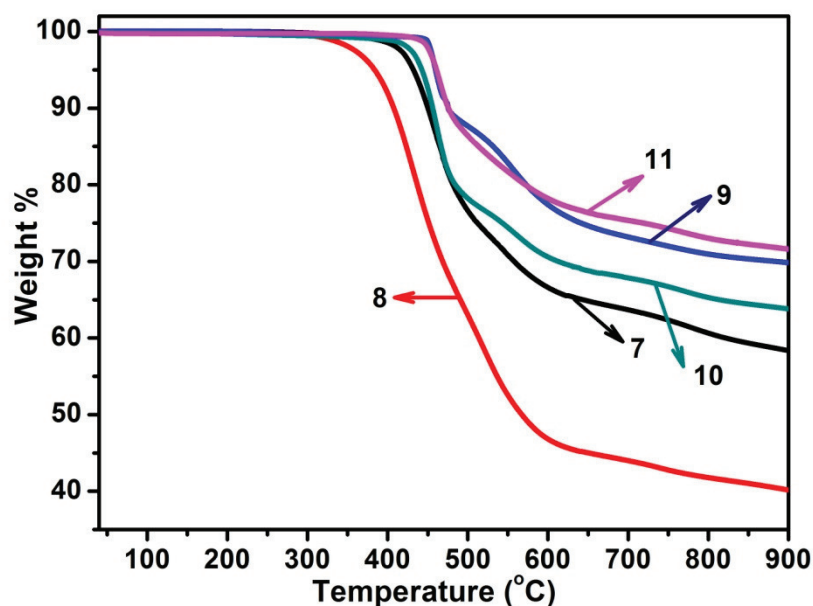


Figure 4.9: TGA curves of **7-11** at heating rate of 10 °C/min.

All these compounds showed very high thermal stability with decomposition temperature (T_{d5}) (corresponds to 5% weight loss) of compounds **7**, **8**, **9**, **10** and **11**

are 432, 383, 459, 442 and 460 (Figure 4.9), respectively. All the five compounds exhibited melting point above 300 °C (Figure 4.10).

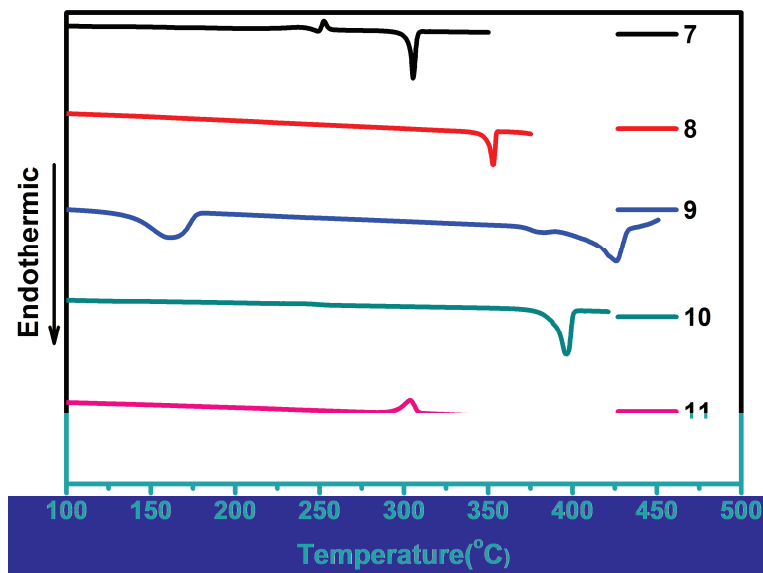


Figure 4.10: DSC curves of 7-11 at heating rate of 10 °C/min.

4.2.5 Electrochemical studies

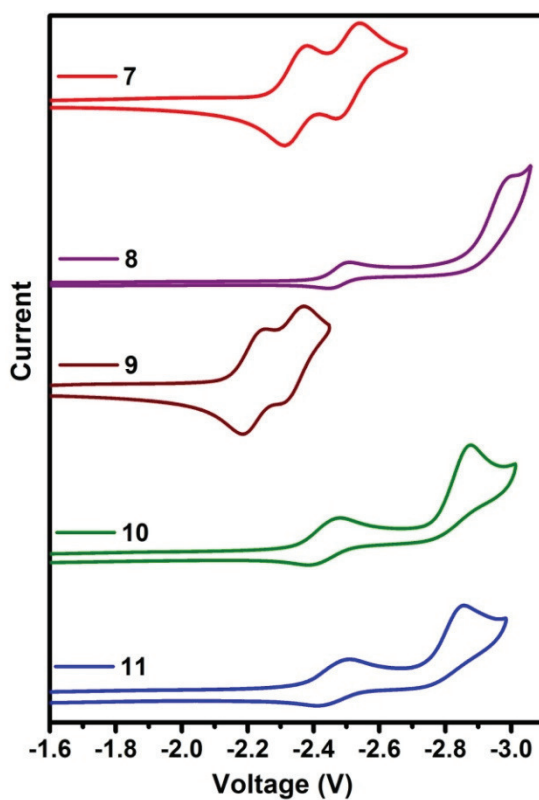


Figure 4.11: Cyclic voltammograms of 7-11 recorded in DMF containing 0.1M $n\text{Bu}_4\text{N}(\text{PF}_6)$ as supporting electrolyte; scan rate 100 mV/s. Referenced relative to Fc/Fc^+ couple.

The electrochemical properties of compounds **7-11** were studied by cyclic voltammetry at a scan rate of 100 mV/s using $t\text{Bu}_4\text{NPF}_6$ as a supporting electrolyte (0.1 M) in DMF solution under nitrogen atmosphere. The cyclic voltammograms of compounds **7-11** are shown in Figure 4.11. Compounds **8, 10, 11** displayed two quasi-reversible reduction peaks whereas compound **7, 9** displayed two reversible reduction peaks. Compound **9** exhibited less negative reduction potentials as compared the compounds **7,8, 10** and **11**.

4.3 Conclusions

In conclusion, we have synthesised a series of phenanthrene imidazole based dinuclear boron compounds (**7-11**). The absorbance and emission maxima of these compounds were greatly depends on π - conjugation spacer. These compounds were exhibited fluorescence emission both in solution and solid state. Furthermore these compounds exhibit high thermal stability. The electrochemical and rich photophysical properties, suggesting the possibility of these diboron compounds as emitters and/or electron transporting materials in OLEDs.

4.4 Experimental Section

4.4.1. General Information

All reagents and starting materials were purchased from Sigma-Aldrich, Alfa Aesar and Spectrochem chemical companies and used as received unless otherwise noted. THF and toluene were distilled from Na/benzophenone prior to use. Dichloromethane, N,N-Dimethylformamide and acetonitrile were distilled from CaH_2 . 1,4-Dibromo-2,5-bis(hexyloxy)benzene, 2,7-dibromo-9,9-dihexyl-9H-fluorene, 2,7-dibromo-9-hexyl-9H-carbazole, were prepared by following literature reported methods.³⁶⁻³⁸ All 400 MHz ^1H , 100 MHz ^{13}C and 128 MHz ^{11}B NMR spectra were recorded on a Bruker ARX 400 spectrometer operating at 400 MHz. All ^1H and ^{13}C

NMR spectra were referenced internally to solvent signals. ^{11}B NMR spectra were referenced externally to $\text{BF}_3 \cdot \text{Et}_2\text{O}$ in CDCl_3 ($\delta = 0$). ESI mass spectra were recorded using a Bruker microTOF-QII mass spectrometer. The absorbance spectra were recorded with a JASCO V-730 UV-Visible spectrometer. The fluorescence spectra were recorded using Edinburgh FS5 spectrofluorometer. Fluorescence quantum yields of **7-11** in various solvents were measured by using quinine sulfate as reference and fluorescence quantum yields of their solid powders were measured by integrating sphere technique using Edinburgh FS5 spectrofluorometer. In compound **7**, electron density resulting from one disordered solvent molecule was removed using OLEX solvent mask.

Single-crystal X-ray diffraction data were collected on a Bruker APEX-II diffractometer equipped with an Oxford Instruments low-temperature attachment. Mo-K α radiation (0.71073 Å). SADABS absorption corrections were applied. The structures were solved and refined with SHELX suite of programs. All non-hydrogen atoms were refined with anisotropic displacement coefficients. The H atoms were placed at calculated positions and were refined as riding atoms.

4.4.2. Synthetic procedure and spectral characterization

4.4.2.1 Synthesis of compound 1

A mixture of 9,10-phenanthrenequinone (3.68 g, 17.67 mmol), aniline (1.93 mL, 21.20 mmol), 4-bromobenzaldehyde (3.27 g, 17.67 mmol), ammonium acetate (6.81 g, 83.35 mmol), and acetic acid (175 mL) was refluxed for 24 h under nitrogen. After cooling to room temperature, the reaction mixture was then poured into water and the solid was filtered. The solid product was washed with water, methanol and dried under vacuum. The resultant solid was recrystallized from $\text{CH}_2\text{Cl}_2/n$ -hexane mixture to obtain the pure product. Yield: 6.36 g, (80%). mp: 250 °C. ^1H NMR (400 MHz,

CDCl₃): δ = 8.87 (d, J = 8 Hz, 1H), 8.74 (dd, J = 24, 8 Hz, 2H), 7.76 (t, J = 8 Hz, 1H), 7.68 – 7.60 (m, 4H), 7.53 – 7.41 (m, 7H), 7.27 (t, J = 8 Hz, 1H), 7.17 (d, J = 8 Hz, 1H) ppm. ¹³C NMR (100 MHz, CDCl₃): δ = 149.82, 138.66, 137.55, 131.55, 130.91, 130.41, 130.10, 129.58, 129.47, 129.13, 128.43, 128.41, 127.47, 127.23, 126.44, 125.85, 125.16, 124.25, 123.47, 123.26, 123.04, 122.81, 120.95 ppm. HR-MS (ESI): calcd. for C₂₇H₁₈Br₁N₂ ([M + H]⁺): 449.0648, found : 449.0649.

4.4.2.2 Synthesis of compound 2

A mixture of 9,10-phenanthrenequinone (3.00 g, 14.41 mmol), 4-hexylaniline (3.61 mL, 18.73 mmol), 4-bromobenzaldehyde (2.66 g, 14.41 mmol), ammonium acetate (5.55 g, 72.05 mmol), and acetic acid (150 mL) was refluxed for 24 h under nitrogen. The reaction mixture was poured into water and extracted with dichloromethane (2 x 100 mL). The combined organic layers were washed with aqueous NaHCO₃ and then with brine solution, dried over Na₂SO₄ and concentrated. The resultant residue was purified by silica gel column chromatography using *n*-hexane/dichloromethane mixture as eluent. Yield: 7.68 g, (75%). mp: 141 °C. ¹H NMR (400 MHz, CDCl₃): δ = 8.87 (d, J = 8 Hz, 1H), 8.73 (dd, J = 24, 8 Hz, 2H), 7.75 (t, J = 8 Hz, 1H), 7.66 (t, J = 8 Hz, 1H), 7.53 – 7.37 (m, 9H), 7.29 – 7.21 (m, 2H), 2.81 (t, J = 8 Hz, 2H), 1.78 – 1.74 (m, 2H), 1.41 (s, 6H), 0.97 (t, J = 6.5 Hz, 3H) ppm. ¹³C NMR (100 MHz, CDCl₃): δ = 149.84, 145.20, 137.47, 136.07, 131.48, 130.87, 130.33, 129.68, 129.43, 128.78, 128.48, 128.40, 127.41, 127.27, 126.36, 125.77, 125.08, 124.19, 123.36, 123.24, 123.14, 122.78, 121.00, 35.77, 31.80, 31.20, 28.87, 22.79, 14.24 ppm. HR-MS (ESI): calcd. for C₃₃H₃₀Br₁N₂ ([M + H]⁺): 533.1587, found : 533.1579.

4.4.2.3 Synthesis of compound 3

To a stirred solution of compound 1 (4.50 g, 10.01 mmol), and N,N-diisopropylethylamine (*i*-Pr₂NEt (1.74 mL, 10.01 mmol) in 150 mL of

dichloromethane at 0 °C was added BBr₃ (1.0 M in dichloromethane, 30.03 mL, 30.03 mmol) under nitrogen. After being stirred at room temperature for 24 h, saturated K₂CO₃ aqueous solution was added to the reaction mixture and extracted with CH₂Cl₂. The combined organic layers were washed with water, dried over MgSO₄ and concentrated under vacuum to afford the crude product **3a**. Under nitrogen atmosphere AlMe₃ (2.0 M in toluene, 10.01 mL, 20.02 mmol) was added to the crude product **3a** at room temperature in CH₂Cl₂ and toluene (80 mL : 80 mL). After being stirred at this temperature for 0.5 h, the reaction was quenched by adding water and extracted with CH₂Cl₂. The combined organic layers were washed with water, brine, dried over Na₂SO₄ and concentrated. The residue was purified by silica gel column chromatography using *n*-hexane/dichloromethane mixture as eluent. Yield: 2.70 g, (55%). mp: 253 °C. ¹H NMR (400 MHz, CDCl₃): δ = 9.31 (d, *J* = 8 Hz, 1H), 8.72 (d, *J* = 8 Hz, 2H), 7.88 (t, *J* = 8 Hz, 3H), 7.80 (t, *J* = 8 Hz, 2H), 7.74 – 7.69 (m, 3H), 7.55 – 7.51 (m, 1H), 7.31 (t, *J* = 8 Hz, 1H), 7.23 (d, *J* = 8 Hz, 1H), 7.14 (d, *J* = 8 Hz, 1H), 6.31 (d, *J* = 8 Hz, 1H), 0.55 (s, 6H) ppm. ¹³C NMR (100 MHz, CDCl₃): δ = 176.27, 152.66, 136.63, 132.35, 131.52, 131.19, 130.99, 129.32, 129.06, 129.00, 128.35, 127.97, 127.55, 127.02, 126.80, 126.11, 126.03, 125.78, 125.54, 124.15, 123.41, 123.38, 122.35, 122.19, 120.54, 7.07 ppm. ¹¹B NMR (128 MHz, CDCl₃): δ = 0.90 (s) ppm. HR-MS (ESI): calcd. for C₂₉H₂₃B₁Br₁N₂ ([M + H]⁺): 489.1137, found : 489.1138.

4.4.2.4 Synthesis of compound 4

Compound **4** was prepared following a procedure similar to that used for compound **3**. The quantities involved are as follows: Compound **2** (5.80 g, 10.87 mmol), *N,N*-diisopropylethylamine (*i*-Pr₂NEt) (1.89 mL, 10.87 mmol), BBr₃ (1.0 M in dichloromethane, 32.61 mL, 32.61 mmol) and AlMe₃ (2.0 M in toluene, 10.87 mL,

21.74 mmol). Yield: 3.74 g, (60%). mp: 171 °C. ^1H NMR (400 MHz, CDCl_3): δ = 9.29 (d, J = 8.0 Hz, 1H), 8.70 (t, J = 8.0 Hz, 2H), 7.87 (t, J = 8 Hz, 2H), 7.73 (t, J = 8 Hz, 1H), 7.55 – 7.48 (m, 5H), 7.31 – 7.24 (m, 2H), 7.14 (d, J = 8 Hz, 1H), 6.33 (d, J = 8 Hz, 1H), 2.92 (t, J = 8 Hz, 2H), 1.88 – 1.84 (m, 2H), 1.48 (s, 6H), 1.03 (s, 3H), 0.54 (s, 6H) ppm. ^{13}C NMR (100 MHz, CDCl_3): δ = 176.26, 152.76, 146.78, 133.98, 132.30, 131.03, 130.93, 129.28, 129.12, 128.98, 127.96, 127.50, 126.94, 126.72, 126.02, 125.95, 125.88, 125.53, 124.07, 123.46, 123.36, 122.41, 122.28, 120.59, 35.85, 31.75, 31.14, 28.92, 22.76, 14.25, 7.07 ppm. ^{11}B NMR (128 MHz, CDCl_3): δ = 1.17 (s) ppm. HR-MS (ESI): calcd. for $\text{C}_{35}\text{H}_{35}\text{B}_1\text{Br}_1\text{N}_2$ ($[\text{M} + \text{H}]^+$): 573.2077, found : 573.2074.

4.4.2.5 Synthesis of compound 5

Degassed 1,4-dioxane was added to a mixture of compound **3** (4.29 g, 8.77 mmol), potassium acetate (2.58 g, 26.31 mmol), bis(pinacolato)diboron (2.67 g, 10.52 mmol), $\text{Pd}(\text{dppf})\text{Cl}_2$ (192 mg, 0.263 mmol, 3 mol%) under nitrogen atmosphere in a two necked round bottom flask fitted with refluxing condenser. After being stirred at 100 °C temperature for 12 h, the reaction mixture was poured into water, extracted with CH_2Cl_2 . The combined organic layers were washed with brine solution, dried over Na_2SO_4 and concentrated. The residue was purified by silica gel column chromatography using *n*-hexane/ethyl acetate mixture as eluent. Yield: 4.00 g, (85%). mp: >300 °C. ^1H NMR (400 MHz, CDCl_3): δ = 9.31 (d, J = 8 Hz, 1H), 8.77 – 8.73 (m, 2H), 8.15 (d, J = 4.2 Hz, 1H), 7.88 – 7.71 (m, 7H), 7.55 (t, J = 8 Hz, 1H), 7.47 – 7.44 (m, 1H), 7.32 – 7.24 (m, 2H), 6.42 (d, J = 8 Hz, 1H), 1.37 (s, 12H), 0.49 (s, 6H) ppm. ^{13}C NMR (101 MHz, CDCl_3): δ = 172.05, 153.42, 136.90, 135.51, 131.48, 131.34, 131.22, 131.05, 130.31, 129.59, 129.34, 129.11, 128.98, 128.50, 127.50, 126.94, 126.73, 126.00, 125.76, 124.14, 123.60, 123.32, 122.33, 120.65, 120.10, 83.78, 24.99, 7.17 ppm. ^{11}B NMR (128 MHz, CDCl_3): δ = 32.75 (Boronate, s), 0.75

(BMe₂, s) ppm. HR-MS (ESI): calcd. for C₃₅H₃₅B₂N₂O₂ ([M + H]⁺): 537.2891, found : 537.2915.

4.4.2.6 Synthesis of compound 6

Compound **6** was prepared following a procedure similar to that used for compound **5**. The quantities involved are as follows: Compound **4** (3.02 g, 5.27 mmol), potassium acetate (1.55 g, 15.81 mmol), bis(pinacolato)diboron (1.60 g, 6.32 mmol), Pd(dppf)Cl₂ (116 mg, 0.158 mmol, 3 mol%). Yield: 2.94 g, (90%). mp: 237 °C. ¹H NMR (400 MHz, CDCl₃): δ = 9.29 (d, *J* = 4 Hz, 1H), 8.75 (t, *J* = 8 Hz, 2H), 8.13 (d, *J* = 4 Hz, 1H), 7.84 (t, *J* = 8 Hz, 1H), 7.72 (t, *J* = 8 Hz, 1H), 7.62 – 7.53 (m, 5H), 7.46 – 7.43 (m, 1H), 7.31 – 7.29 (m, 2H), 6.42 (d, *J* = 4 Hz, 1H), 2.90 (t, *J* = 8 Hz, 2H), 1.84 – 1.79 (m, 2H), 1.48 – 1.43 (m, 6H), 1.36 (s, 12H), 1.00 (s, 3H), 0.48 (s, 6H). ¹³C NMR (100 MHz, CDCl₃): δ = 171.95, 153.52, 146.61, 135.45, 134.24, 131.46, 131.13, 130.89, 130.20, 129.69, 129.25, 129.13, 128.93, 128.09, 127.43, 126.85, 126.63, 125.90, 125.71, 124.03, 123.63, 123.29, 122.38, 120.67, 120.15, 83.73, 35.86, 31.75, 31.33, 28.94, 24.98, 22.75, 14.23, 7.22. ¹¹B NMR (128 MHz, CDCl₃): δ = 38.56 (Boronate, s), 3 (BMe₂, s) ppm. HR-MS (ESI): calcd. for C₄₁H₄₇B₂N₂O₂ ([M + H]⁺): 621.3832, found : 621.3827.

4.4.2.7 Synthesis of compound 7

Degassed, 1,2-dimethoxyethane : H₂O (50 mL : 17 mL) was added to a mixture of compound **4** (1.07 g, 1.86 mmol), compound **6** (1.50 g, 2.42 mmol), Pd(PPh₃)₄ (64 mg, 0.055 mmol, 3 mol%), Na₂CO₃ (591 mg, 5.58 mmol) under nitrogen atmosphere. The reaction mixture was heated to reflux for 18 h. The reaction mixture was cooled to room temperature then distilled water was added to the reaction mixture and extracted with dichloromethane (3 × 30 mL). The combined organic layers were washed with brine solution, dried over Na₂SO₄ and concentrated. The residue was

purified by silicagel column chromatography using *n*-hexane/ethyl acetate mixture as eluent. Yield: 0.92 g, (50%). mp: 305 °C. ¹H NMR (400 MHz, CDCl₃): δ = 9.36 (d, *J* = 8 Hz, 1H), 8.73 (t, *J* = 8 Hz, 2H), 8.02 (s, 1H), 7.89 (t, *J* = 8 Hz, 1H), 7.75 (t, *J* = 8 Hz, 1H), 7.61 (q, *J* = 8 Hz, 4H), 7.53 – 7.49 (m, 1H), 7.41 (d, *J* = 8 Hz, 1H), 7.30 (d, *J* = 4 Hz, 2H), 6.60 (d, *J* = 8 Hz, 1H), 2.94 (t, *J* = 8 Hz, 2H), 1.92 – 1.84 (m, 2H), 1.54 – 1.46 (m, 6H), 1.04 (t, *J* = 8 Hz, 3H), 0.59 (s, 6H) ppm. ¹³C NMR (100 MHz, CDCl₃): δ = 174.06, 153.64, 146.62, 143.18, 134.34, 131.21, 130.99, 129.21, 129.08, 128.96, 128.19, 128.13, 127.47, 126.88, 126.60, 126.46, 125.83, 125.71, 124.48, 124.09, 123.69, 123.34, 122.48, 121.34, 120.67, 35.90, 31.80, 31.20, 28.97, 22.81, 14.27, 7.41 ppm. ¹¹B NMR (128 MHz, CDCl₃): δ = -2.16 (s) ppm.

4.4.2.8 Synthesis of compound 8

1,4-Dibromo-2,5-bis(hexyloxy)benzene (553 mg, 1.27 mmol) and Pd(PPh₃)₄ (88 mg, 0.076 mmol, 6 mol%) were dissolved in 75 mL of degassed 1,2-dimethoxyethane under nitrogen atmosphere at room temperature. After being stirred at this temperature for 30 min, compound **5** (1.5 g, 2.8 mmol) and freshly prepared degassed solution of Na₂CO₃ (807 mg, 7.62 mmol) in water were added. The reaction mixture was heated to reflux for 18 h and cooled to room temperature. Distilled water was added to the reaction mixture and extracted with CH₂Cl₂. The combined organic layers were washed with brine solution, dried over sodium sulfate and concentrated. The residue was purified by silica gel column chromatography using *n*-hexane/dichloromethane mixture as eluent. Yield: 973 mg, (70%). mp: 352 °C. ¹H NMR (400 MHz, CDCl₃): δ = 9.32 (d, *J* = 8.0 Hz, 2H), 8.78 (t, *J* = 8.0 Hz, 4H), 7.94 (s, 2H), 7.89 – 7.72 (m, 14H), 7.56 (t, *J* = 8.0 Hz, 2H), 7.33 – 7.22 (m, 6H), 7.06 (s, 2H), 6.50 (d, *J* = 8.0 Hz, 2H), 3.95 (t, *J* = 6.4 Hz, 4H), 1.76 – 1.69 (m, 4H), 1.42 – 1.37 (m, 4H), 1.29 – 1.26 (m, 8H), 0.87 (t, *J* = 8.0 Hz, 6H), 0.52 (s, 12H) ppm. ¹³C

NMR (100 MHz, CDCl₃): δ = 153.77, 150.59, 140.20, 137.16, 131.49, 131.36, 131.13, 130.49, 129.35, 129.01, 128.75, 127.57, 126.96, 126.68, 126.40, 125.83, 124.25, 123.75, 123.35, 122.55, 120.70, 120.54, 116.55, 69.83, 31.68, 29.51, 26.00, 22.73, 14.23, 7.29. ¹¹B NMR (128 MHz, CDCl₃): δ = -2.13 ppm. HR-MS (ESI): calcd. for C₇₆H₇₂B₂N₄O₂Na([M + Na]⁺): 1117.5756, found : 1117.5758.

4.4.2.9 Synthesis of compound 9

Compound **9** was prepared following a procedure similar to that used for compound **8**. The quantities involved are as follows: 2,5-Dibromothiophene (405 mg, 1.50 mmol), Pd(PPh₃)₄ (115 mg, 0.1 mmol, 6 mol%), compound **5** (1.89 g, 3.51 mmol) and Na₂CO₃ (1.06 g, 10.02 mmol). Yield: 2.57 g, (81%). mp: 425 °C. ¹H NMR (400 MHz, CDCl₃): δ = 9.27 (d, *J* = 8.0 Hz, 2H), 8.77 (t, *J* = 8 Hz, 4H), 7.92 – 7.81 (m, 10H), 7.78 – 7.72 (m, 6H), 7.58 – 7.54(m, 2H), 7.39 (s, 2H), 7.31 (t, *J* = 8 Hz, 2H), 7.26 – 7.24 (m, 5H), 6.42 (d, *J* = 8 Hz, 2H), 0.49 (s, 12H) ppm. ¹³C NMR (100 MHz, CDCl₃): δ = 153.30, 144.79, 137.06, 135.60, 135.33, 131.43, 131.34, 131.19, 129.39, 129.08, 129.03, 128.69, 127.59, 127.00, 126.75, 126.38, 125.97, 125.79, 124.80, 124.26, 123.65, 123.37, 122.62, 122.46, 121.44, 120.71, 7.31. ¹¹B NMR (128 MHz, CDCl₃): δ = -4.51 ppm. HR-MS (ESI): calcd. for C₆₂H₄₆B₂N₄S₁K([M + K]⁺): 939.3280, found : 939.3245.

4.4.2.10 Synthesis of compound 10

Compound **10** was prepared following a procedure similar to that used for compound **8**. The quantities involved are as follows: 2,7-Dibromo-9,9-dihexyl-9H-fluorene (561 mg, 1.14 mmol), Pd(PPh₃)₄ (90 mg, 0.068 mmol, 6 mol%), compound **5** (1.28 g, 2.39 mmol), Na₂CO₃ (724 mg, 6.84 mmol). Yield: 920 mg, (70%). mp: 396 °C. ¹H NMR (400 MHz, CDCl₃): δ = 9.36 (d, *J* = 8 Hz, 2H), 8.77 (d, *J* = 8 Hz, 4H), 8.03 (s, 2H), 7.92 – 7.68 (m, 20H), 7.56 (t, *J* = 7.2 Hz, 2H), 7.36 – 7.27 (m, 6H), 6.57 (d, *J* = 8.0

Hz, 2H), 2.13 – 2.09 (m, 4H), 1.18 – 1.13 (m, 12H), 0.82 (t, $J = 6.9$ Hz, 10H), 0.61 (s, 12H) ppm. ^{13}C NMR (101 MHz, CDCl_3): $\delta = 174.32, 153.52, 151.76, 143.23, 140.68, 140.36, 137.08, 131.38, 131.31, 131.15, 129.32, 129.05, 129.01, 128.65, 127.74, 127.57, 126.98, 126.73, 126.50, 126.16, 125.95, 125.76, 124.33, 124.22, 123.66, 123.39, 122.44, 121.94, 121.34, 120.65, 120.06, 40.64, 31.61, 29.84, 23.93, 22.72, 14.16, 7.42$ ppm. ^{11}B NMR (128 MHz, CDCl_3): $\delta = 0.19$ (s) ppm. HR-MS (ESI): calcd. for $\text{C}_{83}\text{H}_{76}\text{B}_2\text{N}_4\text{Na}([\text{M} + \text{Na}]^+)$: 1173.6172, found : 1173.6156.

4.4.2.11 Synthesis of compound 11

Compound **11** was prepared following a procedure similar to that used for compound **8**. The quantities involved are as follows: 2,7-Dibromo-9-hexyl-9H-carbazole (573 mg, 1.40 mmol) and $\text{Pd}(\text{PPh}_3)_4$ (97 mg, 0.084 mmol, 6 mol%), compound **5** (1.72 g, 3.22 mmol), Na_2CO_3 (890 mg, 8.4 mmol). Yield: 913 mg, (61%). mp: 425 °C. ^1H NMR (400 MHz, CDCl_3): $\delta = 9.31$ (d, $J = 8$ Hz, 2H), 8.78 (t, $J = 8$ Hz, 4H), 8.15 (d, $J = 8$ Hz, 2H), 8.02 (s, 2H), 7.90 – 7.79 (m, 12H), 7.75 (t, $J = 8$ Hz, 2H), 7.65 (s, 2H), 7.59 – 7.54 (m, 4H), 7.36 – 7.28 (m, 6H), 6.55 (d, $J = 8$ Hz, 2H), 4.40 (t, $J = 8$ Hz, 4H), 1.97 – 1.90 (m, 2H), 1.48 – 1.44 (m, 4H), 1.38 – 1.30 (m, 2H), 0.89 (t, $J = 8$ Hz, 3H), 0.54 (s, 12H) ppm. ^{13}C NMR (100 MHz, CDCl_3): $\delta = 174.35, 153.60, 143.83, 141.66, 139.79, 137.14, 131.41, 131.35, 131.20, 129.37, 129.07, 129.03, 128.73, 128.30, 127.59, 127.00, 126.74, 126.12, 125.95, 125.80, 124.72, 124.26, 123.70, 123.38, 122.50, 122.18, 121.33, 120.70, 120.62, 119.18, 107.66, 43.23, 31.74, 29.85, 29.15, 27.14, 22.72, 14.20, 7.39$ ppm. ^{11}B NMR (128 MHz, CDCl_3): $\delta = -3.09$ (s) ppm. HR-MS (ESI): calcd. for $\text{C}_{76}\text{H}_{63}\text{B}_2\text{N}_5\text{Na}([\text{M} + \text{Na}]^+)$: 1090.5184, found : 1090.5151.

4.5 References

- (1) Grimsdale, A. C.; Leok Chan, K.; Martin, R. E.; Jokisz, P. G.; Holmes, A. B. *Chem. Rev.***2009**, *109*, 897.
- (2) Cicoira, F.; Santato, C. *Adv. Funct. Mater.***2007**, *17*, 3421.
- (3) Samuel, I. D. W.; Turnbull, G. A. *Chem. Rev.***2007**, *107*, 1272.
- (4) Dale, T. J.; Rebek, J. *J. Am. Chem. Soc.***2006**, *128*, 4500.
- (5) Rao, Y.-L.; Wang, S. *Inorg. Chem.***2011**, *50*, 12263.
- (6) Li, D.; Zhang, H.; Wang, Y. *Chem. Soc. Rev.***2013**, *42*, 8416.
- (7) Frath, D.; Massue, J.; Ulrich, G.; Ziessel, R. *Angew. Chem. Int. Ed. Engl.***2014**, *53*, 2290.
- (8) Rao, Y.-L.; Amarne, H.; Wang, S. *Coord. Chem. Rev.***2012**, *256*, 759.
- (9) Wong, H.-L.; Wong, W.-T.; Yam, V. W.-W. *Org. Lett.***2012**, *14*, 1862.
- (10) Yoshino, J.; Kano, N.; Kawashima, T. *Dalton Trans.***2013**, *42*, 15826.
- (11) Pais, V. F.; Alcaide, M. M.; Lopez-Rodriguez, R.; Collado, D.; Najera, F.; Perez-Inestrosa, E.; Alvarez, E.; Lassaletta, J. M.; Fernandez, R.; Ros, A.; Pischel, U. *Chem. - Eur. J.***2015**, *21*, 15369.
- (12) Wakamiya, A.; Taniguchi, T.; Yamaguchi, S. *Angew. Chem. Int. Ed. Engl.***2006**, *45*, 3170.
- (13) Job, A.; Wakamiya, A.; Kehr, G.; Erker, G.; Yamaguchi, S. *Org. Lett.***2010**, *12*, 5470.
- (14) Yang, D.-T.; Mellerup, S. K.; Peng, J.-B.; Wang, X.; Li, Q.-S.; Wang, S. *J. Am. Chem. Soc.***2016**, *138*, 11513.
- (15) Mellerup, S. K.; Yuan, K.; Nguyen, C.; Lu, Z.-H.; Wang, S. *Chem. Eur. J.***2016**, *22*, 12464.
- (16) Rao, Y.-L.; Amarne, H.; Chen, L. D.; Brown, M. L.; Mosey, N. J.; Wang, S. *J. Am. Chem. Soc.***2013**, *135*, 3407.

- (17) Rao, Y. L.; Amarne, H.; Chen, L. D.; Brown, M. L.; Mosey, N. J.; Wang, S. *J. Am. Chem. Soc.* **2013**, *135*, 3407.
- (18) Rao, Y.-L.; Amarne, H.; Lu, J.-S.; Wang, S. *Dalton Trans.* **2013**, *42*, 638.
- (19) Yoshino, J.; Kano, N.; Kawashima, T. *J. Org. Chem.* **2009**, *74*, 7496.
- (20) Yoshino, J.; Kano, N.; Kawashima, T. *Chem. Commun.* **2007**, 559.
- (21) Li, D.; Zhang, Z.; Zhao, S.; Wang, Y.; Zhang, H. *Dalton Trans.* **2011**, *40*, 1279.
- (22) Dou, C.; Ding, Z.; Zhang, Z.; Xie, Z.; Liu, J.; Wang, L. *Angew. Chem. Int. Ed.* **2015**, *54*, 3648.
- (23) Zhang, Z. J.; Ding, Z. C.; Dou, C. D.; Liu, J.; Wang, L. X. *Polym. Chem.* **2015**, *6*, 8029.
- (24) Ishida, N.; Moriya, T.; Goya, T.; Murakami, M. *J. Org. Chem.* **2010**, *75*, 8709.
- (25) Zhu, C.; Guo, Z. H.; Mu, A. U.; Liu, Y.; Wheeler, S. E.; Fang, L. *J. Org. Chem.* **2016**, *81*, 4347.
- (26) Zhao, Z.; Chang, Z.; He, B.; Chen, B.; Deng, C.; Lu, P.; Qiu, H.; Tang, B. Z. *Chem. Eur. J.* **2013**, *19*, 11512.
- (27) Yusuf, M.; Liu, K.; Guo, F.; Lalancette, R. A.; Jakle, F. *Dalton Trans.* **2016**, *45*, 4580.
- (28) Wong, B. Y.-W.; Wong, H.-L.; Wong, Y.-C.; Chan, M.-Y.; Yam, V. W.-W. *Chem. Eur. J.* **2016**, *22*, 15095.
- (29) Shaikh, A. C.; Ranade, D. S.; Thorat, S.; Maity, A.; Kulkarni, P. P.; Gonnade, R. G.; Munshi, P.; Patil, N. T. *Chem. Commun.* **2015**, *51*, 16115.
- (30) He, B.; Chang, Z.; Jiang, Y.; Chen, B.; Lu, P.; Kwok, H. S.; Qin, A.; Zhao, Z.; Qiu, H. *Dyes Pigm.* **2014**, *101*, 247.

- (31) Crossley, D. L.; Vitorica-Yrezabal, I.; Humphries, M. J.; Turner, M. L.; Ingleson, M. J. *Chem. Eur. J.* **2016**, *22*, 12439.
- (32) Crossley, D. L.; Cid, J.; Curless, L. D.; Turner, M. L.; Ingleson, M. J. *Organometallics* **2015**, *34*, 5767.
- (33) Crossley, D. L.; Cade, I. A.; Clark, E. R.; Escande, A.; Humphries, M. J.; King, S. M.; Vitorica-Yrezabal, I.; Ingleson, M. J.; Turner, M. L. *Chem. Sci.* **2015**, *6*, 5144.
- (34) Yuan, Y.; Li, D.; Zhang, X.; Zhao, X.; Liu, Y.; Zhang, J.; Wang, Y. *New J. Chem.* **2011**, *35*, 1534.
- (35) Entwistle, C. D.; Collings, J. C.; Steffen, A.; Palsson, L.-O.; Beeby, A.; Albesa-Jove, D.; Burke, J. M.; Batsanov, A. S.; Howard, J. A. K.; Mosely, J. A.; Poon, S.-Y.; Wong, W.-Y.; Ibersiene, F.; Fathallah, S.; Boucekkine, A.; Halet, J.-F.; Marder, T. B. *J. Mater. Chem.* **2009**, *19*, 7532.
- (36) Pal, B.; Yen, W.-C.; Yang, J.-S.; Su, W.-F. *Macromolecules* **2007**, *40*, 8189.
- (37) Rice, N. A.; Adronov, A. *Macromolecules* **2013**, *46*, 3850.
- (38) Norris, B. N.; Zhang, S.; Campbell, C. M.; Auletta, J. T.; Calvo-Marzal, P.; Hutchison, G. R.; Meyer, T. Y. *Macromolecules* **2013**, *46*, 1384.

CHAPTER 5A

Tetraaryl pyrazole polymers: Versatile synthesis, aggregation induced emission enhancement and detection of explosives

5A.1 Introduction	201
5A.2 Results and discussion	202
5A.2.1 Synthesis and characterization	202
5A.2.2 Thermal studies	206
5A.2.3 Photophysical studies	208
5A.3 Conclusions	215
5A.4 Experimental section	215
5A.4.1 General information	215
5A.4.2 Synthetic procedure and spectral characterization	216
5A.5 References	221

5A.1 Introduction

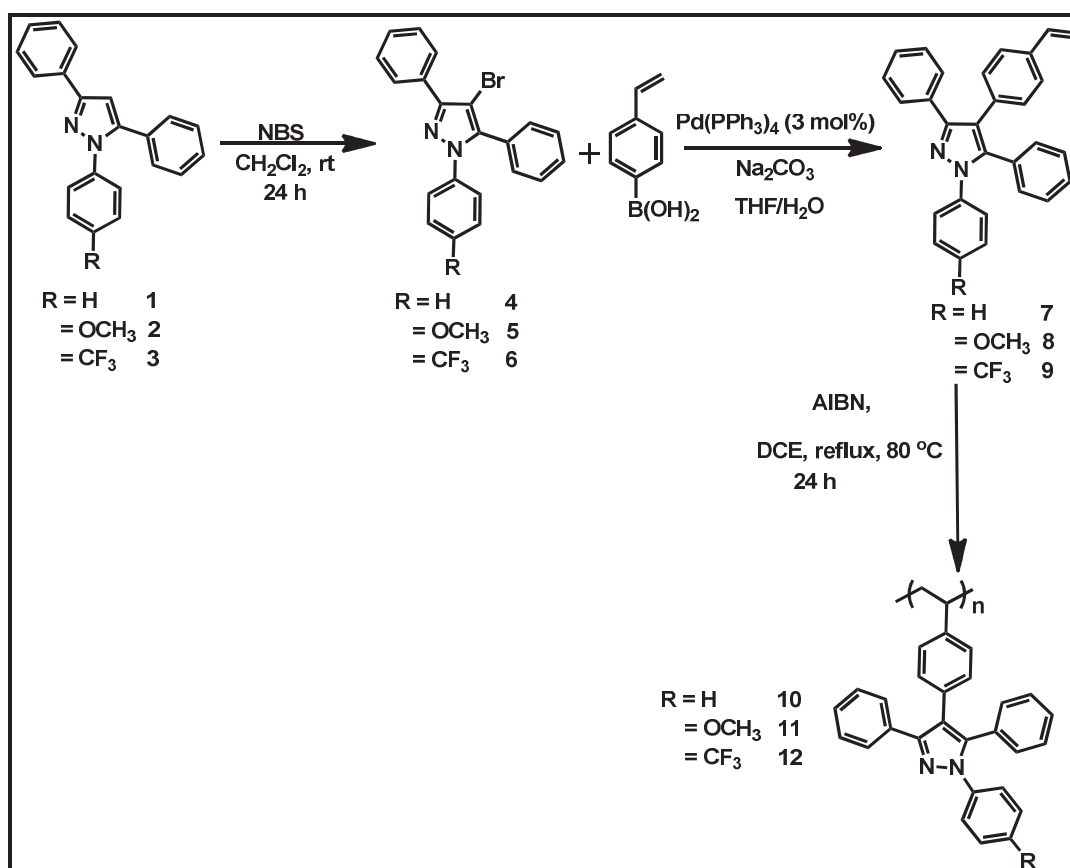
Pyrazoles are an important family of heterocyclic ring systems and have attracted interest because of their applications in pharmaceutical and medicinal chemistry and their versatility to form different coordination and organometallic compounds.^{1,2} Furthermore, pyrazoles have also served as useful ligands in catalysis,³⁻⁵ as building blocks for the synthesis of different heterocycles^{6,7} and supramolecules,^{8,9} as photoinduced electron transfer systems¹⁰, as optical brighteners¹¹ and as efficient blue emitters in organic light emitting diodes.^{12,13} The respective pyrazole polymeric analogues are particularly interesting due to their high thermal stability, the opportunity of using solution processing techniques for device fabrication and their potential to be utilized as reusable catalysts. Several methodologies have been reported for the incorporation of pyrazole moieties into the backbone of the polymers.¹⁴⁻¹⁶ However, in comparison with polymers that contain pyrazoles in main chain, polymers with pyrazoles as side-chain have received far less attention.¹⁷⁻¹⁹ In spite of the added advantages of polymer side chain approach like (a) molecular weight control by choice of polymerization techniques (b) synthesis of copolymers with different functionalities; the side chain functionalization of pyrazoles has not been systematically studied.

Aggregation induced emission (AIE)²⁰ and aggregation-induced emission enhancement (AIEE)²¹ are intriguing phenomena reported by Tang and coworkers and Park and coworkers which is opposite to the aggregation quenching effect. These phenomena have received considerable attention in the past few years due to their potential applications in the fabrication of organic LEDs, in biological probes, in chemical sensors and in stimuli-responsive nanomaterials.²²⁻²⁵ This breakthrough research initiated the development of new AIE and (or) AIEE luminogens with

versatile functionalities and diverse applications.²⁶⁻³² Among the AIE luminogens, hexaphenylsilole³³⁻³⁷ and tetraphenylethene³⁸⁻⁴¹ and their derivatives have been extensively studied for applications in organic light emitting diodes and as chemosensors for explosives. Recently it was realized that tetraaryl pyrazoles show significant enhancement in light emission upon aggregation.⁴² We envisioned that the pyrazolyl polymers might also show AIEE phenomenon. In this chapter, we describe the synthesis of pyrazolyl polymers which exhibit the AIEE phenomenon and their application towards picric acid sensing.

5A.2 Results and discussion

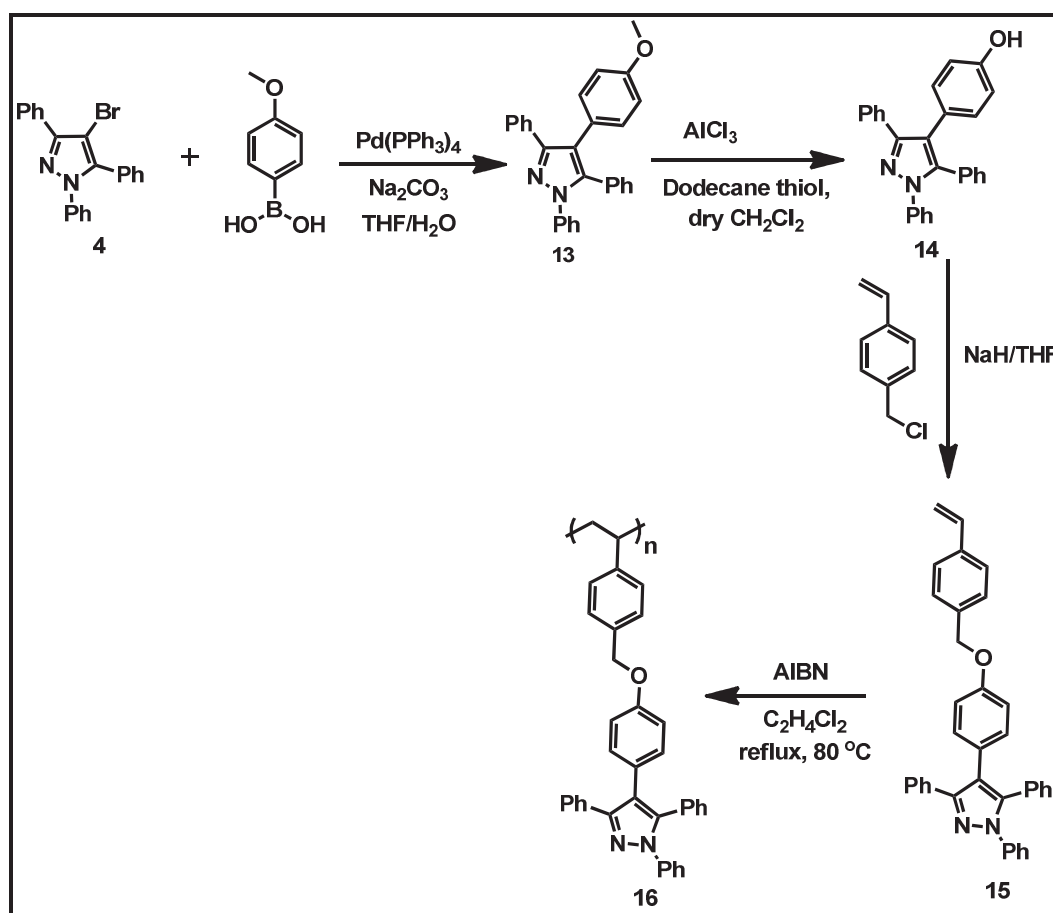
5A.2.1 Synthesis and characterization



Scheme 5A.1: Synthetic route for the preparation of poly(tetraaryl pyrazole)s (10-12).

The styryl containing pyrazoles were prepared according to the synthetic route shown in scheme 5A.1. The triaryl pyrazoles were synthesized according to the literature-reported procedure,⁴³ which involves the condensation of 1,3-dicarbonyl

and substituted hydrazines. The triaryl pyrazoles were brominated using *N*-bromosuccinimide in dichloromethane. The target monomers (**7-9**) were synthesized *via* Suzuki coupling between brominated triaryl pyrazoles (**4-6**) and styreneboronic acid (Scheme 5A.1). The flexible linker substituted monomer (**15**) was synthesized from **14** as described in scheme 5A.2. Compound **14** was obtained in 95 % yield by demethylation of **13** using AlCl_3 .



Scheme 5A.2: Synthetic route for the preparation of flexible poly(tetraaryl pyrazole).

The monomers **7-9** & **15** were polymerized under typical free radical polymerization conditions using 2, 2'-azobis(isobutyronitrile) (AIBN) as an initiator. The resultant polymers (**10-12** & **16**) were isolated by precipitation into hexane in 80-85% yield. High resolution LC-MS, ^1H and ^{13}C NMR established the successful synthesis of the monomers **7-9** & **15**. Figure 5A.1 represents the HRMS spectrum of monomer **7**. In

the ^1H NMR spectrum of **8**, the vinyl protons give rise to the expected AMX pattern between 5.3-6.8 ppm. A representative ^1H NMR spectrum is given in Figure 5A.3.

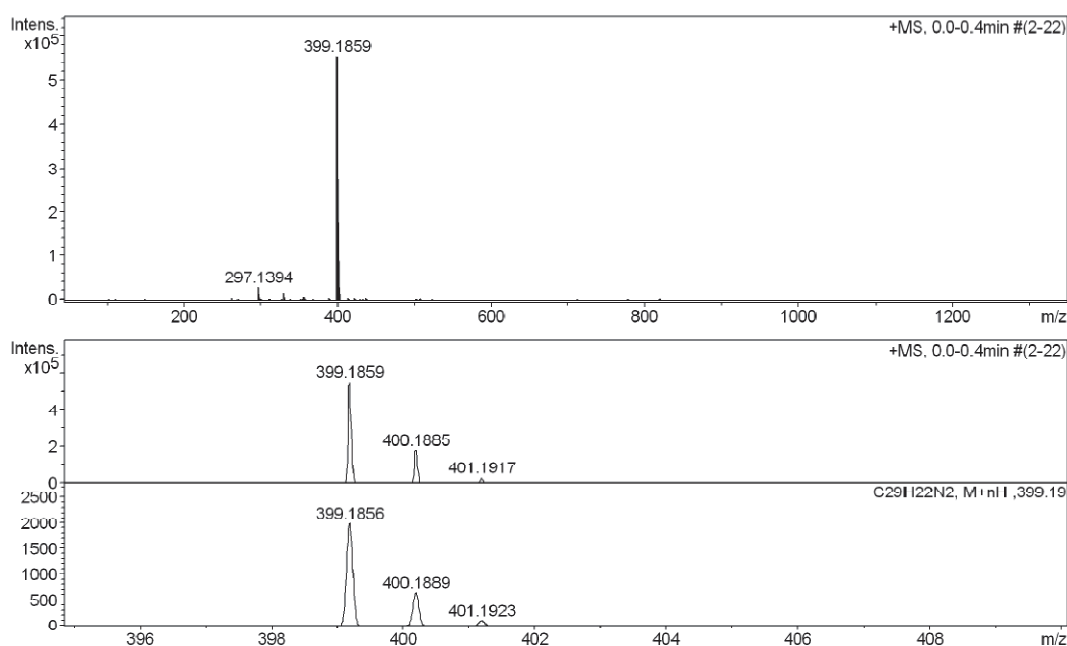


Figure 5A.1: HRMS spectrum of compound **7**.

The structure of **9** was further confirmed by X-ray crystallography (Figure 5A.2). The crystallographic data for monomer **9** is given in table 5A.1. The phenyl rings around pyrazole are arranged in a propeller fashion with a torsion angle ranging from 20.91 to 65.94°. The packing pattern of monomer **9** will be discussed later *vide infra*. The polymers **10-12** & **16** were fully characterized by ^1H & ^{13}C NMR spectroscopy. The ^1H NMR spectra of **10-12** & **16** show complete disappearance of the AMX multiplet due to the vinyl protons and characteristic broadening features associated with the polymers were observed (Figure 5A.3). The molecular weights of the polymers were studied by gel-permeation chromatography (GPC) in tetrahydrofuran using narrow polystyrene standards. The number-average molecular weights of the polymers **10-12** & **16** are 13,000; 10,500; 17,200 and 15,200 respectively with polydispersity indices (PDIs) ranging from 2.28 to 2.38 (Table 5A.2).

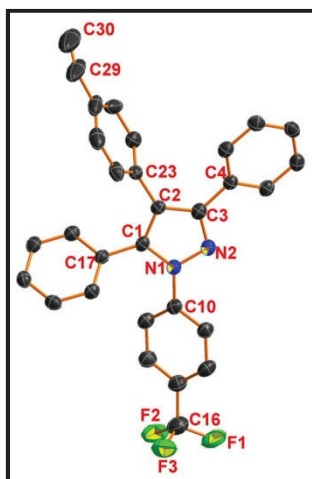


Figure 5A.2: Molecular structure of **9**, thermal ellipsoids are drawn at the 50% probability level (Hydrogen atoms are omitted for clarity). Selected bond distances (Å) and bond angles (°) are as follows: N1–N2 1.361(3), N1–C1 1.380(3), N1–C10 1.424(4), N2–C3 1.333(4), C1–C2 1.384(4), C2–C3 1.420(4), C2–C23 1.480(4), C1–C17 1.474(4), C3–C4 1.478(4), C29–C30 1.056(7), N2–N1–C1 111.9(2), N1–C1–C2 106.0(2), C1–C2–C3 105.6(2), N2–C3–C2 110.9(2), C30–C29–C26 145.2(9). Torsion angles between the pyrazole core and the neighbouring phenyl groups are 20.91, 38.47, 44.59 & 65.94.

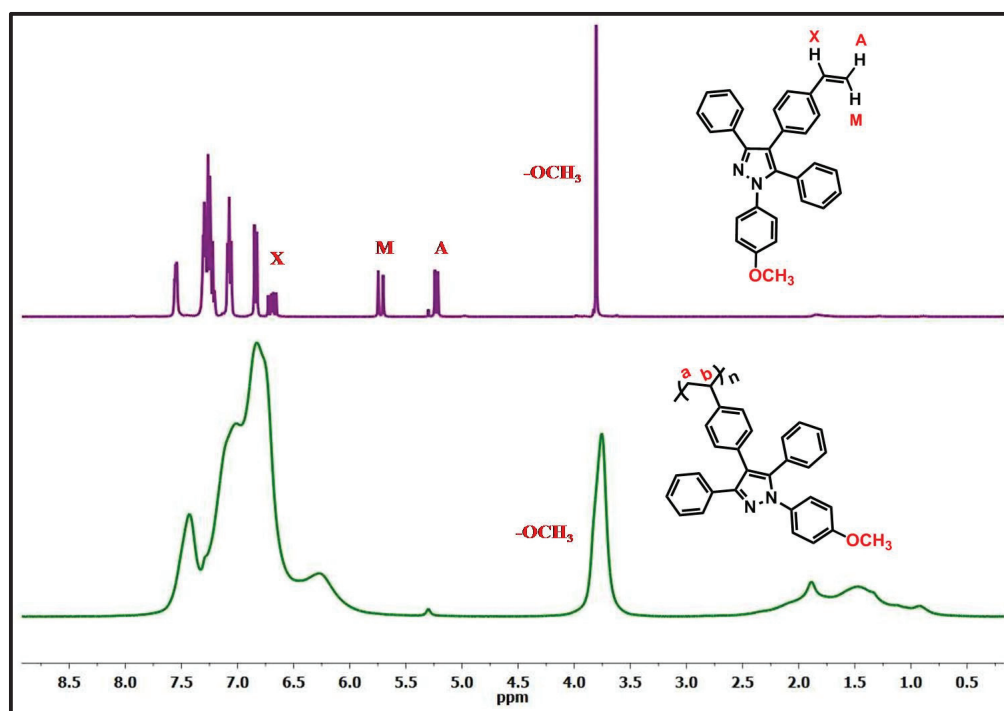


Figure 5A.3: ^1H NMR spectra of (top) monomer **8** & (bottom) polymer **11** in CDCl_3 .

Table 5A.1: Crystal data and structure refinement parameters for compounds **9**.

Compound	9
Empirical formula	C ₃₀ H ₂₁ F ₃ N ₂
Formula weight	466.49
Temperature/K	296(2)
Crystal system	Monoclinic
Space group	<i>C2/c</i>
<i>a</i> /Å	28.3793(16)
<i>b</i> /Å	8.2635(4)
<i>c</i> /Å	21.2253(14)
α /°	90
β /°	112.455(7)
γ /°	90
Volume/Å ³	4600.2(5)
Z	8
ρ_{calcd} /g cm ⁻³	1.347
μ (MoK α)/mm ⁻¹	0.096
<i>F</i> (000)	1936
θ range for data collection/°	1.55 to 25.80
Index ranges	-34 ≤ <i>h</i> ≤ 34, -10 ≤ <i>k</i> ≤ 9, -25 ≤ <i>l</i> ≤ 25
Reflns. collected	27952
Independent reflns	4370 [<i>R</i> (int) = 0.0873]
Data/restraints/ parameters	4370 / 0 / 316
GOF on <i>F</i> ²	1.076
Final <i>R</i> indices [<i>I</i> > 2σ(<i>I</i>)]	<i>R</i> ₁ = 0.0618 <i>wR</i> ₂ = 0.1703
<i>R</i> indices (all data)	<i>R</i> ₁ = 0.1000 <i>wR</i> ₂ = 0.2030
Largest diff. peak /hole [e Å ⁻³]	0.700/ -0.487

Table 5A.2: Molecular weight data for polymers **10-12** & **16**.

Polymer	<i>M</i> _w , Da ^a	<i>M</i> _n , Da ^a	PDI ^a
10	31 000	13 000	2.38
11	24 700	10 500	2.35
12	40 200	17 200	2.34
16	34 700	15 200	2.28

^a GPC-RI in THF vs polystyrene standards, PDI-polydispersity index (PDI = *M*_w/*M*_n)

5A.2.2 Thermal studies

The thermal properties of the poly(pyrazole)s (**10-12** & **16**) were studied by thermogravimetric analysis (TGA) and differential scanning calorimetry (DSC) and the relevant data are summarized in Table 5A.3. TGA analysis of polymers **10-12** & **16** reveal that these polymers are thermally stable upto *ca.* 345°C (Figure 5A.4). DSC analysis revealed high glass transition temperature ranging from 137 to 202 °C (Figure 5A.5).

Table 5A.3: Thermal data for polymers **10-12** & **16**.

Polymer	PDT, °C	T_g , °C
10	375	137
11	390	200
12	380	202
16	345	145

PDT-polymer decomposition temperature,
 T_g -glass transition temperature

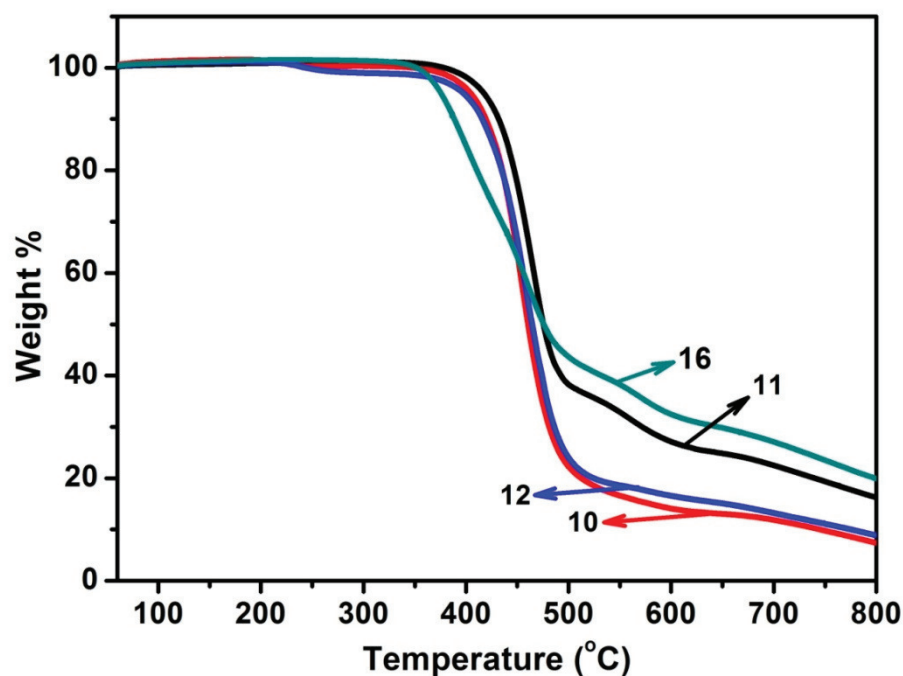


Figure 5A.4: TGA curves of polymers **10-12** & **16** at heating rate of 20 °C/min.

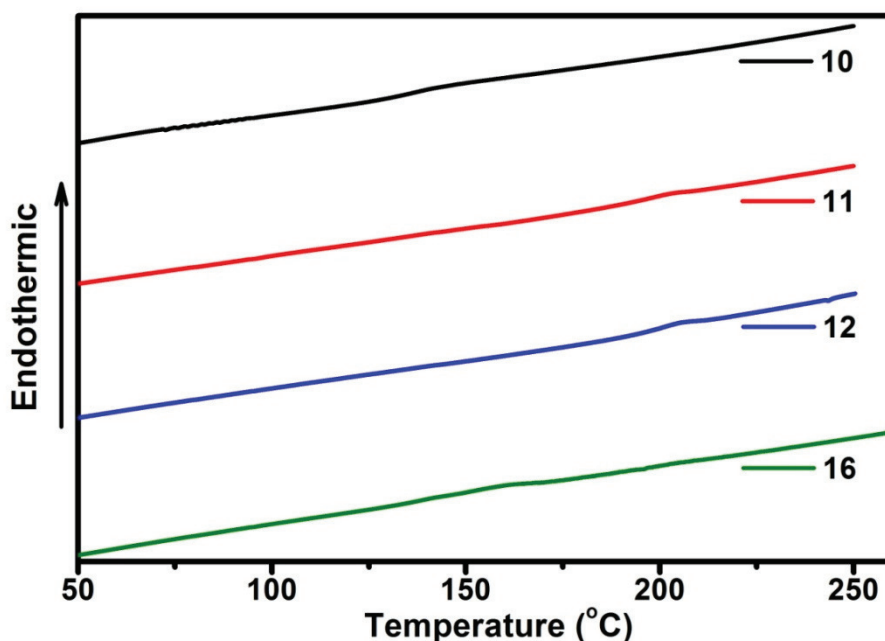


Figure 5A.5: DSC curves of polymer **10-12** & **16** at a heating rate of 20 °C/min.

5A.2.3 Photophysical studies

The optical properties of the polymers **10-12** & **16** were investigated in THF solution. As shown in figure 5A.6, all poly(tetraaryl pyrazole)s exhibit absorption maxima (λ_{max}) around 281-296 nm, and emission maxima around 379-396 nm. Tetraaryl pyrazoles are AIEE active,¹⁶ to know such phenomenon be preserved in the poly(tetraaryl pyrazole)s, we investigated the emission behaviour of the polymers **10-12** & **16** in solution and aggregate states. The polymers are weakly fluorescent in tetrahydrofuran solution with fluorescence quantum yields (Φ) of 0.32 (**10**), 0.35 (**11**), 0.52 (**12**) and 0.42 (**16**) (Table 5A.4). However, when water is added into the solution keeping the concentration of the polymer same, the emission intensity continuously increased with gradual addition of water under the same measurement conditions (Figure 5A.8 and Table 5A.4). Polymer **16** was synthesized to analyse the effect of the flexible linker on the AIEE feature. As envisioned, polymer **16** exhibited a pronounced AIEE effect till 90:10 (H₂O:THF) composition whereas the emission

intensity of polymer **10** decreased at 90:10 (H₂O:THF) composition which may be due to precipitation of the polymer **10** at that composition (Figure 5A.8).

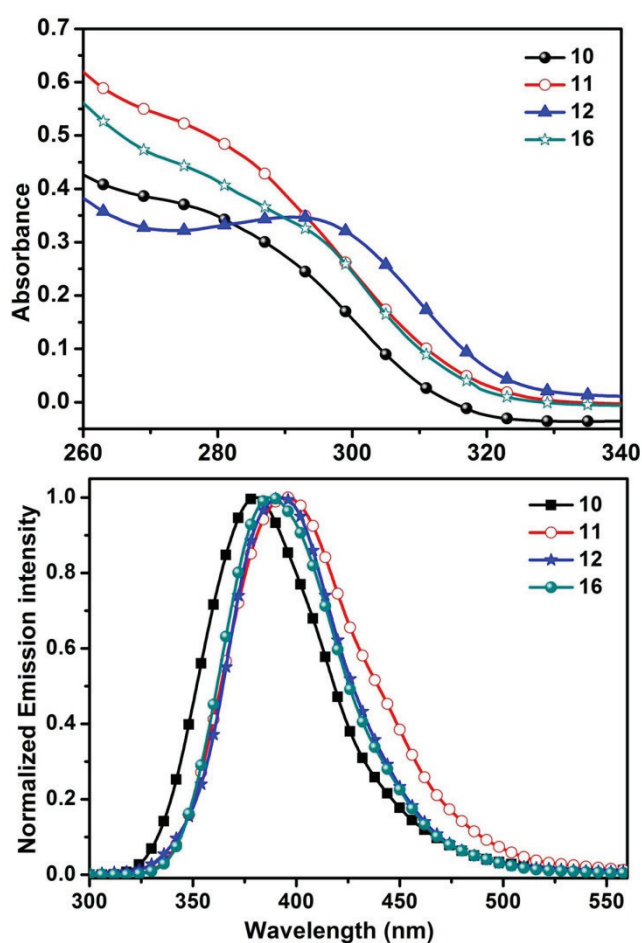


Figure 5A.6: (top) UV-Vis absorption spectra of polymers **10-12** & **16** (2.2×10^{-5} M) in THF solution. (bottom) Fluorescence spectra of polymers **10-12** & **16** (2.2×10^{-5} M) in THF solution.

Table 5A.4: Optical properties of the monomers (**7-9** & **15**) and polymers (**10-12** & **16**) in the solution and aggregated state.

Compound	λ_{ab}/nm	λ_{em}/nm	$\Phi_F(\text{THF})^a$	$\Phi_{F,agg}^{a,b}$
7	282	379	0.34	0.64
8	282	392	0.33	0.58
9	281	394	0.53	0.93
15	295	387	0.38	0.76
10	281	379	0.32	0.68
11	282	394	0.35	0.55
12	281	396	0.52	0.95
16	296	387	0.42	0.80

^a Measured using *p*-terphenyl in cyclohexane ($\Phi_F = 0.82$). ^b Aggregates formed in THF/water mixture (20:80).

Similar photoluminescence behaviours were observed for polymers **11** and **12** (Figure 5A.8). The quantum yields of the aggregates of polymers **10-12** & **16** at 80:20 (H₂O:THF) composition increased to 0.68 (**10**), 0.55 (**11**), 0.95 (**12**) and 0.80 (**16**) which is about 2 times higher than that in pure THF (Figure 5A.7 & Table5A.4).

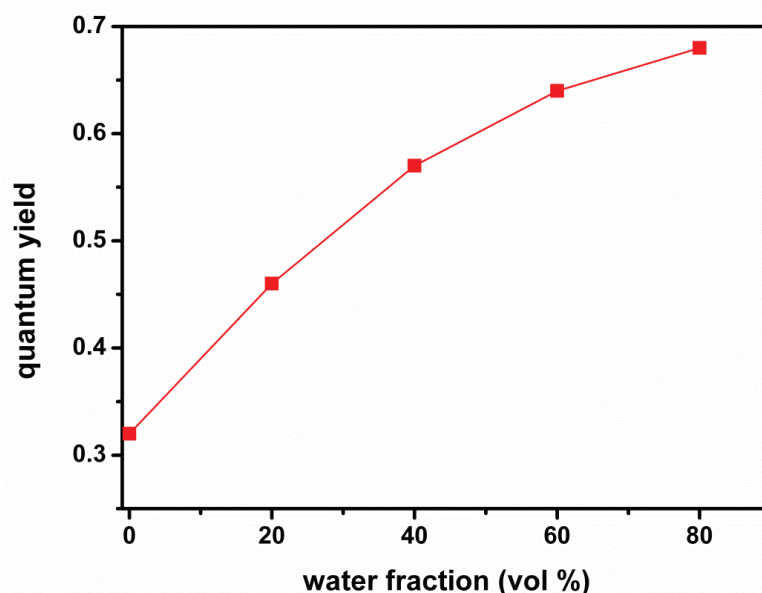


Figure 5A.7: Variation of quantum yields of polymer **10** with water fraction in the THF/H₂O mixture.

The emission intensity of the monomers (**7-9** & **15**) remain unchanged up to 70:30 (H₂O:THF) composition. Upon further increase in the water fraction in the mixture, the PL intensity rises rapidly (Figure 5A.9). On the other hand the emission intensity of the polymers **10-12** & **16** gradually increased with an increase in the water content. This may be explicated by the fact that the motions of the polymers are controlled by both internal (polymer chain entanglement) and external factors (H₂O addition) whereas in case of monomers the motions are restricted by physical aggregation which is controlled by external factors (water addition). As observed in hexaphenylsilole,³³⁻³⁷ tetraphenylethene³⁸⁻⁴¹ and other systems, the enhancement in emission in tetraaryl pyrazoles is due to the restricted intramolecular rotation caused by aggregation.

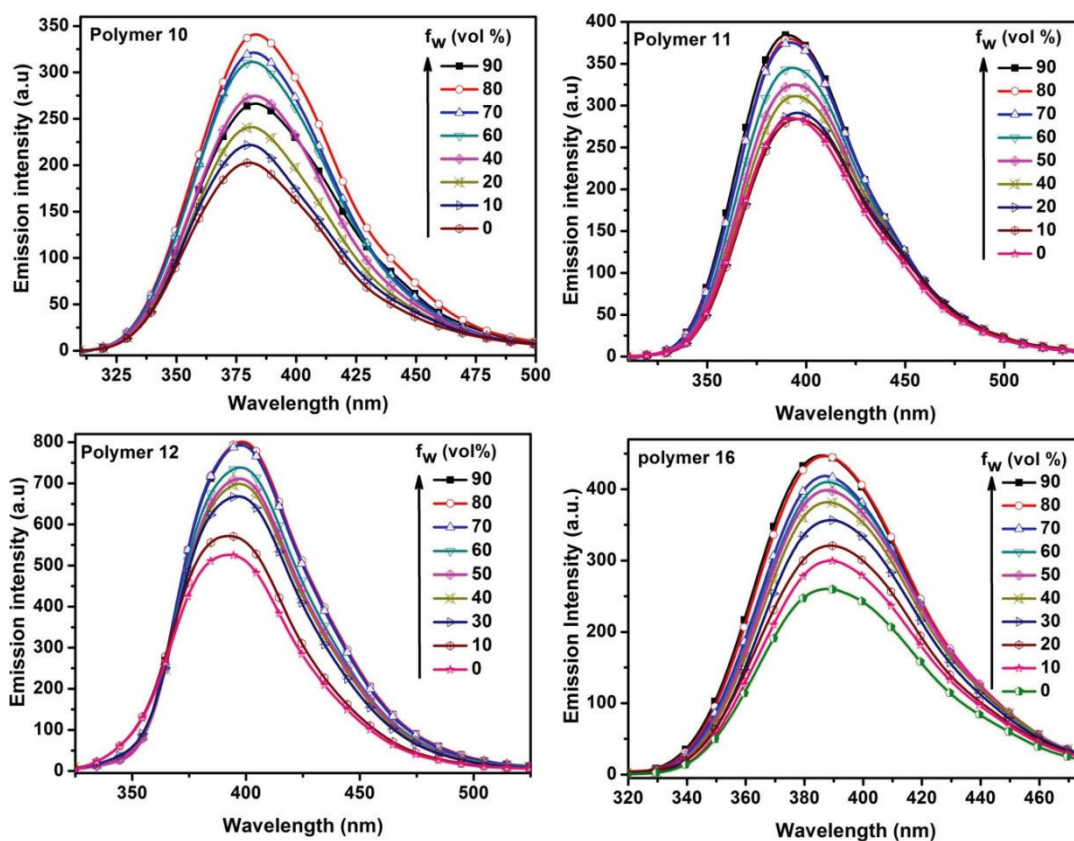


Figure 5A.8: Fluorescence spectra of polymers **10-12** & **16** in in THF/water mixtures with different water fraction (f_w). (Concentration = 2.2×10^{-5} M).

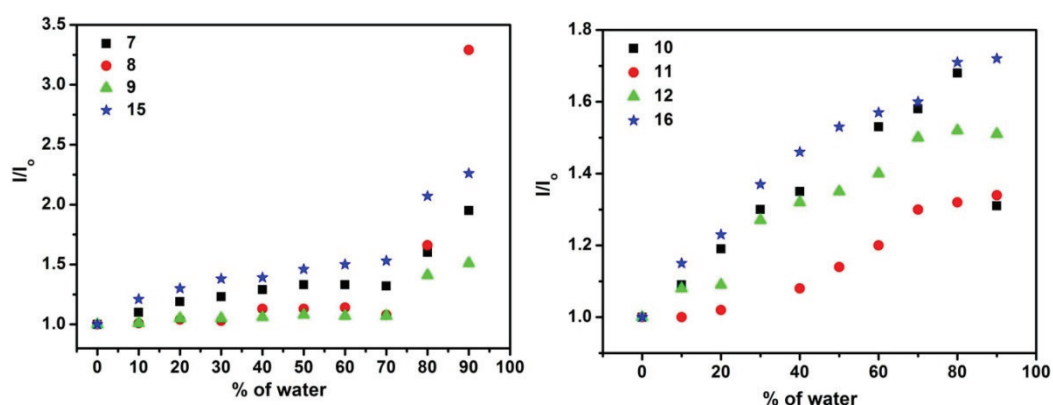


Figure 5A.9: Effects of water addition on Fluorescence Intensity (I) of Monomers (left) and polymers (right).

To better understand the photoluminescence properties of the tetraaryl pyrazole system, we investigated the packing pattern of the monomer **9**. As depicted in Figure 5A.10, the molecule adopts a twisted conformation, which hinders the close stacking of the molecule. Weak interactions like C-H \cdots π hydrogen bonds (2.774 to 2.885 Å) work to restrict the intramolecular rotation process and promote radiative

relaxation of the excited state. The cumulative effect of restricted intramolecular rotation and radiative relaxation of the excited state causes the molecules to fluoresce strongly.

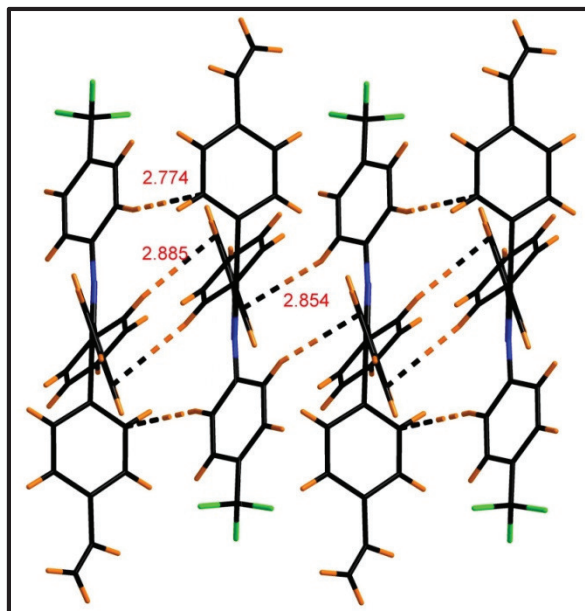


Figure 5A.10: Packing diagram with intermolecular C-H... π interactions (capped stick model).

We further supported the effect of restricted intramolecular rotation by carrying out temperature dependent studies of polymer **10** in THF solution. As shown in Figure 5A.11, the fluorescence peak intensity progressively increased with a decrease in temperature, indicating that cooling is limiting the intramolecular rotation thus helps to enhance the emission intensity.

To explore the potential use of these polymers we subjected polymer **10** for picric acid detection. Detection of picric acid is very important as this compound acts as an explosive in warfare and possesses acute health effects such as skin allergy, skin irritation, cancer and liver damage.^{33,34,44-46} The aggregates of polymer **10** in THF/H₂O (30:70) were used as the probe. Upon addition of aliquots of picric acid in water

to aggregates of polymer **10** (Figure 5A.12), its fluorescence emission got effectively quenched.

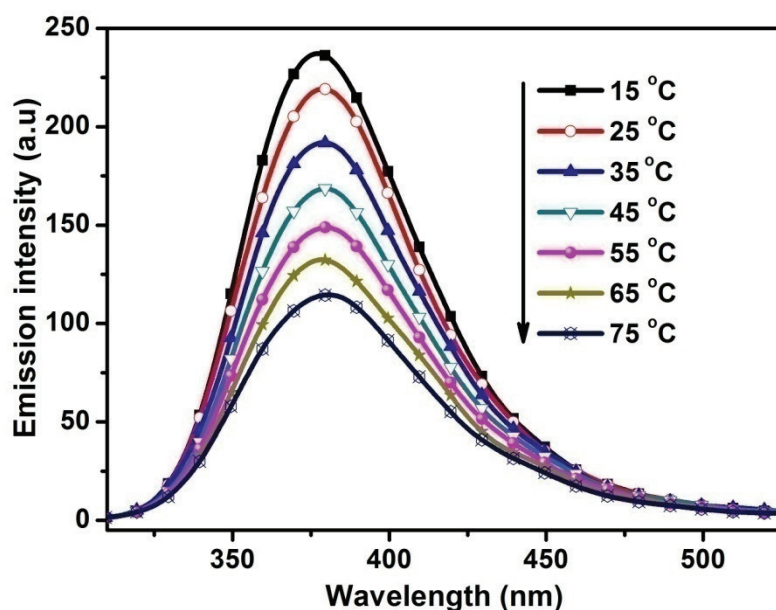


Figure 5A.11: Fluorescence spectra of polymer **10** (2.2×10^{-5} M) at different temperatures.

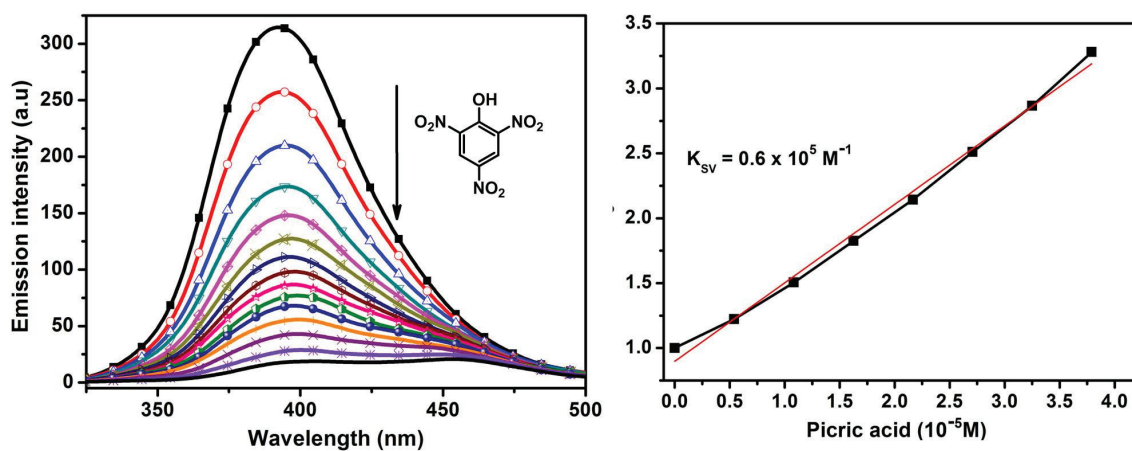


Figure 5A.12: (left) Fluorescence quenching of Polymer **10** (2.2×10^{-5} M) in THF/water mixture (70:30) with various concentrations of picric acid (0, 0.25, 0.50, 0.75, 1.00, 1.25, 1.50, 1.75, 2.00, 2.25, 2.50, 3.00, 3.50, 4.50, 5.50 equiv). Stern - Volmer plot for polymer **10** using picric acid as quencher at lower concentration.

The photoluminescence data of picric acid quenching were analyzed using Stern-Volmer plot. At low concentrations of picric acid, the Stern-Volmer plot is linear and gives a quenching constant of $0.60 \times 10^5 \text{ M}^{-1}$. However, the curve deviates from linearity when the picric acid concentration increased further. This is suggestive of super-quenching due to self-adsorption and (or) energy transfer.⁴⁷ Time resolved

fluorescence studies of polymer **10** were found to be invariant at different concentrations of picric acid indicating that the mechanism of quenching is static (Figure 5A.13).

To realize practical applicability of the polymers we adsorbed polymer **10** onto filter papers. Picric acid solutions with different concentration (10^{-3} , 10^{-4} and 10^{-5} M) were spotted onto the polymer coated filter papers along with a blank (Figure 5A.14). The minimum amount of picric acid detectable was ~ 23 ng, which is comparable with other literature reported AIE/AIEE based polymers.^{33,34,44}

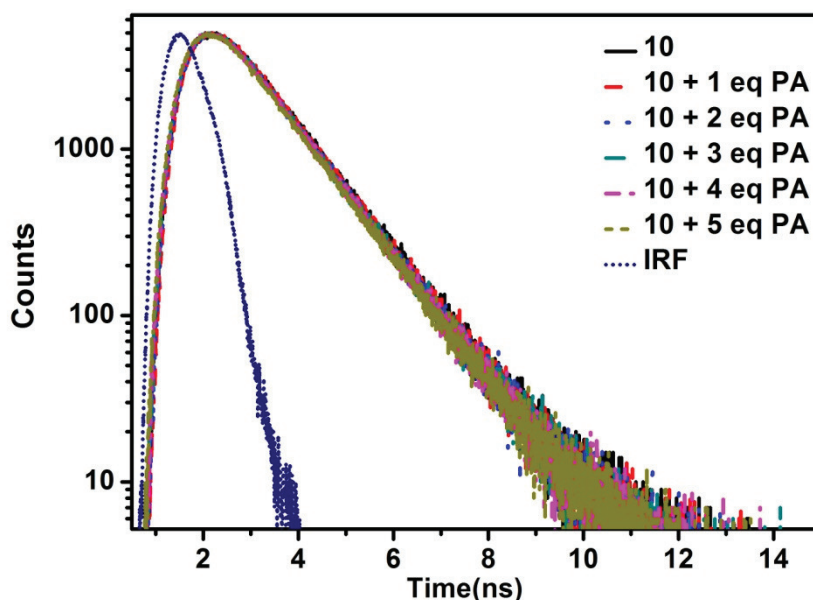


Figure 5A.13: Fluorescence lifetime decay profile of polymer **10** (2.2×10^{-5} M) in THF/H₂O (30:70) mixture for different concentrations of picric acid (PA). IRF = instrument response function. $\lambda_{\text{ex}} = 280$ nm.

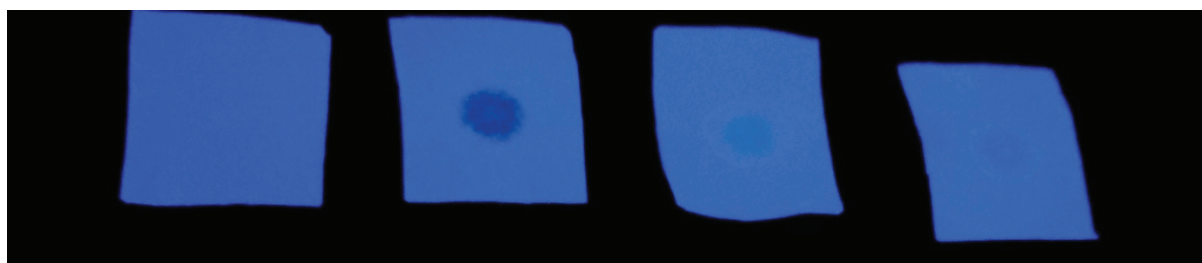


Figure 5A.14: Colour of fluorescent strips under UV light before and after addition of different concentration of picric acid (from left to right: blank, 10^{-3} , 10^{-4} , 10^{-5} M (PA)).

5A.3 Conclusion

In summary, a versatile route is developed for the synthesis of tetraaryl pyrazole containing polymerizable vinyl functional group. The poly(tetraaryl pyrazole)s, with moderate molecular weights were prepared by the standard free radical initiator, AIBN. All the polymers are thermally stable ($T_d > 300$ °C) and readily soluble in organic solvents like THF, CH_2Cl_2 and CHCl_3 . Our new poly(tetraaryl pyrazole)s are less-emissive when dissolved in THF solution but become more emissive when aggregated, divulging that they are AIEE active. Utilizing this novel AIEE effect of the poly(tetraaryl pyrazole)s we exploited them as chemosensors for the detection of explosives (picric acid) in the aggregate state. We expect that our results will have significant impact on the development of luminescent materials for organic electronics and in the area of biological imaging.

5A.4 Experimental section

5A.4.1 General information

Reagents and starting materials were purchased from Alfa-Aesar, Sigma-Aldrich and Spectrochem chemical companies and used as received unless otherwise noted. Chlorinated solvents were distilled from CaH_2 . Tetrahydrofuran was distilled from Na/benzophenone prior to use. 1,3,5-triphenyl-1*H*-pyrazole was prepared according to literature reported procedure.¹ All 400 MHz ^1H and 100 MHz ^{13}C NMR spectra were recorded on a Bruker ARX 400 spectrometer operating at 400 MHz and referenced internally to solvent signals. ESI mass spectra were recorded on a Bruker, microTOF-QII mass spectrometer. The absorbance spectra were recorded on a Perkin Elmer Lambda 750 UV–visible spectrometer. The fluorescence spectra were recorded on a Perkin Elmer LS-55 Fluorescence Spectrometer. The fluorescence spectra were corrected for instrumental response. Thermogravimetric analyses (TGA) were

recorded on a PerkinElmer Pyris 6 TGA model in a nitrogen atmosphere at a heating rate of 20 °C min⁻¹. Differential scanning calorimetric (DSC) analyses were recorded on a PerkinElmer Pyris 6 DSC model in nitrogen atmosphere at a heating rate of 20 °C min⁻¹. Gel-permeation chromatography (GPC) analyses were performed on a Shimadzu-LC20AD system referenced to poly(styrene) standards. THF was used as the mobile phase with a flow rate of 1.0 mL min⁻¹. Single-crystal X-ray diffraction data were collected on a Bruker APEX-II diffractometer equipped with an Oxford Instruments low-temperature attachment. The data were collected at 296 K using Mo-K α radiation (0.71073 Å). The structures were solved and refined with SHELX suite of programs. All non-hydrogen atoms were refined with anisotropic displacement coefficients. The H atoms were placed at calculated positions and were refined as riding atoms.

5A.4.2 Synthetic procedure and spectral characterization

5A.4.2.1 Synthesis of tetraaryl pyrazole (7)

Under nitrogen atmosphere, a biphasic solution of compound **4** (1.88 g, 5.02 mmol), 4-styrene boronic acid (0.89 g, 6.02 mmol), sodium carbonate (1.60 g, 15.06 mmol) and [Pd(PPh₃)₄] (3 mol%) in tetrahydrofuran and water (20:8; 56 mL) was heated at reflux for 12 hours. The organic layer was separated and the aqueous layer was extracted with ethyl acetate (2 x 20 mL). The combined organic phase was dried with sodium sulfate and concentrated under vacuum. The product was purified by column chromatography to afford compound **7**. Yield: 1.00 g (50%). mp: 160 °C. ¹H NMR (400 MHz, CDCl₃): δ = 5.22 (d, J = 8 Hz, 1H), 5.71 (d, J = 16 Hz, 1H), 6.68 (dd, J = 18 & 8 Hz, 1H), 7.04-7.08 (m, 4H), 7.19-7.34 (m, 13H), 7.53-7.55 (m, 2H) ppm. ¹³C NMR (100 MHz, CDCl₃): δ = 113.67, 120.45, 125.50, 126.24, 127.42, 127.85, 128.38, 128.47, 128.63, 128.92, 130.17, 130.59, 130.90, 132.75, 133.18, 135.87,

136.75, 140.00, 141.54, 150.36 ppm. HR-MS (ESI): calcd. For $C_{29}H_{22}N_2$ ($[M+H]^+$) : 399.1856, found : 399.1859. IR (KBr): $\nu(\text{cm}^{-1})$ = 3054 (s), 1595 (s), 1549 (m), 1495 (s), 1445 (s), 1399 (m), 1361 (s), 1294 (m), 1175 (m), 1065 (m), 1029 (m), 989 (m), 967 (s), 913 (s), 846 (s), 757 (s), 688 (s), 527 (m), 507 (m).

5A.4.2.2 Synthesis of tetraaryl pyrazole (8)

Compound **8** was prepared following a procedure similar to that used for **7**. The quantities involved are as follows: Compound **5** (3.14 g, 7.75 mmol), 4-styrene boronic acid (1.37 g, 9.30 mmol), sodium carbonate (2.46 g, 23.25 mmol) and $[Pd(PPh_3)_4]$ (3 mol%). Yield: 1.82 g (55%). mp: 168 °C. 1H NMR (400 MHz, $CDCl_3$): δ = 3.80 (s, 3H), 5.22 (d, J = 8 Hz, 1H), 5.72 (d, J = 20 Hz, 1H), 6.68 (dd, J = 18 & 8 Hz, 1H), 6.83 (d, J = 8 Hz, 2H), 7.05-7.08(m, 4H), 7.19-7.31 (m, 10H), 7.53-7.55 (m, 2H) ppm. ^{13}C NMR (100 MHz, $CDCl_3$): δ = 55.47 (O- CH_3), 113.49, 113.97, 119.86, 126.11, 126.76, 127.62, 128.11, 128.23, 128.30, 128.49, 130.09, 130.48, 130.76, 132.78, 133.16, 133.18, 135.66, 136.63, 141.40, 149.86, 158.69 ppm. HR-MS (ESI): calcd. For $C_{30}H_{24}N_2O$ ($[M+H]^+$) : 429.1961, found : 429.1947. IR (KBr): $\nu(\text{cm}^{-1})$ = 3056 (m), 2932 (m), 1608 (m), 1513 (s), 1451 (m), 1364 (m), 1299 (m), 1248 (s), 1175 (m), 1028 (m), 990 (m), 970 (m), 912 (m), 851 (m), 834 (m), 761 (m), 725 (m), 698 (m), 539 (m).

5A.4.2.3 Synthesis of tetraaryl pyrazole (9)

Compound **9** was prepared following a procedure similar to that used for **7**. The quantities involved are as follows: Compound **6** (3.63 g, 8.18 mmol), 4-styrene boronic acid (1.45 g, 9.82 mmol), sodium carbonate (2.60 g, 24.56 mmol) and $[Pd(PPh_3)_4]$ (3 mol%). Yield: 2.60 g (68 %). mp: 148 °C. 1H NMR (400 MHz, $CDCl_3$): δ = 5.24 (d, J = 12 Hz, 1H), 5.74 (d, J = 16 Hz, 1H), 6.69 (dd, J = 20 & 12 Hz, 1H), 7.06 (d, J = 8 Hz, 2H), 7.12 (d, J = 8 Hz, 2H), 7.26-7.35 (m, 8H), 7.45-7.48

(m, 2H), 7.54-7.59 (m, 4H) ppm. ^{13}C NMR (100 MHz, CDCl_3): δ = 113.93, 121.49, 122.71, 125.01, 125.45, 125.42, 126.15, 126.35, 128.18, 128.52, 128.61, 128.87, 129.19, 129.91, 130.57, 130.89, 132.30, 132.89, 136.16, 136.71, 141.69, 142.83, 151.27 ppm. HR-MS (ESI): calcd. For $\text{C}_{30}\text{H}_{21}\text{N}_2\text{F}_3$ ($[\text{M}+\text{H}]^+$) : 467.1730, found : 467.1724. IR (KBr): $\nu(\text{cm}^{-1})$ = 3045 (m), 1615 (m), 1521 (m), 1438 (m), 1365 (m), 1324 (s), 1166 (s), 1123 (s), 1106 (m), 1072 (m), 1058 (m), 968 (m), 912 (m), 844 (m), 731 (m), 698 (m), 526 (m), 503 (m).

5A.4.2.4 Synthesis of monomer 15

To a suspension of NaH (57% oil suspension, 0.12 g, 2.82 mmol) in anhydrous tetrahydrofuran (20 mL) at 0 °C 4-(1,3,5-triphenyl-1*H*-pyrazol-4-yl)phenol (1.00 g, 2.57 mmol) in anhydrous tetrahydrofuran (10 mL) was added while stirring. The reaction mixture was warmed to room temperature and refluxed for 2 h. The resulting solution was cooled to 0 °C in an ice bath and 1-(chloromethyl)-4-vinylbenzene (0.39 g, 2.57 mmol) in anhydrous tetrahydrofuran (5 mL) was added. The reaction mixture was refluxed for 24 h, cooled to room temperature and filtered. The filtrate was removed under vacuum; the resultant crude product was purified by silica gel column chromatography using ethyl acetate and hexane as eluent to afford the corresponding product as a white solid. Yield: 1.03 g (80%). mp: 154 °C. ^1H NMR (400 MHz, CDCl_3): δ = 5.00 (s, 2H), 5.27 (d, J = 12 Hz, 1H), 5.77 (d, J = 16 Hz, 1H), 6.74 (dd, J = 16 & 12 Hz, 1H), 6.84 (d, J = 8 Hz, 2H), 7.03 (d, J = 8 Hz, 2H), 7.07 (d, J = 8 Hz, 2H), 7.19-7.35 (m, 11H), 7.39-7.43 (m, 4H), 7.54-7.57 (m, 2H) ppm. ^{13}C NMR (100 MHz, CDCl_3): δ = 69.87, 114.27, 114.81, 120.45, 125.54, 125.59, 126.54, 127.47, 127.87, 128.00, 128.32, 128.37, 128.44, 128.57, 128.93, 130.14, 130.58, 131.93, 133.02, 133.59, 136.61, 137.51, 139.86, 141.58, 150.17, 157.83 ppm. HR-MS (ESI): calcd. For $\text{C}_{36}\text{H}_{28}\text{N}_2\text{O}_1$ ($[\text{M} + \text{H}]^+$) : 505.2274, found : 505.2240. IR (KBr): $\nu(\text{cm}^{-1})$ =

3052 (m), 2911 (m), 1596 (m), 1551 (m), 1510 (s), 1497 (s), 1450 (m), 1407 (m), 1362 (m), 1280 (m), 1242 (s), 1175 (m), 1006 (m), 970 (m), 913 (m), 835 (m), 768 (m), 696 (s), 540 (m).

5A.4.2.5b Synthesis of Polymer 10

A Schlenk tube was charged with monomer **7** (0.50 g, 1.25 mmol) and free radical initiator azobisisobutyronitrile (2 mol%). The system was purged with nitrogen and degassed dichloroethane (1.0 mL) was added. The reaction mixture was stirred at 80 °C for 24 h. The mixture was then slowly added to hexane to precipitate the polymer. The resulting solid was redissolved in dichloromethane (1 mL) and reprecipitated from hexane. The precipitation was repeated three times. The solid was collected and dried under high vacuum to obtain the polymer **10** as a white solid. Yield = 0.40 g (80%), ¹H NMR (400 MHz, CDCl₃): δ = 0.88-2.20 (b, polymer backbone), 6.21-7.38 (aromatic H) ppm. ¹³C NMR (100 MHz, CDCl₃): δ = 39-40 (polymer backbone), 120.38, 125.17, 127.19-128.74, 130.23, 133.28, 139.81, 141.10, 150.06 ppm. IR (KBr): ν(cm⁻¹) = 3052 (m), 2919 (m), 1596 (m), 1496 (s), 1449 (m), 1361 (s), 1176 (m), 1073 (m), 1028 (m), 969 (m), 914 (m), 839 (m), 758 (m), 695 (s), 656 (m), 563 (m), 524 (m).

5A.4.2.6 Synthesis of Polymer 11

Polymer **11** was prepared following a procedure similar to that used for polymer **10**. The quantities involved are as follows: Monomer **8** (0.50 g, 1.17 mmol), azobisisobutyronitrile (2 mol%) Yield = 0.42 g, (85%), ¹H NMR (400 MHz, CDCl₃): δ = 0.88 -2.20 (b, polymer backbone), 3.70 (s, OMe), 6.19-7.37 (aromatic H) ppm. ¹³C NMR (100 MHz, CDCl₃): δ = 39-41 (polymer backbone), 55.41 (-OCH₃), 113.92, 119.90, 126.63, 127.56-128.34, 130.30, 132.96-133.28, 141.15, 149.66, 158.55 ppm. IR (KBr): ν(cm⁻¹) = 3055 (m), 3024 (m), 2927 (m), 2836 (m), 1604 (m), 1511 (s),

1444 (m), 1364 (m), 1299 (s), 1248 (s), 1170 (m), 1065 (m), 1030 (m), 970 (m), 832 (s), 771 (m), 722 (m), 697 (s), 563 (m), 532 (m).

5A.4.2.7 Synthesis of Polymer 12

Polymer **12** was prepared following a procedure similar to that used for polymer **10**. The quantities involved are as follows: Monomer **3c** (0.60 g, 1.29 mmol), azobisisobutyronitrile (2 mol%). Yield = 0.49 g (83%), ^1H NMR (400 MHz, CDCl_3): δ = 0.85 -2.10 (b, polymer backbone), 6.26-7.45 (aromatic H) ppm. ^{13}C NMR (100 MHz, CDCl_3): δ = 39-40 (polymer backbone), 119.82, 121.04, 122.45, 124.59, 125.17, 126.06, 128.27-129.18, 128.27-129.18, 129.97-130.35, 132.98, 141.22, 142.47, 150.84 ppm. IR (KBr): $\nu(\text{cm}^{-1})$ = 3058 (m), 2921 (m), 2850 (m), 1616 (s), 1522 (s), 1448 (m), 1444 (m), 1410 (m), 1363 (m), 1329 (s), 1166 (m), 1129 (s), 1072 (m), 1058 (m), 1018 (m), 968 (s), 843 (s), 755 (m), 732 (m), 696 (m), 564 (m), 523 (m).

5A.4.2.8 Synthesis of Polymer 16

Polymer **16** was prepared following a procedure similar to that used for polymer **10**. The quantities involved are as follows: Monomer **15** (0.50 g, 0.99 mmol), azobisisobutyronitrile (2 mol%). Yield = 0.42 g (85%), ^1H NMR (400 MHz, CDCl_3): δ = 0.78 -2.00 (b, polymer backbone), 4.72 (s, $-\text{CH}_2-$), 6.50 -7.48 (aromatic H) ppm. ^{13}C NMR (100 MHz, CDCl_3): δ = 39-40 (polymer backbone), 69.89 ($-\text{CH}_2-$), 114.54, 120.30, 125.31, 125.61, 127.26-128.27, 128.84, 130.18-130.43, 131.86, 133.30, 134.22, 140.03, 141.20, 144.79, 150.19, 157.79 ppm. IR (KBr): $\nu(\text{cm}^{-1})$ = 3051 (m), 2919 (m), 1596 (m), 1549 (m), 1508 (s), 1497 (s), 1449 (m), 1361 (s), 1281 (m), 1226 (s), 1172 (s), 1015 (m), 969 (m), 912 (m), 835 (m), 763 (m), 735 (m), 695 (s), 540 (m).

5A.5 References

- (1) Fustero, S.; Sánchez-Roselló, M.; Barrio, P.; Simón-Fuentes, A. *Chem. Rev.***2011**, *111*, 6984.
- (2) Fustero, S.; Antonio, S. F.; Sanz-Cervera, J. F. *Org. Prep. Proced. Int.***2009**, *41*, 253.
- (3) Chandrasekhar, V.; Deria, P.; Krishnan, V.; Athimoolam, A.; Singh, S.; Madhavaiah, C.; Srivatsan, S. G.; Verma, S. *Bioorg. Med. Chem. Lett.***2004**, *14*, 1559.
- (4) Chandrasekhar, V.; Athimoolam, A.; Krishnan, V.; Azhakar, R.; Madhavaiah, C.; Verma, S. *Eur. J. Inorg. Chem.***2005**, 1482.
- (5) Chandrasekhar, V.; Athimoolam, A.; Srivatsan, S. G.; Sundaram, P. S.; Verma, S.; Steiner, A.; Zacchini, S.; Butcher, R. *Inorg. Chem.***2002**, *41*, 5162.
- (6) Harb, A. F. A.; Abbas, H. H.; Mostafa, F. H. *J. Iran. Chem. Soc.***2005**, *2*, 115.
- (7) Harb, A. F. A.; Abbas, H. H.; Mostafa, F. H. *chem.pap.***2005**, *59*, 187.
- (8) Maeda, H.; Ito, Y.; Kusunose, Y.; Nakanishi, T. *Chem. Commun.***2007**, 1136.
- (9) Chandrasekhar, V.; Azhakar, R.; Krishnan, V.; Athimoolam, A.; Pandian, B. *M. J. Am. Chem. Soc.***2006**, *128*, 6802.
- (10) Karatsu, T.; Shiochi, N.; Aono, T.; Miyagawa, N.; Kitamura, A. *Bull. Chem. Soc. Jpn.***2003**, *76*, 1227.
- (11) Dorlars, A.; Schellhammer, C. W.; Schroeder, J. *Angew. Chem. Int. Ed.***1975**, *14*, 665.
- (12) He, Z.; Milburn, G. H. W.; Baldwin, K. J.; Smith, D. A.; Danel, A.; Tomasik, P. *J. Lumin.***2000**, *86*, 1.
- (13) Tao, Y. T.; Balasubramaniam, E.; Danel, A.; Tomasik, P. *Appl. Phys. Lett.***2000**, *77*, 933.

- (14) Xiao, L.; Cai, S.; Liu, Q.; Liao, L.; Guo, X.; Li, Y.; Jia, X.; Li, F.; Liu, L. *Polym. Chem.***2014**, *5*, 607.
- (15) Matsumoto, F.; Chujo, Y. *Macromolecules***2003**, *36*, 5516.
- (16) Moore, J. A.; Mehta, P. G. *Macromolecules***1988**, *21*, 2644.
- (17) Qin, Y.; Cui, C.; Jäkle, F. *Macromolecules***2008**, *41*, 2972.
- (18) Lu, C.; Liu, Q.; Gu, P.; Chen, D.; Zhou, F.; Li, H.; Xu, Q.; Lu, J. *Polym. Chem.***2014**, *5*, 2602.
- (19) Gu, P. Y.; Lu, C. J.; Xu, Q. F.; Ye, G. J.; Chen, W. Q.; Duan, X. M.; Wang, L. H.; Lu, J. M. *J. Polym. Sci., Part A: Polym. Chem.***2012**, *50*, 480.
- (20) Luo, J.; Xie, Z.; Xie, Z.; Lam, J. W. Y.; Cheng, L.; Chen, H.; Qiu, C.; Kwok, H. S.; Zhan, X.; Liu, Y.; Zhu, D.; Tang, B. Z.; Tang, B. Z.; Tang, B. Z. *Chem. Commun.***2001**, *18*, 1740.
- (21) An, B. K.; Kwon, S. K.; Jung, S. D.; Park, S. Y. *J. Am. Chem. Soc.***2002**, *124*, 14410.
- (22) Ding, D.; Li, K.; Liu, B.; Tang, B. Z. *Acc. Chem. Res.***2013**, *46*, 2441.
- (23) Hu, R.; Leung, N. L. C.; Tang, B. Z. *Chem. Soc. Rev.***2014**, *43*, 4494.
- (24) Mei, J.; Leung, N. L. C.; Kwok, R. T. K.; Lam, J. W. Y.; Tang, B. Z. *Chem. Rev.***2015**, *115*, 11718.
- (25) Hong, Y.; Lam, J. W. Y.; Tang, B. Z. *Chem. Soc. Rev.***2011**, *40*, 5361.
- (26) Xie, Z.; Yang, B.; Xie, W.; Liu, L.; Shen, F.; Wang, H.; Yang, X.; Wang, Z.; Li, Y.; Hanif, M.; Yang, G.; Ye, L.; Ma, Y. *J. Phys. Chem. B***2006**, *110*, 20993.
- (27) Lai, C. T.; Hong, J. L. *J. Phys. Chem. B***2010**, *114*, 10302.
- (28) Chen, M.; Li, L.; Nie, H.; Tong, J.; Yan, L.; Xu, B.; Sun, J. Z.; Tian, W.; Zhao, Z.; Qin, A.; Tang, B. Z. *Chem. Sci.***2015**, *6*, 1932.

- (29) Chen, M.; Li, L.; Nie, H.; Shi, Y.; Mei, J.; Wang, J.; Sun, J. Z.; Qin, A.; Tang, B. Z. *Chem. Commun.***2015**, *51*, 10710.
- (30) Zhang, X.; Chi, Z.; Zhou, X.; Liu, S.; Zhang, Y.; Xu, J. *J. Phys. Chem. C***2012**, *116*, 23629.
- (31) Yan, X.; Cook, T. R.; Wang, P.; Huang, F.; Stang, P. J. *Nat. Chem.***2015**, *7*, 342.
- (32) Liu, J.; Zhong, Y.; Lu, P.; Hong, Y.; Lam, J. W. Y.; Faisal, M.; Yu, Y.; Wong, K. S.; Tang, B. Z. *Polym. Chem.***2010**, *1*, 426.
- (33) Zhang, L. H.; Jiang, T.; Wu, L. B.; Wan, J. H.; Chen, C. H.; Pei, Y. B.; Lu, H.; Deng, Y.; Bian, G. F.; Qiu, H. Y.; Lai, G. Q. *Chem. - Asian J.***2012**, *7*, 1583.
- (34) Zhao, Z.; Guo, Y.; Jiang, T.; Chang, Z.; Lam, J. W. Y.; Xu, L.; Qiu, H.; Tang, B. Z. *Macromol. Rapid Commun.***2012**, *33*, 1074.
- (35) Liu, J.; Lam, J. W. Y.; Tang, B. Z. *J. Inorg. Organomet. Polym. Mater.***2009**, *19*, 249.
- (36) Chen, L.; Jiang, Y.; Nie, H.; Lu, P.; Sung, H. H. Y.; Williams, I. D.; Kwok, H. S.; Huang, F.; Qin, A.; Zhao, Z.; Tang, B. Z. *Adv. Funct. Mater.***2014**, *24*, 3621.
- (37) Mei, J.; Wang, J.; Sun, J. Z.; Zhao, H.; Yuan, W.; Deng, C.; Chen, S.; Sung, H. H. Y.; Lu, P.; Qin, A.; Kwok, H. S.; Ma, Y.; Williams, I. D.; Tang, B. Z. *Chem. Sci.***2012**, *3*, 549.
- (38) Zhao, Z.; Lam, J. W. Y.; Tang, B. Z. *J. Mater. Chem.***2012**, *22*, 23726.
- (39) Huang, J.; Sun, N.; Dong, Y.; Tang, R.; Lu, P.; Cai, P.; Li, Q.; Ma, D.; Qin, J.; Li, Z. *Adv. Funct. Mater.***2013**, *23*, 2329.
- (40) Ghosh, K. R.; Saha, S. K.; Wang, Z. Y. *Polym. Chem.***2014**, *5*, 5638.
- (41) Dong, W.; Fei, T.; Palma-Cando, A.; Scherf, U. *Polym. Chem.***2014**, *5*, 4048.

- (42) Mukherjee, S.; Salini, P. S.; Srinivasan, A.; Peruncheralathan, S. *Chem. Commun.***2015**, *51*, 17148.
- (43) Mamidala, R.; Mukundam, V.; Dhanunjayarao, K.; Venkatasubbaiah, K. *Dalton Trans.***2015**, *44*, 5805.
- (44) Zhao, Z.; Jiang, T.; Guo, Y.; Ding, L.; He, B.; Chang, Z.; Lam, J. W. Y.; Liu, J.; Chan, C. Y. K.; Lu, P.; Xu, L.; Qiu, H.; Tang, B. Z. *J. Polym. Sci., Part A: Polym. Chem.***2012**, *50*, 2265.
- (45) Vishnoi, P.; Sen, S.; Patwari, G. N.; Murugavel, R. *New J. Chem.***2015**, *39*, 886.
- (46) Feng, H. T.; Zheng, Y. S. *Chem. Eur. J.***2014**, *20*, 195.
- (47) Thomas, S. W.; Joly, G. D.; Swager, T. M. *Chem. Rev.***2007**, *107*, 1339.

CHAPTER 5B

Synthesis, Characterization and Aggregation Induced Enhanced Emission Properties of Tetraaryl Pyrazole Decorated Cyclophosphazenes

5B.1 Introduction	227
5B.2 Results and discussion	228
5B.2.1 Synthesis and characterization	228
5B.2.2 Photophysical studies	233
5B.3 Conclusions	245
5B.4 Experimental section	246
5B.4.1 General information	246
5B.4.2 Synthetic procedure and spectral characterization	248
5B.5 References	252

5B.1 Introduction

Organic fluorophores generally show strong emission in dilute solutions, however more often exhibit relatively weak emission in solid state due to aggregation of molecules in the solid state. This phenomenon is known as aggregation caused quenching (ACQ) which has become an obstacle in the fabrication of light-emitting devices.¹ The trouble caused by ACQ has driven researchers to develop unconventional anti ACQ luminophoric systems. The recent discovery of aggregation induced emission (AIE) by Tang's group² and aggregation induced enhanced emission (AIEE) by Park's group³ have attracted much attention owing to their potential applications in different fields. Since these pioneering works, a series of interesting molecules with AIE or AIEE property have been reported and used as bioprobes, stimuli responsive nanomaterials, chemosensors and active layers in the construction of efficient organic light emitting diodes.⁴⁻¹³

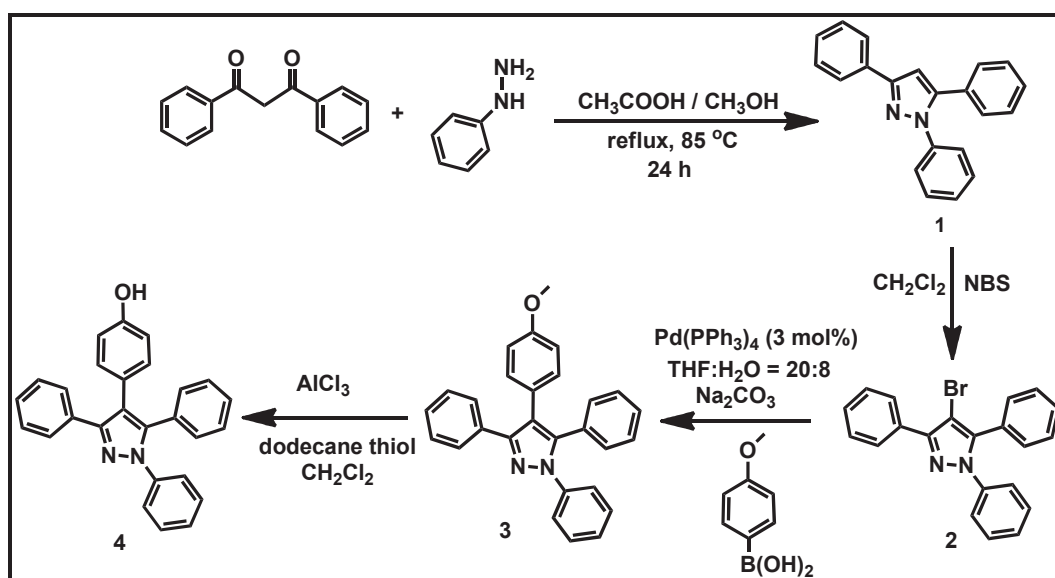
Among the inorganic heterocycles,¹⁴ cyclophosphazenes¹⁵⁻¹⁸ have attracted interest because of their use as scaffolds for the design and construction of a wide variety of functional and speciality materials.¹⁹⁻²⁸ Another added advantage of the hexachlorocyclotriphosphazene is its ability to serve as a small-molecule model system for high polymeric phosphazenes.²⁹⁻³¹ The properties studied with hexachlorocyclotriphosphazene could be transposed to the high polymeric phosphazenes. Grafting fluorescent probes to hexachlorocyclotriphosphazene have received increasing attention owing to their application in medicinal imaging, organic light-emitting diodes and organic nanodots.³²⁻³⁷ In this chapter, we describe tetraaryl pyrazole decorated cyclophosphazenes, their AIEE properties and sensing ability towards the explosive like picric acid. It is worth noting that we also varied the

number of AIEE luminogen on the periphery of the cyclophosphazene from one to six and studied their AIEE properties.

5B.2 Results and discussion

5B.2.1 Synthesis and characterization

The AIEE active tetraaryl pyrazole **3** was prepared according to the synthetic route shown in Scheme 5B.1. The triaryl pyrazole **1** was synthesised by the condensation of 1,3-diphenyl-1,3-propanedione and phenylhydrazine in refluxing methanol/acetic acid. The triaryl pyrazole³⁸**1** was brominated using N-bromosuccinimide in dichloromethane to form compound **2**. Compound **3** was synthesized from brominated triphenyl pyrazole (**2**) and 4-methoxy phenyl boronic acid under Suzuki coupling reaction condition. Demethylation of **3** by AlCl_3 gave hydroxylated tetraaryl pyrazole derivative **4**. The formation of **4** from **3** was confirmed by the absence of methoxyl protons in the ^1H NMR spectrum of the product **4** (Figure 5B.1).



Scheme 5B.1: Synthetic pathway for compound **4**

As shown in Scheme 5B.2, the reaction of **4** with $\text{N}_3\text{P}_3\text{Cl}_6$ in the presence of NaH as a base in tetrahydrofuran (THF) resulted in the formation of $\text{N}_3\text{P}_3(\text{O}-\text{C}_6\text{H}_4-\text{C}_3\text{N}_2-$

(C₆H₅)₃)₆ (**5**). A similar protocol was used for the synthesis of N₃P₃(O₂C₁₂H₈)(O-C₆H₄-C₃N₂-(C₆H₅)₃)₄ (**6**) and N₃P₃(O₂C₁₂H₈)₂(O-C₆H₄-C₃N₂-(C₆H₅)₃)₂ (**7**) starting from N₃P₃(O₂C₁₂H₈)Cl₄, N₃P₃(O₂C₁₂H₈)₂Cl₂ respectively (Scheme 5B.2). Compound **9** was synthesized as shown in Scheme 5B.3. For this purpose first, compound **8** was synthesized by the reaction of **4** with N₃P₃Cl₆ in dry acetone using K₂CO₃ as a base. The resultant mono substituted N₃P₃Cl₅(O-C₆H₄-C₃N₂-(C₆H₅)₃) is reacted with excess of phenol in the presence of the base NaH in THF to obtain compound **9** in 65 % yield. All compounds were characterized with ¹H, ¹³C NMR, high resolution mass spectroscopy (HRMS) and elemental analysis. A representative HRMS for compounds **6** and **7** are shown in Figure 5B.2.

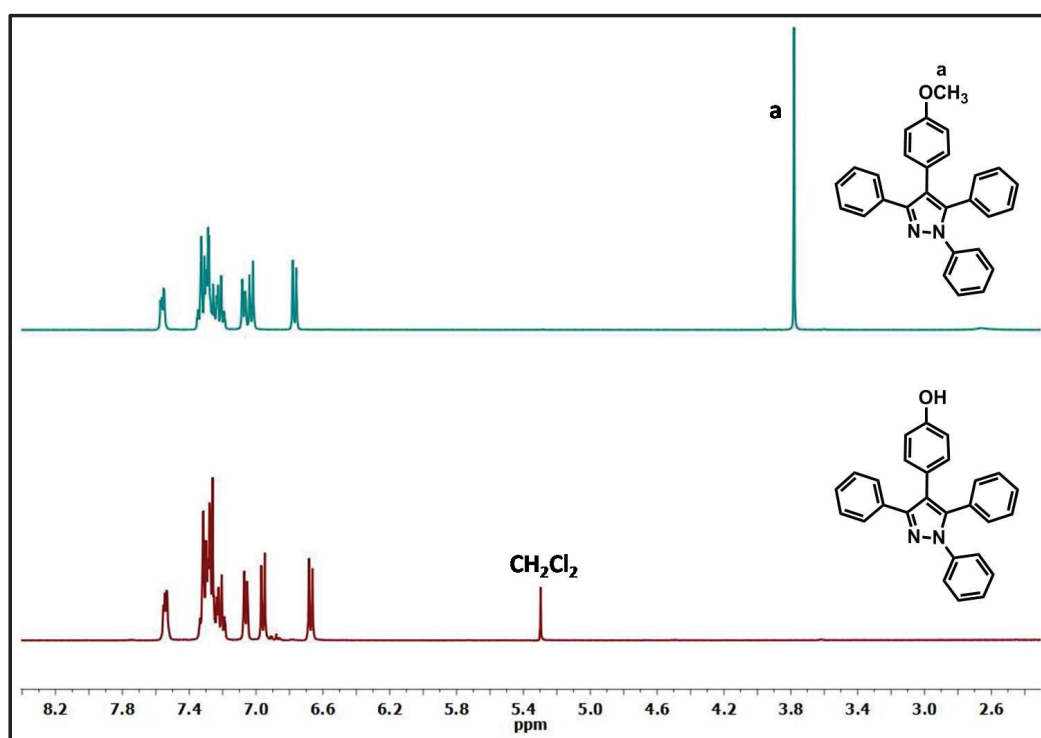


Figure 5B.1: ¹H NMR spectrum of compound **3**(top) and **4** (bottom) recorded in CDCl₃

Compound **5**, **6**, **7**, **8** and **9** were further characterised by ³¹P[¹H]NMR spectroscopy. As shown in Figure 5B.3, the ³¹P[¹H]NMR spectrum shows a singlet (8.5 ppm) for compound **5**, AX₂/A₂X type first-order pattern were observed for compounds **6**, **7** and **8**. Compound **9** shows a non-first order ³¹P[¹H]NMR spectrum.

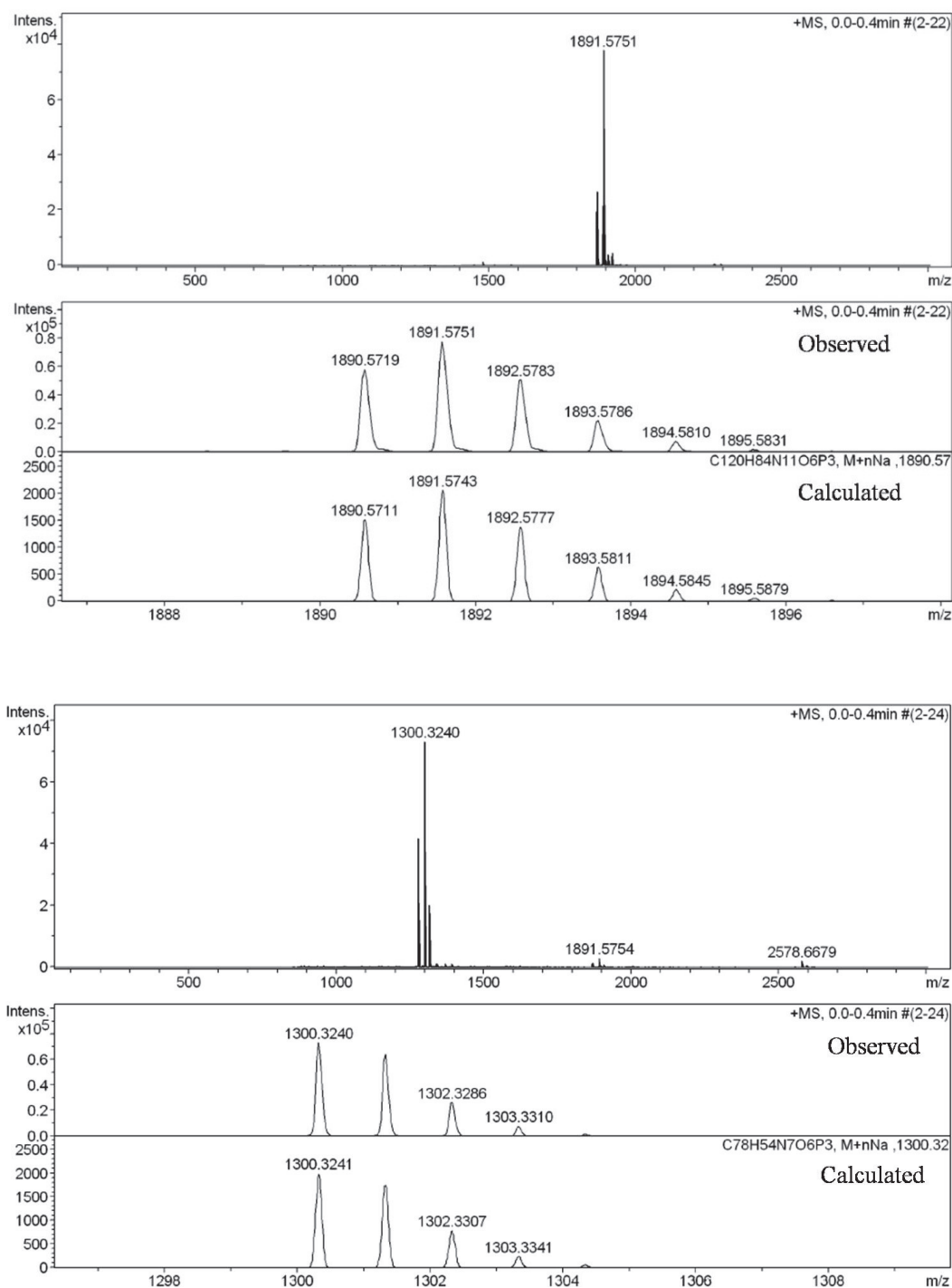
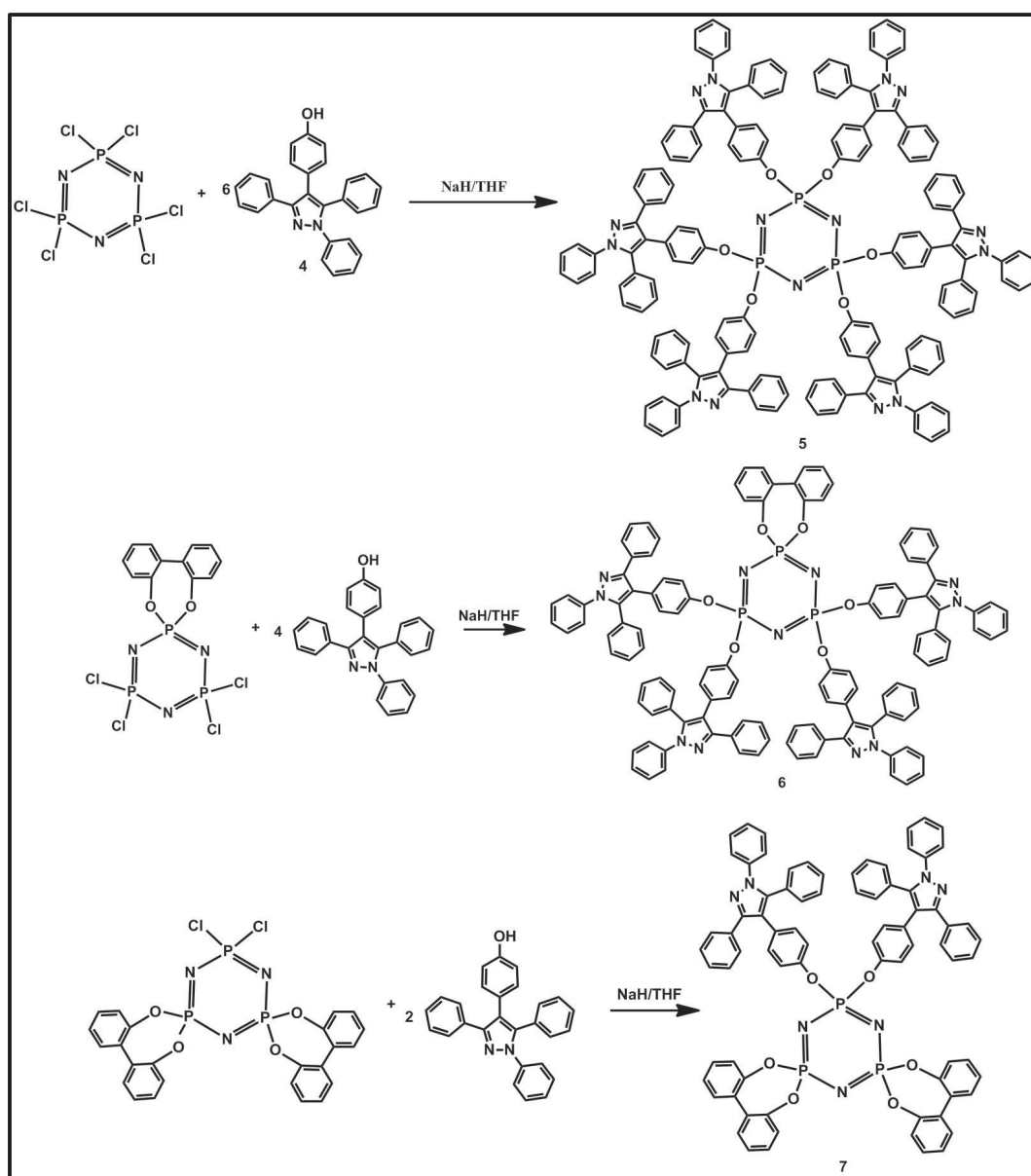


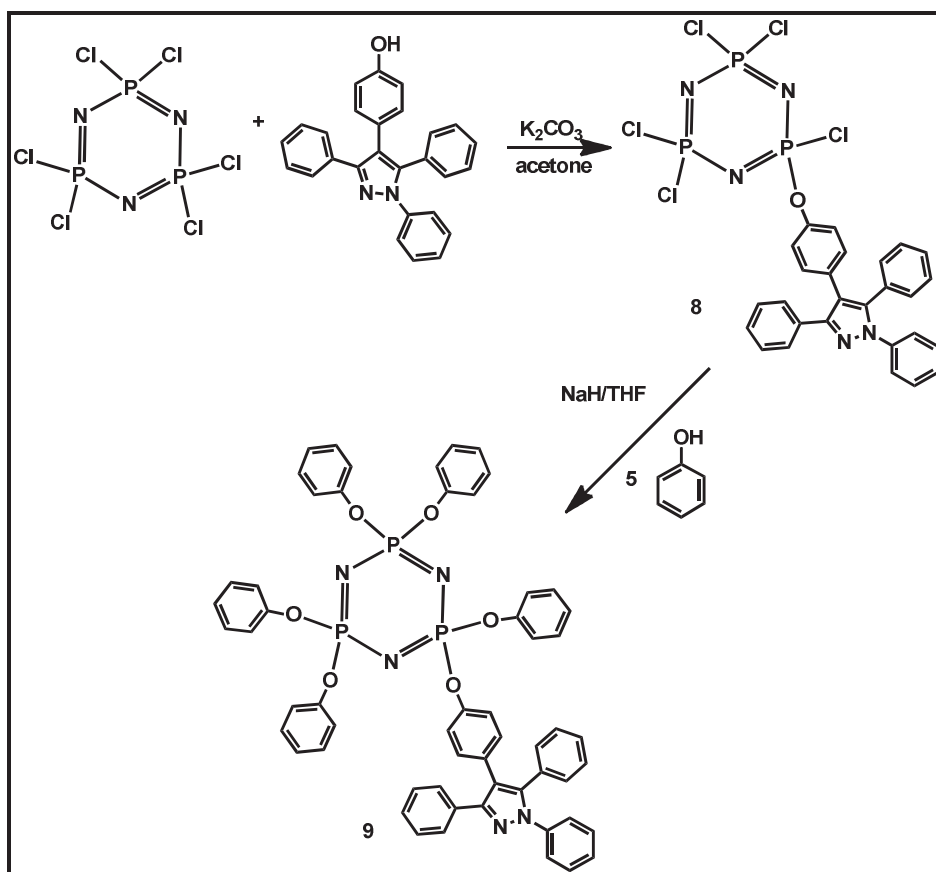
Figure 5B.2: HRMS of compound **6** (top) and **7** (bottom)

Recently it was realized that tetraaryl substituted pyrazoles exhibit AIEE phenomenon.³⁹ The question raised in our mind is, does the pyrazole decorated cyclophosphazenes still retain the AIEE characteristics of the tetraaryl pyrazoles? To

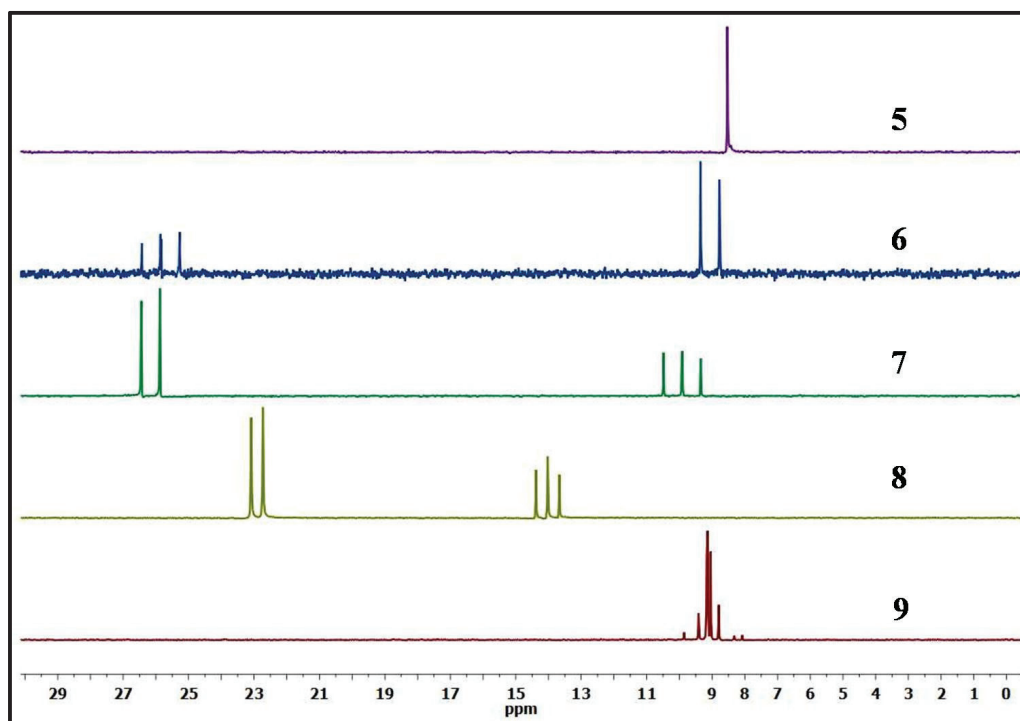
answer this question, we studied the photoluminescence behaviour of compounds **5**, **6**, **7** & **9** in solution and aggregate state.



Scheme 5B.2: Synthetic pathway for compound **5**, **6** and **7**



Scheme 5B.3: Synthetic pathway for compound 9

Figure 5B.3: ^{31}P NMR spectrum of compound 5, 6, 7, 8 and 9 recorded in $CDCl_3$

5B.2.2 Photophysical studies

The optical properties of the newly synthesized cyclotriphosphazene derivatives were investigated by UV-Vis absorption and fluorescence spectroscopy in THF solution.

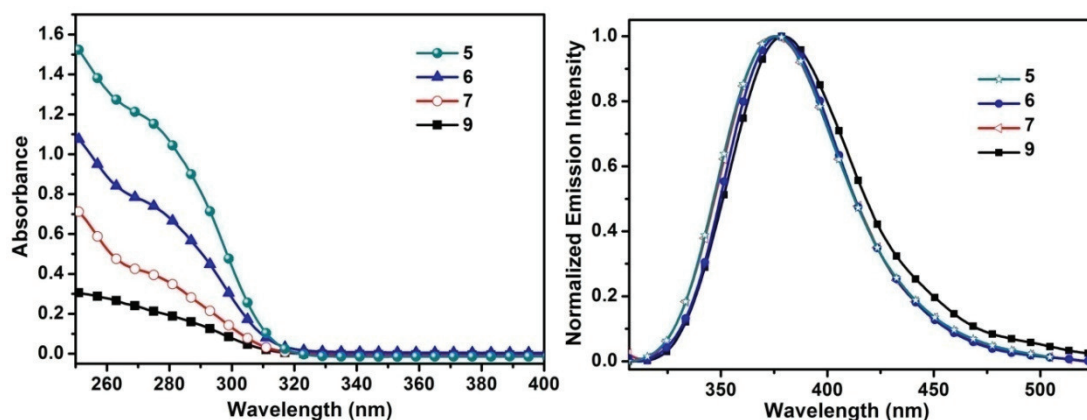


Figure 5B.4: (left) UV-Visible spectra of compounds **5**, **6**, **7** & **9**; (right) Normalized photoluminescence spectra (excited at 280 nm) of compounds **5**, **6**, **7** & **9** recorded using 9.6×10^{-6} M tetrahydrofuran solutions.

As shown in Figure 5B.4, the shapes of the UV-Vis spectra of the compounds **5**, **6**, **7** & **9** recorded under similar concentration reveal a linear decrease in the ϵ values. Thus compound **9** shows the lowest ϵ value of 19900 while compound **5** with six pyrazole arms show high ϵ value (110800). All compounds showed broad band centred at 376 nm in the emission spectra (Table 5B.1).

Table 5B.1: Optical properties of the compounds **5**, **6**, **7** & **9**.

Compound	λ_{ab} [nm] (ϵ , $M^{-1}cm^{-1} \times 10^3$)	λ_{em} [nm]	Φ_F (THF) ^a	Φ_F (agg) ^{a,b}
5	280 (110.8)	376	0.11	0.22
6	280 (69.5)	377	0.12	0.21
7	280 (36.8)	376	0.09	0.20
9	280 (19.9)	379	0.09	0.19

^a Measured using *p*-terphenyl in cyclohexane ($\Phi_F = 0.82$). ^b Aggregates formed in THF/water mixture (10:90).

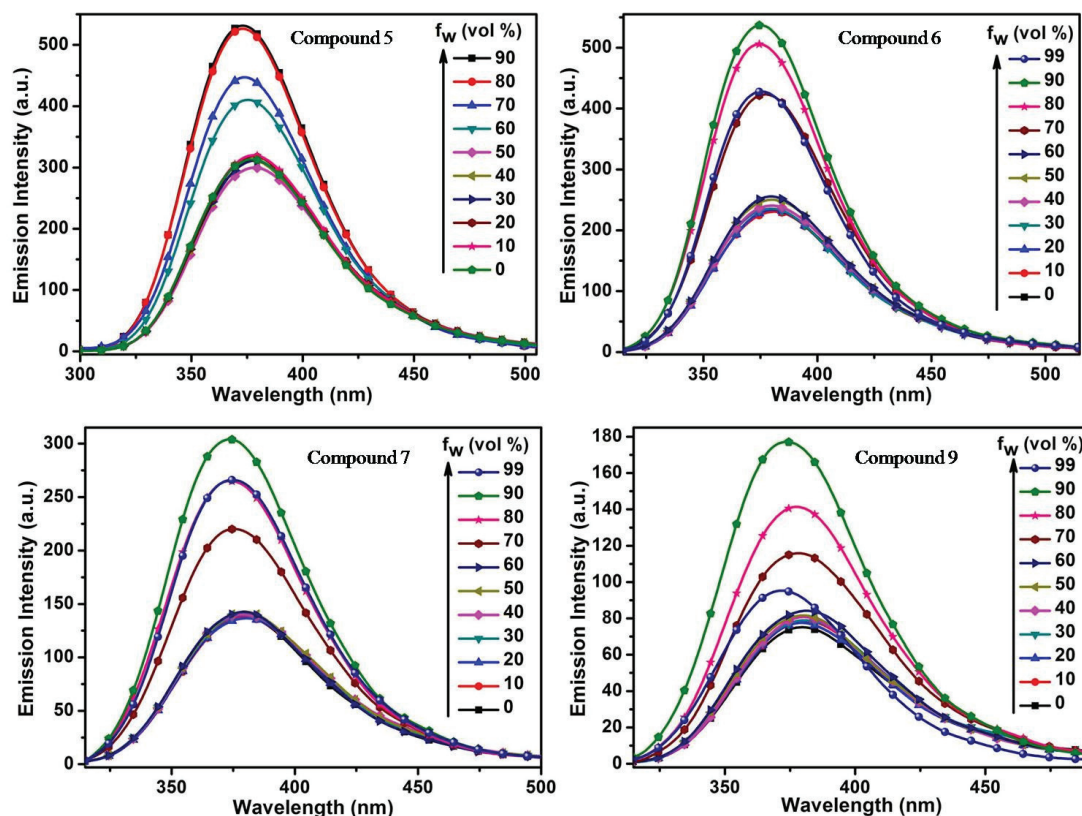


Figure 5B.5: Fluorescence spectra of compound **5**, **6**, **7** & **9** (4.8×10^{-6} M, excited at 280 nm) in THF/H₂O mixture with different water fraction (f_w).

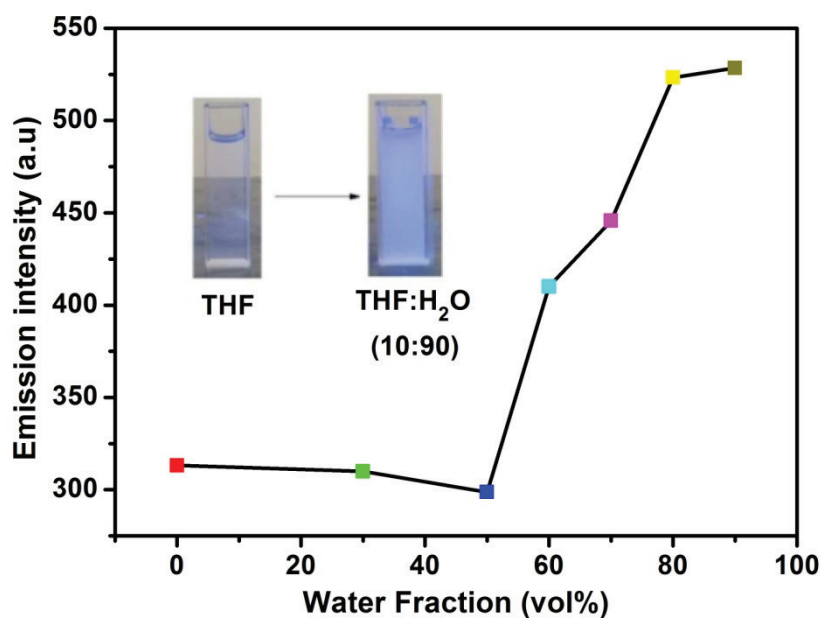


Figure 5B.6: Relationship between PL intensity of compound **5** and different water fraction (Insets: fluorescence photograph under UV light; THF:H₂O ratio 10:90).

The tetraaryl pyrazole decorated cyclophosphazenes (**5**, **6**, **7** & **9**) are soluble in common organic solvents such as dichloromethane, chloroform and tetrahydrofuran,

but insoluble in water. The emission spectrum of **5**, **6**, **7** & **9** (Figure 5B.5) in well dissolved THF solution showed a maximum peak at 376, 377, 376, 379 nm with a quantum yield of 11 %, 12%, 9% and 9% respectively. To examine the AIEE property of all the pyrazole decorated cyclophosphazenes (**5**, **6**, **7** & **9**) we gradually increased the water fraction (f_w) keeping the concentration of the solution same. As expected, a remarkable enhancement of emission is observed for the 40:60 (v/v) THF:H₂O mixture (Figure 5B.6). The emission starts increasing continually and reaches a maximum at 10:90 (v/v) THF:H₂O mixture with a quantum efficiency of 22 %, 21%, 20% & 19% respectively which is about 2 times higher than the quantum yield observed in the pure THF solvent (Table 5B.1). As water is a nonsolvent (or) poor solvent for pyrazole decorated cyclophosphazenes (**5**, **6**, **7** & **9**), with increase in water content, the molecules must have aggregated which leads to restriction of intramolecular rotations.

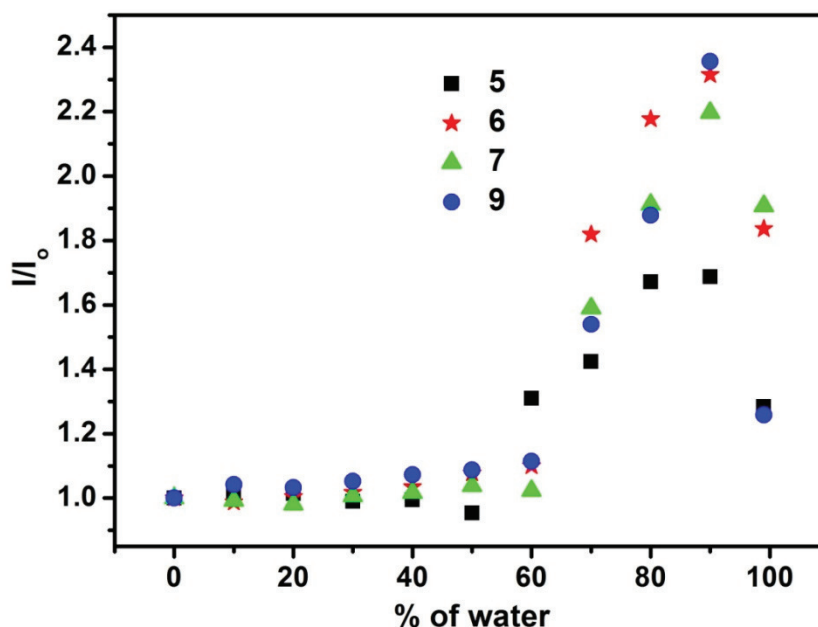


Figure 5B.7: Effects of water addition on fluorescence intensity (I) of the compound **5**, **6**, **7** & **9**.

This restriction of intramolecular rotation leads to increased fluorescent emission which is called as AIEE effect.⁴⁰ The photoluminescence peak intensities

(I/I_0) vs water content of the mixture were plotted to visually realize the emission intensity changes of the compounds **5**, **6**, **7** & **9**. As shown in Figure 5B.7, each pyrazole decorated cyclophosphazenes (**5**, **6**, **7** & **9**) has an instantaneous point for the emission enhancement, however when the water composition increased beyond 95%, the emission of all compounds decreased which may be due to precipitation of the compounds at that composition.

To further verify the AIEE phenomenon, the emission spectrum of compound **5** at different temperature was studied. When the solution temperature is increased, the emission intensity dramatically decreased (Figure 5B.8); at low temperature the molecular rotations will be lower and increases with increase in temperature. This result supports that restriction of intramolecular rotations play a very important role in the AIEE process.

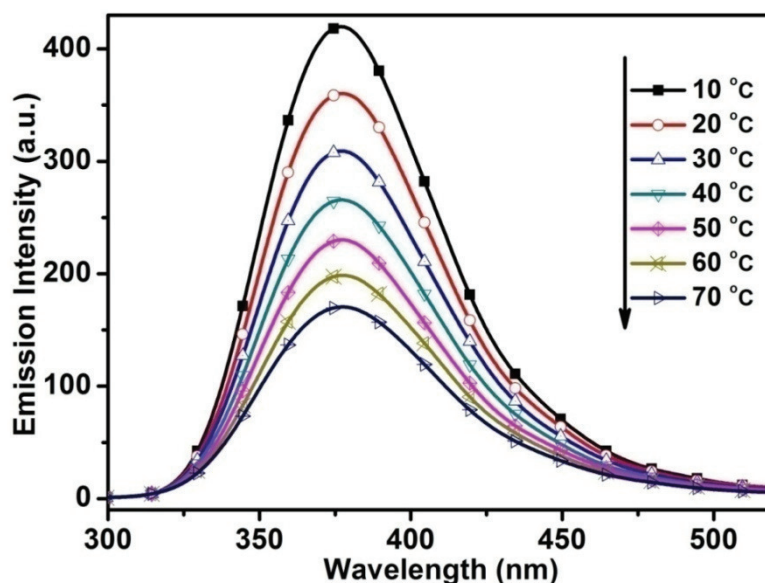


Figure 5B.8: Fluorescence spectra of compound **5** (4.8×10^{-6} M; excited at 280 nm) at different temperature.

We then measured the emission spectra of compound **7** in a solution of different viscosities. We prepared solutions of different viscosities by blending glycerol with methanol.⁴¹ Although there is insignificant emission enhancement from 0 to 40 %; the

emission became stronger upon increasing the viscosity of the solution and reaches a maximum when the glycerol fraction is about 80 % (Figure 5B.9). The observed emission enhancement is due to viscosity effect which further supports that the AIEE-phenomenon is caused by the restricted intramolecular rotations of the aromatic rings.

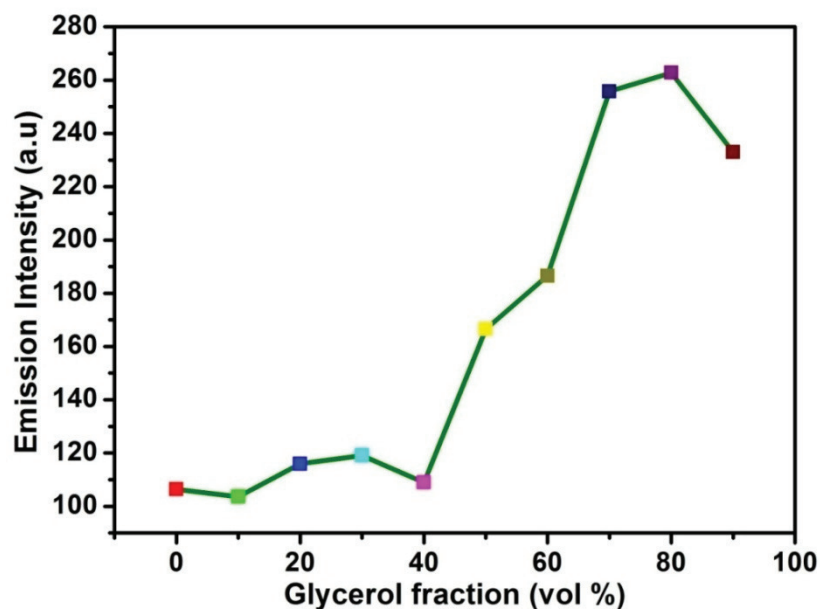


Figure 5B.9: Photoluminescence peak intensity of compound 7 (1.9×10^{-5} M; excited at 280 nm) vs composition of glycerol/methanol mixtures.

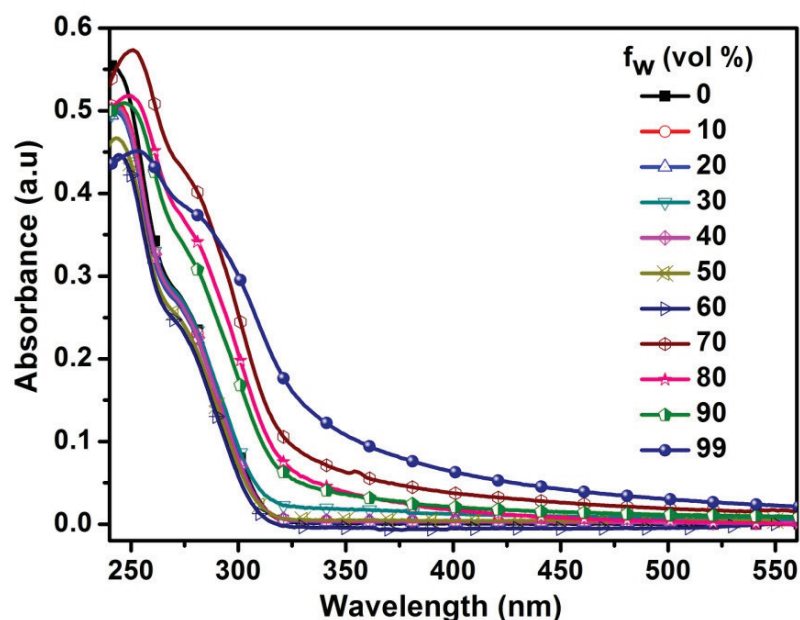


Figure 5B.10: UV –Vis absorption spectra of compound 7 (4.8×10^{-6} M) in H₂O/THF mixtures with different volume fractions of water.

However, the absorption spectra of compound **7** in THF-water mixtures do not exhibit any trend in the absorbance in the spectral region (Figure 5B.10).

The AIEE behaviour of the compounds **5**, **6**, **7** & **9** have also been investigated by the time resolved fluorescence technique (Figure 5B.11). All four compounds show longer fluorescence life time at 90:10 (H₂O:THF) composition (0.88 ns (**5**), 1.06 ns (**6**), 0.81 ns (**7**), 0.81 ns (**9**)) than that in pure THF solvent (0.46 ns (**5**), 0.49 ns (**6**), 0.35 ns (**7**), 0.37 ns (**9**)), which further supports the AIEE mechanism through aggregates.

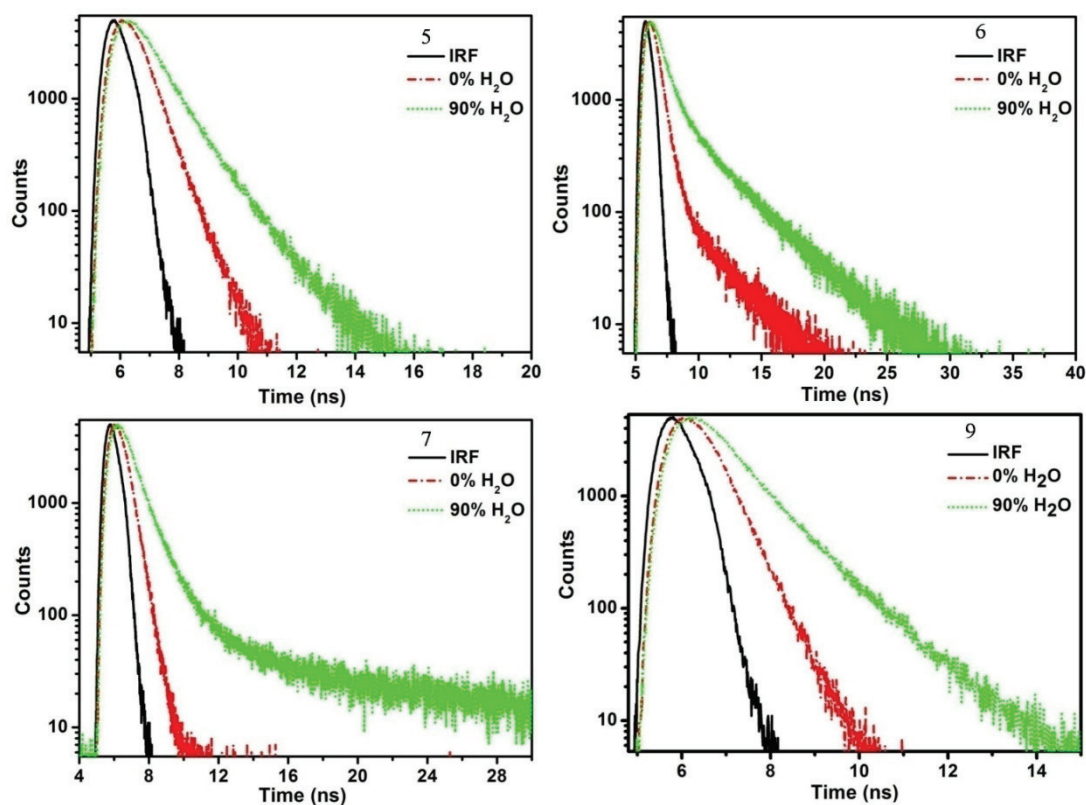


Figure 5B.11: Fluorescence decay of compound **5**, **6**, **7** & **9** in THF (red) solution and THF:H₂O (10:90; blue) aggregates. (2.28×10^{-5} M; excited at 280 nm).

To better understand the photoluminescence properties of the tetraaryl pyrazole (**3**) and pyrazole decorated cyclophosphazenes, attempts were made to obtain single crystals. Delightfully, single crystals of tetraaryl pyrazole (**3**) and di-pyrazole decorated cyclophosphazene (**7**) were obtained and analysed using single

crystal X-ray diffraction technique (Table 5B.2). Compound **3** and **7** are crystallized in the Orthorhombic and Triclinic system respectively.

Table 5B.2: Crystal data and structure refinement parameters for compounds **3** & **7**

Compound	3	7
Empirical formula	C ₂₈ H ₂₂ N ₂ O	C ₁₆₄ H ₁₂₄ N ₁₄ O ₁₇ P ₆
Formula weight	402.48	2748.59
Temperature/K	296(2)	296(2)
Crystal system	Orthorhombic	Triclinic
Space group	<i>P</i> 2 ₁ 2 ₁ 2 ₁	<i>P</i> -1
<i>a</i> /Å	9.4128(2)	12.6054(3)
<i>b</i> /Å	10.2247(2)	17.2285(4)
<i>c</i> /Å	22.8025(6)	18.9581(5)
α /°	90	64.2940(10)
β /°	90	89.5010(10)
γ /°	90	80.5230(10)
Volume/Å ³	2194.58(9)	3649.95(15)
Z	4	1
ρ_{calcd} /g cm ⁻³	1.218	1.250
μ /mm ⁻¹	0.074	0.144
F(000)	848	1432
θ range [°]	1.79 – 28.33	1.64 – 26.05
Index ranges	-12 ≤ <i>h</i> ≤ 12 -13 ≤ <i>k</i> ≤ 13 -30 ≤ <i>l</i> ≤ 30	-15 ≤ <i>h</i> ≤ 13 -21 ≤ <i>k</i> ≤ 21 -23 ≤ <i>l</i> ≤ 23
Reflns. collected	35656	46528
Independent reflns	5470 [<i>R</i> (int) = 0.0741]	14371 [<i>R</i> (int) = 0.0471]
Data/restraints/ parameters	5470 / 0 / 282	14371 / 0 / 909
GOF on <i>F</i> ²	1.011	1.045
Final <i>R</i> indices [<i>I</i> > 2σ(<i>I</i>)]	<i>R</i> ₁ = 0.0502 <i>wR</i> ₂ = 0.1024	<i>R</i> ₁ = 0.0705 <i>wR</i> ₂ = 0.2206
<i>R</i> indices (all data)	<i>R</i> ₁ = 0.1002 <i>wR</i> ₂ = 0.1294	<i>R</i> ₁ = 0.1145 <i>wR</i> ₂ = 0.2620
Largest diff. peak and hole [e Å ⁻³]	0.333 and -0.365	1.359 and -0.357

In the crystal, the phenyl rings around the pyrazole positioned in a non planar, propeller shaped arrangement. The observed torsion angles between the pyrazole unit and the neighbouring phenyl groups are 47.61 (8), 41.18 (8), 54.93 (7) and 47.99 (7) ° (for compound **3**) (Figure 5B.12), 65.78 (1), 54.82 (2), 40.99 (1) and 24.33 (1) °; 52.97 (1), 74.97 (2), 34.13 (2) and 25.28 (2) ° (for compound **7**) (Figure 5B.13). This

twisted conformation hampers the ability of molecules to pile in a face-to-face fashion.

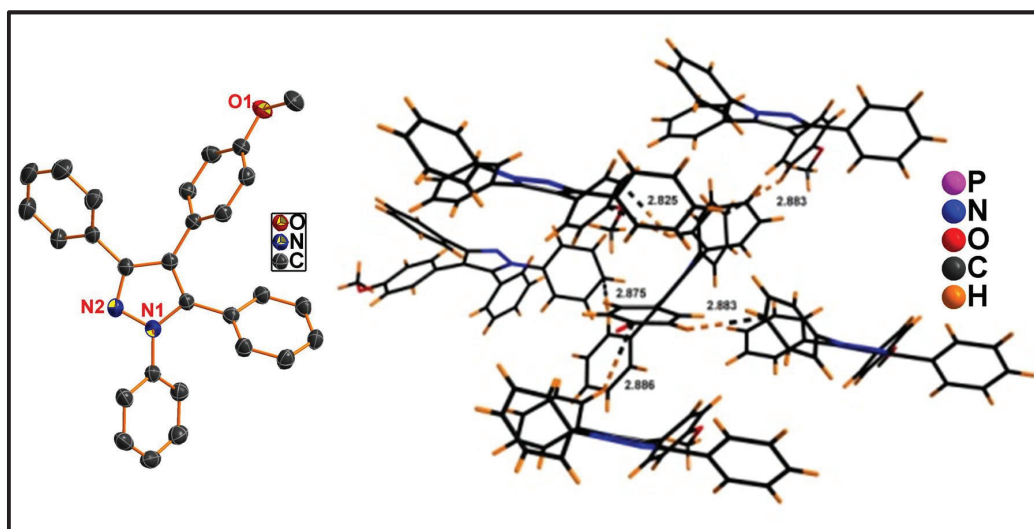


Figure 5B.12: (left) Molecular structure of compound **3**. Thermal ellipsoids are drawn at 50% probability level (Hydrogen atoms are omitted for clarity). (right) Packing diagram with intermolecular C-H... π interactions (capped stick model).

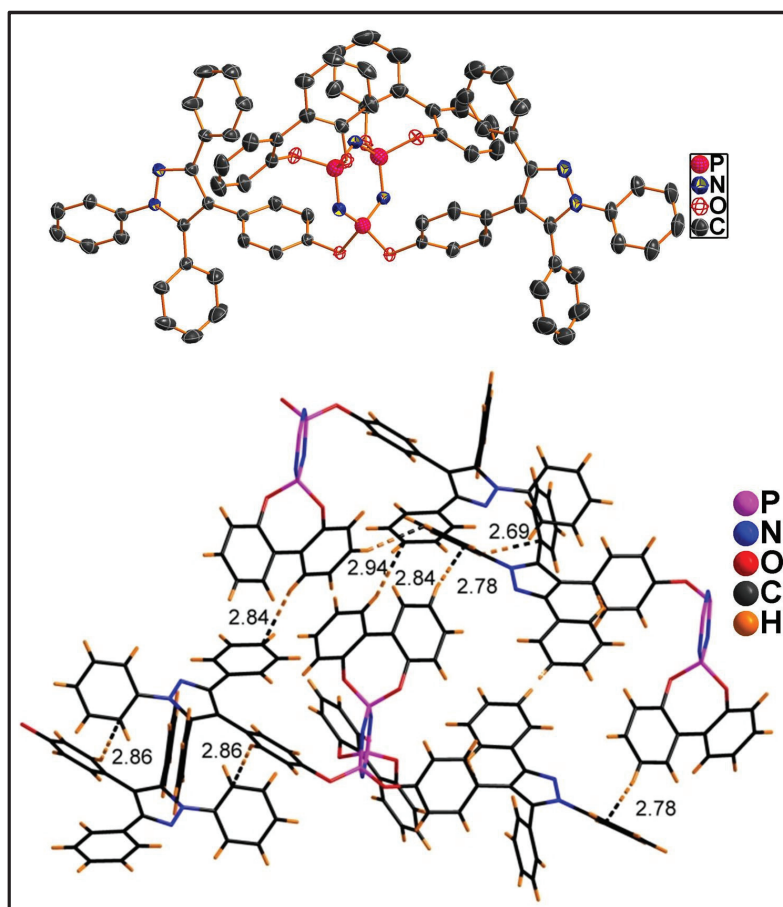


Figure 5B.13: (top) Molecular structure of compound **7**. (bottom) Packing diagram with intermolecular C-H... π interactions (capped stick model).

Compound **3** and **7** showed multiple C-H... π hydrogen bonds as shown in Figure 5B.12 & 5B.13. These intrinsic intermolecular supramolecular interactions are most important structural features that promote radiative relaxation of the excited state, making the molecules to fluoresce strongly in the aggregated state.

To better comprehend the relationship between the structure and the emission properties, computations were conducted.

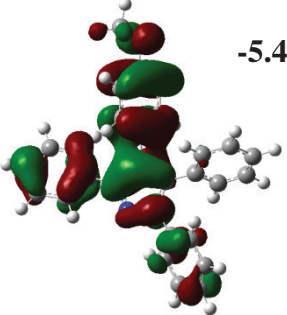
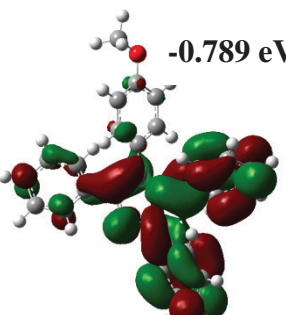
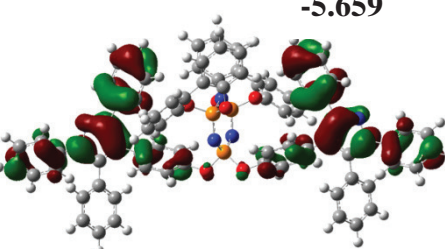
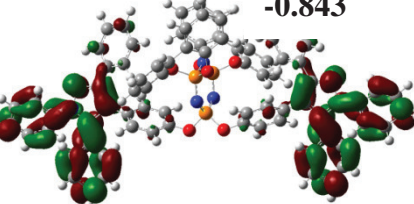
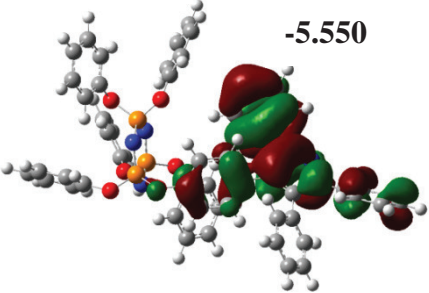
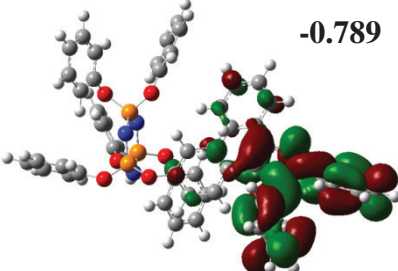
Compound	HOMO	LUMO
3	 -5.414 eV	 -0.789 eV
7	 -5.659	 -0.843
9	 -5.550	 -0.789

Figure 5B.14: Computed orbitals for compound **3**, **7** & **9**.

The geometry of the molecule **3** was optimized using DFT of B3LYP with 6-31G(d) basis set. The orbital distribution of the HOMO and LUMO energy levels of the

optimized structure **3** is shown in Figure 5B.14. The filled π -orbitals (or HOMOs) are dominated by the orbitals originating from pyrazole core and 1,3 & 4-phenyl, while the unfilled orbitals (or LUMOs) are mainly dominated from the pyrazole core and phenyl groups at the 1,3 & 5-positions (Figure 5B.14). Since the cyclophosphazene only acts as a support, we believe that the computation results derived from **3** can be transposed to **5**, **6**, **7**, & **9**. To verify this we also optimized structures of compound **7** & **9** as described *vide supra*. As expected the HOMO and LUMO of compounds **7** and **9** dominated by the orbitals originating from pyrazole unit and there is no conjugation between cyclophosphazene core and the pyrazole unit (Figure 5B.14).

To explore the potential use of the luminogen decorated cyclotriphosphazenes, we subjected the pyrazole decorated cyclophosphazenes (**5**, **6**, **7** & **9**) for the detection of picric acid. Picric acid is one of the powerful explosive and environmental pollutant; detection of the same is highly desirable.^{42,43} The fluorescence spectrum of aggregates of compound **5**, **6**, **7** & **9** in THF/H₂O (30:70) exhibits an intense emission at 376 nm upon excitation at 280 nm. The emission of the aggregates of **5**, **6**, **7** & **9** are effectively quenched upon addition of picric acid (Figure 5B.15). At low concentration the Stern-Volmer plot is linear and gave a quenching constant of $0.50 \times 10^5 \text{ M}^{-1}$ (**5**), $0.39 \times 10^5 \text{ M}^{-1}$ (**6**), $0.53 \times 10^5 \text{ M}^{-1}$ (**7**), & $0.60 \times 10^5 \text{ M}^{-1}$ (**9**); however at higher concentration of picric acid the curve deviate from linearity and bend upward which may be due to “super-quenching” effect ; an effect observed in the high concentration region. The fluorescence life time of compound **5**, **6**, **7** and **9** were studied with gradual addition of picric acid to ascertain whether the quenching mechanism is dynamic or static (Figure 5B.16). The fluorescence life time of **5**, **6**, **7** and **9** remain unchanged upon addition of picric acid which is indicative of static quenching.

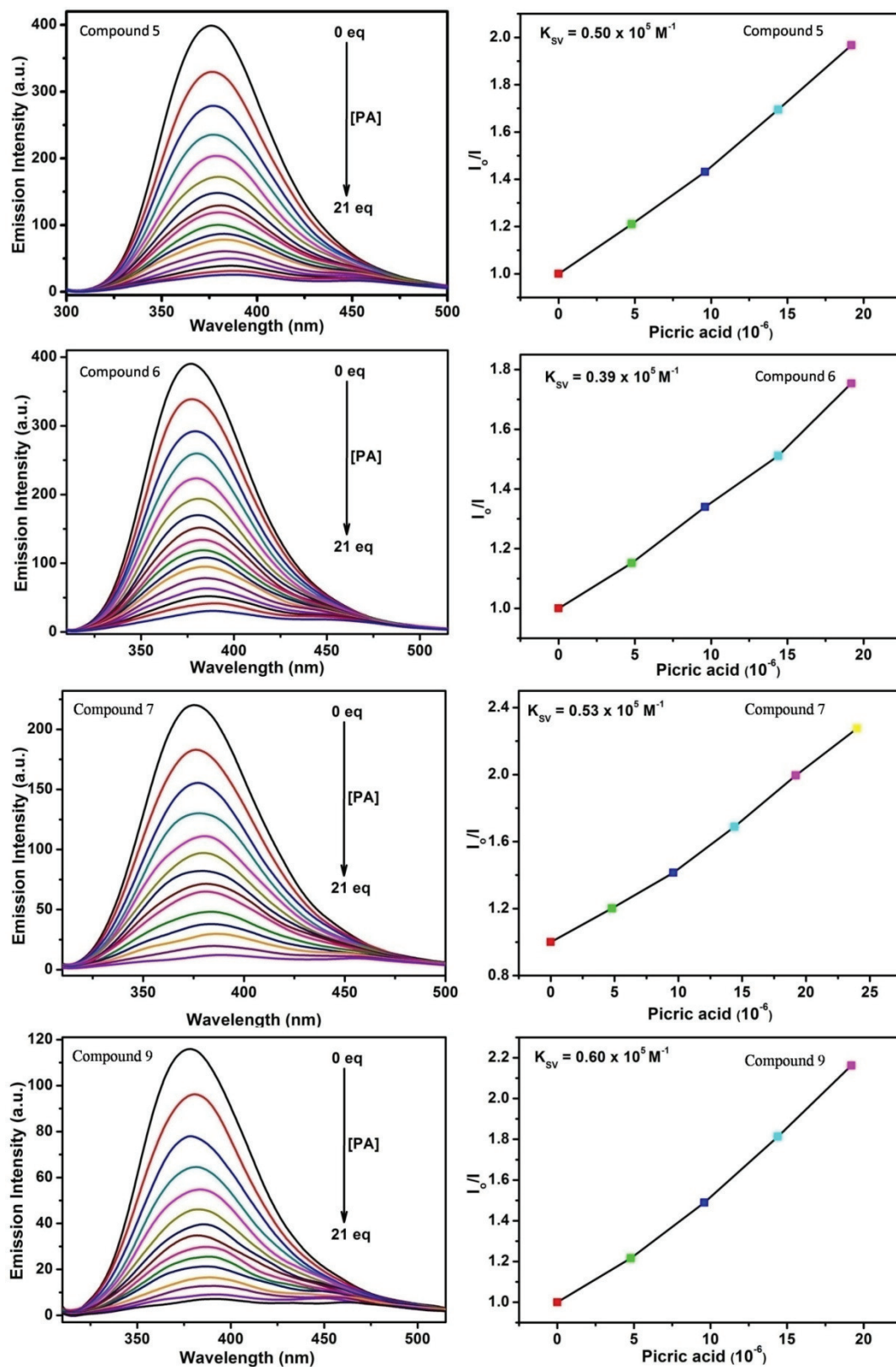


Figure 5B.15: (left) Fluorescence quenching of compound 5, 6, 7 and 9 (4.8×10^{-6} M; excited at 280 nm) in THF/water mixture (30:70). (right) Stern–Volmer plot for compound 5, 6, 7 and 9 using PA as quencher at lower concentration.

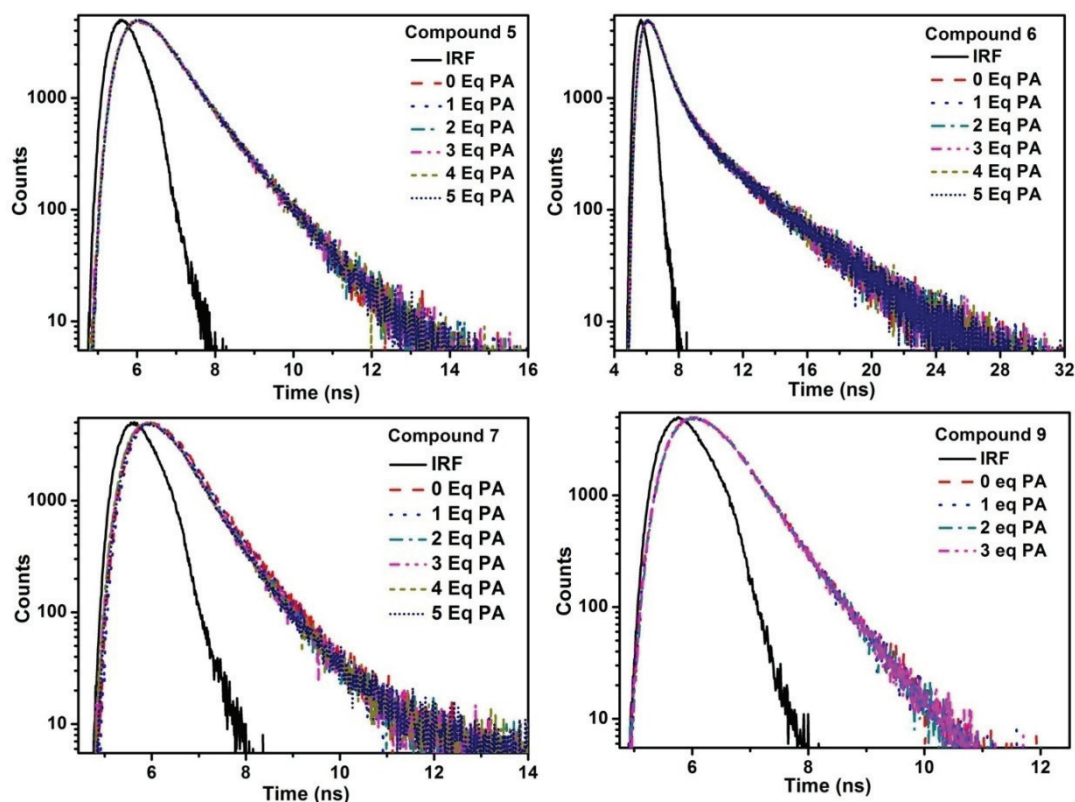


Figure 5B.16: Fluorescence lifetime decay profiles for compound **5**, **6**, **7** & **9** in THF/water mixture (30:70) (4.8×10^{-6} M ; $\lambda_{\text{ex}} = 280$ nm).

To examine the selectivity of our system, we took compound **5** and tested against different analytes like 2,6-dinitrotoluene (2,6-DNT), 4-nitrophenol (4-NP), 4-nitroanisole (4-NA), nitrobenzene (NB), nitromethane (NM), phenol, 2,3-dichloro-5,6-dicyano-1,4-benzoquinone (DDQ). Interestingly, the quenching efficiency for picric acid was found to be 90%, indicates its effectiveness to detect picric acid over other tested analytes (Figure 5B.17). To perceive the use of our system, we prepared filter paper strips of compound **5** by dipping a filter paper in the solution of compound **5** in THF followed by drying it by exposure to air. In order to check the sensitivity of the test strip coated with compound **5**, solution with different concentrations of picric acid were spotted on the test strips (Figure 5B.18). After drying the test strips, we visualized the same under UV light; our test strip method readily allowed us to visually

detect picric acid of ~20 ng, which is comparable with other literature reported reports.^{42,44-49}

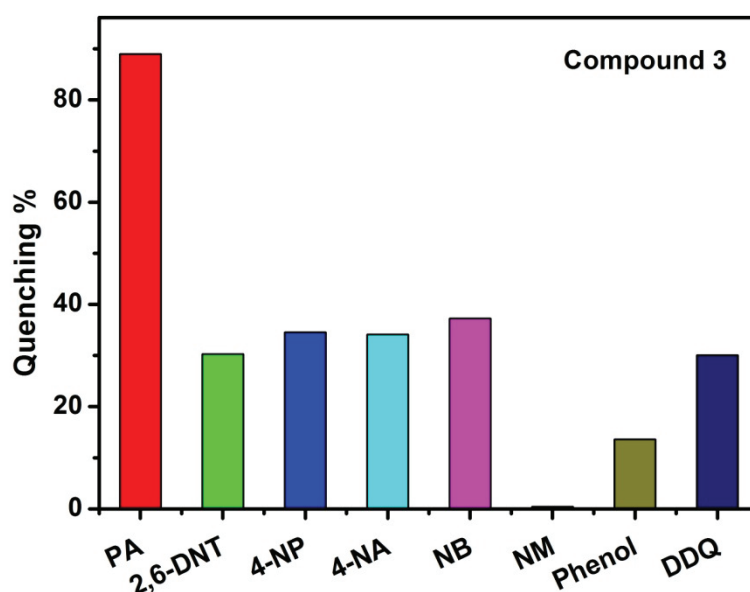


Figure 5B.17: Fluorescence quenching efficiencies of compound **5** in THF:H₂O (30:70) mixture (4.8×10^{-6} M; excited at 280 nm) toward different analytes (12 eq).

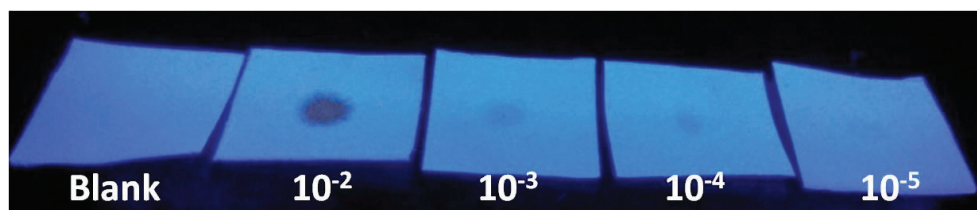


Figure 5B.18: Colour of fluorescent strips under UV light after the addition of different concentration of picric acid.

5B.3 Conclusion

In summary, we synthesized a new AIEE active tetraaryl pyrazolyl motif that can be supported in cyclophosphazene. We have shown that tetraaryl pyrazole decorated cyclophosphazenes **5**, **6**, **7** & **9** shows intense emission when aggregated in THF:H₂O mixture which is a typical aggregation induced emission enhancement process. The crystal structure of **3** and **7** and the theoretical analysis of the model compound **3** show the existence of nonplanar propeller shaped arrangement which may be responsible for the above discussed AIEE phenomenon observed in **3** as well as in tetraaryl pyrazole

substituted cyclophosphazenes **5**, **6**, **7&9**. We envisage that this proof of concept will be useful for further development of wide range of cyclophosphazene based AIEE or AIE active materials and also poly(phosphazene) based AIEE or AIE active material that are of interest as advanced optical materials.

5B.4 Experimental section

5B.4.1 General information

Reagents and starting materials were purchased from Alfa-Aesar, Sigma-Aldrich and Spectrochem chemical companies and used as received unless otherwise noted. Dichloromethane was distilled from CaH₂. THF was distilled from Na/benzophenone prior to use. 1,3,5-triphenyl-1*H*-pyrazole was prepared according to literature procedure.¹ All 400 MHz ¹H, 100 MHz ¹³C and 81 MHz ³¹P NMR spectra were recorded on a Bruker ARX 400 spectrometer operating at 400 MHz. ¹H & ¹³C NMR spectra were referenced internally to solvent signals and ³¹P spectrum was referenced externally to H₃PO₄ in D₂O ($\delta = 0$). All NMR spectra were recorded at ambient temperature. ESI mass spectra were recorded on Bruker, micrOTOF-QII mass spectrometer. The absorbance spectra are recorded on a Perkin Elmer Lambda 750 UV–visible spectrometer. The fluorescence spectra are recorded on a Perkin Elmer LS-55 fluorescence spectrometer. The fluorescence spectra are corrected for the instrumental response. The quantum yield was calculated by measuring the integrated area under the emission curves and by using the following equation. $\Phi_{\text{sample}} = \Phi_{\text{standard}} \times (I_{\text{sample}}/I_{\text{standard}}) \times (\text{OD}_{\text{standard}}/\text{OD}_{\text{sample}}) \times (\eta_{\text{sample}}^2/\eta_{\text{standard}}^2)$ where, ‘ Φ ’ is the quantum yield, ‘I’ the integrated emission intensity, ‘OD’ the optical density at the excitation wavelength, and ‘ η ’ the refractive index of the solvent. The subscripts “standard” and “sample” refer to the fluorophore of reference and unknown respectively. In this case unknowns are **5**, **6**, **7&9**, reference is *p*-terphenyl (quantum

yield of *p*-terphenyl in cyclohexane is 0.82). Optically matched solutions with very similar optical densities of the “sample” and “standard” at a given absorbing wavelength were used for quantum yield calculations. A time-correlated single-photon counting (TCSPC) spectrometer (Edinburgh, OB920) with a light emitting diode (LED) source ($\lambda_{\text{exc}} = 280$ nm) was used for all time-resolved measurements. A micro channelplate (MCP) photomultiplier (Hamamatsu R3809U-50) was used as the detector for all time resolved measurements. The instrument response function (IRF) was recorded by scatterer (dilute ludox solution in water) in place of the sample. Decay curves were analyzed using the nonlinear least-squares interation process using F900 decay analysis software. The quality of the fit was judged using the chi square (χ^2) values. Elemental analyses were carried out by using a Thermo quest CE instrument model EA/110 CHNS-O elemental analyzer. Single-crystal X-ray diffraction data were collected on a Bruker APEX-II diffractometer equipped with an Oxford instruments low-temperature attachment. The data were collected at 296 K using, Mo-K α radiation (0.71073 Å). The structures were solved and refined with SHELX suite of programs.³ All non-hydrogen atoms were refined with anisotropic displacement coefficients. The H atoms were placed at calculated positions and were refined as riding atoms. DFT calculations were performed with the Gaussian03 program.⁴ The structures were optimized using 6-31G(d) (B3LYP) as the basis set. The input files were generated using X-ray data (for compound **3** and **7**). Excitation data were determined using TD-DFT (B3LYP) calculations.

5B.4.2 Synthetic procedure and spectral characterization**5B.4.2.1 Synthesis of 4-(4-methoxyphenyl)-1,3,5-triphenyl-1H-pyrazole (3)**

4-bromo-1,3,5-triphenyl-1H-pyrazole (7.50 g, 20 mmol), (4-methoxy phenyl) boronic acid (3.95 g, 26 mmol), sodium carbonate (6.36 g, 60 mmol), tetrakis(triphenylphosphine) palladium(0) (0.69 g, 0.60 mmol) were placed in 500 mL round bottom flask under nitrogen atmosphere and degassed mixture of THF/Water (150/50 mL) was added. The reaction mixture was refluxed for 36 h, cooled and filtered through celite pad. The solvent was removed under vacuum and 100 mL of ethyl acetate and 100 mL of water was added. After separating organic layer, the aqueous layer was extracted with ethyl acetate (3 × 15 mL). The combined organic phases were washed with brine and dried over Na₂SO₄. The solvent was removed under reduced pressure, and the product was purified by silica gel column chromatography using mixture of ethyl acetate and hexane as eluent to afford the corresponding product as a white solid. Yield: 5.63 g, (70 %). mp: 166 °C. ¹H NMR (400 MHz, CDCl₃): δ = 3.78 (s, 3H, -OCH₃), 6.77 (d, *J* = 8 Hz, 2H, ArH), 7.02-7.08 (m, 4H, ArH), 7.21-7.33 (m, 11H, ArH), 7.55-7.57 (m, 2H, ArH) ppm. ¹³C NMR (100 MHz, CDCl₃): δ = 55.23, 113.84, 120.47, 125.32, 125.47, 127.37, 127.77, 128.24, 128.33, 128.39, 128.51, 128.89, 130.23, 130.56, 131.88, 133.18, 139.98, 141.47, 150.22, 158.52 ppm. HR-MS (ESI): calcd. for C₂₈H₂₂N₂O₁ ([M +H]⁺): 403.1805, found: 403.1787. Elemental analysis calcd (%) for C₂₈H₂₂N₂O₁: C 83.56, H 5.51, N 6.96; found: C 83.43, H 5.56, N 6.88.

5B.4.2.2 Synthesis of 4-(1,3,5-triphenyl-1H-pyrazol-4-yl)phenol (4):

To a mixture of dodecanethiol (5 mL) and dichloromethane (150 mL) was added aluminium chloride (5.96 g, 45 mmol) at 0 °C. The resulting solution was warmed to room temperature and compound **3** (4.56 g, 11 mmol) was added with stirring. After

being stirred for 24 h, the reaction mixture was cooled to 0 °C and 100 mL of water was slowly added. The aqueous layer was extracted with dichloromethane (3 × 20 mL). The combined organic phases were washed with brine and dried over Na₂SO₄. The solvent was removed under reduced pressure, and the product was washed with hexane twice to remove the dodecanethiol. The resultant crude product was purified by silica gel column chromatography using mixture of ethyl acetate and hexane as eluent to afford the corresponding product as a white solid. Yield: 4.12 g, (95 %). mp: 260 °C. ¹H NMR (400 MHz, CDCl₃): δ = 6.67 (d, *J* = 8 Hz, 2H, ArH), 6.96 (d, *J* = 8 Hz, 2H, ArH), 7.06 (d, *J* = 8 Hz, 2H, ArH), 7.18- 7.34 (m, 11H, ArH), 7.53-7.55 (m, 2H, ArH) ppm. ¹³C NMR (100MHz, CDCl₃): δ = 115.44, 120.44, 125.47, 125.51, 127.43, 127.82, 128.28, 128.35, 128.40, 128.47, 128.52, 128.92, 130.18, 130.56, 132.08, 133.12, 139.94, 141.53, 150.25, 154.58 ppm. HR-MS (ESI): calcd. for C₂₇H₂₀N₂O₁ ([M +H]⁺) :389.1648, found : 389.1631. Elemental analysis calcd (%) for C₂₇H₂₀N₂O₁ : C 83.48, H 5.19, N 7.21; found: C 83.40, H 5.56, N 7.08.

5B.4.2.3 Synthesis of compound 5

Under nitrogen, 4-(1,3,5-triphenyl-1*H*-pyrazol-4-yl)phenol (1.00 g, 2.57 mmol) in anhydrous tetrahydrofuran (10 mL) was added to a suspension of NaH (57 % oil suspension, 0.11 g, 2.67 mmol) in anhydrous tetrahydrofuran (20 mL) at 0 °C with stirring. The reaction mixture was warmed to room temperature and refluxed for 2 h. The resulting solution was cooled to 0 °C in ice bath and P₃N₃Cl₆ (0.12 g, 0.34 mmol) in anhydrous tetrahydrofuran (5 mL) was added. The reaction mixture was refluxed for 24 h, cooled to room temperature and filtered. The filtrate was removed under vacuum; the resultant crude product was purified by silica gel column chromatography using ethyl acetate and hexane as eluent to afford the corresponding product as a white solid. Yield: 0.41g (49 %). mp: 241 °C. ¹H NMR (400 MHz,

CDCl_3): $\delta = 6.70$ - 6.78 (m, 23H, ArH), 6.91-6.93 (m, 12H, ArH), 6.98-7.04 (m, 19H, ArH), 7.11-7.12 (m, 18H, ArH), 7.29 (s, 29H, ArH), 7.41-7.42 (m, 12H, ArH) ppm. ^{13}C NMR (100 MHz, CDCl_3): $\delta = 119.79$, 120.79, 125.39, 127.44, 127.80, 128.31, 128.36, 128.43, 128.93, 129.86, 130.10, 130.36, 131.84, 132.99, 139.96, 141.36, 149.60, 150.33 ppm. ^{31}P NMR (162 MHz, CDCl_3): $\delta = 8.5$. HR-MS (ESI): calcd. for $\text{C}_{162}\text{H}_{114}\text{N}_{15}\text{O}_6\text{P}_3$ ($[\text{M} + \text{H}]^+$) : 2459.8394, found : 2459.8313. Elemental analysis calcd (%) for $\text{C}_{162}\text{H}_{114}\text{N}_{15}\text{O}_6\text{P}_3$: C 79.11, H 4.67, N 8.54; found: C 79.02, H 4.58, N 8.44.

5B.4.2.4 Synthesis of compound 6

Compound **6** was prepared by following a procedure similar to that used for **5**. The quantities involved are as follows: Compound **4** (2.30 g, 5.92 mmol), NaH (57 % oil suspension, 0.30 g, 7.15 mmol), $\text{P}_3\text{N}_3\text{Cl}_4$ ($\text{C}_{12}\text{H}_8\text{O}_2$) (0.50 g, 1.08 mmol). Yield: 0.80 g, (40 %). mp: 209 °C. ^1H NMR (400 MHz, CDCl_3): $\delta = 6.81$ (d, $J = 8$ Hz, 2H, ArH), 6.88 - 7.00 (m, 24H, ArH), 7.05-7.10 (m, 12H, ArH), 7.17-7.19 (m, 12H, ArH), 7.27-7.31 (m, 24H, ArH), 7.48-7.54 (m, 10H, ArH) ppm. ^{13}C NMR (100 MHz, CDCl_3): $\delta = 119.86$, 120.98, 122.02, 125.47, 126.18, 127.54, 127.92, 128.42, 128.48, 128.82, 128.95, 129.66, 129.77, 130.08, 130.39, 131.87, 132.77, 139.79, 141.57, 148.06, 148.15, 149.62, 149.66, 149.70, 150.23 ppm. ^{31}P NMR (162 MHz, CDCl_3): $\delta = 9.1$ (d, $J = 92.3$ Hz), 25.8 (t, $J = 93.9$ Hz) ppm. HR-MS (ESI): calcd. for $\text{C}_{120}\text{H}_{84}\text{N}_{11}\text{O}_6\text{P}_3$ ($[\text{M} + \text{Na}]^+$) : 1891.5743, found : 1891.5751. Elemental analysis calcd (%) for $\text{C}_{120}\text{H}_{84}\text{N}_{11}\text{O}_6\text{P}_3$: C 77.12, H 4.53, N 8.24; found: C 77.01, H 4.59, N 8.43.

5B.4.2.5 Synthesis of compound 7

Compound **7** was prepared by following a procedure similar to that used for **5**. The quantities involved are as follows: Compound **4** (1.01 g, 2.61 mmol), NaH (57 % oil suspension, 0.13 g, 3.13 mmol), $\text{P}_3\text{N}_3\text{Cl}_2(\text{C}_{12}\text{H}_8\text{O}_2)_2$ (0.60 g, 1.04 mmol). Yield: 0.72 g (54 %). mp: 290 °C. ^1H NMR (400 MHz, CDCl_3): $\delta = 7.03$ - 7.06 (m, 8H, ArH),

7.12-7.17 (m, 10H, ArH), 7.23-7.35 (m, 28H, ArH), 7.51-7.56 (m, 8H, ArH) ppm. ^{13}C NMR (100 MHz, CDCl_3): δ = 119.94, 121.23, 121.28, 122.07, 125.57, 125.61, 126.18, 127.64, 128.05, 128.49, 128.53, 128.57, 128.88, 128.96, 129.71, 129.84, 130.48, 131.88, 132.57, 139.63, 141.83, 148.16, 148.21, 148.25, 149.84, 150.16, 171.29. ^{31}P NMR (162 MHz, CDCl_3): δ = 9.9 (t, J = 91.5 Hz), 26.1 (d, J = 90.7 Hz) ppm. HR-MS (ESI): calcd. for $\text{C}_{78}\text{H}_{54}\text{N}_7\text{O}_6\text{P}_3$ ($[\text{M} + \text{Na}]^+$) : 1300.3241, found : 1300.3240. Elemental analysis calcd (%) for $\text{C}_{78}\text{H}_{54}\text{N}_7\text{O}_6\text{P}_3 \cdot \text{C}_4\text{H}_8\text{O}_2$: C 72.08, H 4.57, N 7.18; found: C 72.29, H 4.68, N 7.04.

5B.4.2.6 Synthesis of compound 8

A mixture of $\text{P}_3\text{N}_3\text{Cl}_6$ (1.34 g, 3.86 mmol), 4-(1,3,5-triphenyl-1*H*-pyrazol-4-yl)phenol (1.50 g, 3.86 mmol), K_2CO_3 (0.64 g, 4.63 mmol) was stirred in dry acetone at 0 °C under nitrogen atmosphere and then the reaction mixture was allowed to stir at room temperature for 48 h. The solvent was removed under vacuum. The residue was extracted with CH_2Cl_2 (3 × 20 mL). After the solvent was removed, the resultant crude product was purified by silica gel column chromatography using mixture of ethyl acetate and hexane as eluent to afford the corresponding product as a white solid. Yield: 1.30 g, (48 %). mp: 140 °C. ^1H NMR (400 MHz, CDCl_3): δ = 7.04 (d, J = 8 Hz, 2H), 7.13 (s, 4H), 7.20-7.32 (m, 11H), 7.49 (s, 2H) ppm. ^{13}C NMR (100 MHz, CDCl_3): δ = 119.48, 121.63, 121.68, 125.52, 127.64, 128.07, 128.50, 128.58, 128.61, 128.99, 129.71, 130.51, 132.07, 132.10, 132.31, 132.33, 132.66, 139.70, 141.80, 148.04, 148.15, 150.21 ppm. ^{31}P NMR (162 MHz, CDCl_3): δ = 14.0 (t, J = 58.3 Hz), 22.9 (d, J = 58.3 Hz) ppm. HR-MS (ESI): calcd. for $\text{C}_{27}\text{H}_{19}\text{Cl}_5\text{N}_5\text{O}_1\text{P}_3$ ($[\text{M} + \text{H}]^+$) : 697.9318, found: 697.9373.

5B.4.2.7 Synthesis of compound 9

Compound **9** was prepared by following a procedure similar to that used for **5**. The quantities involved are as follows: Phenol (0.86 g, 9.14 mmol), NaH (57 % oil suspension, 0.42 g, 10.06 mmol), compound **6** (0.80 g, 1.14 mmol). Yield: 0.73 g, (65 %). mp: 150 °C. ¹H NMR (400 MHz, CDCl₃): δ = 6.78 (d, *J* = 8 Hz, 2H), 6.86 (d, *J* = 8 Hz, 2H), 6.92-7.06 (m, 14H), 7.09-7.32 (m, 24H), 7.50-7.51 (m, 2H) ppm. ¹³C NMR (100 MHz, CDCl₃): δ = 119.91, 120.60, 121.07, 121.12, 121.18, 121.29, 124.98, 125.07, 125.42, 127.39, 127.84, 128.39, 128.48, 128.52, 128.90, 129.54, 129.78, 130.06, 130.51, 131.79, 133.12, 140.02, 141.49, 149.70, 150.38, 150.73 ppm. ³¹P NMR (162 MHz, CDCl₃): δ = 8.0, 8.3, 8.8, 9.0, 9.1, 9.2, 9.4, 9.8 ppm. HR-MS (ESI): calcd. for C₅₇H₄₄N₅O₆P₃ ([M +H]⁺) : 988.2577, found : 988.2600. Elemental analysis calcd (%) for C₅₇H₄₄N₅O₆P₃ : C 69.30, H 4.49, N 7.09; found: C 69.35, H 4.57, N 6.94.

5B.5 References

- (1) Birks, J. B. *Photophysics of Aromatic Molecules* **1970**.
- (2) Luo, J.; Xie, Z.; Xie, Z.; Lam, J. W. Y.; Cheng, L.; Chen, H.; Qiu, C.; Kwok, H. S.; Zhan, X.; Liu, Y.; Zhu, D.; Tang, B. Z.; Tang, B. Z.; Tang, B. Z. *Chem. Commun.* **2001**, *18*, 1740.
- (3) An, B. K.; Kwon, S. K.; Jung, S. D.; Park, S. Y. *J. Am. Chem. Soc.* **2002**, *124*, 14410.
- (4) Ding, D.; Li, K.; Liu, B.; Tang, B. Z. *Acc. Chem. Res.* **2013**, *46*, 2441.
- (5) Hu, R.; Leung, N. L. C.; Tang, B. Z. *Chem. Soc. Rev.* **2014**, *43*, 4494.
- (6) Hong, Y.; Lam, J. W. Y.; Tang, B. Z. *Chem. Soc. Rev.* **2011**, *40*, 5361.
- (7) Mei, J.; Leung, N. L. C.; Kwok, R. T. K.; Lam, J. W. Y.; Tang, B. Z. *Chem. Rev.* **2015**, *115*, 11718.

- (8) Zhao, Q.; Sun, J. Z. *J. Mater. Chem. C***2016**, *4*, 10588.
- (9) Yui, G.; Yin, S.; Liu, Y.; Chen, J.; Xu, X.; Sun, X.; Ma, D.; Zhan, X.; Peng, Q.; Shuai, Z.; Tang, B.; Zhu, D.; Fang, W.; Luo, Y. *J. Am. Chem. Soc.***2005**, *127*, 6335.
- (10) Chen, M.; Li, L.; Nie, H.; Tong, J.; Yan, L.; Xu, B.; Sun, J. Z.; Tian, W.; Zhao, Z.; Qin, A.; Tang, B. Z. *Chem. Sci.***2015**, *6*, 1932.
- (11) Chi, Z.; Zhang, X.; Xu, B.; Zhou, X.; Ma, C.; Zhang, Y.; Liu, S.; Xu, J. *Chem. Soc. Rev.***2012**, *41*, 3878.
- (12) Yang, Z.; Chi, Z.; Xu, B.; Li, H.; Zhang, X.; Li, X.; Liu, S.; Zhang, Y.; Xu, J. *J. Mater. Chem.***2010**, *20*, 7352.
- (13) Gu, X. G.; Yao, J. J.; Zhang, G. X.; Zhang, C.; Yan, Y. L.; Zhao, Y. S.; Zhang, D. Q. *Chem.-Asian J.***2013**, *8*, 2362.
- (14) Chivers, T.; Manners, I. *Inorganic Rings and Polymers of the P-Block Elements***2009**.
- (15) Allcock, H. R. *Phosphorus-Nitrogen Compounds***1972**.
- (16) Allen, C. W. *Chem. Rev.***1991**, *91*, 119.
- (17) Allcock, H. R. *Chem. Rev.***1972**, *72*, 315.
- (18) Steiner, A.; Zacchini, S.; Richards, P. I. *Coord. Chem. Rev.***2002**, *227*, 193.
- (19) Beşli, S.; Mutlu, C.; Ibişoğlu, H.; Yuksel, F.; Allen, C. W. *Inorg. Chem.***2015**, *54*, 334.
- (20) Kagit, R.; Yildirim, M.; Ozay, O.; Yesilot, S.; Ozay, H. *Inorg. Chem.***2014**, *53*, 2144.
- (21) Li, X.; Jiang, F.; Chen, L.; Wu, M.; Chen, Q.; Bu, Y.; Hong, M. *Dalton Trans.***2012**, *41*, 14038.
- (22) Richards, P. I.; Steiner, A. *Inorg. Chem.***2005**, *44*, 275.

- (23) Lawson, G. T.; Rivals, F.; Tascher, M.; Jacob, C.; Bickley, J. F.; Steiner, A. *Chem. Commun.***2000**, 341.
- (24) Beşli, S.; Coles, S. J.; Davies, D. B.; Erkovan, A. O.; Hursthouse, M. B.; Kiliç, A. *Inorg. Chem.***2008**, *47*, 5042.
- (25) Chandrasekhar, V.; Krishnan, V.; Steiner, A.; Bickley, J. F. *Inorg. Chem.***2004**, *43*, 166.
- (26) Chandrasekhar, V.; Deria, P.; Krishnan, V.; Athimoolam, A.; Singh, S.; Madhavaiah, C.; Srivatsan, S. G.; Verma, S. *Bioorg. Med. Chem. Lett.***2004**, *14*, 1559.
- (27) Chandrasekhar, V.; Athimoolam, A.; Krishnan, V.; Azhakar, R.; Madhavaiah, C.; Verma, S. *Eur. J. Inorg. Chem.***2005**, 1482.
- (28) Chandrasekhar, V.; Athimoolam, A.; Srivatsan, S. G.; Sundaram, P. S.; Verma, S.; Steiner, A.; Zacchini, S.; Butcher, R. *Inorg. Chem.***2002**, *41*, 5162.
- (29) Chandrasekhar, V. *Inorganic and Organometallic Polymers***2005**.
- (30) Allcock, H. R. *Chemistry and Applications of Polyphosphazenes***2003**.
- (31) Gleria, M.; De Jaeger, R. *Applicative Aspects of Cyclophosphazenes***2004**.
- (32) He, Q.; Dai, H.; Tan, X.; Cheng, X.; Liu, F.; Tschierske, C. *J. Mater. Chem. C.***2013**, *1*, 7148.
- (33) Krishna, T. R.; Parent, M.; Werts, M. H. V.; Moreaux, L.; Gmouh, S.; Charpak, S.; Caminade, A. M.; Majoral, J. P.; Blanchard-Desce, M. *Angew. Chem. Int. Ed.***2006**, *45*, 4645.
- (34) Franc, G.; Mazères, S.; Turrin, C. O.; Vendier, L.; Duhayon, C.; Caminade, A. M.; Majoral, J. P. *J. Org. Chem.***2007**, *72*, 8707.
- (35) Mongin, O.; Krishna, T. R.; Werts, M. H. V.; Caminade, A. M.; Majoral, J. P.; Blanchard-Desce, M. *Chem. Commun.***2006**, 915.

- (36) Rao, M. R.; Bolligarla, R.; Butcher, R. J.; Ravikanth, M. *Inorg. Chem.***2010**, *49*, 10606.
- (37) Hu, X. M.; Che, Q.; Zhou, D.; Cao, J.; He, Y. J.; Han, B. H. *Polym. Chem.***2011**, *2*, 1124.
- (38) Mamidala, R.; Mukundam, V.; Dhanunjayarao, K.; Venkatasubbaiah, K. *Dalton Trans.***2015**, *44*, 5805.
- (39) Mukherjee, S.; Salini, P. S.; Srinivasan, A.; Peruncheralathan, S. *Chem. Commun.***2015**, *51*, 17148.
- (40) Mei, J.; Hong, Y.; Lam, J. W. Y.; Qin, A.; Tang, Y.; Tang, B. Z. *Adv. Mater.***2014**, *26*, 5429.
- (41) Chen, J.; Law, C. C. W.; Lam, J. W. Y.; Dong, Y.; Lo, S. M. F.; Williams, I. D.; Zhu, D.; Tang, B. Z. *Chem. Mater.***2003**, *15*, 1535.
- (42) Vishnoi, P.; Sen, S.; Patwari, G. N.; Murugavel, R. *New J. Chem.***2015**, *39*, 886.
- (43) Feng, H. T.; Zheng, Y. S. *Chem. - Eur. J.***2013**, *20*, 195.
- (44) Zhao, Z.; Jiang, T.; Guo, Y.; Ding, L.; He, B.; Chang, Z.; Lam, J. W. Y.; Liu, J.; Chan, C. Y. K.; Lu, P.; Xu, L.; Qiu, H.; Tang, B. Z. *J. Polym. Sci., Part A: Polym. Chem.***2012**, *50*, 2265.
- (45) Mukundam, V.; Kumar, A.; Dhanunjayarao, K.; Ravi, A.; Peruncheralathan, S.; Venkatasubbaiah, K. *Polym. Chem.***2015**, *6*, 7764.
- (46) Bereau, V.; Duhayon, C.; Sutter, J. P. *Chem. Commun.***2014**, *50*, 12061.
- (47) Madhu, S.; Bandela, A.; Ravikanth, M. *RSC Adv.***2014**, *4*, 7120.
- (48) Roy, B.; Bar, A. K.; Gole, B.; Mukherjee, P. S. *J. Org. Chem.***2013**, *78*, 1306.
- (49) Bhalla, V.; Gupta, A.; Kumar, M. *Org. Lett.***2012**, *14*, 3112.

Summary

